



This work is licensed under a [Creative Commons Attribution-NonCommercial-ShareAlike 4.0 International License](https://creativecommons.org/licenses/by-nc-sa/4.0/).

How to cite this thesis / dissertation (APA referencing method):

Surname, Initial(s). (Date). *Title of doctoral thesis* (Doctoral thesis). Retrieved from [http://scholar.ufs.ac.za/rest of thesis URL on KovsieScholar](http://scholar.ufs.ac.za/rest_of_thesis_URL_on_KovsieScholar)

Surname, Initial(s). (Date). *Title of master's dissertation* (Master's dissertation). Retrieved from [http://scholar.ufs.ac.za/rest of thesis URL on KovsieScholar](http://scholar.ufs.ac.za/rest_of_thesis_URL_on_KovsieScholar)

Simulating Future Rangeland Production in Central South Africa

by

Catherine Odendaal

Submitted in partial fulfilment for the degree

Magister Scientiae Agriculturae in Agrometeorology

in the

Department of Soil, Crop and Climate Sciences

Faculty of Natural and Agricultural Sciences

University of the Free State

Supervisor: Mr. A.S. Steyn

Co-Supervisor: Dr. H.J. Fouché

Bloemfontein

2018

Table of Contents

TABLE OF CONTENTS.....	I
DECLARATION	V
ABSTRACT	VI
OPSOMMING	VIII
ACKNOWLEDGEMENTS.....	X
LIST OF ABBREVIATIONS AND SYMBOLS	XI
LIST OF FIGURES AND TABLES.....	XV
CHAPTER 1 INTRODUCTION	1
1.1 Background.....	1
1.2 Climatic Climax Grassland.....	6
1.3 Research Questions and Objectives of the Research	9
1.4 Organisation of Chapters.....	13
CHAPTER 2 LITERATURE REVIEW	15
2.1 Factors Influencing Rangeland Production.....	15
2.1.1 Climatic Factors	15
2.1.1.1 Solar Radiation	15
2.1.1.2 Temperature.....	17
2.1.1.3 Moisture.....	18
2.1.2 Rangeland Condition.....	21
2.1.3 Rangeland Management.....	23
2.1.4 Fire	24
2.1.5 Soil Properties.....	26
2.2 Biophysical Simulation Models	28
2.2.1 Introduction	28
2.2.2 Models in use.....	32
2.3 A Changing Climate, A Changing Land	40
2.3.1 Climate Change Science	40
2.3.2 Climate Predictions	41
2.3.3 Effects of Climate Change	44
2.3.4 Representative Concentration Pathways	49

2.4	El Niño – Southern Oscillation.....	55
CHAPTER 3	METHODOLOGY	59
3.1	Study Area.....	59
3.1.1	Botanical and Pedological Description.....	60
3.1.2	Climatological Description.....	64
3.2	Data Sources.....	66
3.2.1	Rangeland Production Data.....	66
3.2.2	Historically Observed Climate Data	67
3.2.3	Future Simulated Climate Data	67
3.3	PUTU VELD Model	69
3.3.1	The Operations of the PUTU VELD Model	70
3.3.1.1	Plant Physiological Parameters and their initial values.....	71
3.3.1.2	Inputs and Initial Values.....	73
3.3.1.2.1	Meteorological Observations	73
3.3.1.2.2	Initial Values of the Different Plant Parts	73
3.3.1.3	The Soil Water Balance	75
3.3.1.3.1	Calculation of the Soil Water Potential.....	75
3.3.1.3.2	Radiation Relationships	76
3.3.1.3.3	Evapotranspiration.....	79
3.3.1.3.4	Hydraulic Conductance and Leaf Water Potential.....	82
3.3.1.3.5	Soil Water Withdrawal.....	84
3.3.1.3.6	Soil Water Replenishment and Drainage	86
3.3.1.4	Influence of Environmental Driving Forces on Production	86
3.3.1.4.1	Calculation of Leaf Area	86
3.3.1.4.2	Environmental Limiting Factors.....	86
3.3.1.4.3	Photosynthetic Efficiency	88
3.3.1.4.4	Assimilation, Respiration and Net Production of Dry Material....	89
3.3.1.5	Phenology and Growth Functions	90
3.3.1.5.1	Vegetative Growth Stage	92
3.3.1.5.2	Reproductive Growth Stage	93
3.3.1.5.3	Seed Formation Growth Stage.....	93
3.3.1.5.4	Seed-Fall Growth Stage	94
3.3.1.5.5	Dormant Growth Stage	94
3.3.1.6	Translocation in the Plant.....	95

3.3.1.6.1	Maximum Growth Rates and Actual Translocation Rates	95
3.3.1.6.2	The Mass Flow Variables	96
3.3.1.6.3	Mass Balance of the Different Plant Parts.....	97
3.3.1.6.4	Plant Reserves.....	97
3.3.1.7	Iteration and Output	98
3.4	Assumptions	103
3.5	Analysis of PUTU VELD Output Data	105
3.5.1	Validation of the PUTU VELD model	105
3.5.1.1	Mean Absolute Error (MAE)	106
3.5.1.2	Root Mean Square Error (RMSE).....	106
3.5.1.3	Index of agreement (d)	107
3.5.1.4	Correlation Coefficient (r)	107
3.5.1.5	Coefficient of Determination (R^2)	107
3.5.2	Cumulative Distribution Function (CDF).....	108
3.6	Seasonal Prediction of Maximum Dry Matter Production	108
3.7	Process Description	109
CHAPTER 4	RESULTS AND DISCUSSIONS.....	111
4.1	Validation of the PUTU VELD Model	111
4.2	Simulated Rangeland Production during the Historical Base Period (1980/81 – 2009/10).....	114
4.2.1	Maximum Dry Matter Production.....	114
4.2.2	Date of Occurrence of Maximum Dry Matter Production	117
4.2.3	Number of Moisture Stress Days.....	120
4.2.4	Seasonal Prediction of Maximum Dry Matter Production	122
4.3	Simulated Future Rangeland Production	123
4.3.1	Maximum Dry Matter Production.....	123
4.3.2	Date of Occurrence of Maximum Dry Matter Production	133
4.3.3	Number of Moisture Stress Days.....	140
CHAPTER 5	CONCLUSIONS AND RECOMMENDATIONS	146
5.1	Validation of PUTU VELD	147
5.2	Maximum Dry Matter Production.....	148
5.3	Date of Occurrence of Maximum Dry Matter Production	149
5.4	Number of Moisture Stress Days.....	149
5.5	Seasonal Prediction of Maximum Dry Matter Production	150

5.6 Recommendations.....	150
REFERENCES.....	153
APPENDIX A	181
APPENDIX B	216
APPENDIX C	224
APPENDIX D	227
APPENDIX E.....	228

DECLARATION

I declare that the dissertation hereby submitted for the degree of Magister Scientiae Agriculturae in Agrometeorology at the University of the Free State is my own independent work and has not previously been submitted by me at another university or faculty. I further more cede copyright of this dissertation in favour of the University of the Free State.

Catherine Odendaal

Signature: 

Date: January 2018

Place: Bloemfontein, South Africa

ABSTRACT

A large part (69%) of South Africa's surface is suitable for grazing resulting in livestock farming being the largest agricultural sector in the country. Rangelands are an important resource for a stock farmer as it provides a cheap food source for the livestock midst it is in a good condition. In order to feed an ever-increasing population, better rangeland management practices are needed to ensure food security. Adaptation strategies should address climate variability and change, which is already suspected to be the main cause for variable crop yields and rangeland production. It is therefore imperative to investigate what the effect of climate change will be on rangeland production in the long run. Thus, the main aim of this study was to assess the historical and future rangeland production in the Bloemfontein area of South Africa, which falls within the dry *Themeda-Cymbopogon* veld type and is deemed representative of the central grassland biome.

Observed climate data was sourced from the South African Weather Service (SAWS) station at Bloemfontein Airport for the historical base period (1980/81 – 2009/10). Simulated climate data was also obtained for the base and three future periods (i.e. current period (2010/11 – 2039/40), near future (2040/41 – 2069/70) and distant future (2070/71 – 2098/99)) from five Global Climate Models (GCMs) using two Representative Concentration Pathways (RCPs). Here RCP 4.5 and 8.5 respectively represented intermediate and high greenhouse gas emission pathways. Measured rangeland production data was obtained from the Sydenham Experimental Farm outside Bloemfontein for the historical base period. PUTU VELD (PV) was used to simulate rangeland production for the base and future time periods. Inputs included rainfall (mm), minimum and maximum temperature (°C), sunshine hours (h) and evapotranspiration ($\text{mm}\cdot\text{d}^{-1}$) at daily intervals, where the latter was estimated using the Hargreaves-Samani method. PV outputs included maximum dry matter production (DMPmax), the date of occurrence of DMPmax (Dtp) and the number of moisture stress days (MSD).

Results showed a weak positive trend in measured DMPmax over the historical base period. It should be stressed that the results of this study should not be interpreted or extrapolated outside the context of this document since the validation of PV over the historical base period yielded poor results ($R^2 = 0.28$), revealing possible serious

overfitting issues. PV was also found to generally underestimate DMPmax when using GCM data as input when compared to runs employing SAWS data. Dtp showed a weak negative trend, implying a tendency for Dtp to occur slightly earlier in the season with time, while MSD revealed weak linear trends over the base period. Using 3-month running means of the Niño 3.4 anomalies as predictor of standardized DMPmax showed real promise as approximately 17.5% of the variation in DMPmax could be explained by the variation in the July-August-September (JAS) Niño 3.4.

With respect to the future periods, the results showed that on average DMPmax will decrease slightly over time under RCP 4.5, while it will increase under RCP 8.5. In terms of grazing capacity, both RCPs revealed that more land will be needed per animal for sustainable farming. The Dtp showed a general shift to later in the growing season under both RCPs. It was also noted that although both RCPs had more MSDs when compared to the base period, there were larger differences observed under RCP 8.5.

It was suggested that active monitoring and good rangeland improvement techniques be utilised by livestock farmers to ensure a good rangeland condition with adequate food supply for livestock. Future work should focus on evaluating other rangeland production models for this region.

Keywords: *climate change, global climate models, PUTU VELD, rangeland production model, Themeda-Cymbopogon veld*

OPSOMMING

'n Groot deel (69%) van Suid-Afrika se oppervlakte is geskik vir weiding, met die gevolg dat veeboerdery die grootste landbousektor in die land is. Weiveld is 'n belangrike hulpbron vir 'n veeboer aangesien dit 'n goedkoop voedselbron vir vee kan wees mits dit in 'n goeie toestand is. Om aan die toenemende bevolking voedsel te verskaf, word beter veldbestuurspraktyke benodig om voedselsekerheid te waarborg. Aanpassingstrategieë behoort klimaatveranderlikheid en -verandering aan te spreek, wat reeds aangevoer word as die hooforsaak vir veranderlike gewasopbrengste en weidingproduksie. Dit is dus noodsaaklik om ondersoek in te stel na die langtermyn uitwerking van klimaatverandering op weidingproduksie. Die hoofdoel van hierdie studie was dus om die historiese en toekomstige veldproduksie in die Bloemfontein-gebied van Suid-Afrika, wat binne die droë *Themeda-Cymbopogon*-veldtipe val en as verteenwoordigend van die sentrale graslandbloom beskou word, te evalueer.

Waargenome klimaatdata was verkry vanaf die Suid-Afrikaanse Weerdiens (SAWS) se stasie op Bloemfontein Lughawe vir die historiese basistydperk (1980/81 – 2009/10). Gesimuleerde klimaatdata is ook verkry vir die basis en drie toekomstige tydperke (d.w.s. huidige tydperk (2010/11 – 2039/40), nabye toekoms (2040/41 – 2069/70), en verre toekoms (2070/71 – 2098/99)) vanaf vyf globale klimaatmodelle (GKM'e) deur gebruik te maak van twee verteenwoordigende konsentrasiepaaie (VKP's). Hier verteenwoordig VKP 4.5 en 8.5 onderskeidelik intermediêre en hoë kweekhuisgasvrystellings. Gemete weidingproduksiedata is verkry van die Sydenham Proefplaas buite Bloemfontein vir die historiese basistydperk. PUTU VELD (PV) is gebruik om weidingproduksie te simuleer vir die basis en toekomstige tydperke. Insette sluit in reënval (mm), minimum en maksimum temperatuur (°C), sonskynure (h) en evapotranspirasie (mm.d⁻¹), waar laasgenoemde volgens die Hargreaves-Semani-metode geraam is. PV uitsette sluit in maksimum droëmateriaalproduksie (DMPmax), die datum van die voorkoms van DMPmax (Dtp) en die aantal vogstremmingsdae (VSD).

Resultate het 'n swak positiewe tendens in gemete DMPmax oor die historiese basistydperk getoon. Dit moet egter beklemtoon word dat die resultate van hierdie studie nie buite die konteks van hierdie dokument geïnterpreteer en geëkstrapoleer moet word nie, aangesien die validering van PV oor die historiese basistydperk swak

resultate opgelewer het ($R^2 = 0.28$), wat moontlike ernstige oorpasingsprobleme toon. Daar was ook gevind dat PV oor die algemeen DMPmax onderskat wanneer GKM-data as insette gebruik word in vergelyking met lopies wat SAWS-data gebruik. Dtp het 'n swak negatiewe neiging getoon, wat daarop dui dat Dtp mettertyd effens vroeër in die seisoen plaasvind, terwyl VSD 'n swak lineêre tendens oor die basistydperk getoon het. Die gebruik van 3-maand lopende gemiddelde van die Niño 3.4-anomalieë as voorspeller van gestandaardiseerde DMPmax het werklike belofte getoon, aangesien ongeveer 17.5% van die variasie in DMPmax verklaar kon word deur die variasie in die Julie-Augustus-September (JAS) Niño 3.4

Met betrekking tot die toekomstige tydperke het die resultate getoon dat DMPmax oor die algemeen mettertyd sal afneem onder VKP 4.5, terwyl dit onder VKP 8.5 sal toeneem. Wat weidingskapasiteit betref, het beide VKPs getoon dat meer grond per dier benodig word vir volhoubare boerdery. Die Dtp het 'n algemene verskuiwing tot later in die groeiseisoen onder beide VKPs getoon. Daar is ook opgemerk dat hoewel beide VKPs meer VSDs gehad het in vergelyking met die basistydperk, was daar groter verskille waargeneem onder VKP 8.5.

Daar is voorgestel dat aktiewe monitering en goeie veldverbeteringstegnieke deur veeboere aangewend moet word om 'n goeie veldtoestand te verseker met voldoende voedselvoorsiening vir vee. Toekomstige werk moet fokus op die evaluering van ander weidingproduksiemodelle vir hierdie streek.

Sleutelwoorde: *globale klimaatmodelle, klimaatsverandering, PUTU VELD, Themeda-Cymbopogon veld, weidingproduksiemodel*

ACKNOWLEDGEMENTS

Many thanks and appreciation to:

- ⌘ Mrs L. Molope and her team from the Agricultural Research Council for financial support during my studies from 2013 to middle 2017 as a part of the Professional Development Program.
- ⌘ Inkaba ye Africa for financial support during the early years of the project.
- ⌘ My supervisor, Mr A.S. Steyn for his valuable help, guidance and friendship.
- ⌘ My co-supervisor, Dr H.J. Fouché for his valuable suggestions.
- ⌘ The staff of the Agrometeorology division at the University of the Free State for their encouragements throughout the study period.
- ⌘ The staff of the Agrometeorology division at the Agricultural Research Council – Institute for Soil, Climate and Water for their encouragements and suggestions while employed in the Professional Development Program.
- ⌘ My fellow office mate, Phumzile Maluleke for her help and suggestions and for being an ear when it was needed during the rants and raves.
- ⌘ The Almighty Father for His strength and guidance during my studies, for being with me every step of the way and the awesome nature that He created for me to admire and study.
- ⌘ My amazing parents, Golly and Marius, for being there for me and for encouraging me all the way to never give up.
- ⌘ My loving best friend and husband, Heinrich, for helping me when times got tough, being there for me and encouraging me to never give up.
- ⌘ Lastly, my two cats, Elsa and Tigger, for keeping me sane and merry during the tough times.

Cultivators of the earth are the most valuable citizens. They are the most vigorous, the most independent, the most virtuous, and they are tied to their country and wedded to its liberty and interests by the most lasting bands.

– Thomas Jefferson

Agriculture is not crop production as popular belief holds - it's the production of food and fiber from the world's land and waters. Without agriculture, it is not possible to have a city, stock market, banks, university, church or army. Agriculture is the foundation of civilization and any stable economy.

– Allan Savory

LIST OF ABBREVIATIONS AND SYMBOLS

AgMIP	Agricultural Model Intercomparison and Improvement Project
AIM	Asian-Pacific Integrated Model
AMJ	April-May-June
APSIM	Agricultural Production Systems Simulator
AR4	IPCC Forth Assessment Report
AR5	IPCC Fifth Assessment Report
ARC	Agricultural Research Council
ASO	August-September-October
ATP	Adenosine triphosphate
BACROS	Basic Crop Simulator
BFN	Bloemfontein
CCSM4	Community Climate System Model 4.0
CDF	Cumulative distribution function
CERES	Crop Environment Resource Synthesis
CO ₂	Carbon dioxide
CropSyst	Cropping Systems Simulation Model
CSAG	Climate Systems Analysis Group
CSIR	Council for Scientific and Industrial Research
CSIRO	Commonwealth Scientific and Industrial Research Organization
d	Index of agreement
DEA	Department of Environmental Affairs
DJF	December-January-February
DMPmax	Maximum dry matter production (kg.ha ⁻¹)
DSSAT	Decision Support System for AgroTechnology Transfer

Dtp	Date that maximum dry matter production occurs
e.g.	For example
ELCROS	Elementary Crop Growth Simulator
ELM	Ecological Model
EN	El Niño
ENSO	El Niño - Southern Oscillation
ET	Evapotranspiration
ET _o	Reference evapotranspiration
FAO	Food and Agricultural Organization of the United Nations
FORTTRAN	Formulation Translation programming language
GC	Grazing capacity (ha.AU ⁻¹ or ha.LSU ⁻¹)
GCAM	Global Change Assessment Model
GCM	Global climate model
GDP	Gross domestic product
Gemini	Grassland Ecosystem Model with Individual centred Interactions
GFDL-ESM2M	Geophysical Fluid Dynamics Laboratory - Earth System Model 2M
GHG	Greenhouse gases
GRAM	Grassland Statistical Model
GRASIM	Grazing Simulation Model
HadGEM2-ES	Hadley Centre Global Environmental Model 2 - Earth System
i.e.	In essence
IBP	International Biological Program
IFSM	Integrated Farm System Model
IMAGE	Integrated Model to Assess the Global Environment
IPCC	Intergovernmental Panel on Climate Change

IRI	International Research Institute for Climate and Society
JAS	July-August-September
JJA	June-July-August
LN	La Niña
LSU	Large stock unit
MAE	Mean absolute error
MAM	March-April-May
MESSAGE	Model for Energy Supply Strategy Alternatives and their General Environmental Impacts
MIROC5	Model for Interdisciplinary Research on Climate 5.0
MJJ	May-June-July
MPI-ESM-MR	Max-Planck Institute - Earth System Model - MR
MSD	Total number of moisture stress days (d)
NASA	National Aeronautics and Space Administration
NDJ	November-December-January
NOAA	National Oceanic and Atmospheric Administration
O ₂	Oxygen
OND	October-November-December
ONI	Oceanic Niño Index
P1	Current period
P2	Near future period
P3	Distant future period
PV-AgMIP	Output data from runs utilising climate data from AgMIP
PV-AgMIP DMPmax	Maximum dry matter production obtained using AgMIP climate data (kg.ha ⁻¹)
PV-AgMIP Dtp	Date of occurrence of DMPmax using AgMIP climate data
PV-AgMIP MSD	Number of moisture stress days using AgMIP climate data
PV-Fouché	Initial validation of PUTU 11 done by Fouché (1992)

PV-SAWS	Output data from runs utilising climate data from SAWS
PV-SAWS DMPmax	Maximum dry matter production obtained using SAWS climate data ($\text{kg}\cdot\text{ha}^{-1}$)
PV-SAWS Dtp	Date of occurrence of DMPmax using SAWS climate data
PV-SAWS MSD	Number of moisture stress days using SAWS climate data
r	Correlation coefficient
R ²	Coefficient of determination
RCP	Representative Concentration Pathways
RMSE	Root mean square error
RP	Rangeland production ($\text{kg}\cdot\text{ha}^{-1}$)
RPM	Rangeland production model
SA	South Africa
SANBI	South African National Biodiversity Institute
SAWS	South Africa Weather Service
SON	September-October-November
SPAM	Soil-Plant-Atmosphere Model
SPUR	Simulation of Production and Utilisation of Rangelands
SR	Stocking Rate ($\text{ha}\cdot\text{AU}^{-1}$)
SRES	Special Report on Emissions Scenarios
SST	Sea surface temperatures
SYMFOY	Simulator for Forage Yield
TAR	IPCC Third Assessment Report
Tn	Minimum temperature ($^{\circ}\text{C}$)
Tx	Maximum temperature ($^{\circ}\text{C}$)
USA	United States of America
UV-A	Ultraviolet A (long-wave)
UV-C	Ultraviolet C (short-wave)

LIST OF FIGURES AND TABLES

Figure 1.1	Sweetveld with <i>Themeda triandra</i> in the foreground.....	1
Figure 1.2	South Africa's biomes (geographical areas comprising a number of ecosystems with related plants and animals).....	2
Figure 1.3	A field of climatic climax grassland.....	7
Figure 1.4	Graph illustrates the change in global surface temperature relative to 1951 – 1980 average temperatures.....	10
Figure 1.5	Projections of biome shifts under low-, medium- and high-risk climate scenarios until approximately 2050.....	11
Figure 1.6	Schematic outline of the first research objective.....	12
Figure 1.7	Schematic outline of the second research objective.....	13
Figure 2.1	Typical theorized relationships between cumulated aboveground biomass and cumulated intercepted solar radiation for C ₄ and C ₃ species.....	17
Figure 2.2	Schematic illustration of the effect of temperature on major physiological processes of plants.....	18
Figure 2.3	Effects of drought and flooding on growth and physiology of forage plants. A and B denotes the changes in shoot physiology under drought and flood conditions, respectively. C and D denotes the changes in root and crown physiology under drought and flood conditions, respectively.....	20
Figure 2.4	Yield of recovery growth from Tall Grassveld burnt in early August and after the first spring rains.....	26
Figure 2.5	The relationship between simulation, field- and laboratory studies and actual measurements in the field.....	31
Figure 2.6	Mean atmospheric CO ₂ concentration at Mauna Loa Observatory, Hawaii, measured since 1960.....	40
Figure 2.7	Trends in annual (a) mean daily maximum temperature (°C) and (b) mean daily minimum temperature (°C). The value of tau represents the direction and relative strength of the trend. Non-filled triangles indicate changes that are not statistically different (5% level). The larger the triangle, the larger the increase/decrease. The red triangles indicate an increase in mean daily temperature (max or min) (1960 to 2010) and the blue triangles indicate a decrease in mean daily temperature (max/min) (1960 to 2010).....	42

Figure 2.8	Trends in annual mean rainfall (mm). The value of tau represents the direction and relative strength of the trend. The green triangles indicate an increase in mean rainfall between 1960 and 2010. Non-filled triangles indicate an increase that is not statistically significantly (5% level). The larger the triangle, the larger the increase. Brown triangles indicate a decrease.....	43
Figure 2.9	Roots of the common <i>Acacia karoo</i> (sweet thorn) exposed to different levels of CO ₂ . A and B: pre-industrial conditions, C: high CO ₂ of late 1990s, D: current CO ₂ levels.....	45
Figure 2.10	Changes in radiative forcing relative to pre-industrial conditions. Bold coloured lines show the four RCPs.....	52
Figure 2.11	Global population and GDP projections of the four scenarios underlying the RCPs. Grey area for A indicates the range of the UN scenario (low and high) (UN, 2004). Grey area for B indicates the 98 th and 90 th percentiles (light/dark grey) of the IPCC AR4 database.....	52
Figure 2.12	Land use (cropland and use of grassland) across the RCPs. Grey area indicates the 90 th percentile of scenarios reported in literature. Vegetation is defined as the part not covered by cropland or anthropogenically used grassland.....	55
Figure 2.13	Maps of sea-surface temperature anomalies in the Pacific Ocean during a strong La Niña and El Niño.....	56
Figure 2.14	Global El Niño impacts.....	57
Figure 2.15	Global La Niña impacts.....	57
Figure 2.16	Niño index regions.....	58
Figure 2.17	Historical record of sea surface temperature anomaly in the Niño 3.4 region.....	58
Figure 3.1	Map of South Africa highlighting the Free State Province in orange. INSERT: Map of Africa highlighting the Republic of South Africa.....	59
Figure 3.2	Map highlighting the major land use systems of South Africa.....	60
Figure 3.3	Biomes of South Africa.....	61
Figure 3.4	The seed heads of <i>Themeda triandra</i> (red grass).....	61
Figure 3.5	Vegetation map of South Africa.....	63
Figure 3.6	Annual wind rose for Bloemfontein Airport.....	66

Figure 3.7	Google Earth image showing location of the data points in and around Bloemfontein.....	68
Figure 3.8	The different segments of the soil water retention curve for the total profile of a Sherock soil series of the Hutton form at Sydenham.....	77
Figure 3.9	Daily variation in solar radiant flux at the outermost limits of the atmosphere above Bloemfontein.....	79
Figure 3.10	Graph of $GS \left(\frac{s}{s + \gamma} \right)$ as a function of air temperature.....	81
Figure 3.11	Influence of temperature and radiant flux density upon computed potential evapotranspiration.....	82
Figure 3.12	Dependence of the hydraulic limiting factor (FW) upon leaf water potential.....	84
Figure 3.13	Decrease in soil water evaporation rate factor (FG) with time following a rainfall event of greater than 5 mm.d ⁻¹	85
Figure 3.14	Dependence of the radiation limiting factor (FI) upon leaf area index at a 10% basal cover.....	87
Figure 3.15	Variation of the temperature limiting factor (FT) with temperature.....	88
Figure 3.16	Diagrammatic representation of translocation and mass flow inside the plant as seen in the PUTU VELD model. DMG = The days dry matter gain (kg CHO.ha ⁻¹ .d ⁻¹); GD = Grain dead; GL = Grain living; CD = Culm dead; CL = Culm living; BD = Leaves dead; BL = Leaves living; SD = Stubble dead; SL = Stubble living; RD = Roots dead; RL = Roots living; TR = Trash dead; RES = Carbohydrate reserves; DA = Above ground dead; BA = Above ground living; DB = Below ground dead; BB = Root biomass; CA = Above ground standing crop; CB = Below ground standing crop; Rn = Translocated masses; Xn = Mass flow variables.....	91
Figure 3.17	Relationship between translocation rate multiplier and the relative desired proportion decrement.....	91
Figure 3.18	Detailed Forrester diagram explaining the PUTU VELD.....	99
Figure 4.1	Time series comparison between simulated rangeland production data from PV-Fouché, PV-SAWS and the measured rangeland production data from Sydenham Experimental Farm.....	113
Figure 4.2	Scatterplot of the PUTU VELD simulated maximum dry matter production in Bloemfontein over the historical base period (1980/81 – 2009/10) using observed climate data (PV-SAWS) and GCM-derived climate data (PV-AgMIP).....	114

Figure 4.3	Cumulative distribution functions of the PUTU VELD simulated maximum dry matter production in Bloemfontein over the historical base period (1980/81 – 2009/10) using observed climate data (PV-SAWS) and GCM-derived climate data (PV-AgMIP).....	115
Figure 4.4	Time series comparison of PUTU VELD simulated maximum dry matter production in Bloemfontein using observed climate data (PV-SAWS) and GCM-derived climate data (PV-AgMIP).....	116
Figure 4.5	Accumulated maximum dry matter production in Bloemfontein for the historical base period (1980/81 – 2009/10) using observed climate data (PV-SAWS) and GCM-derived climate data (PV-AgMIP).....	117
Figure 4.6	Basic growth curve of a grass plant.....	118
Figure 4.7	Daily dry matter production simulated by PUTU VELD for Bloemfontein during a typical growing season (2009/10).....	118
Figure 4.8	Cumulative distribution functions of the PUTU VELD simulated date (Dtp) on which maximum dry matter production occurred in Bloemfontein for the base period (1980/81 – 2009/10) using observed climate data (PV-SAWS) and GCM-derived climate data (PV-AgMIP). The two vertical lines demarcate the optimal period (244 – 304) for Dtp to occur.....	119
Figure 4.9	Time series comparison for the date (Dtp) on which maximum dry matter production occur in Bloemfontein for the base period (1980/81 – 2009/10) using observed climate data (PV-SAWS) and GCM-derived climate data (AgMIP). The two horizontal purple lines demarcate the optimal period (244 – 304) for Dtp to occur.....	120
Figure 4.10	Cumulative distribution functions of the PUTU VELD simulated number of moisture stress days (MSD) in Bloemfontein for the base period (1980/81 – 2009/10) using observed climate data (PV-SAWS) and GCM-derived climate data (PV-AgMIP).....	121
Figure 4.11	Time series of the PUTU VELD simulated number of moisture stress days in Bloemfontein for the base period (1980/81 – 2009/10) using observed climate data (PV-SAWS) and GCM-derived climate data (PV-AgMIP).....	121
Figure 4.12	Scatterplot showing the correlation between the 3-month Niño 3.4 anomalies for July-August-September (JAS) and simulated standardized maximum dry matter production using historical climate data using historical climate data (PV-SAWS DMPmax) for Bloemfontein during the base period (1980/81 – 2009/10).....	123
Figure 4.13	Cumulative distribution functions of simulated dry matter production in Bloemfontein for each GCM and time period under RCP 4.5. The purple vertical line represents a threshold of 750 kg.ha ⁻¹ which equates to the norm grazing capacity for the Free State of 6 ha.LSU ⁻¹ . P1 = current period; P2 = near future; and P3 = distant future.....	127

Figure 4.14	Cumulative distribution functions of simulated dry matter production in Bloemfontein for each GCM and time period under RCP 8.5. The purple vertical line represents a threshold of 750 kg.ha ⁻¹ which equates to the norm grazing capacity for the Free State of 6 ha.LSU ⁻¹ . P1 = current period; P2 = near future; and P3 = distant future.....	128
Figure 4.15	Cumulative distribution functions of ensemble-averaged simulated maximum dry matter production in Bloemfontein for each time period under RCP 4.5. The vertical line represents a threshold of 750 kg.ha ⁻¹ which equates to the norm grazing capacity for the Free State of 6 ha.LSU ⁻¹	129
Figure 4.16	Cumulative distribution functions of ensemble-averaged simulated maximum dry matter production in Bloemfontein for each time period under RCP 8.5. The vertical line represents a threshold of 750 kg.ha ⁻¹ which equates to the norm grazing capacity for the Free State of 6 ha.LSU ⁻¹	130
Figure 4.17	Accumulated PUTU VELD simulated maximum dry matter production (DMPmax) for Bloemfontein for 10 ensemble members (five GCMs and two RCPs). The averaged RCP 4.5 and RCP 8.5 values are also included, along with those for the base period (black horizontal line).....	131
Figure 4.18	Average grazing capacity for Bloemfontein for 10 ensemble members (five GCMs and two RCPs) and the averaged RCP 4.5 and RCP 8.5 values, compared to the base period (black solid line) and the norm (purple dashed line).....	133
Figure 4.19	Cumulative distribution functions of date of occurrence of maximum dry matter production (Dtp) in Bloemfontein for each GCM and time period under RCP 4.5. The two vertical lines demarcate the optimal period (244 – 304) for Dtp to occur. P1 = current period; P2 = near future; and P3 = distant future.....	136
Figure 4.20	Cumulative distribution functions of date of occurrence of maximum dry matter production (Dtp) in Bloemfontein for each GCM and time period under RCP 8.5. The two vertical lines demarcate the optimal period (244 – 304) for Dtp to occur. P1 = current period; P2 = near future; and P3 = distant future.....	137
Figure 4.21	Cumulative distribution functions of ensemble-averaged date of occurrence of maximum dry matter production (Dtp) in Bloemfontein for each time period under RCP 4.5. The two vertical lines demarcate the optimal period (244 – 304) for Dtp to occur.....	138
Figure 4.22	Cumulative distribution functions of ensemble-averaged date of occurrence of maximum dry matter production (Dtp) in Bloemfontein for each time period under RCP 8.5. The two vertical lines demarcate the optimal period (244 – 304) for Dtp to occur.....	139

Figure 4.23	Cumulative distribution functions of the number of moisture stress days in Bloemfontein for each GCM and time period under RCP 4.5. P1 = current period; P2 = near future; and P3 = distant future.....	141
Figure 4.24	Cumulative distribution functions of the number of moisture stress days in Bloemfontein for each GCM and time period under RCP 8.5. P1 = current period; P2 = near future; and P3 = distant future.....	142
Figure 4.25	Cumulative distribution functions of ensemble-averaged number of moisture stress days in Bloemfontein for each time period under RCP 4.5.....	144
Figure 4.26	Cumulative distribution functions of ensemble-averaged number of moisture stress days in Bloemfontein for each time period under RCP 8.5.....	145
Table 2.1	The PUTU-series models for the mathematical simulation of the growth of crops.....	39
Table 2.2	Summary of the characteristics of the different Representative Concentration Pathways. ^a IMAGE – Integrated Model to Assess the Global Environment; GCAM – Global Change Assessment Model; AIM – Asian-Pacific Integrated Model; MESSAGE – Model for Energy Supply Strategy Alternatives and their General Environmental Impact.....	53
Table 3.1	Botanical composition of the experimental plots at Sydenham Experimental Farm, Bloemfontein, when the rangeland is in a good condition.....	62
Table 3.2	Climate data for Bloemfontein International Airport for the period 1980/81 – 2009/2010.....	65
Table 3.3	Information about the global climate models used.....	69
Table 3.4	The percentage distribution of total biomass (C) of the different plant parts at the beginning of the simulation.....	74
Table 3.5	Maximum growth rate for each plant part during each growth stage. Where an AGR- value is not specified for a certain growth stage, the value is taken as nil. G, C, B, S and R stands for seeds, culms, leaves, stubbles and roots respectively. DBL stands for leaf mass change demand. All values are consistent with a basal cover of 100%.....	96
Table 4.1	Validation statistics for the original nine years (1980/81 – 1988/89) and the extended 30-year base period (1980/81 – 2009/10) (n = number of years, Min. Prod. = minimum dry matter production, Max. Prod. = maximum dry matter production, MAE = mean absolute error, RMSE = root mean square error, d = index of agreement, r = correlation coefficient and R ² = coefficient of determination; * indicates value obtained using PUTU VELD and climate data from Glen).....	112
Table 4.2	Summary of coefficient of determination obtained using various combinations of the Niño 3.4 anomalies as predictor of measured	

standardized maximum dry matter production and simulated standardized maximum dry matter production using historical climate data in Bloemfontein during the base period (1980/81 – 2009/10)...**122**

Table 4.3	The approximate 33.3 rd and 66.6 th percentiles for simulated dry matter production for Bloemfontein for 10 ensemble members (five GCMs and 2 RCPs) for each simulated time period.....	124
Table 4.4	Ensemble-average 33.3 rd and 66.6 th percentiles of the PUTU VELD simulated maximum dry matter production for Bloemfontein for each of the time periods and emission scenario.....	126
Table 4.5	The 33.3 rd and 66.6 th percentiles for date of occurrence of maximum dry matter production in Bloemfontein for 10 ensemble members (five GCMs and 2 RCPs) for each time period.....	134
Table 4.6	Ensemble-averaged 33.3 rd and 66.6 th percentiles for the date of occurrence of maximum dry matter production in Bloemfontein for each of the time periods and emission scenarios.....	135
Table 4.7	The 33.3 rd and 66.6 th percentiles for number of moisture stress days in Bloemfontein for the various GCMs and time periods under both RCP 4.5 and 8.5.....	143
Table 4.8	Ensemble-averaged 33.3 rd and 66.6 th percentiles for the number of moisture stress days in Bloemfontein for each of the time periods and emission scenarios.....	143

CHAPTER 1

INTRODUCTION

1.1 Background

Approximately 69% of South Africa's surface is suitable for grazing of which 30% is covered by pastoral grasslands, resulting in livestock farming being the largest agricultural sector in the country (Goldblatt, 2015). Most of the grasslands occur in the eastern half of the country, corresponding to higher annual rainfall values (Grassland Programme, 2012; Goldblatt, 2015). The sweetveld (Figure 1.1) of the climatic climax grasslands occupy 45% (\pm 44 million ha) of the potential grassveld area. Less than 35% of the sweetvelds remain open grasslands, with the majority having been invaded by karoo pioneer species (Acocks, 1988).



Figure 1.1 Sweetveld with *Themeda triandra* in the foreground (Fish, 2012).

Grasslands provide various natural resources for man but the only real potential it has for food production is as a feed source for animal production (Fogel & Manuel, 1980; cited by Fouché, 1992). In South Africa, the Grassland Biome is found mainly on the high central plateau and the inland areas of KwaZulu Natal and the Eastern Cape (Figure 1.2). A single layer of grass dominates grasslands, also known locally as veld or rangeland. The amount of cover depends on rainfall and the degree of grazing (McDonald, 2012). An extremely variable intra- and inter-annual rainfall epitomizes the semi-arid grasslands. Annual dry matter production therefore varies considerably from season to season and from year to year (Hatch, 1999).

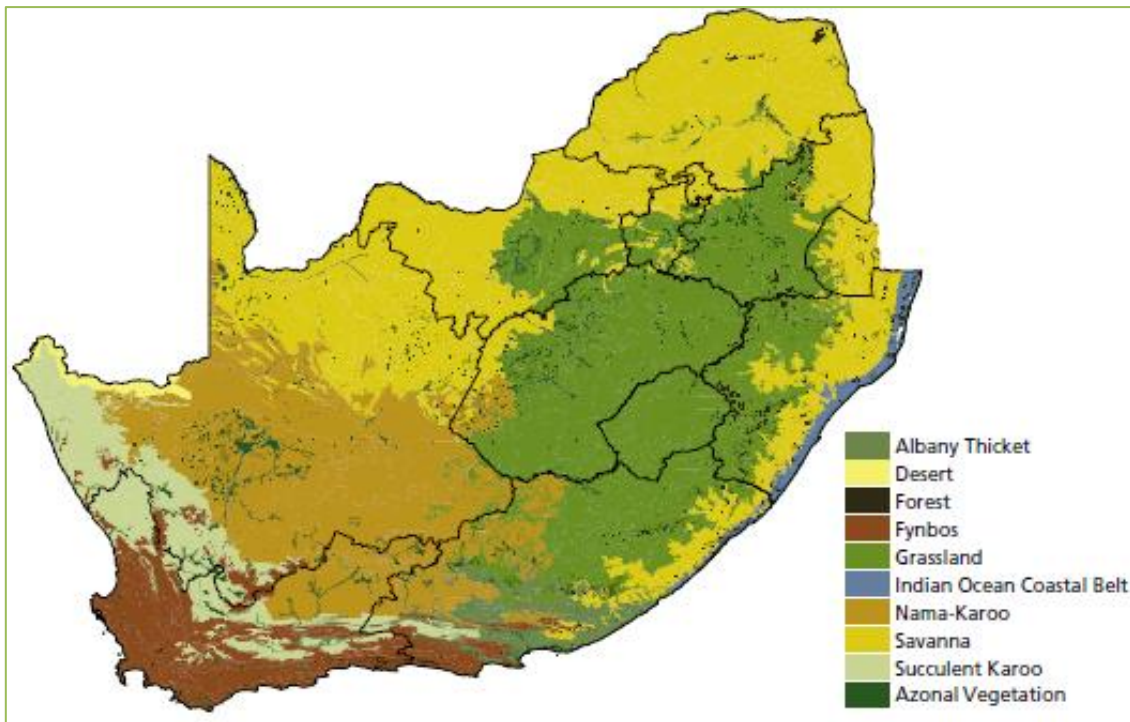


Figure 1.2 South Africa's biomes (geographical areas comprising a number of ecosystems with related plants and animals) (Cadman *et al.*, 2010).

Rangeland is an animal farmer's most precious resource and the cheapest resource if it is in a good condition (Snyman & Fouché, 1991; Snyman & Fouché, 1993). It seems as if the real value of this has not yet been comprehended by many farmers who have been warned for years against the increase in rangeland degradation (Fouché, 1992). South African soils are characteristically exceptionally vulnerable to degradation and have low recovery potential (Goldblatt, 2015). Therefore, even small mistakes in rangeland management can be devastating. Wind erosion is a big cause of degradation with an estimate of 25% of the soils highly susceptible (Goldblatt, 2015). This is more noticeable with the sandy soils of the North West and the Free State (Goldblatt, 2015).

A great number of farmers are under the impression that their rangelands are in a good condition and that they use the correct rangeland management practices (Fouché, 1992). Apparently, there isn't a need for more information regarding the rangeland management practices that are available. However, it was already pointed out in 1986 in a study by De Klerk (cited by Fouché, 1992) that this does not coincide with the results obtained from the study. It was found that 52.8% of the sheep farmers, and 61.4% of the cattle farmers, were overestimating the grazing capacity of their land by 6 – 50%. It is thus understood that the existing grazing capacity norms are either

not correct, are not understood or are not accepted. The same problem is seen with the overestimation of the production potential of the rangelands. There is still a serious concern regarding the condition of the rangelands (Fouché, 1992). The total area of grazing land (land available for animals to graze) has declined over time owing to expanding human settlements and activities (such as crop farming, forestry and mining) (Goldblatt, 2015). A major part of this grazing land is being stocked beyond its long-term grazing capacity (Gbetibouo & Ringler, 2009).

According to Meissner *et al.* (1983):

“Grazing capacity (GC) is defined as the area of land required to maintain a single animal unit (AU) over an extended number of years without deterioration of the soil or vegetation. An animal unit (AU), also commonly referred to as a large stock unit (LSU), is defined as an animal with a mass of 450 kg, which gains $0.5 \text{ kg}\cdot\text{d}^{-1}$ on forage with a digestible energy percentage of 55%. Stocking rate (SR) is defined as the area of land in the system of management, which the manager has allocated to each animal unit in the system per length of the grazeable period of the year ($\text{ha}\cdot\text{AU}^{-1}$).”

Simply put, the GC refers to the true number of animals that the vegetation can sustain. Commonly, SR refers to the number of animals the manager perceived that the vegetation could sustain (Smit, 2009). Selection of the sustainable stocking rate is the most vital of all grazing management choices, and is based on ecological use of livestock and wildlife production, economic return and vegetation (Danckwerts & Tainton, 1996; Snyman, 1998). Although it is very problematic to determine GC for rangelands, it is critical to estimate GC as it can aid as a benchmark for sustainable rangeland utilisation (Van der Westhuizen *et al.*, 2001). Environmental characteristics can account for less than 25% of the variation in GC (van der Westhuizen *et al.*, 2001). The general grazing capacity for a red grass rangeland in the central Free State is $6 \text{ ha}\cdot\text{LSU}^{-1}$ but can vary in practice between five and 25 depending on the rangeland conditions (van der Westhuizen, *et al.*, 2001). Overstocking occurs more in the communal rangelands where over half of the local herd is farmed. It can cause crusting and trampling of the soil, strip the rangeland of vegetation, reduce soil fertility, reduce productivity and lead to erosion (Smit, 2009). A considerable 91% of South Africa is defined as arid or semi-arid where land degradation (compounded by climate change)

can lead to desertification and the irreversible loss of productive land (Gbetibouo & Ringler, 2009).

South Africa's population is growing at an alarming rate of 2% per annum, compared to the global growth rate of 1.13% per annum (Worldometers, 2016), and is estimated to reach 82 million by the year 2035 (Goldblatt, 2015). In order to feed the ever-increasing population, better rangeland management practices are needed together with food imports which need to double. As more people become wealthier and there is a shift in the demands for certain food types, the production of foodstuff needs to increase while still using the same or fewer available natural resources.

The shift to other food types is also due to price increases. Until recently (early 2000s), the price of food in South Africa has either declined or stayed stable, which benefits both the national and household economies (Goldblatt, 2015). Currently the situation has changed with prices increasing at an alarming rate due to an increase in labour, electricity, transport and fertiliser costs. This increase in food prices is a big burden for the poor population, who spend about 33% of their income on food compared to 2% of the wealthier population's salary. Food security is not only about food prices and availability, but it is also an unemployment issue. The government needs to create jobs to ensure that the people can buy food for their tables (Goldblatt, 2015).

South Africans have already shown a change in their food consumption since the 1970s with a decrease in staples (e.g. maize and bread) (Goldblatt, 2015). Sustainable farming is about meeting the needs of South Africans today and in the future. The recent global rise in food prices and repeated reports of social unrest in a large number of countries reveal the strategic and basic importance of the agricultural sector for social and economic stability.

The South African national cattle herd has increased by approximately 6 million heads to a stable 14 million since the 1970s (Palmer & Ainslie, 2006a; Brandt, 2014). The composition of the herd has changed somewhat during the past 10 years with the commercial component staying steady at 60% of the national herd and the non-commercial herd increasing since the late 1990's (Brandt, 2014). The production of beef has increased over time from 672 000 tonnes in 2005 to 855 000 tonnes in 2013. This has allowed for the local demand in red meat to almost be met. The annual consumption of beef per capita has also increased over the same period from 15.5 kg

to 17 kg. This growth is thought to be the result of the observed increase in the middle class of the population (Brandt, 2014). A trend that is likely to continue is one where chicken consumption exceeds that of red meat. The local sheep herd has been decreasing at a steady rate over the past few years, mainly due to factors such as stock theft and labour problems. Despite this, the production has increased over the past few years (Brandt, 2014). Over South Africa, rainfall generally increases from west to east, so too does the carrying capacity (i.e. potential stocking rate) of the land. Cattle farming is more concentrated in the eastern, wetter regions of the country as well as in the Northern Cape and North West Province. Sheep prefer a drier climate and therefore are more concentrated in the drier western and central regions of the country. Owing to expanding human settlements and other agricultural activities (crop farming and forestry), the total grazable land area has declined over time (Goldblatt, 2015).

Rainfall is not only critical to animal production but also to agronomical crops. This is noted in the correlation of South African maize production from the drought conditions in 2012 (12.1 million tonnes) to the wet conditions in 2014 (14 million tonnes) (Brandt, 2014). Profitability and production risk of wheat led to a decrease in production areas in the central parts of the country. Production predominantly occurs in the Western Cape and in the irrigation areas of the central parts of the country. Due to current economic conditions, the consumption of wheat will likely decrease in the short term but remains fairly stable at 3 million tonnes (Brandt, 2014).

Rangeland as a resource is difficult to manage. This is truer in areas with a low production potential. Poorly managed intensive farming has many negative impacts on the natural environment, on people's well-being and on a farmer's ability to adapt to change (Goldblatt, 2015). Economic and climatological restrictions are placed on the intensity of the management and therefore the manipulation of animals is the main operational variable. The success of the management in terms of rangeland improvement is often slow and difficult to measure due to the spatial and temporal variation in the rangeland composition and production (Fouché, 1992). Rangeland management is essentially applied plant conservationism, which endeavours to optimise quality and quantity of plant production over the short- and long-term (Snyman, 1998). The gratification from using the correct management practices is thus not often felt by the farmer. It is also in the central areas of the country that periodic

droughts are experienced and where the degradation of the rangeland is the biggest problem (Fouché, 1992). A sustainable approach to farming is needed in South Africa, or the welfare of our nation – both current and future generations – is at risk (Goldblatt, 2015). Mismanaged agricultural industrialisation and growth could compromise food safety and increase unemployment and environmental degradation.

Sustainable agricultural practices should aim to (Goldblatt, 2015):

- a) Contribute to the economic and social well-being of all;
- b) Mitigate and adapt to climate change;
- c) Safeguard the livelihood and well-being of farmers, farm workers and their families;
- d) Change the way land and water resources are managed, so that their long-term productivity is optimised and sustained;
- e) Ensure a high quality and safe supply of agricultural products; and
- f) Maintain functioning, healthy agricultural ecosystems rich in biodiversity.

The likely reason for the slow progress with research regarding the environmental impacts and that farmers do not accept the recommendations, lies with the complexity of the interaction between the animal- and rangeland production systems (Fouché, 1992; Sinclair & Seligman, 1996; Fourcaud *et al.*, 2008). A variety of environmental influences from outside, for example droughts, further complicates the description of the system. With the introduction of contemporary computer technology, this interaction can be dealt with in simulation models. These models can then be used as artificial “laboratories” where the interactions are investigated. The information generated by these models can thus point out any gaps and open new research fields (Fouché, 1992; Sinclair & Seligman, 1996; Fourcaud *et al.*, 2008; Poorter *et al.*, 2013).

1.2 Climatic Climax Grassland

Climatic climax grassland of South Africa is the portion of the grassland biome that is found on the great inland plateau west of the Drakensberg escarpment, and on the Drakensberg escarpment itself. The term climatic climax grassland is used to describe this area, as it is too arid or too cold to permit the development of woody communities, even in the absence of fire (Tainton, 1999a). The decline in rainfall over the area from east (700 to 1000 mm.y⁻¹) to west (about 400 mm.y⁻¹) is accompanied by a drop in

altitude from approximately 3200 m in the east, to 1200 m in the west (Tainton, 1999a). These areas are strongly dominated by grasses. As the rainfall is relatively low, the soils are not highly leached (they are eutrophic) and the western part of the area is thus dominated by the so-called sweet grasses, species which provide year-round grazing (Tainton, 1999a).

The rangeland is dominated by tropical and subtropical (C₄) grasses (Figure 1.3). The most important of these are *Themeda triandra*, *Heteropogon contortus*, *Microchloa caffra*, *Elionurus muticus*, *Setaria sphacelata*, *Tristachya leucothrix*, a number of species of *Eragrostis* (*Eragrostis chloromelas*, *E. curcula* and *E. racemosa*), *Brachiaria serrata* and *Cymbopogon pospischilii* (Fouché, 1992).



Figure 1.3 A field of climatic climax grassland (Fish, 2012).

The grass is typically fairly tall (0.75 to 2 m) and forms a relatively uniform stand and are perennial (Morgan, 1999; Tainton, 1999a). They form a continuous basal cover ranging from about 6% to 15%. The arid and semi-arid areas have already undergone serious degradation, and bare areas are common. (Tainton, 1999a). At low altitudes, grasslands are potentially productive compared to the grasslands in other parts of the world. However, scientific and advanced management is essential if they are to produce to their potential. Dry matter production (DMP) range from 1 t DMP.ha⁻¹.y⁻¹ in the drier regions to 3 t DMP.ha⁻¹.y⁻¹ in the higher rainfall eastern region (Tainton, 1999a). The rainfall in this region occurs mainly during the summer months. The active growing season normally starts in September, when the temperature of the upper 5 cm of soil reaches about 12°C, and ends in April. The winter months are too dry and cold for growth, while the warmer summer and autumn months results in rapid

increase in vegetation. Infiltration rates are low and runoff rates high during midsummer when most of the rain falls during heavy thunderstorms. Because temperatures are high at this time, evaporation and transpiration rates are high. Moisture stress therefore limits growth for most of the midsummer period (Tainton, 1999a).

In South Africa, rangeland can be described as either sweet, mixed or sour. By definition, sweetveld is rangeland which remains palatable and nutritious when it is mature, whereas sourveld provides palatable material only during the growing season (Scott, 1947). Mixed veld is intermediate between these two extremes, and ranges from sweet-mixed veld, which provides grazing for about 9 – 11 months of the year, to sour-mixed veld, which provides grazing for between 6 – 8 months (Tainton, 1999b).

The main characteristics of sweetveld in summer rainfall areas are (Tainton, 1999b):

- This rangeland is generally found in low elevations which are almost frost-free, but may also occur at higher altitudes, where frosts can be severe;
- Because rainfall is limited and uncertain, growth is erratic. The carrying capacity of sweetveld is normally less than that of sourveld;
- The cover is relatively sparse;
- The rangeland is easily damaged by persistent grazing during the growing season, mainly due to destruction of the edible species, which often causes a drastic reduction in cover;
- It has the capacity for recovering its composition and density rapidly, provided erosion has not been excessive and enough soil remains;
- It is prone to encroachment by bushveld trees and/or karroid shrubs;
- As spring rains are usually late, the spring period is often critical because of a lack of grazeable material; and
- Typically, it is a moderate to tall grassland at low altitudes in the eastern areas.

The functions of the grazing lands in South Africa are extremely variable. For this reason, the ability of the vegetation to support different types of livestock, and the best management procedures for the vegetation, are likely to vary widely from place to place. It should be noted that the majority of these grazing lands are extremely productive relative to natural vegetation in most other parts of the world. The grasslands and savanna, in particular, can support large numbers of livestock, and

deserve careful management, as they contribute substantially to the agriculture economy of South Africa (Tainton, 1999b).

1.3 Research Questions and Objectives of the Research

Climate change is referred to by the Intergovernmental Panel on Climate Change (IPCC, 2007) as “a change in the state of the climate that can be identified by changes in the mean climatic variability of its properties and that persists for an extended period, typically decades or longer. Climate change may be due to natural internal processes or external forcing, or to persistent anthropogenic changes in the composition of the atmosphere or changes in land use”. Climate change affects many sectors but agriculture is one of the most vulnerable as it is dependent on weather conditions. Climate variability from year to year is one of the main causes for the variable crop yields. In future, extreme weather events such as storms, heavy rains, droughts, floods, etc. are generally expected to be more frequent and have a negative effect on agricultural yields (IPCC, 2007; Polley *et al.*, 2013).

The IPCC described that a rainfall change and variability is very likely to lead to a global reduction in cover and productivity in grasslands in response to the observed drying trend of about 8 mm.yr⁻¹ since 1970. Thus, the agriculture sector should make further efforts to minimise the effects of climate change (IPCC, 2007). The enhanced greenhouse effect that is associated with increasing concentrations of greenhouse gases anthropogenic activities has result in an increase in the global atmospheric temperature by 1°C since 1750 and could cause an additional 2°C increase by mid-century (Polley *et al.*, 2013). During the strong El Niño conditions, the average global land and ocean surface temperature for 2016 was 0.94°C above the 20th century average of 13.9°C. This surpassed the previous year’s record by 0.04°C (NOAA, 2017). Figure 1.4 shows the global mean surface temperature anomalies from NASA (2017b) since 1880. Their calculations show a difference of 0.99°C for 2016 relative to the average temperature from 1951 – 1980. It can be noted that 16 of the 17 warmest years in the 136-year record have all occurred since 2001 (except 1998) with 2016 being the warmest on record (NASA, 2017b).

The upside to an elevated atmospheric carbon dioxide (CO₂) is an increase in plant growth and a reduction of the negative effects of drying in warmer climates due to an increase in water use efficiency (Polley *et al.*, 2013). However, the effect of the CO₂ is

facilitated by the environmental conditions, especially soil water availability (Polley *et al.*, 2013). Rangeland is one of the sources of feed for cattle and if the rangeland production is affected, the livestock production will be affected. As climate change affects the amount and duration of rainfall, the temperature variation and the degree of solar intensity, it stands to reason that climate change will affect the rangelands. In a previous climate modelling study, it was found that the net primary rangeland production is only slightly affected by the anticipated change in the climate (Kiker, 2015).

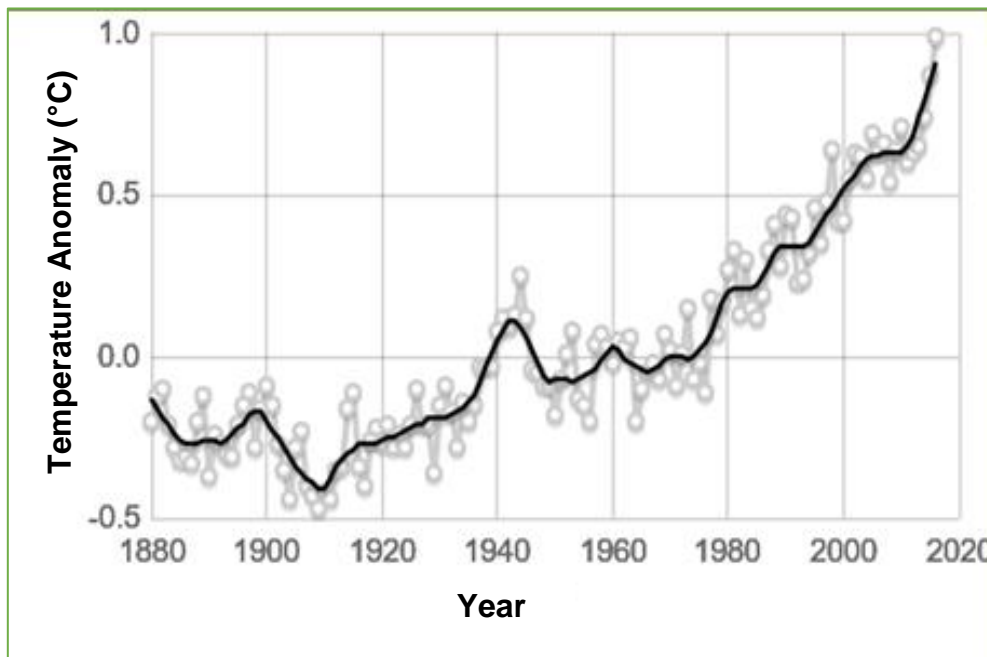


Figure 1.4 Graph illustrates the change in global annual mean surface temperature anomalies relative to 1951 – 1980 (NASA, 2017b).

This was thought to be due to the fact that the rise in temperature and slight decrease in rainfall are counterbalanced by the rise in CO₂ levels. As increased drainage and runoff are possible in the wetter parts of the country, elsewhere the increased water use efficiency will explain the longer growing season that will be experienced (Kiker, 2015). Lastly, it was found that the conditions for tree growth (higher temperatures and elevated CO₂ levels) will become more favourable in the grassland biome (Kiker, 2015). This was also evident in a study done by the South African National Biodiversity Institute (SANBI) in collaboration with the Department of Environmental Affairs on climate change and biodiversity (DEA, 2013b). During this study, the effects of climate change on South Africa's biomes was determined by processing global climate projections downscaled to a specific local condition. The results from several different

climate models were combined to form “low”, “intermediate” and “high” risk climate scenarios. The “low-risk” scenario represented a combination of wettest and coolest projections while the “high-risk” scenario represented a combination of driest and warmest projections. It was concluded that the grassland is the most threatened and vulnerable biome under all the climate scenarios as large portions of the biome is expected to be replaced by savannah and forests (Figure 1.5). This means that grasslands are in need of stronger protection, restoration and research to ensure adaptation benefits for vulnerable communities under future climate conditions (DEA, 2013b; SANBI, 2013).

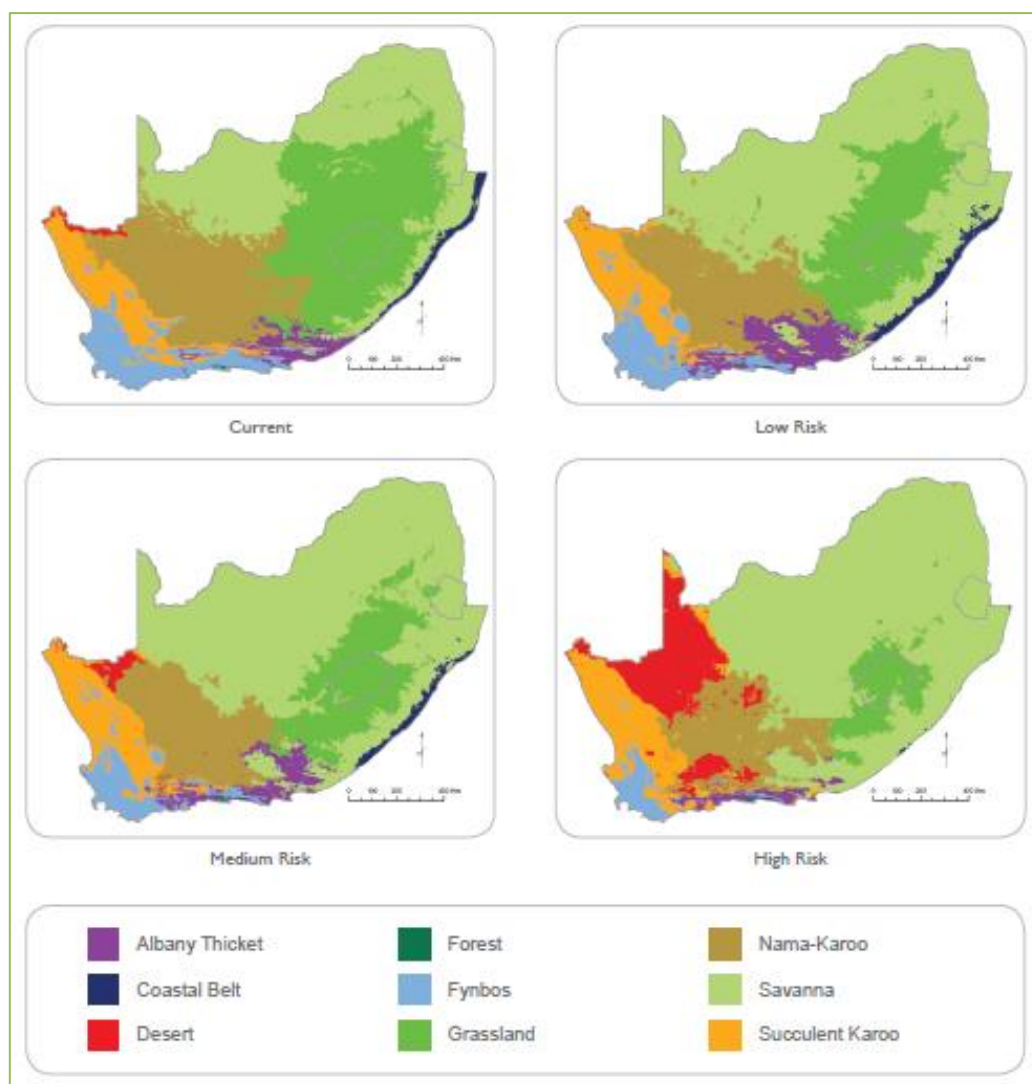


Figure 1.5 Projections of bioclimatic envelopes under statistically downscaled climate scenarios, looking ahead to approximately 2050. Low Risk map simulates impacts of wet/cool future climate projections, High Risk the impacts of dry/hot projections, and Medium Risk the median temperature and rainfall projections (DEA, 2013b).

More research needs to be done to ensure the continued existence of grasslands. The research questions that arose from the uncertainty of how the rangeland production could ultimately respond to the changing climate in the distant future and how climate change has affected the grassland production in the past are:

- 1) Can PUTU VELD (a biophysical rangeland production model) accurately simulate historical rangeland production?
- 2) Will rangeland production differ significantly under future climate scenarios?

There are two main objectives for the study:

- 1) To assess the historical rangeland production within the study area; and
- 2) To simulate the rangeland production within the study area under future climate scenario(s).

More information on the study area is provided in Section 3.1.

Specific objectives under Objective 1 include (Figure 1.6):

- a) To validate a rangeland production model in the form of PUTU VELD against historical data (done to some degree by Booyesen, 1983 and Fouché, 1992);
- b) To simulate rangeland production (RP) using PUTU VELD and observed climate data for the historical base period (1980/81 – 2009/10); and
- c) To evaluate the simulated RP for the historical base period.

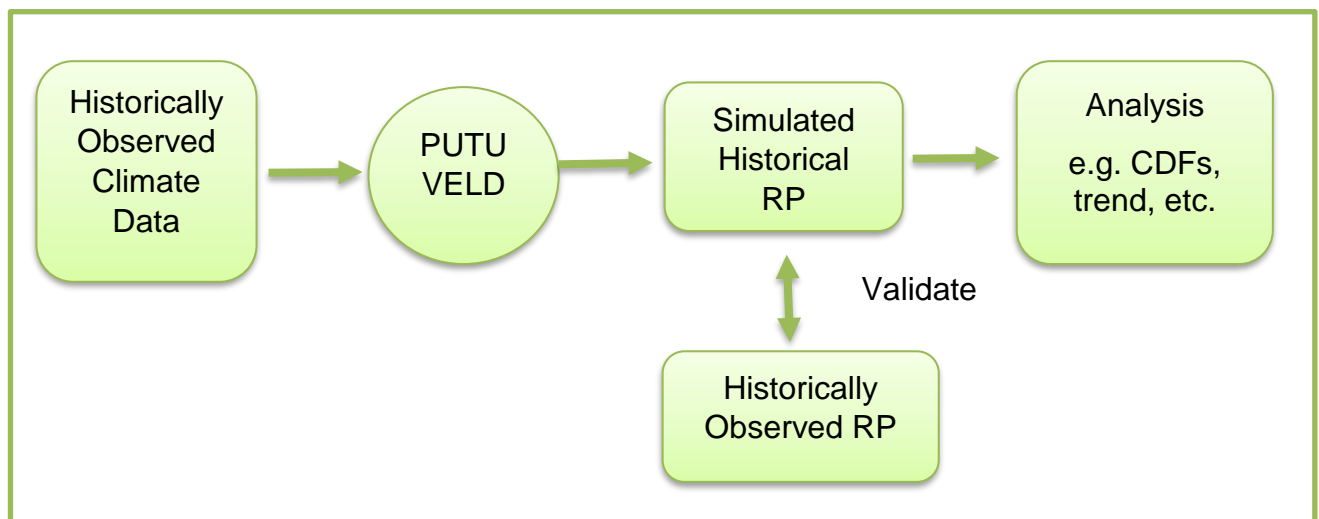


Figure 1.6 Schematic outline of the first research objective.

Specific objectives under Objective 2 include (Figure 1.7):

- a) To simulate RP using PUTU VELD and global climate model (GCM) data for the historical base period (1980/81 – 2009/10);

- b) To compare RP using observed and GCM generated climate data for the historical base period;
- c) To simulate rangeland production using PUTU VELD and GCM generated climate data for three future periods under two greenhouse gas emission scenarios:
 - 2010/11 – 2039/40 (current period)
 - 2040/41 – 2069/70 (near future)
 - 2070/71 – 2098/99 (distant future); and
- d) To evaluate the differences between the various time periods in order to describe the expected changes in RP.

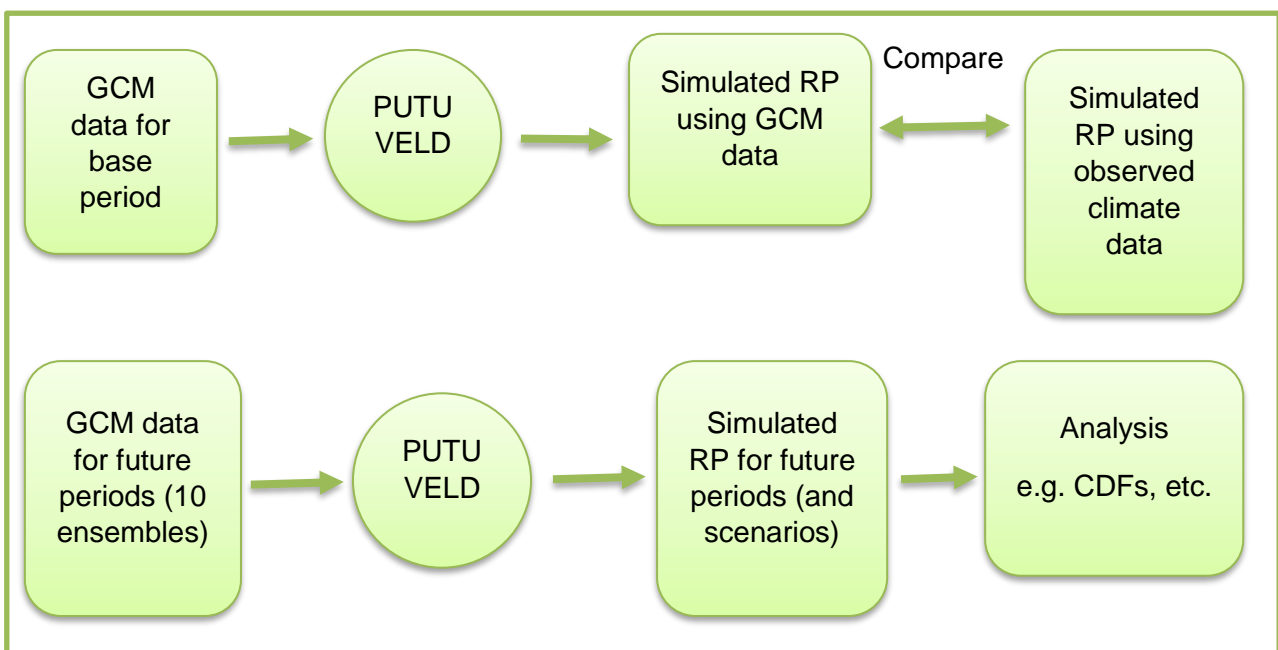


Figure 1.7 Schematic outline of the second research objective.

1.4 Organisation of Chapters

As mentioned in Section 1.3, grasslands are dependent on climate variables and how they change. Chapter 2 deals with why these climate variables affect grasslands and their role in the plant. Other factors that influence the production of rangelands are also discussed such as soil and fire. Different biophysical models in use and their advance over time are reviewed. The development path to the current PUTU VELD model is also outlined.

The elements of the study area and sources of data follows in Chapter 3. A detailed discussion on the PUTU VELD model follows, highlighting key aspects of the model and how it operates. The process of validation and how the data was analysed is

discussed. The results are highlighted in Chapter 4 with the use of graphs and tables and subsequently discussed.

We conclude in Chapter 5 with highlighting points from the document. Recommendations and further study discussions end the thesis.

CHAPTER 2

LITERATURE REVIEW

2.1 Factors Influencing Rangeland Production

To properly manage rangelands, a thorough understanding of how grass plants grow and develop is critical (Stichler, 2002). When one understands how and why plant processes work, then astute management decisions can be made based on the conditions of the rangeland rather than striving to follow an “average” set of guidelines. As every rangeland and the animals on it are different, depending on the situation it should be managed accordingly. Basic knowledge of the biology of plant growth and diligent monitoring can result in an improved stewardship of plant, soil and water as well as profitability (Stichler, 2002). The following discussion will focus on the various factors that influence rangeland production (viz. climatic factors, rangeland condition, rangeland management, fire and soil properties).

2.1.1 Climatic Factors

The rate of growth of grass plants and therefore the subsequent production of grasslands depends on the size of the photosynthetic (leaf) area available for trapping sunlight and the efficiency with which this leaf can photosynthesise. Photosynthetic efficiency is dependent on the environmental factors as well as the availability of the raw materials of photosynthesis and the age of the plant’s leaf system. Solar radiation, temperature and moisture are amongst the most important variables affecting leaf growth (Wolfson & Tainton, 2000; Volenec & Nelson, 2003).

2.1.1.1 Solar Radiation

Plant growth responses to radiation can be separated into those due to quality (wavelength or colour), density (intensity) and duration of radiation (photoperiod). Under field conditions these factors are often interrelated, e.g. density of radiation is usually highest during the same season that duration is longest (Volenec & Nelson, 2003). Quality refers to the wavelength of the rays contributing to the radiation spectrum. Plant development is enhanced under the full spectrum of sunlight (solar radiation) than under any single portion thereof. Photosynthetically active radiation (PAR) occurs in the visible range (400 – 700 nm) and is where photosynthesis is most active (Volenec & Nelson, 2003; Campillo *et al.*, 2012). A wavelength of longer than

800 nm (infrared) will result in heat affecting the plant and therefore water loss will be increased (Volenec & Nelson, 2003; Campillo *et al.*, 2012). Between 320 and 400 nm (UV-A) the leaf shape is affected and the plants will be shorter and the leaves thicker (Volenec & Nelson, 2003; Campillo *et al.*, 2012). Wavelengths shorter than 280 nm (UV-C) will result in rapid death of the plant (Volenec & Nelson, 2003; Campillo *et al.*, 2012).

When water supply and nutrients are adequate, growth rate of plants (amount of dry matter produced by the plant) is a direct function of radiation density via the influence on photosynthesis (Figure 2.1) (Campillo *et al.*, 2012). The quantity of solar radiation intercepted by the plant cover is influenced by various factors such as the properties of the leaf surface affecting light reflection, the thickness and chlorophyll concentration, which affects the light transmission, the angle of the leaf, its size and shape and the elevation of the sun together with the distribution of direct and diffuse solar radiation (Campillo *et al.*, 2012). Until extensive leaf area accumulates following cutting or grazing, forage rate is related more to percent radiation interception than to photosynthetic activity per unit of leaf area (Campillo *et al.*, 2012). In spaced plants grown at low light intensity, the products of photosynthesis are retained by the shoot at the expense of the root. In this way leaf area is maximized (Campillo *et al.*, 2012). In a closed crop community, however, where light intensities falling on individual leaves are further reduced by self-shading, the greater allocation of resources to produce leaves will normally not increase light interception sufficiently to offset the effects of low light intensity. Total plant photosynthesis is lowered, and so too is total dry matter production (Holmes, 1989). Most production plans are directed towards maximizing the interception of solar radiation (Campillo *et al.*, 2012).

Photosynthesis and growth are generally highest during the longest days of summer when the maximum radiation per day is received (Volenec & Nelson, 2003). Photoperiod also affects the vegetative growth form of many forage species. Leaf and stem growth in spring and summer are often erect under long photoperiods, but growth under short photoperiods in autumn tend to be flat and branched. Perennial forage grasses require exposure to low temperatures (less than 4.5°C) for an extended period (4 weeks or more) in a process called vernalization. This is why many perennial grasses flower only once each year (Volenec & Nelson, 2003).

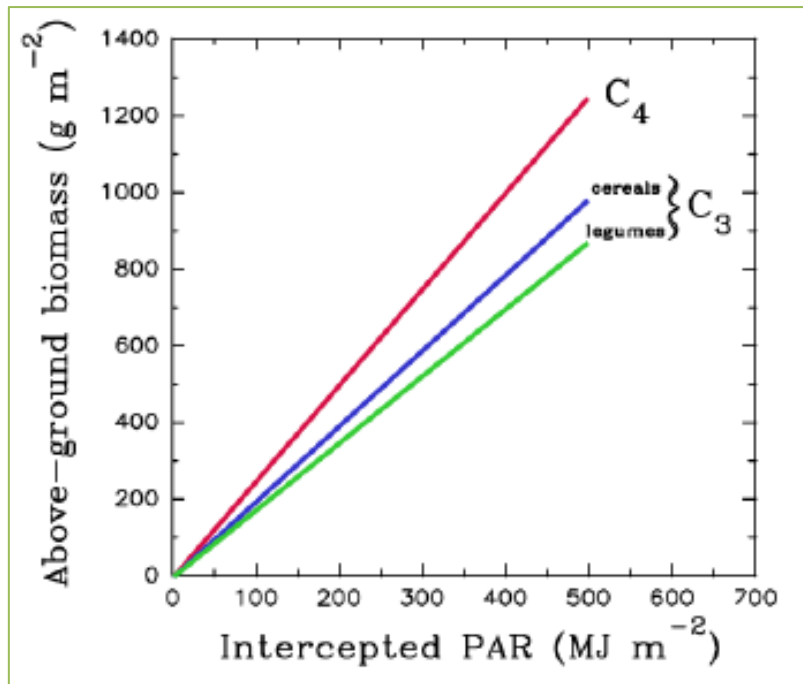


Figure 2.1 Typical theorized relationships between cumulated aboveground biomass and cumulated intercepted solar radiation for C₄ and C₃ species (Campillo *et al.*, 2012).

2.1.1.2 Temperature

Rates of growth and other processes depend on the temperature patterns a plant is exposed to (including variation between day and night temperatures) (Volenc & Nelson, 2003). The rate of extension of a growing leaf is extremely sensitive to the ambient temperature and responds to changes in temperature within minutes (Wolfson & Tainton, 2000). Grasses fall into two categories, either cool-season or warm-season types (Rodriguez, 2017). Plants are subjected to rapid daily changes in temperature and stress occurs when the temperature is above or below the optimal range for that particular species (Volenc & Nelson, 2003; Hasanuzzaman *et al.*, 2013). Cool-season grasses are subjected to root damage if the soil temperatures rise to 29°C or more, while warm-season grasses are easily damaged by consistently cold temperatures below 13°C and frost, where the grass leaves cannot use the nutrients and moisture efficiently and root growth is stunted (Rodriguez, 2017).

Severity of damage depends on the stage of development and on stress intensity and duration. As high temperature stress often occurs concurrently with moisture stress, it is difficult to separate the two effects (Bade *et al.*, 1985). Excessively high temperatures can induce flower sterility, especially pollen abortion, leading to poor seed production (Figure 2.2) (Volenc & Nelson, 2003; Thorvaldsson *et al.*, 2007).

Low temperature stress (temperatures slightly above 0°C) can cause chilling injury of some plants, mainly by affecting membranes or metabolism (Figure 2.2) (Volenc & Nelson, 2003; Thorvaldsson *et al.*, 2007; Hasanuzzaman, 2013). The rate of extension of a growing leaf is extremely sensitive to the ambient temperature, responding to temperature changes within minutes (Holmes, 1989).

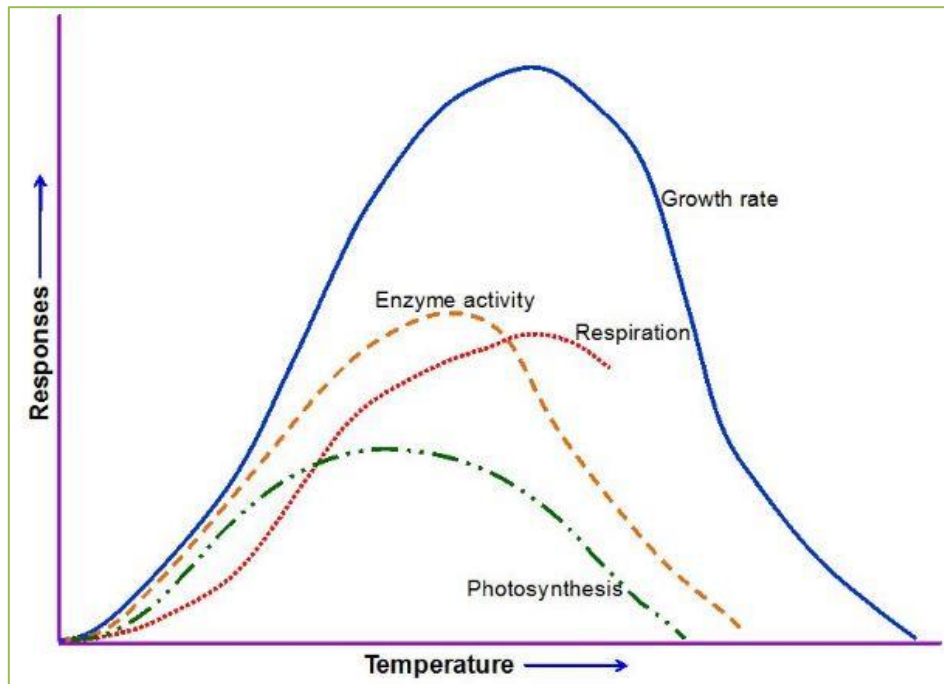


Figure 2.2 Schematic illustration of the effect of temperature on major physiological processes of plants (Hasanuzzaman, 2013).

2.1.1.3 Moisture

Probably few climatic factors are as important to the survival and growth of rangeland plants as is the availability of water (Brown, 1977). Water is essential for the maintenance of turgidity and cell enlargement and growth in plants. It is also an important medium for the absorption and dissipation of heat as well as plant nutrients from the soil (Brown, 1977; Stichler, 2002). Actively growing grasses are 70 to 95% water, yet grasses use or combine only about 2% of the water that actually passes through the plant. The other 98% is lost through transpiration which is also a cooling mechanism for the plant (Stichler, 2002). The effects of moisture stress on the growth and development of grasses will vary among different plant species. This is due to the growth stage of the plant, the duration of the moisture stress period and management prior to (e.g. tillage or no tillage) and during the stress period (e.g. mulching or no mulching) (Stichler, 2002). Seedlings are generally more susceptible to water deficit

mortality than mature plants primarily because of their less extensive root systems (Johnson, 1980). As water deficit intensity and duration persists, leaf growth and shoot development are the first to be restricted (Brown, 1995). First signs of moisture stress are the reduction in cell enlargement and the rate of cell division which can be visibly seen as a slowing down of the leaf growth and shoot development (Wolfson & Tainton, 2000; Stichler, 2002). Cell division and cell enlargement are affected by even a slight decrease in water potential (the ability of water to move from one area to another (Volenc & Nelson, 2003)) and directly reduce shoot growth (Figure 2.3). Shoot growth slows well before water stress becomes severe enough to cause stomatal closure and a decline in photosynthesis. Some cool-season grasses that experience drought stress during summer may have enhanced growth during autumn and the following spring. During severe drought, leaf growth ceases, leaves curl to reduce the exposed area, stomata remain closed and photosynthesis and transpiration declines markedly (Figure 2.3). In order to maintain or improve water status as soils become drier, many plants reduce shoot growth but maintain root growth under moderate drought stress conditions (Figure 2.3) (Volenc & Nelson, 2003).

Figure 2.3 illustrates the effect of extreme water stress (drought and flood) on plant physiology. Under drought conditions (block A, Figure 2.3), leaf temperature (······) increases with an increase in air temperature (Barfield & Normal, 1983; Feller & Vaseva, 2014) while photosynthesis and transpiration (- - - -) decreases (Arve *et al.*, 2011; Tardieu, 2013). This is due to the leaf overheating and while the plant tries to cool itself down, moisture is lost through transpiration via the fully open stomata (Arve *et al.*, 2011; Tardieu, 2013). As photosynthesis is restricted during a drought, the growth of shoots (———) is inhibited and new shoots are not produced (Tardieu, 2013). Under flood conditions (block B, Figure 2.3), photosynthesis (←——) is reduced as the stomatal conductance is decreased and thus shoot growth is decreased (Chen *et al.*, 2005; Liu *et al.*, 2014).

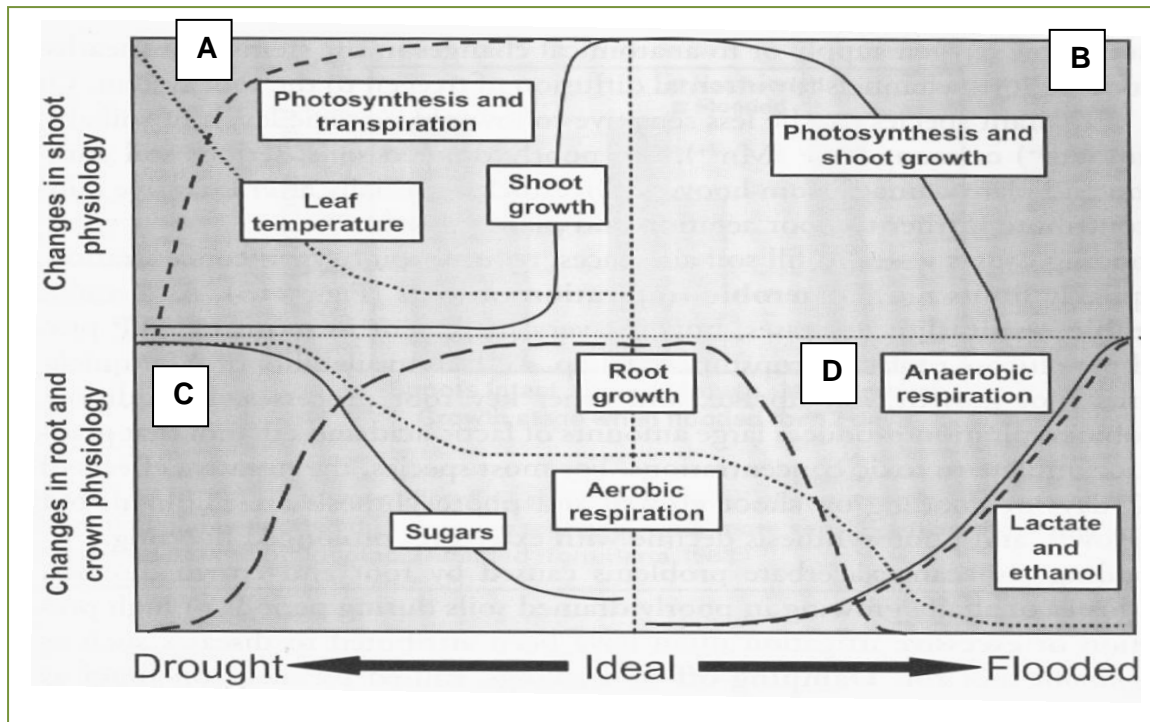


Figure 2.3 Effects of drought and flooding on growth and physiology of forage plants (Volencic & Nelson, 2003). A and B denotes the changes in shoot physiology under drought and flood conditions, respectively. C and D denotes the changes in root and crown physiology under drought and flood conditions, respectively.

During drought conditions (block C, Figure 2.3) sugar storage (—) is increased (Shi *et al.*, 2016). The plant relocates its sugar/carbohydrate supply to the roots for storage so that after the recovery phase, during which the stress conditions have lessened, they can be used for new shoot and fruit growth (Krasensky & Jonak, 2012; Shi *et al.*, 2016). Root growth (- - -) is highest during ideal conditions and lowest during drought (block C, Figure 2.3) and flood conditions (block D, Figure 2.3) when there is too little or too much water, respectively, for the roots to utilise (Chen *et al.*, 2005; Liu *et al.*, 2014; Koevoets *et al.*, 2016; Rowe *et al.*, 2016). Aerobic respiration (.....) by the roots are highest during drought conditions (block C, Figure 2.3) when the sugar content of the roots are high and therefore more sugars can be utilised and broken down into energy (32 molecules of adenosine phosphate (ATP)), CO₂ and water (Martin *et al.*, 2009; Bange *et al.*, 2016). During floods (block D, Figure 2.3), the soil is saturated and respiration cannot occur optimally and thus it becomes anaerobic respiration (Chen *et al.*, 2005). Anaerobic respiration (—) in plants only occur during high water levels (block D, Figure 2.3) when low or no levels of oxygen (O₂) is available within the roots to efficiently break down the sugars. The sugar molecules are not broken down completely but changed into ethanol, lactate and CO₂ and only produce two molecules of ATP (energy). Roots can only withstand these conditions for short periods or they

start decaying. Thus, anaerobic respiration and levels of lactate and ethanol (----) in block D (Figure 2.3) increases during flood conditions and the root growth decreases to such an extent that the roots start dying off (Sousa & Sodek, 2002; Maricle *et al.*, 2014).

Relatively short moisture stress periods during any phonological phase have been shown to cause significant increases in the root mass of *T. triandra* plants (Figure 1.1), as well as significant increases in the total available carbohydrate content of roots and stubble (Opperman & Human, 1976). Snyman (1989) demonstrated that, in terms of water use efficiency, i.e. the amount of above ground material produced in relation to the water transpired over a specified period, plants in the climax community in semi-arid areas were most efficient while those in the pioneer community were least efficient. However, *T. triandra* dominated rangeland receiving 20% less than normal rainfall was found to change to rangeland dominated by species of *Tragus* and *Aristida* over three seasons, suggesting that species of the climax community are intolerant of extended periods of moisture stress (Snyman & Opperman, 1983).

Poorly drained soils in high rainfall climates provide an unfavourable environment for growth of many forage species. Flooding causes water to fill soil air spaces and reduces soil oxygen concentrations. This limits normal aerobic respiration of roots (Figure 2.3) and as a result, anaerobic respiration increases. Anaerobic respiration is very inefficient in terms of ATP produced per glucose molecule consumed. Low availability of ATP quickly limits the root growth, ion uptake and other key root processes. During anaerobic respiration, large amounts of lactic acid and ethanol are produced which can gradually accumulate to toxic concentrations (Figure 2.3). Flooding can also increase the chance for root and crown diseases (Volencic & Nelson, 2003).

2.1.2 Rangeland Condition

In the present context, the term “rangeland condition” is used to describe vegetation in relation to its long-term potential for livestock production. It has been defined as the “state of health of the rangeland in terms of its ecological status, resistance to soil erosion and its potential for producing forage for sustained optimum livestock production” (Trollope *et al.*, 1990). Soil loss may be regarded as an absolute measure of the “health” of grazing lands (Wilson *et al.*, 1984; Snyman, 2009a; Snyman, 2009b)

since it is irreversible except over extremely long periods of time, and results in a reduction in productivity and affects future land use options. Vegetation is usually used to quantify rangeland condition since it is a more sensitive indicator of ecosystem change and is easier to measure than the soil (Teague & Danckwerts, 1989).

There are three main objectives of assessing rangeland condition. These are (Tainton, 1999c):

- a) To evaluate rangeland condition relative to its potential in that ecological zone;
- b) To evaluate the effects of current management on rangeland condition and to monitor changes over time; and
- c) To classify the different vegetation types on the farm and quantify their condition.

Most of the environmental variables responsible for vegetation pattern cannot be manipulated. However, defoliation by grazing and fire can be controlled by the farmer and both variables will influence the dynamics of plant communities (Bosch & van Rensburg, 1987; Morris *et al.*, 1992; Hurt *et al.*, 1993). Certain species respond differently to the same grazing impacts as a result of, for example, differences in soils (Bosch & van Rensburg, 1987). Hence the need to assess vegetation within a specific ecological zone where spatial variation in the abiotic environment (e.g. soils, temperature and rainfall) is kept to a minimum and where the grassland is therefore relatively homogeneous. In these homogeneous grasslands, several studies have shown that grazing and fire are of prime importance in determining the “state of health” of an area of rangeland (Hardy & Mentis, 1986; Bosch & van Rensburg, 1987).

Characteristics of the grass species can determine the ability of that plant to grow during short periods of moisture stress and is to a large degree proportional to root development, number of roots and depth of root penetration (Stichler, 2002). The larger the root system, the greater the capacity of the roots to absorb available moisture and nutrients. The ability of grass to survive long term drought is also dependent upon the amount of leaf area to maintain. Generally, tall grasses are replaced by medium size and short grasses as these grasses require less water for maintenance due to less transpiration (Stichler, 2002). Rangeland condition is an important factor controlling water-use efficiency and runoff which subsequently influence rangeland production (Snyman & Fouché, 1991). The high runoff from a rangeland in a poor condition and the ensuing low production results in a poor

consumption of rainfall, leading to droughts to occur even when there is reasonable rainfall (Snyman & Fouché, 1991).

A Study conducted by Palmer *et al.* (2001) found that a commercial rangeland management system had more vegetative cover than the communal rangeland management system, which meant that the commercial site had a stronger shield against nutrient and water movement across the landscape. It was noted, however, that the communal site had more fertile soils with higher organic carbon, phosphorus and nitrogen content than the commercial site (Palmer *et al.*, 2001).

2.1.3 Rangeland Management

The number one cause of poor DMP is improper grazing management (Stichler, 2002). It is critical to maintain a sufficient number of leaves through proper management (e.g. rotational grazing, correct stocking rate, fertilization and weed control, high density short duration grazing) or the rangeland will begin to deteriorate (Stichler, 2002). Rangelands can be harvested extensively during the vegetative growth stage, but it is important to reduce grazing or harvest pressure to allow for sufficient regrowth of leaves and for carbohydrate production to rebuild the plant and root system. This is in order to maintain healthy rangelands (Ferraro & Oesterheld, 2002; Swemmer & Knapp, 2008). Increasing grazing frequency or the severity of it has been noted to have a negative impact on *T. triandra* (the dominant grass species of the study area) (Snyman *et al.*, 2013). When rangelands are not permitted to regrow leaves and roots before being defoliated again, they will eventually die. This is due to the supply of energy from leaves and culms to the roots that becomes depleted and the root system begins to shrink and eventually leads to natural mortality. If drought occurs when the grass is energy stressed and unable to replenish the leaves, it may die. During such periods, the stocking rates must be reduced by either increasing the land area per animal, decreasing the number of animals on the rangeland or by decreasing the duration of grazing by the animals (Stichler, 2002). Properly grazed rangelands will produce more DMP than non-grazed rangelands. Grasses need to have the top growth removed occasionally so plants continue to produce new shoot growth. Short duration high intensity grazing causes grasses to be rejuvenated and develop new shoots when allowed to rest following defoliation (rotational grazing) (Ferraro & Oesterheld, 2002; Stichler, 2002; Swemmer & Knapp, 2008). A study conducted by Snyman *et al.* (2013)

showed that *T. triandra* rangelands should be grazed rotationally. It has also been noted that maximum utilization of the rangeland can be achieved when the rangeland is grazed during the dormant stage although grazing early in the dormant stage may lead to loss of plant vigor (Rethman & Booysen, 1968; Snyman *et al.*, 2013).

An important rangeland management practice is to always maintain a sufficient number of leaves to provide energy for regrowth and recovery of roots and leaves after harvest, to return organic matter back to the soil and cover the soil to prevent rainfall runoff and increase water absorption into the soil (Stichler, 2002; Boval & Dixon, 2012; Yan *et al.*, 2013). A concern for climax grasslands is that *T. triandra* is relatively sensitive to poor rangeland management and that loss of this species is regularly the first sign that degradation of the rangeland is occurring, most often leading to soil erosion, species changes and lower production (Snyman *et al.*, 2013).

2.1.4 Fire

Fire is thought to be a long-established natural factor of the environment of southern Africa (Tainton, 1999d). There is a widespread belief that fire is harmful to vegetation, that it upsets the natural balance between vegetation, insects, birds and animals and causes soil erosion, and should therefore be prevented wherever possible. Various South African writers have condemned rangeland burning, but most ecologists accept it as a natural part of the environment. They argue that complete elimination of fire would lead to extensive and often undesirable changes in the vegetation (Tainton & Hardy, 1999). The fire climax grassveld owes its nature to its long association with fire. In spite of this, the general attitude to its use in rangeland management tends to be negative, except in conservation areas. This attitude can be ascribed, firstly, to the fact that the first researchers to report on fire effects in South Africa were foresters, who understandably opposed its use, and secondly, because of the damaging effects that fire can have on grassveld when used imprudently (Tainton, 1999d).

Any discussion of rangeland burning in South Africa must take into account the objectives of using fire in management programs. These objectives, in both agricultural and conservation areas, are (Trollope, 1999):

- To burn off unpalatable growth left over from previous season's production which would be unacceptable as forage and, if it is not removed, would tend to smother the plant;

- To control the encroachment of undesirable plants;
- To stimulate out-of-season growth to provide green feed when it does not occur naturally;
- To contribute to fire control by reducing fuel loads; and
- To maintain or develop grass cover for soil and water conservation.

Grassland areas are prone to fire and support many plant and animal species which have evolved adaptations in response to fire (Mentis & Bigalke, 1979). Fires are a natural phenomenon in these areas because Africa is so prone to lightning storms. During the dry period lightning-induced fires can burn plant fuels that have accumulated during the wet rainy period (Everson, 1999). Edwards (1984) showed that grassland areas coincide with regions where the density of lightning flashes is greater than four strikes per square kilometre per year. Therefore, fire is regarded as a central component in the management of grasslands (Everson, 1999). Commercial livestock farms burn extensively from mid-August to early spring to promote early growth for feeding their livestock (Everson, 1999).

There should be no real need to remove accumulated ungrazed material by means other than grazing in the sweetveld areas. Since they are climatic climax grasslands they are not subject to rapid deterioration if under-utilised, although individual plants may be ruined if they are left unutilised for long periods (Everson, 1999). If burned regularly in late autumn or winter for many years, the density of the cover of these grasslands declines and susceptibility of the soil to erosion increases (Mentis & Tainton, 1984; Snyman, 2006). *T. triandra* rangelands flourish under annual or biennial fire regimes than when occasionally or not burnt (Fyn 2003; Raitt, 2005; Mopipi, 2012). Depending on the intensity and type of the fire, there can be substantial loss of above ground material, although much of it can be dead matter (Bennett *et al.*, 2002).

Usually after a fire event there is a decrease in biomass production for one or more seasons (Bennett *et al.*, 2002; Fyn, 2003; Snyman, 2004b). A decrease in the biomass production can also be caused by the negative influence fire has on soil water content and water infiltration, and loss of soil nutrients (Fyn *et al.*, 2003; Snyman, 2003b; Snyman, 2003a). Unplanned or accidental fires in the drier sweetveld areas can cause considerable fodder flow problems for stock farmers which can result in mismanagement of the rangeland (Snyman, 2006). Communal livestock farmers in

these drier areas widely burn only from mid-August to early spring (Figure 2.4) to encourage early growth for feed for their livestock (Snyman, 2002; Snyman, 2003b). Rangelands in the semi-arid regions should preferably be rested for a full growing season after a fire event and not be utilised for the first part of the following growth season. This is to ensure sustainable utilisation of the rangeland (Snyman, 2006). It was found in studies by Snyman (2003a; 2006) and Tainton and Mentis (1984) that a fire event does not greatly change the composition of the rangeland.

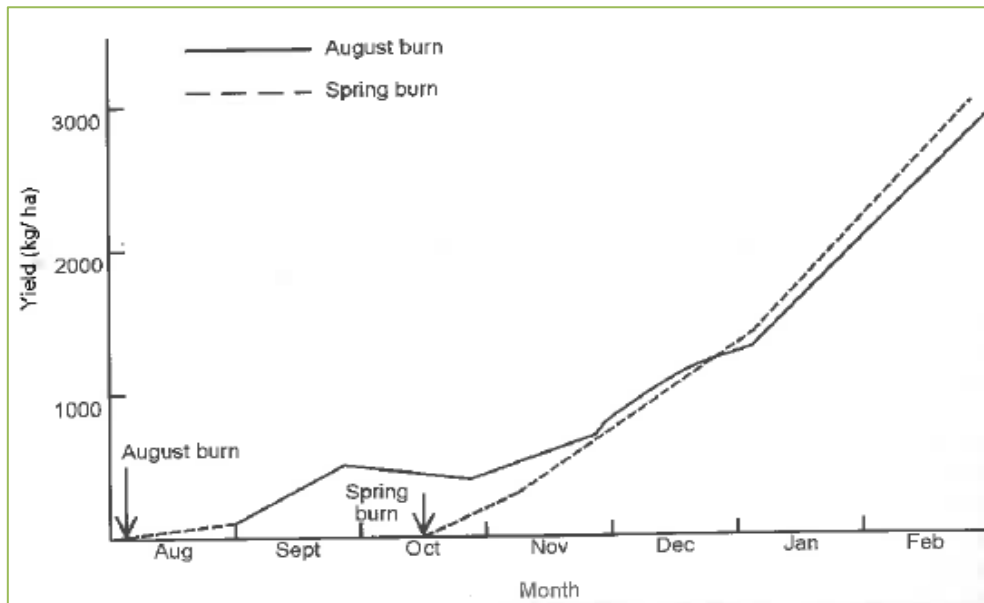


Figure 2.4 Yield of recovery growth from Tall Grassveld burnt in early August and after the first spring rains (Tainton *et al.*, 1977).

2.1.5 Soil Properties

Soil depth determines the root depth, as well as grass species differences such as shallow or deep root systems. Shallow soils will restrict root development and the roots will not penetrate beyond restrictive layers such as bedrocks that water seldom penetrates. Too many grass plants on shallow soils will cause precipitous loss of available soil moisture and those that have smaller, shallow roots will die. The effects of drought or floods on both the grasses and soil can be minimized with properly managed rangelands (Myburgh *et al.*, 1996; Stichler, 2002; Hirzel & Matus, 2013).

Soil texture (proportion of sand, silt and clay) affects the amount of water that can be stored in a soil (water holding capacity) within the root zone. Typically, clay soils have higher water holding capacity and less aeration, whereas, sandy soils have lower water holding capacity and greater aeration (Passioura, 1991; Stichler, 2002; Jalota

et al., 2010). Soil texture also affects fertility of the soil. Sandy soils have a lower capacity to hold cations (positively charged minerals/ions such as calcium, magnesium, etc.), and have a low cation exchange capacity (CEC). Clay particles have a high CEC and are generally more fertile and hold more water. Soil texture also affects the amount of O₂ available for root growth. A lack of O₂ can be caused by flood conditions or soil compaction in the deeper soil layers (Mitsui & Ueda, 1963; Stichler, 2002; Saidi, 2012).

Plant nutrients are minerals necessary for plant growth. Minerals such as nitrogen (N), phosphorus (P), potassium (K), magnesium (Mg), sulphur (S) and calcium (Ca) are used in large quantities in the plant. Small amounts of boron (B), manganese (Mn), molybdenum (Mo), iron (Fe), copper (Cu), zinc (Zn) and other nutrients are also used (Arvidsson, 1999; Prinzenberg *et al.*, 2010; Ormeño & Fernandez, 2012; Marimuthu & Surendran, 2015). These raw materials come from the soil but only make up about 5% of the total dry weight of the plant parts. Carbon (C), hydrogen (H) and O₂ from the air and water in the form of carbohydrates make up most of the remaining 95% (Stichler, 2002). If a plant lacks any nutrient, the growth of the plant will not be more than what is allowed by the most limiting nutrient. Of all the nutrients, nitrogen is the most vital because of the amount needed by the plant and the one most often deficient. It is highly mobile (moves easily between the soil particles) and cannot be stored in the soil (easily leached) (Riley *et al.*, 2001; Cameron *et al.*, 2013; Letey & Vaughan, 2013). It is most essential for cell division and growth, because N is the building blocks of proteins. It is critical for the formation of chlorophyll (used in photosynthesis) and the more N and water (H₂O) available, the higher the growth potential. N is absorbed by plant roots generally in the nitrate (NO₃) form and to a lesser amount as ammonium (NH₄) molecules. Sources of N are rainfall (released into the atmosphere by lightning and carried into the soil), organic matter (decomposed insects and plants), commercial fertilizer (LAN), manure or other waste products, and legumes (rhizobium bacteria in nodes on the roots convert atmospheric N to a useable form in the soil) (Uchida, 2002; Stichler, 2002; Leghari *et al.*, 2016; Tajer, 2016).

Soil pH is an important part of plant nutrition. When the pH of the soil is either too high or too low, the availability of some nutrients is reduced and root uptake is lessened. Soil minerals and applied fertilizers are not efficiently used and reduced plant growth is the result. Different plant species prefer different soil pH for optimum growth (Kidd

& Proctor, 2001; Stichler, 2002). High salinity (salt) levels will affect root growth and cause drought symptoms to occur. Soil salts affect plants by competing with roots for available water. Under drought conditions, salt pulls water out of roots causing them to dehydrate or desiccate. High concentrations of salts will also burn young tender roots and prevent them from developing normally (Stichler, 2002; Shrivastava & Kumar, 2015; Machado & Serralheiro, 2017).

2.2 Biophysical Simulation Models

2.2.1 Introduction

By definition, a model is a “simplified representation of the perception of a system or a set of equations, which symbolize the behavior of a system, with the purpose of assisting, understanding and improving the functioning of the system” (Rauff & Bello, 2015). This simplification makes models valuable because they offer an extensive description of a problem situation. However, the generality is, at the same time, the greatest weakness of the process. It is a difficult task to construct a comprehensible, functioning representation of a part of reality, which understands the essential elements and mechanisms of that real-world system. It is even more demanding, when the complex arrangements encountered are in environmental management (Murthy, 2002).

Simulations are mathematical models that describe computationally a system process. They are our best intellectual representation of multifaceted reality (Vallverdú, 2014). Simulations are a usable experimental technique for scientific research (Bosch, 1978; De Bruin, 1980). Modelling must start with the identification of the processes and variables that the system describes (Loomis *et al.*, 1979; Selirio & Brown, 1979). There must also be a continual compromise between the amount of detail that is included and the limits that it results in, not only regarding its measurable accountability, but also the programming accountability, the detection and correction of functions and the meaning of the influence of the process on the total system (Christiaan *et al.*, 1978).

Loomis *et al.* (1979) divides the variables into the following categories:

- a) State variables (e.g. mass of organs) which are adjusted at the end of each iteration period;
- b) Rate variables (e.g. rate of flow of carbon dioxide in the photosynthesis process);

- c) Driving force variables (e.g. climate inputs); and
- d) Internal auxiliary variables (e.g. meristematic state of the organ).

The number of state variables involved reflects the current state of information about the system. There are, for example, more than 100 state variables found in the model of the BACROS group (Basic Crop Simulator) (Du Pisani, 1979). Relationships and constants are derived from experimental results such as found for most of the processes involved. The relationships must be defined mathematically.

The choice of a time interval for iteration in the model depends on the aim of the model (Makkink & Van Heemst, 1975; Loomis *et al.*, 1979). A good guideline is that an iteration-interval must be no longer than 10 – 20% of the time needed by the system to recover after a small disturbance. If the iteration period is too long, then it causes an oscillation in the over- and under estimation of the values of the state variables. At this stage, it is advised to proceed to the development of a computer program.

Choosing a programming language is determined by the computer system that is used, incorporation of the algorithms and subroutines from other programs, the testing of the model by other researchers at various institutes and the universal use of the program at a later stage (Du Pisani, 1979). However, there is no uniform computer language that is used in simulation model development and this leads to models being developed that pursue the same objectives but have different standard program modules (Loomis *et al.*, 1979). As a result of this there were attempts at developing special simulation systems, e.g. SIMSCRIPT on a CDC-system (Freer *et al.*, 1970), DYNAMO and CSMP/360C (Continuous System Modelling Program) at Wageningen (Baier, 1977), Swarm simulation system (Minar *et al.*, 1996) and Simics system (Magnusson *et al.*, 2002). The actions and activities involved in the creation of a simulation model is shown in Figure 2.5.

There are many types of models, depending on the purpose for which it has been designed. A few of them are (Murthy, 2004):

- a) Descriptive models: These models define the behaviour of a system in a simple manner. The model reflects little or none of the mechanisms that are the causes of phenomena. However, they consist of one or more mathematical equations. An example of such an equation is the one derived from successfully measured

weights of a crop. The equation is helpful to determine quickly the weight of the crop where no observation was made.

- b) Deterministic models: These models estimate the exact value of the yield or dependent variable and have defined coefficients.
- c) Dynamic models: In these models, time is a variable. Both independent and dependent variables have values, which remain constant over a given period.
- d) Explanatory models: These consist of quantitative descriptions of the processes that cause the actions of the system. To create this model, a system is analysed and its mechanisms are quantified separately. The model is developed by incorporating these descriptions for the entire system. It contains descriptions of well-defined processes such as leaf area expansion, tiller production, etc., as crop growth is a consequence of these processes.
- e) Mechanistic models: These models explain not only the relationship between yield and weather parameters, but also the mechanisms of these models (explains the connexion of influencing dependent variables). These models are based on physical selection.
- f) Simulation models: Computer models, in general, are a mathematical representation of a real-world system. One of the main goals of these models is to guesstimate agricultural production as a function of weather and soil conditions as well as crop management. These models use one or more sets of differential equations, and calculate both rate and state variables over time, normally from planting until final harvest.
- g) Static models: In these models, time is not included as a variable. Independent and dependent variables' values remain constant over a given period.
- h) Statistical models: These models express the relationship between weather parameters and yield. Statistical techniques (e.g. correlation, cumulative distribution functions, step down regressions, etc.) are used to measure the relationships in a system.
- i) Stochastic models: In these models, a probability element is attached to each output. For each set of inputs, different outputs are given along with

probabilities. State of dependent variables or yields at a given rate are defined in these models.

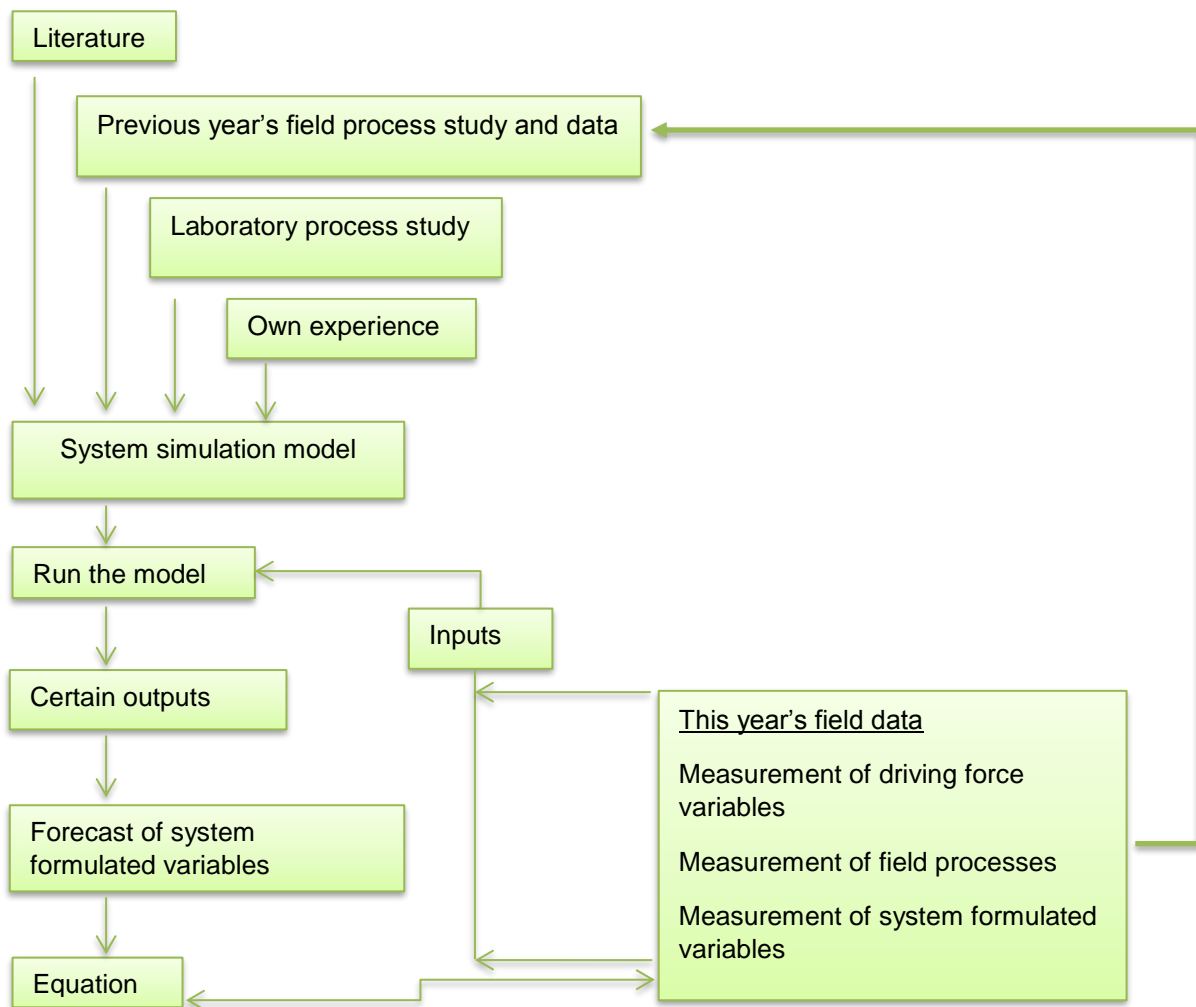


Figure 2.5 The relationship between simulation, field- and laboratory studies and actual measurements in the field (Innis, 1978).

Growth models or production models may have various meanings (Fouché, 1992). In the context of this study its meaning is the integration of mathematical equations and algorithms which describe the interaction of the biotic and abiotic components of the grassland ecosystem. Modelling is thus a process of organizing, synthesizing, conceptualizing and integrating in a realistic description of the prototype (Wight, 1988; cited by Fouché, 1992). Crop modelling has advanced considerably over the past 40 years in corresponding advances in crop and environmental sciences and in computer technologies. A wide range of crop models are used, incorporating different approaches and levels of complexity and highlighting different aspects of the soil-plant-atmosphere system (e.g. DSSAT (Jones *et al.*, 2003), APSIM (Keating *et al.*, 2003), and CropSyst (Stöckle *et al.*, 2003).

The potential uses of models can be grouped under (a) crop management, (b) research and (c) policy analysis (Boote *et al.*, 1996). Models enable researchers to explore scientific hypotheses and investigate the impact of unparalleled agricultural and ecological conditions. They can also be used to amalgamate knowledge and data across disciplines, assisting the synthesis of new knowledge (Singels *et al.*, 2010).

Proper understanding of the effects of climate change helps scientists to guide farmers to make crop management decisions such as selection of crops, cultivars, sowing dates and irrigation scheduling to minimise the risks (Murthy, 2004). Crop models are remarkable in predicting crop performance and resource dynamics and thus provide exceptional information for planning and management assessments over both the long and short term (Singels *et al.*, 2010). The application of crop models to study the potential impacts of climate change and variability provides a direct link between models, Agrometeorology and the concerns of the society. As climate change deals with future issues, the use of General Circulation Models and crop simulation models provide a more scientific approach to study the impact of climate change on agricultural production and world food security compared to other surveys (Murthy, 2004; Rauff & Bello, 2015).

2.2.2 Models in use

The development and use of crop growth models demands multi-discipline research and it is here that Prof De Wit and his team of colleagues from the Netherland University of Agriculture in Wageningen made a big contribution to the current knowledge of simulation techniques (Baier, 1979). The crop growth simulator, Elementary CROp growth Simulator (ELCROS), is a typical example of a dynamic model that was developed and published in 1974. The model simulates processes such as photosynthesis, respiration, translocation and transpiration. The model determines the total dry mass production and the transpiration of a growing crop during the vegetative growth stage from physical, physiological and chemical plant components and macro-meteorological data (Baier, 1979). Further developments focused on aspects such as the simulation of a) ecological processes (De Wit & Goudriaan, 1978); b) water use and the growth of grasslands in arid areas (Van Keulen, 1975); c) the water balance from arable lands and grasslands (Makkink *et al.*,

1975; cited by Booyesen, 1983); d) grassland systems (Christiaan *et al.*, 1978); and e) a simulation study concerning crop-micrometeorology (Goudriaan, 1977).

A few of the older crop models were developed in the United States of America such as the SPAM (Soil-Plant-Atmosphere) model (Stewart & Lemon, 1969; cited by Shawcroft *et al.*, 1974). This model simulates the plant- and environmental interactions over the short term. Du Pisani (1979) summed up deterministic modelling in the USA as follows: The counterpart of ELCROS, namely BACROS (Basic Crop Simulator) was developed at Davis University in California by Prof Loomis. It simulates the growth of various crops and was thoroughly tested for maize and wheat (Du Pisani, 1979). Two other models that were also developed in California, is SUBGOL for simulation of growth for sugar beets and the potatoes simulation model with the appropriate name POTATO. From Ohio, the SOYMOD/OARDC was developed for soya beans (Du Pisani, 1979). This model is a system of partial differential equations which describes the mass- and energy balance inside the plant. The mechanisms of the simulation process rests on the basic principles of plant biochemistry. It includes product inhibition, enzyme control, concentration and dilution, mobility of internal nutrient and buffer actions. SORGF was developed in Temple, Texas as a dynamic grain sorghum growth model. It has been widely used by amongst others the US Department of Agriculture, for yield forecasting. An interesting characteristic of the model was that it could be updated during the season with actual measured data, which greatly increased the operational application of the model (Du Pisani, 1979).

The LINTUL-POTATO model was developed in the early 1990s by Kooman and Haverkort (1994). The model describes the dry matter accumulation as a function of solar radiation interception and light use efficiency (Spitters, 1990; Spitters & Schapendonk, 1990). A more robust but less complex LINTUL-POTATO-DSS model was derived from the LINTUL-POTATO model in order to compare the influence of environmental conditions on crop production (Haverkort *et al.*, 2015). Pereira *et al.* (2008) tested the LINTUL-POTATO model based on different climatic elements and cultivar characteristics in Brazil. The results showed a good performance of the model with an underestimation of irrigated potato productivity of less than 10%.

A major model system is the Decision Support System for AgroTechnology Transfer (DSSAT), developed in the USA (Murthy, 2004). This system is being used as a

teaching and research tool for a wide variety of applications. As a research tool, its role is to develop recommendations regarding crop management and to explore environmental and sustainability issues. The products enable users to match the biological requirements of crops to the physical characteristics of land to provide them with management options for improved land use planning. DSSAT is also being used as a business tool to increase profitability and to improve input marketing. The DSSAT package consists of the following (Murthy, 2004; Rauff & Bello, 2015): a) a database management system for weather, soil, management inputs and genetic coefficients; b) crop simulation models; c) series of weather generation programs; d) series of utility programs; and e) strategy assessment program to evaluate options including choice of planting date, plant population density, row spacing, cultivar choice, irrigation, fertiliser application, soil type, water stress in a certain growth stage, initial conditions on yield, and net returns.

There are various versions of the Crop Environment Resource Synthesis (CERES) models, where CERES-Maize and CERES-Wheat is more widely known (Wu *et al.*, 1989). CERES is a predictive, deterministic model that is designed to simulate crop growth, soil-water, soil-temperature and soil-nitrogen dynamics at a field scale during one growing season. The model is used for basic and applied research on the effects of climate and management on the growth of a crop. CERES-Maize was used in an experiment in the North China Plain to simulate maize yields for a period of 5 years (Wu *et al.*, 1989). The results showed that the model tended to overestimate the yields during the wet years and underestimate the yields during the dry years. When they simulated the irrigation, the model yields improved. The model was then modified to account for the effects of excess water through the use of a crop moisture index and subsequently the results showed a further improvement in the yields (Wu *et al.*, 1989). Gerçek and Okant (2010) simulated maize yields under irrigation rates with the CERES-maize model in a semi-arid region of Harran Plain of South Eastern Turkey in 2005 and 2006. It was found that for all treatments, yield and biomass were adequately simulated by the model and differences between simulated and measured values were less than 6%. Comparison of the model data with the measured values showed that there was a satisfactory agreement between the measured and simulated values and the model performed well for both biomass and yield (Gerçek & Okant, 2010). In South Africa, CERES-maize, within DSSAT, has been used to find solutions to problems from

farm (Prinsloo *et al.*, 1998; Durand & Du Toit, 2000) to regional scale (Schulze *et al.*, 1993) and to simulate maize yields for a diverse range of applications such as climate change (Du Toit *et al.*, 2000) and drought assessment (De Jager *et al.*, 1998).

The Thünen Institute of Market Analysis (TI-MA) in Germany developed the AnnuGrow model in 2008 (Köchy, 2008). It is a process based model that is used to quantify the effect of different daily rainfall distributions and compare it to the effect of a change in mean annual amount on vegetation. It simulates explicitly the response of individual plants and soil moisture to rainfall variability and can consider the effects of rainfall on different life stages and special interactions (competition dispersal). The daily and annual rainfall amounts are simulated as a stochastic time series with specified means. Köchy (2008) used the AnnuGrow successfully in a study to simulate vegetation in the Mediterranean region, situated between water stressed subtropical and mesic temperate regions.

Most models are focused on agricultural work, particularly on the determination of soil water through the soil profile as well as the simulation of evapotranspiration (Pierce, 1958; Pelton *et al.*, 1960; Jensen *et al.*, 1971; Jones *et al.*, 1972; Saxton *et al.*, 1974; Amerman, 1976; De Jong & Cameron, 1979; Xu & Chen, 2005; Mohawesh, 2011; Li *et al.*, 2016; Muniandy *et al.*, 2016). Grassland growth models are in the minority but as grasslands is one of the major biomes more models are being developed. Christiaan *et al.* (1978) described a complex model for the simulation of grassland systems. The model functions on three levels, namely the simulations of the biological processes involved, the second level is the management and the third level is that of optimization.

At the University of Guelph, Canada, Selirio *et al.* (1978; cited by Booyesen, 1983) established the SYMFOY (Simulator of Forage Yield) model. The model simulates growth according to the sigmoidal curve. Deviations from the potential growth-increments per day are determined by the estimation of the available soil moisture and the number of degree-days above 5°C. The amount of yield at the end of the season is the daily accumulation of growth increments. The daily soil water is estimated for different soil layers by using potential evapotranspiration which is estimated by means of an energy balance method and a withdrawal pattern which is determined by the soil moisture dispersion within the profile as well as the root distribution.

With the American grassveld biome project (US/IBP), which forms part of the International Biological Program (IBP) the complex ecological model, ELM, was developed at Fort Collins, Colorado (Innis, 1978). The ELM-model is also an example of a multi-level explanatory model with different degrees of accuracy which offers good results in the field of guidance and research. The development of the model started in 1968 and is preceded by the PRONG model, the PAWNEE 1 model, the LINEAR 1 model, the SIMOPT model, the PAWNEE 2 model and LINEAR 2 models (Innis, 1978). The mechanisms of the different models ranged from differential equations with the special focus on interseasonal dynamics of plant- and soil components to linear models which described the abiotic and nutritional components of the system.

The Simulation of Production and Utilisation of Rangelands (SPUR) model is one of the most comprehensive grassland models available (Foy *et al.*, 1999). Developed in the USA, in 1987, it is composed of five components, namely climate, hydrology, plant growth, animal production and the economy. It simulates the daily growth of individual plants or plant groups, carbon and nitrogen cycling, soil moisture flux, foraging by wildlife and economics of beef production. The model uses daily rainfall, minimum and maximum temperature, solar radiation, wind speed and direction and dew point temperature. The output can be set for monthly, annual or user selected interval summaries. The model is, however, point-based and is applicable only to a small homogeneous area at a scale of a pasture or smaller, with a basic modelling unit of one soil and one plant type. The SPUR and more recently the SPUR 2.4 model was used successfully by Wight & Skiles (1987), Carlson & Thurrow (1992) and Skirvan & Moran (2003).

The Integrated Farm System Model (IFSM) (Rotz *et al.*, 1999) is a deterministic, process-based model that predicts the effects of weather and management on hydrology and soil nutrient dynamics, forage and crop yields, harvest, handling and feeding of crops, milk or beef production, manure management and farm economics in temperate regions at a whole-farm scale. To simulate pasture plant dynamics, the current IFSM used modified portions of the grazing simulation model GRASIM (Corson *et al.*, 2006). GRASIM estimates daily forage dry matter, daily soil water content and drainage, and daily soil nitrate content and leaching. The Web interface for GRASIM was developed to better deliver this useful computing resource to general users with access to a Web browser, regardless of their computer platform (Mohtar *et al.*, 2000).

The CSIRO Division of Plant Industry in Australia developed the GrassGro Decision Support System in 1997 (Moore *et al.*, 1997). It runs on a daily time step combining the pasture growth module with a module for predicting the intake of herbage of ruminants (sheep and cattle) and their productivity. GrassGro enables users to analyse simplified grazing systems in terms of pasture and animal production, grass margins, and a year to year variability for any specified cultivar, or combination of cultivars, at any specified site. The support system may be used to simulate future predictions from current animal and pasture conditions, for assessing the probability distribution of production outcomes. The user can test management options against a wide range of seasons to achieve a more profitable and sustainable utilisation of grasslands. The CSIRO Division of Plant Industry (Moore *et al.*, 1997) has successfully used the model in Australia.

The Grassland Statistical Model (GRAM) was developed by the Agricultural Research and Education Centre in Austria (Trnka *et al.*, 2006). This model assumes that grass growth is dependent on the soil water content in the active root zone, in combination with global solar radiation, air temperature and management strategies, as well as short- and long-term water stress. The model further assumes that all supply of water can be attributed to rainfall. The water uptake is then divided mainly between the evapotranspiration and the soil evaporation and percolation to deeper soil layers. Schaumberger (2010) used the GRAM model to estimate the forage production in Austria in 2010.

Researchers in France (Soussana *et al.*, 2012) developed the Grassland Ecosystem Model with INdividual centred Interactions (Gemini). The model simulates average individual plants for each population of a multi-species canopy consisting of perennial C₃ grass species. It is parameterized from a large number of shoot and root traits in each plant population. The model is run on a daily time step for temperate grasslands. Inputs include shortwave solar radiation, temperature, rainfall and CO₂ concentration. During a study in France in 2012, Gemini successfully showed it had the ability to simulate, without bias, disturbance and nitrogen responses of net primary productivity and of plant community structure (Soussana *et al.*, 2012).

Until recently, continuous monitoring of global vegetation productivity has not been possible because of technological restrictions (Running *et al.*, 2004). A new satellite

driven monitor of the global environment that regularly calculates daily gross primary production (GPP) and annual net primary production (NPP) was developed (Running *et al.*, 2004). The MOD 17 MODIS (Moderate Resolution Imaging Spectroradiometer aboard the Terra and Aqua satellites) project provides constant estimates of GPP/NPP across Earth's entire vegetation covered surface (Numerical Terradynamic Simulation Group, 2017). It is part of the NASA Earth Observation System program and the outputs are useful for global carbon cycle analysis, ecosystem status assessment, natural resource and land management and environmental change monitoring. The main outputs are the annual NPP, eight-day net photosynthesis and eight-day GPP (Numerical Terradynamic Simulation Group, 2017). Palmer *et al.* (2016) conducted a study in northwest Namibia in an arid/semi-arid rangeland system using the MOD 17 project. They found that even though MOD 17 overestimated the annual NPP, the "measured" mean dry matter production (calculated using samples and regression equations) was 83% of that modelled by MOD 17. They concluded that the results showed the viability of using the MODIS NPP product as a near replacement for dry matter production in wide-ranging semi-arid rangeland systems (Palmer *et al.*, 2016).

The PUTU model system was first developed by De Jager (1984; cited by Booysen, 1983) for the growth and development of maize. The name "PUTU" was adopted after the South African maize meal porridge (Singels *et al.*, 2010). The system explains and computes the growth and development processes of agronomic crops using mathematical equations and the essential laws of chemistry and physics (Singels *et al.*, 2010). The rationalization was that dynamic, deterministic simulations are analytical, precise, repeatable, and hence crucial for practical agricultural problem solving and management decision support (De Jager *et al.*, 2001). In the first "PUTU" active maize crop simulation the efficacy of radiation use in photosynthesis was calculated and converted to carbohydrates (De Jager, 1976; cited by Singels *et al.*, 2010). A generic model was developed for simulating yield and water use of any crop by computing yield response as a function of relative evapotranspiration deficit (De Jager, 1997). Before this, it was adjusted by De Jager, Opperman & Booysen (1980; cited by Fouché, 1992) for the simulation of grassland production (PUTU 2). Due to certain shortfalls in the PUTU 2 model, the PUTU 11 model was developed by Booysen (1983) and applied by Fouché (1984; 1992). The PUTU VELD model (used in this study and discussed further in Section 3.3) was an adaptation of the PUTU 11

model and is included in Appendix A. These two simulation models are part of a series of models that have been developed at the University of the Free State, South Africa (Table 2.1). An important outcome from these models was the PUTU 13 model (Du Pisani, 1992). This model simulates the production of *Cenchrus ciliaris* in the same manner as PUTU 11 does for a *Themeda-Cymbopogon* veld. It is also the first model that can simulate the dry matter production of pasture crops under dryland conditions (Fouché, 1992).

Table 2.1 The PUTU-series models for the mathematical simulation of the growth of crops (Booyesen, 1983; Fouché, 1992)

NAME	DESCRIPTION
PUT EST	Create daily data from monthly values of maximum (Tx) and minimum temperature (Tn), sunshine duration and daily rainfall (1981)
PUT COR	Correct data files created for PUTU from the keyboard from the HP9845 – included in PUTU 6 (1980)
PUT DAT	Test data for PUTU to be used on HP9845
PUTU 1	Guelph – hourly values for maize (De Jager, 1974)
PUTU 2	Grassland – De Jager, Georgia
PUTU 3	Bethlehem maize – hourly values (De Jager, 1976)
PUTU 5	Special version for HP9845 – daily input data
PUTU 6	Wheat – daily input from Tx, Tn, sunshine duration and rainfall (De Jager <i>et al.</i> , 1981; De Jager <i>et al.</i> , 1982)
PUTU 7	Wheat – daily rainfall/monthly Tx, Tn and sunshine duration
PUTU 8	Maize – same as PUTU 6 (De Jager <i>et al.</i> , 1983a)
PUTU 9	Wheat (De Jager <i>et al.</i> , 1983b)
PUTU 989	Wheat – refinement of PUTU 9's phenology, leaf development and grain filling (Singels & De Jager, 1991a; Singels & De Jager, 1991b; Singels & De Jager, 1991c)
PUTU 11	Grassland – improvement of PUTU 2 (Booyesen, 1983; Fouché, 1984)
PUTU 13	Pastures – refinement of PUTU 11 for phenology, translocation, dry matter increase, growth vigour (Du Pisani, 1992)
PUTU - system	Decision support system for maize, wheat, irrigation, “any crop” and grassland (De Jager, 1992)

2.3 A Changing Climate, A Changing Land

2.3.1 Climate Change Science

Climate change, defined in Section 1.3, is not a new phenomenon and occurred at various times throughout the Earth's history under natural forcings (NASA, 2017a). Proxy data (e.g. obtained from ice cores, etc.) show that over the last 800 000 years the Earth has undergone several major climatic shifts which have sometimes resulted in major extinctions (NASA, 2017a). The fluctuation has from time to time been rapid and extreme, with a change of more than 2°C in the mean temperature just 50 to 100 years. The difference between the present and past is that this time round, people are the major cause for the climate change (Stevens *et al.*, 2015; NASA, 2017a). As of November 2017, the CO₂ level have surpassed the 400-ppm mark at 405.58 ppm (Figure 2.6) at the Mauna Loa Observatory in Hawaii (Scripps Institute of Oceanography, 2017).

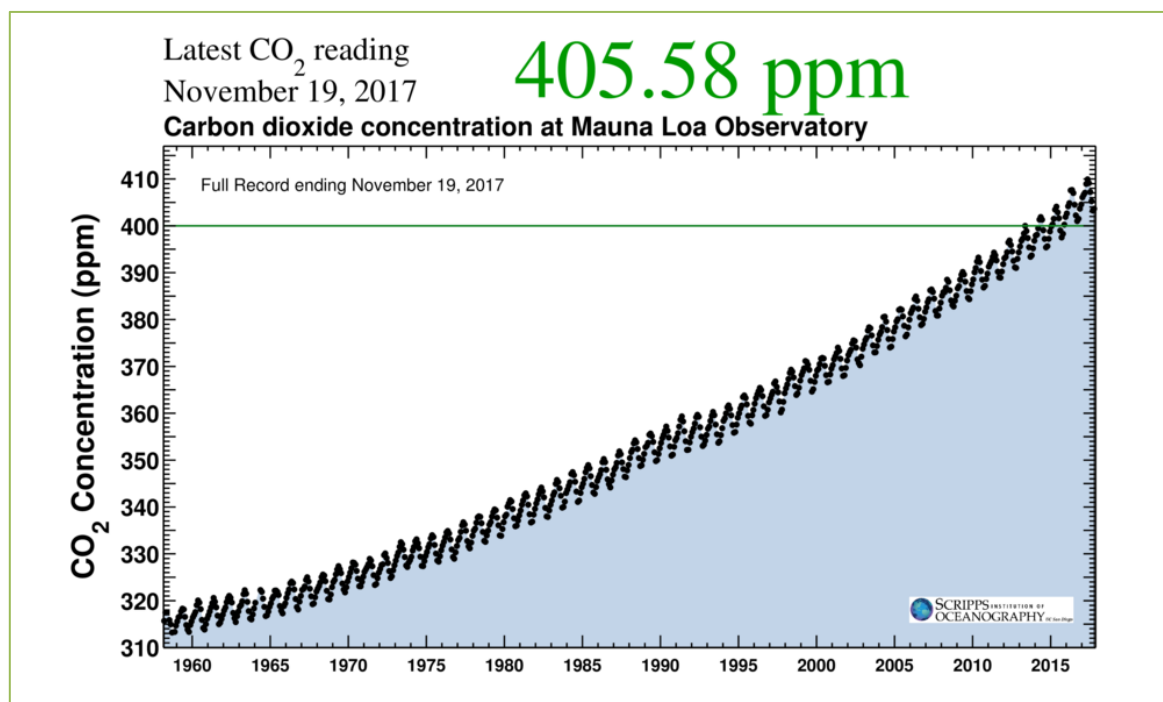


Figure 2.6 Mean atmospheric CO₂ concentration at Mauna Loa Observatory, Hawaii, measured since 1960 (Scripps Institute of Oceanography, 2017).

Human activities such as the burning of fossil fuels and deforestation account for half of the globally observed warming over the past 60 years (Stevens *et al.*, 2015). Thus, temperatures are increasing more rapidly than can be explained by natural forcings such as solar radiation. The rise in temperature is mirrored by the increase in the concentration of greenhouse gases (GHGs) (Stevens *et al.*, 2015). Methane (CH₄) and

CO₂ are natural atmospheric heat trappers, enabling our planet to be habitable. But, since the start of the industrial revolution, when more fossil fuels were being used, the levels of CO₂ have increased by 40%, thus causing extra heat to be trapped and the surface of the Earth become even warmer (Stevens *et al.*, 2015). Due to the atmospheric lifetime of these GHGs, various feedback mechanisms and the probable continued use of fossil fuels, such warming is expected to continue into the near future (Stevens *et al.*, 2015).

2.3.2 Climate Predictions

Predictions are full of uncertainties and climate estimates are no exceptions. Confidence in Global Climate Model (GCM) estimates are lower for some climate variables (e.g. precipitation) than others (e.g. temperature) (IPCC, 2007). During a number of decades of development, GCMs have provided without fail a robust and clear picture of significant climate warming in response to increasing greenhouse gases (IPCC, 2007). Research in climate change is not a precise science. There are a number reasons for this (IPCC, 2007; Stevens *et al.*, 2015):

- a) Computer models of climate are progressively complex, but remain generalizations of reality that do not include all the factors affecting the climate;
- b) Forthcoming levels of greenhouse gases in the atmosphere are governed by trends in human population growth, the use of fossil fuels, and the introduction of mitigating effects of reduced polluting energy technologies;
- c) We still have much to learn about how climate behaves, and some details may be characteristically impossible to model because they are 'chaotic', or very responsive to minor changes;
- d) Climate model estimates are generally made at a global scale; the details of predictions of climate shifts at the regional or local scale are subject to compounding uncertainties; and
- e) We also cannot correctly predict the reaction of animals and plants to changes in climate and CO₂ levels.

GCMs have the ability to simulate important aspects of the current climate (IPCC, 2007). By comparing their simulations with observations of the variables over some historical time period, they are regularly and comprehensively assessed. The main source of errors is that many important small-scale processes cannot be represented

clearly in models, and so must be included in approximate form as they interact with larger-scale features (IPCC, 2007). This is partly due to restrictions in scientific understanding or in the availability of detailed observations of some physical processes (IPCC, 2007). Notwithstanding these uncertainties, GCMs all agree with the prediction of significant warming under greenhouse gases. GCMs can make predictions on a global, regional or local scale depending on the resolution that is needed and are becoming more comprehensive in their capability to represent more physical and biological processes and their interactions (IPCC, 2007).

GCMs are multifaceted computer models used to simulate global climate change (Baker *et al.*, 1993; Stevens *et al.*, 2015). These models have predicted that the changes will not occur homogeneously across the globe: temperatures of coastal zones will rise more slowly than continental interiors, polar latitudes will increase faster than temperate latitudes and land areas will likely warm faster than the oceans. These patterns can already be seen in South Africa where the central interior minimum temperatures have decreased slightly, while the rest of the country has seen an increase in maximum and minimum temperatures (Figure 2.7). A change in the rainfall patterns has also been observed. The central and north-eastern parts of South Africa experiences less days with rain, especially during autumn when less rainfall occurs. In the mountainous regions of the southern Drakensberg, the spring and summer rains have increased (Figure 2.8) (Stevens *et al.*, 2015).

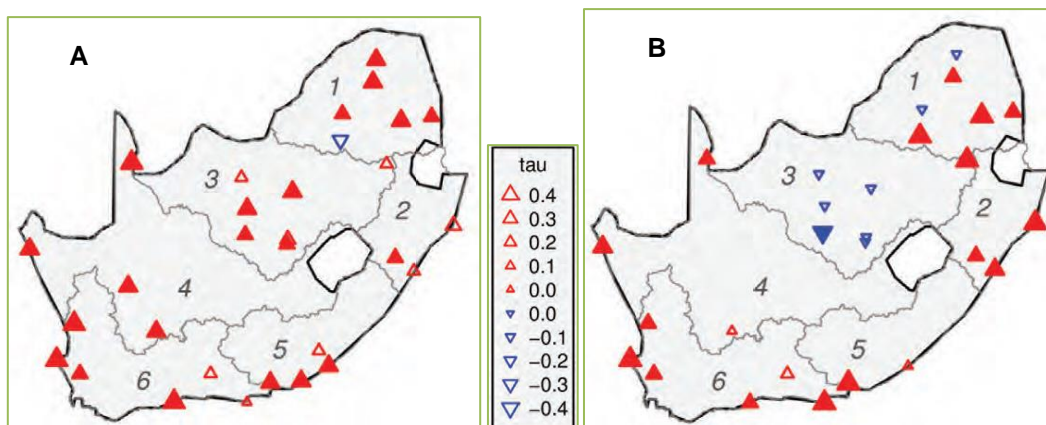


Figure 2.7 Trends in annual (a) mean daily maximum temperature (°C) and (b) mean daily minimum temperature (°C). The value of tau represents the direction and relative strength of the trend. Non-filled triangles indicate changes that are not statistically different (5% level). The larger the triangle, the larger the increase/decrease. The red triangles indicate an increase in mean daily temperature (max or min) (1960 to 2010) and the blue triangles indicate a decrease in mean daily temperature (max/min) (1960 to 2010) (MacKellar *et al.*, 2014).

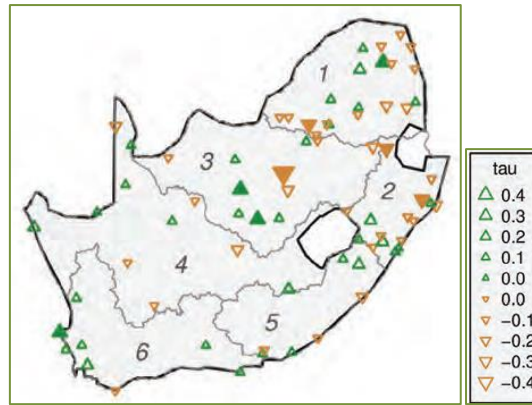


Figure 2.8 Trends in annual mean rainfall (mm). The value of tau represents the direction and relative strength of the trend. The green triangles indicate an increase in mean rainfall between 1960 and 2010. Non-filled triangles indicate an increase that is not statistically significantly (5% level). The larger the triangle, the larger the increase. Brown triangles indicate a decrease (MacKellar *et al.*, 2014).

The projected temperature increase of 4°C, under a “business as usual scenario” (where emissions remain high), is expected to occur over the northern and central interior regions of South Africa during the period 2080 to 2100 (Stevens *et al.*, 2015). It has also been predicted that winter and autumn will warm the most compared to summer and spring (Stevens *et al.*, 2015). As a result of the moderating effect of oceans, the coastal regions will experience the least amount of warming during the same period (Stevens *et al.*, 2015). More certainty is placed on future temperature predictions than on precipitation trends. Simulations predict that there will be a reduction of rainfall over Limpopo and south-western Cape with a moderate to strong increase over the central interior regions extending to the south-east coast. These increases in rainfall are projected to occur during summer and spring. This was also noted by a long-term study done by the Department of Environmental Affairs (2013a) that the south will become drier and the east wetter. Lower wind speeds and a decrease in evaporation have been observed which oppose the model projections for the western Cape regions (Stevens *et al.*, 2015).

Summing up, model confidence comes from their skill in representing observed past climate changes and current climates (IPCC, 2007). GCMs have demonstrated to be exceptionally important tools for simulating and understanding climate, with significant confidence that they will be able to provide credible computable estimates of future climate change. They continue to have certain restrictions but have proven to provide a clear-cut picture of significant climate warming in response to increasing greenhouse gases (IPCC, 2007).

2.3.3 Effects of Climate Change

A change in climate can result in negative or positive effects on plants, animals and humans. Below follows a brief discussion on the impacts of climate change mainly on plants (grasslands, agronomic crops) with some impacts on animals and humans. The economic effect of climate change is dependent on the aggregation rule (Tol, 2002). A 1°C global warming, using a simple sum, would cause a positive 2% growth in the gross domestic product (GDP), while using globally averaged values would cause a negative 3% GDP growth (Tol, 2002). No change in GDP can be calculated using the equity weighting method (Tol, 2002). Large-scale circulation changes such as the El Niño Southern Oscillation (ENSO), short-term natural extremes such as floods and storms and interannual and decadal climate deviations all have important effects on pasture, forest and crop production. ENSO-like conditions across Australia increase the likelihood of farm incomes decreasing below their long-term medians by 75%, with impacts on GDP ranging from 0.75 to 1.6% (Tubiello *et al.*, 2007). During 2003, Europe experienced an extremely risky climate event with temperatures up to 6°C above the long-term means and precipitation shortages up to 300 mm. In Italy, a record maize yield reduction of 36% occurred where extremely high temperatures prevailed (Ciais *et al.*, 2005).

In South Africa, it has been noticed that trees are taking over grassland areas where they have not occurred before, especially on rocky outcrops and near streams and that the boundaries are changing (although at a slow rate) (Stevens *et al.*, 2015). Shifts in changes in vegetation is not only due to changes in plant species composition but also due to a change in fire regimes, number of animals and animal species. It has, however, become clear over the last 15 years that an increase in CO₂ is a major contributor to vegetation changes (Stevens *et al.*, 2015).

Not only does CO₂ affect global warming but it also has a direct effect on plant growth. As the effects of CO₂ on vegetation requires more complex models, it is often ignored in the production models although it is the invisible driver of climate change. Excess CO₂ in the atmosphere is very beneficial to plants in a number of ways (Kimball *et al.*, 2002; Nowak *et al.*, 2004; Stevens *et al.*, 2015). Firstly, it enables the plant to take up CO₂ from the air easier. This means that when the CO₂ is taken in by the leaves, the stomata do not need to be opened wide and therefore less water vapour is lost through

the leaves. This means that secondly, for the same amount of rain, plants will grow more which is a benefit in drought prone regions (Olesen & Bindi, 2002; Tubiello *et al.*, 2002b; Reilly *et al.*, 2003; Morgan *et al.*, 2004; Aydinalp & Gresser, 2008; McKeon *et al.*, 2009; Stevens *et al.*, 2015). Lastly, CO₂ is used in the process of photosynthesis meaning that the more CO₂ is available, the more carbohydrates are produced, and thus an increase in plant production (Ainsworth & Long, 2005; Bond & Midgley, 2012). Figure 2.19 shows the effect of different CO₂ concentrations. One can see that a high CO₂ concentration (D) results in three times more biomass, making massive root systems with increased starch concentrations. These effects will promote rapid resprouting after fire and recovery from browsing. The increases in CO₂ are drastically transforming growing conditions of plants (Bond & Midgley, 2012).



Figure 2.9 Roots of the common *Acacia karoo* (sweet thorn) exposed to different levels of CO₂. A and B: pre-industrial conditions, C: high CO₂ of late 1990s, D: current CO₂ levels (Bond & Midgley, 2012).

Cohn *et al.* (2016) did a study on the effects of different temperatures and precipitation levels on soya beans in the state of Mato Grosso in Brazil. They found that if current trends hold true for the future, that an increase in average temperature of 1°C will cause an overall reduction in soy and maize production of between 9 and 13%. The study also showed that the decrease in production was largely (70%) due to a loss in both total crop area and that the remaining 30% was attributed to crop yield loss.

The potential effects of doubling CO₂ (from 350 to 700 ppm) levels were investigated at two Italian locations (Tubiello *et al.*, 2002a). Different climate scenarios and crops were used with the CropSyst soil-plant growth model. The model was modified to

include the effects of increased CO₂ on photosynthesis and transpiration. The results showed that if current management practices were not changed, the crop yields would decrease by 10 – 40%. Different adaptation strategies were investigated and it was found that a combination of early planting for spring-summer crops and the use of slower-maturing winter cereal cultivars triumphed in maintaining current crop yields. It was also noted that for irrigated crops, more water was needed to keep yields at current levels and that adaptations for climate change may be limited for crops under irrigation (Tubiello *et al.*, 2002a).

A study was done to assess the impacts of potential climate change on grassland and livestock production in the United States (US) using the Simulation of Production and Utilization of Rangelands model (SPUR) and the Colorado Beef Cattle Production Model (Baker *et al.*, 1993). The results indicated that an increase in above ground net primary production was caused by changes in precipitation and temperature trends together with an increase in CO₂. In the northern regions of the US, the animal production increased which implies an increase in economic survivability, while they decreased in the southern regions ensuing uncertainty in the economic survivability (Baker *et al.*, 1993).

The response of grasslands to climate change was also studied using a grassland ecosystem model (Hunt *et al.*, 1991). Simulations were run using observed climate data, with combinations of elevated CO₂, temperature and either increased or decreased precipitation. Increased temperature lengthened the growing season but weakened photosynthesis in summer, with little effect on annual primary production. A two-fold increase in CO₂ caused continual increases in primary production and led to greater storage of carbon in plant residues and soil organic matter. The increased carbon storage was not great enough to keep pace with the present rate of increase in CO₂.

The DEA (2013b) together with a few research institutions (CSIR, ARC, SAWS) did a study on the long-term effects of climate change on various aspects of agriculture. They found that although impacts on livestock have been studied to a lesser extent, the studies do indicate an increase in heat stress as a result of warmer temperatures and less rainfall. This discomfort has known effects on milk yield reductions in dairy cattle, influencing the conception rates across all breeds of livestock. Furthermore,

decreases in rangeland yields due to declines in rainfall would result in negative health impacts for livestock.

Most studies that have looked at the impact of climate change on agriculture have not addressed the problem of adaptation approaches (Reidsma *et al.*, 2010). When these strategies are deliberated, farm management and socio-economic conditions are often ignored, but they clearly influence current farm operations. Reidsma *et al.* (2010) conducted a study on the adaptation methods used by farmers between 1990 and 2003 in various regions of the European Union. Their results showed that impacts on crop yields couldn't directly be translated to impacts on farmers' income, as farmers adapt by implementing different crop rotation schedules and changing inputs. It was also found that there is a difference between the impacts of climate conditions on spatial variability on crop yields and farm income and the impacts of temporal variability in climate (Reidsma *et al.*, 2010). It was noted that actual impacts are largely dependent on farm characteristics (e.g. size, land use, intensity) which has a larger influence on farm management and adaptation. Correct farm management and modifications could reduce the potential impacts of climate change on farm income and crop yields. It was concluded that adaptation strategies should be part of the decision process when simulating crop yields and other indicators related to agricultural performances (Reidsma *et al.*, 2010).

Farmers in South Africa have reported that the following approaches have been used in order to deal with climate change (Benhin, 2006):

a) Adjustments in farming operations

- Shifts in the planting date of some crops have been made;
- Shorter growing season crops have rather been planted; and
- An increase in the use of crop rotations and early harvesting of some crops.

In areas where heavier rainfall, concentrated in shorter periods and starting earlier (previously early September and now late October), farmers have countered by:

- The increased use of modern machinery to take advantage of the shorter planting period;
- The collection of rain water by making furrows near the plants;

- Delaying the start of the plant season; and
- The increased use of irrigation.

In response to higher temperatures, farmers have resorted to using:

- Crop varieties with high water use efficiency;
- Heat tolerant crop varieties; and
- Early maturing crop varieties, and increased crop and livestock farming (mixed farming).

Livestock farmers have also implemented numerous practices aimed at efficient use of water and scarce fodder. There is a general inclination to resort to more heat tolerant breeds rather than the traditional ones, and most livestock farmers now also produce their own fodder, such as Lucerne or maize, and stock it for use during the long dry seasons. In reaction to the long drought periods, farmers have adapted the stocking intensity of their livestock by selling their animals at younger ages. Another practice is to change the timing, duration and location of grazing.

b) Increased chemical application

- With an increase in evapotranspiration due to higher temperatures, farmers have resorted to increased application of chemicals such as Erian to slow down evapotranspiration;
- They also apply more farm manure to keep the soil moister and retain the soil fertility; and
- More lime is also applied to maintain the soil's correct pH balance.

c) Increased use of irrigation

- Farmers shifted from flood irrigation to sprinkler irrigation for an efficient use of the limited water;
- Several farms have sunk their own boreholes to make effective use of underground water; and
- An increase in the use of wetlands for agricultural production.

d) Shade and shelter

- Coverings of shade nets, grass and plastics are used to protect plants against dryness and heat, cold and frost;

- In hot areas, farmers plant trees for natural shade for livestock or as a wind or hail storm break; and
- Heating provided by firewood and paraffin heaters is also used to protect animals against the cold.

e) Conservation practices

- Farmers have built many small dams or planted trees around their farms to predominantly fight erosion;
- Farmers have increased their fallow periods by as much as one to two growing seasons (instead of continuous cropping), to allow the land to restore its nutrients;
- To prevent nutrients to be excessively extracted from the soil, farmers reduced the density of crops or livestock on the land; and
- To preserve soil moisture, cool the soil surface and stabilise soil temperature, mulching (layers of peat, compost or plastics) is used to cover the land.

f) Other practices

- Most large-scale farmers have opted to taking lower risks by reducing their cropping areas to manageable sizes; and
- To reduce the risk of losing income when farm produce decreases as a result of the increased variability in the climate, some (especially large-scale farmers) have insured their farms, while others (especially small-scale farmers) are increasing their involvement in non-farm activities.

2.3.4 Representative Concentration Pathways

When trying to predict how future global warming will contribute to climate change, many factors have to be taken into account (Wayne, 2013). A key variable for this is the amount of future greenhouse gas emissions. Developments in technology, global and regional economic circumstances, changes in energy generation and land use, and population growth must also be considered. In order for research to be complementary and comparable between the different groups, a standard set of scenarios are used to ensure that starting conditions, historical data and projections are employed consistently across the various branches of climate science. The IPCC's

Third and Fourth Assessment Report (TAR & AR4) used the Special Report on Emissions Scenario (SRES) standards. In the Fifth Assessment Report (AR5) these SRES have been replaced with new scenarios called Representative Concentration Pathways (RCPs) (Wayne, 2013).

According to the IPCC Expert Meeting Report (Moss *et al.*, 2008):

“The name ‘representative concentration pathways’ was chosen to emphasize the rationale behind their use. RCPs are referred to as *pathways* in order to emphasize that their primary purpose is to provide time-dependent projections of atmospheric greenhouse gas (GHG) concentrations. In addition, the term *pathways* is meant to emphasize that it is not only a specific long-term concentration or radiative forcing outcome, such as a stabilization level, that is of interest, but also the trajectory that is taken over time to reach that outcome. They are *representative* in that they are one of several different scenarios that have similar radiative forcing and emissions characteristics”.

In order to understand RCPs, one must first understand scenarios and radiative forcing. In terms of climate change research, scenarios (Moss *et al.*, 2008):

“describe plausible trajectories of different aspects of the future that are constructed to investigate the potential consequences of anthropogenic climate change. Scenarios represent many of the major driving forces – including processes, impacts (physical, ecological, and socioeconomic), and potential responses that are important for informing climate change policy. They are used to hand off information from one area of research to another (e.g. from research on energy systems and greenhouse gas emissions to climate modelling). They are also used to explore the implications of climate change for decision making (e.g. exploring whether plans to develop water management infrastructure are robust to a range of uncertain future climate conditions). The goal of working with scenarios is not to predict the future but to better understand uncertainties and alternative futures, in order to consider how robust different decisions or options may be under a wide range of possible futures.”

In terms of climate change, radiative forcing is defined as (ACS, 2015):

“a change in Earth’s energy balance between incoming solar radiation energy and outgoing thermal infrared emission energy when the variable is changed while all other factors are held constant.”

There are four RCPs that were produced from the Integrated Assessment Model (IAM) and are available in published literature: one high pathway for which radiative forcing reaches $>8.5 \text{ W.m}^{-2}$ by 2100 and continues to rise for some amount of time; two intermediate “stabilisation pathways” in which radiative forcing is stabilised at approximately 6 W.m^{-2} and 4.5 W.m^{-2} after 2100; and one pathway where radiative forcing peaks at approximately 3 W.m^{-2} before 2100 and then declines (Van Vuuren *et al.*, 2011). These scenarios include time paths for emissions and concentrations of the full suite of GHGs and aerosols and chemically active gases, as well as land use/land cover (Moss *et al.*, 2008). Each RCP defines a specific emissions trajectory and subsequent radiative forcing. Table 2.2 summarises the characteristics of each RCP.

Figure 2.10 highlights the radiative forcing trajectories for the four RCPs and the modelling groups that were associated with each. It is noted that the forcing trajectories are consistent with socio-economic projections that are unique to each of the RCPs. The worst-case scenario, RCP 8.5, assumes more or less constant emissions while the best-case scenario, RCP 2.6, presumes that through radical policy interventions, greenhouse gas emissions are reduced almost without delay, leading to a slight decrease on today’s level by 2100 (Moss *et al.*, 2010; Wayne, 2013). As mentioned in Table 2.2, the various RCPs are characterized by a growth in population. The United Nations’ (2004) long-term population projections under the various RCP scenarios show that if these predictions become a reality that the population will have to develop new means to ensure food security for all (Figure 2.11a). Projections were also made for the 90th percentile range for the global GDP and according to Figure 2.11b the outlook looks beneficial for the growing population (Hanaoka *et al.*, 2006). With an ever-increasing population, one needs to look at food security and how there will be enough food resources for the people.

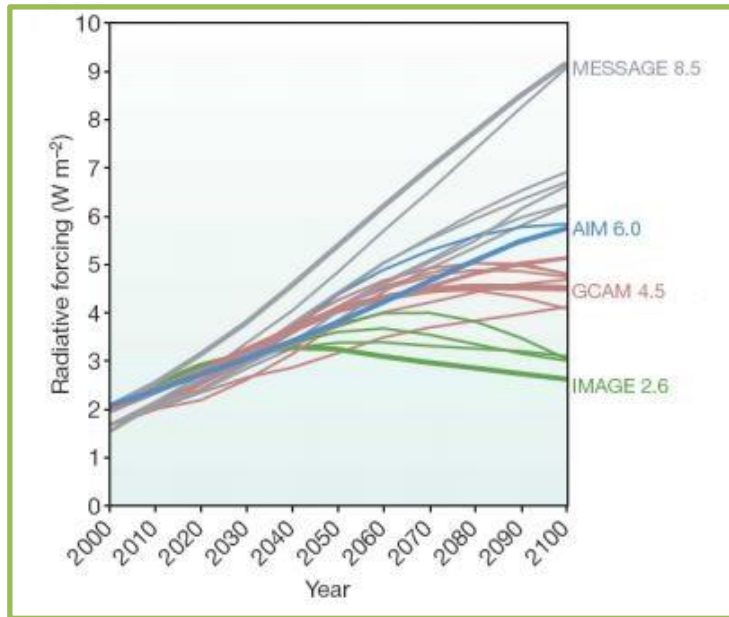


Figure 2.10 Changes in radiative forcing relative to pre-industrial conditions. Bold coloured lines show the four RCPs (Moss *et al.*, 2010).

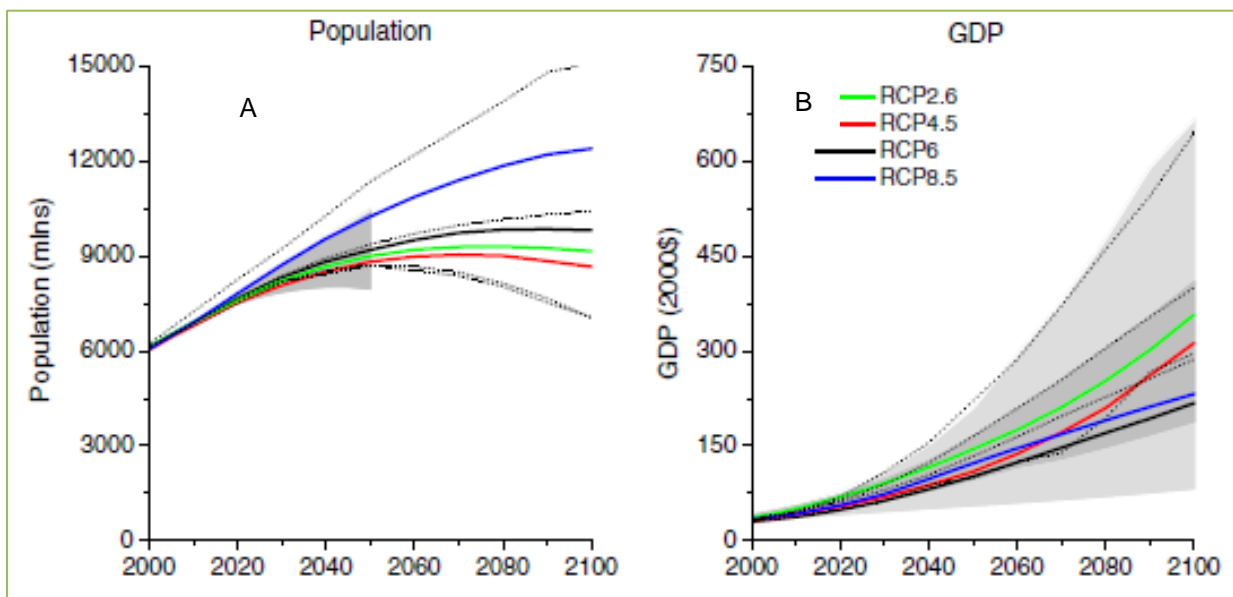


Figure 2.11 Global population and GDP projections of the four scenarios underlying the RCPs. Grey area for A indicates the range of the UN scenario (low and high) (UN, 2004). Grey area for B indicates the 98th and 90th percentiles (light/dark grey) of the IPCC AR4 database (Hanaoka *et al.*, 2006).

Land use influences the climate system in many different ways including hydrological impacts, direct emissions from land-use change, size of the remaining vegetation stock (influencing CO₂ removal from the atmosphere) and the biophysical impacts (such as changes in surface roughness and albedo) (Van Vuuren *et al.*, 2011).

Table 2.2 Summary of the characteristics of the different Representative Concentration Pathways (adapted from Moss *et al.*, 2010; Rogelj *et al.*, 2012; Bjørnæs, 2013)

^a **IMAGE – Integrated Model to Assess the Global Environment; GCAM – Global Change Assessment Model; AIM – Asian-Pacific Integrated Model; MESSAGE – Model for Energy Supply Strategy Alternatives and their General Environmental Impact**

Name	RCP 2.6	RCP 4.5	RCP 6.0	RCP 8.5
Radiative Forcing	3 W.m ⁻² before 2100 declining to 2.6 W.m ⁻² by 2100	4.5 W.m ⁻² in 2100	6.0 W.m ⁻² in 2100	8.5 W.m ⁻² in 2100
Model^a	IMAGE	GCAM	AIM	MESSAGE & IIASA Integrated Assessment Framework
Developed by	PBL Netherlands Environmental Assessment Agency	Pacific Northwest National Laboratory's Joint Global Change Research Institute (JGCRI), U.S.A	National Institute for Environmental Studies (NIES), Japan	International Institution for Applied Systems Analysis (IIASA), Austria
CO₂ Equiv. (ppm)	490	650	850	1370
Temp. anomaly (°C) by 2100	1.5	2.4	3.0	4.9
Pathway	Peak & decline	Stabilization without overshoot	Stabilization without overshoot	Rising
SRES Equiv.	None	SRES B1	SRES B2	SRES A1F1
Future consistent with	<ul style="list-style-type: none"> Methane emissions reduced by 40% A world population of 9bn by year 2100 	<ul style="list-style-type: none"> Stable methane emissions CO₂ emissions increase only slightly before 	<ul style="list-style-type: none"> Stable methane emissions CO₂ emissions peak in 2060 at 75% above today's levels, then 	<ul style="list-style-type: none"> Rapid increase in methane emissions A world population of 12bn by 2100

	<ul style="list-style-type: none"> • CO₂ emissions stay at today's level until 2020, then decline and become negative in 2100 • CO₂ concentrations peak around 2050, followed by a modest decline to around 400 ppm by 2100 • Declining use of oil • Use of croplands increase due to bio-energy production • Low energy intensity • More intensive animal husbandry 	<p>decline commences around 2040</p> <ul style="list-style-type: none"> • Strong reforestation programs • Decreasing use of croplands and grasslands due to yield increases and dietary changes • Lower energy intensity • Stringent climate policies • A world population of 9bn by 2065, declining to 8.7bn by 2100 	<p>decline to 25% above today's levels</p> <ul style="list-style-type: none"> • Heavy reliance on fossil fuels • Increasing use of croplands and declining use of grasslands • Intermediate energy intensity • A world population of 10bn by year 2100 	<ul style="list-style-type: none"> • 3x today's CO₂ emissions by 2100 • Heavy reliance on fossil fuels • Increased use of croplands and grassland which is driven by an increase in population • Lower rate of technology development • High energy intensity • No implementation of climate policies
Reference	Van Vuuren <i>et al.</i> , 2006; Van Vuuren <i>et al.</i> , 2007	Smith & Wigley, 2006; Clarke <i>et al.</i> , 2007; Wise <i>et al.</i> , 2009	Fujino <i>et al.</i> , 2006; Hijioka <i>et al.</i> , 2008	Riahi <i>et al.</i> , 2007

The RCPs encompass a wide-range of land-use scenario projections. This is clarified by the inclinations shown in Figure 2.12. Croplands increases under the RCP 2.6 as a result of bio-energy production. Grassland usage is invariable under RCP 2.6 as the swell in fabrication of animal products is met through a shift from extensive to more intensive animal husbandry. A clear turning point in global land use is seen for RCP 4.5, based on the assumption that carbon in natural vegetation will be valued as part of global climate policy. RCP 6.0 shows a decline in pasture use but an increase in the use of croplands. Finally, due to an expanding global population, the use of cropland and grasslands increases under RCP 8.5 (Van Vuuren *et al.*, 2011).

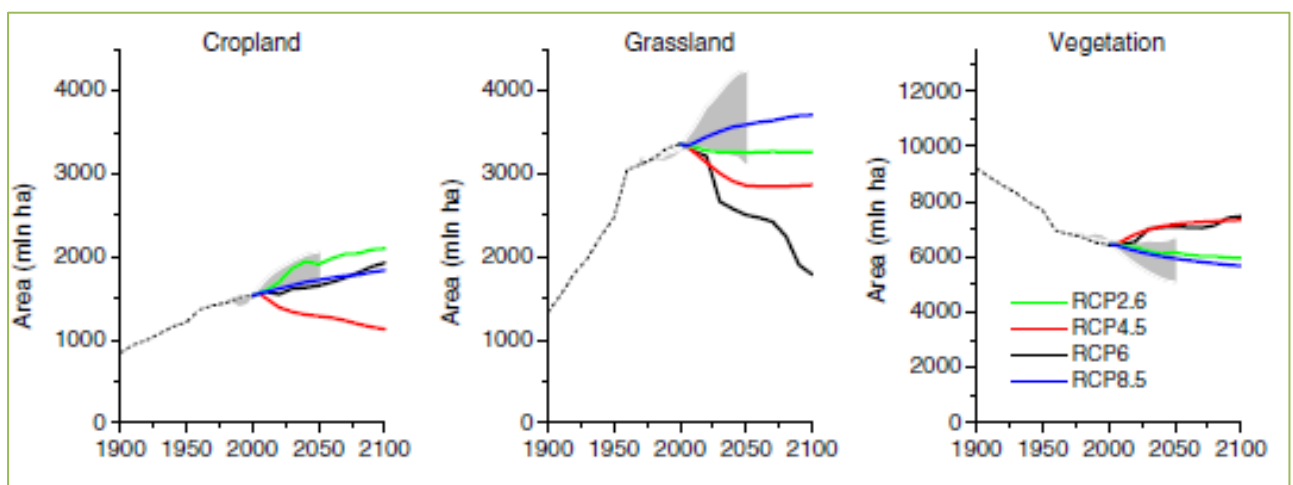


Figure 2.12 Land use (cropland and use of grassland) across the RCPs. Grey area indicates the 90th percentile of scenarios reported in literature. Vegetation is defined as the part not covered by cropland or anthropogenically used grassland (Van Vuuren *et al.*, 2011).

2.4 El Niño – Southern Oscillation

The interaction between the Earth’s atmosphere and oceans has a direct impact on the climate and weather conditions that are experienced. ENSO refers to the El Niño – Southern Oscillation (Stenseth *et al.*, 2003; IRI, 2016; NOAA, 2016a). El Niño (“boy child” in Spanish) events often begin to develop during the austral autumn months with large-scale warming of surface water and reaches a peak during November – January. It can last up to 18 months and occurs every two to seven years (WMO, 2014). La Niña (“little girl” in Spanish) events refer to the large-scale cooling of the ocean surface temperatures. During ENSO-neutral phases, climate drivers control the atmospheric patterns (Figure 2.13) (WMO, 2014).

El Niño (EN) and La Niña (LN) can have an overall effect on the global average sea surface temperatures (SSTs) found in the tropical Pacific Ocean by increasing or decreasing it, respectively (WMO, 2014). While the ocean can have an effect on the atmosphere above it, so too can the atmosphere have an effect on the ocean below it (IRI, 2016). The anomalously cooler or warmer ocean temperatures affects the weather patterns around the world by influencing low and high-pressure systems, precipitation, and winds (NOAA, 2016a).

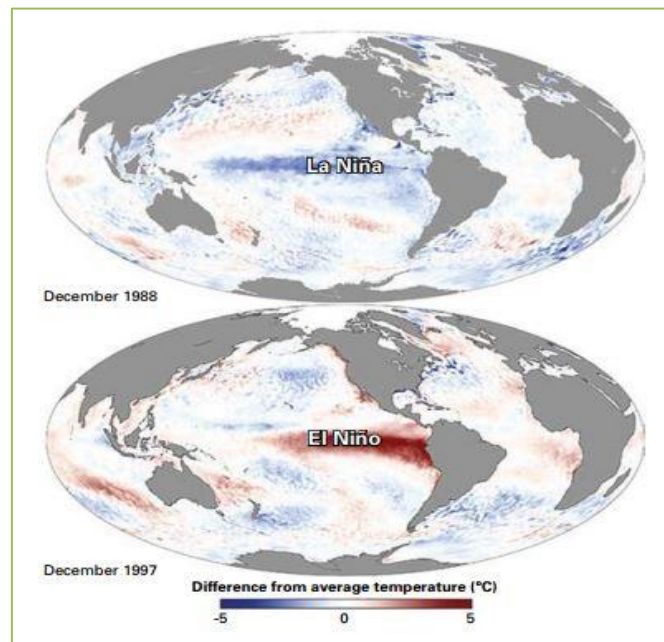


Figure 2.13 Maps of sea-surface temperature anomalies in the Pacific Ocean during a strong La Niña and El Niño (NOAA, 2016b).

LN is characterized by low pressure over southern Africa that produces anomalous mid-tropospheric ascent and increases in precipitation relative to the long-term average (Figure 2.14). EN is characterized by high pressure over southern Africa that produces anomalous mid-tropospheric descent and decreases in precipitation relative to the long-term average (Figure 2.15) (Hoell *et al.*, 2017).

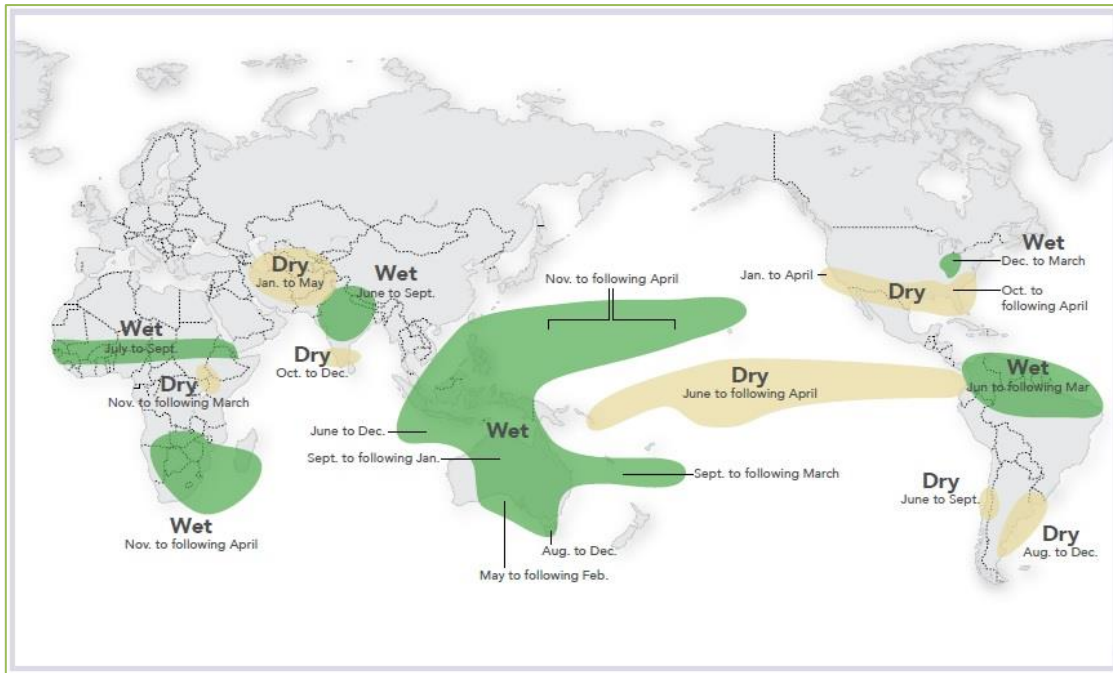


Figure 2.14 Global La Niña impacts (IRI, 2017).

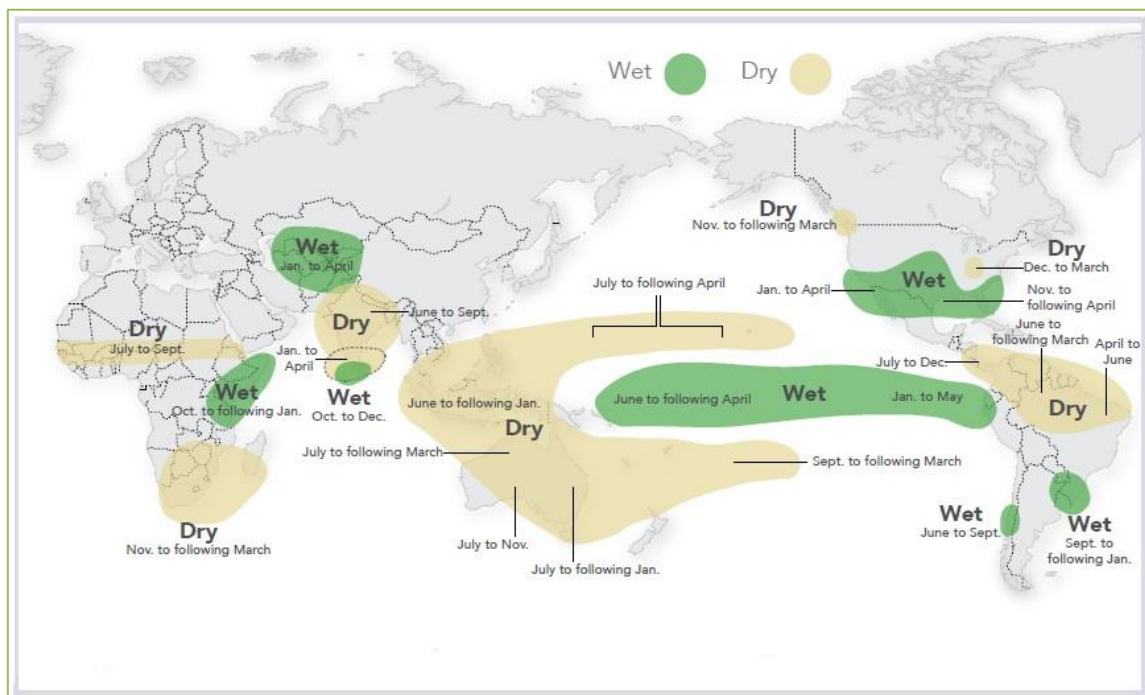


Figure 2.15 Global El Niño impacts (IRI, 2017).

ENSO can be monitored by considering the Oceanic Niño Index (ONI), whereby EN (LN) is defined by the five consecutive 3-month running mean of SST anomalies in the Niño 3.4 region (Figure 2.16) falling above (below) the threshold of + 0.8°C (- 0.8°C) in a certain region of the tropical Pacific (Stenseth *et al.*, 2003; NOAA, 2016b). The

Niño 3.4 region is the most common with a threshold of $\geq + 0.8^{\circ}\text{C}$ (Figure 2.17) (NOAA, 2016b).

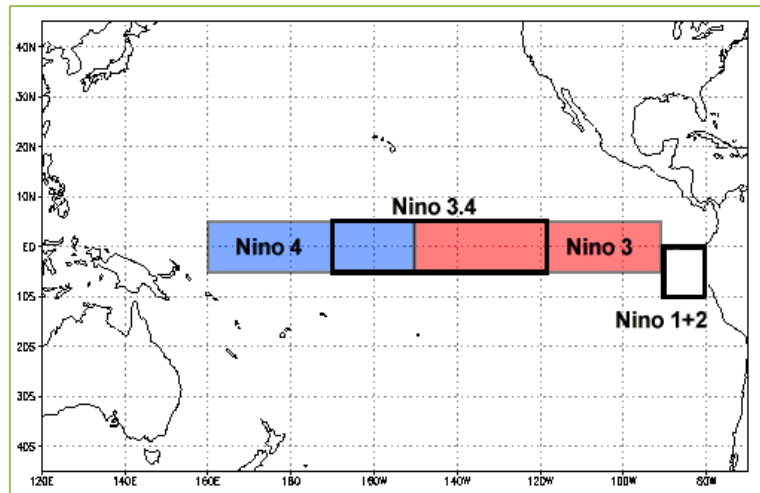


Figure 2.16 Niño index regions (NOAA, 2016b).

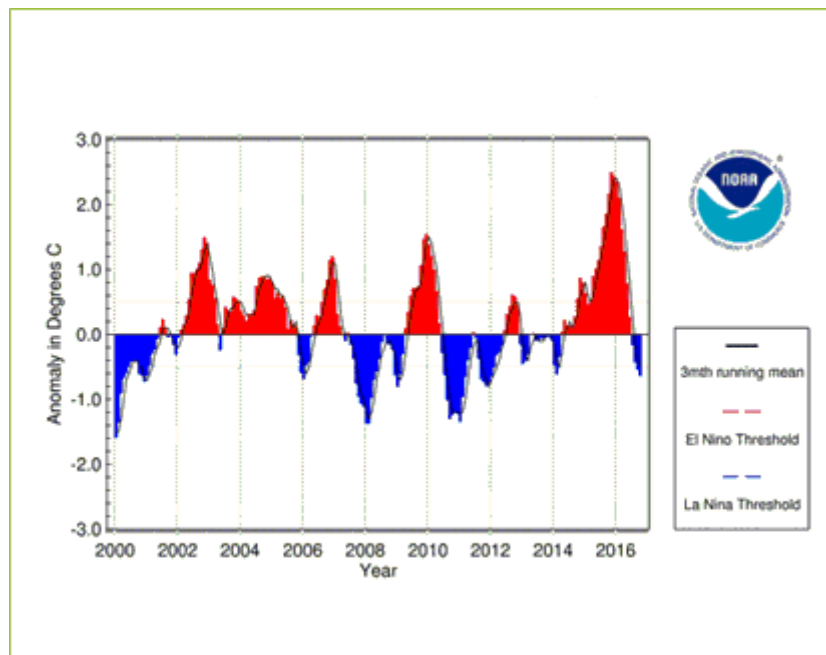


Figure 2.17 Historical record of sea surface temperature anomaly in the Niño 3.4 region (NOAA, 2016b).

CHAPTER 3 METHODOLOGY

3.1 Study Area

Since PUTU VELD was originally calibrated with data from the Bloemfontein area (Section 2.2.2), this study will focus on the same region. Bloemfontein is the judicial capital of South Africa and the provincial capital of the Free State (Figures 3.1).

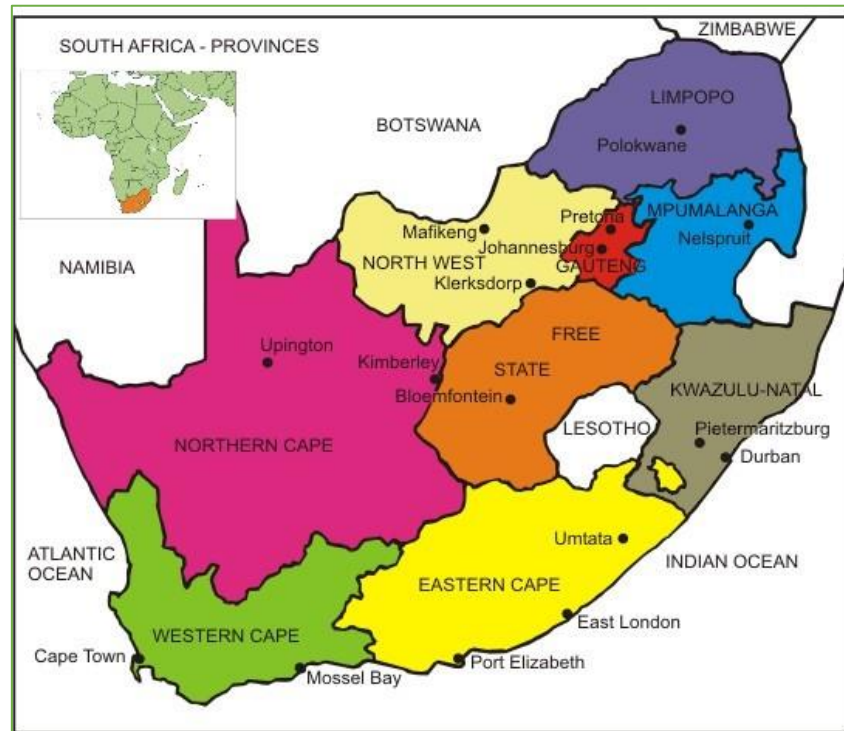


Figure 3.1 Map of South Africa highlighting the Free State Province in orange (Rana, 2016).
INSERT: Map of Africa highlighting the Republic of South Africa (WRM, 2016).

The Free State is a principle producer of winter and summer crops with a quarter of the country's arable land residing within its borders (Macaskill, 2013). A large part of the country's grains and oilseeds are cultivated in the province, namely: wheat (29% of SA's total); maize (39%); groundnuts (32%); grain sorghum (53%); dry beans (25%); sunflower (50%) and soy beans (23%). The eastern mountainous area is prominent for cherry and asparagus farming while the province is also a major producer of eggs (17%). The south is more classified as a karoo/semi-arid vegetation where livestock farming is largely done. Cattle (17%), sheep (20%) and game/wildlife are farmed in that area (Macaskill, 2013).

3.1.1 Botanical and Pedological Description

Land cover is dominated by grassland (Figure 3.2) (FAO, 2010). The terrain can be described as undulating to flat. Approximately 25% of the surface is covered by terrain unit 3 (slopes) and 55% by terrain unit 4 (plains). It is evident that 38% of the slopes are formed by rocks, while the most important soil forms that occur are Mispah, Milkwood, Swartland and Sterkspruit. About 70% of the plains are made up of Milkwood (with a clay content of more than 35%), Arcadia (35% clay content) and Valsrivier (55% clay content). It can be seen that the soil has relatively high clay content. Therefore, these soils are generally fertile and do not (according to depth) negatively affect the rangeland production (Fouché, 1992).

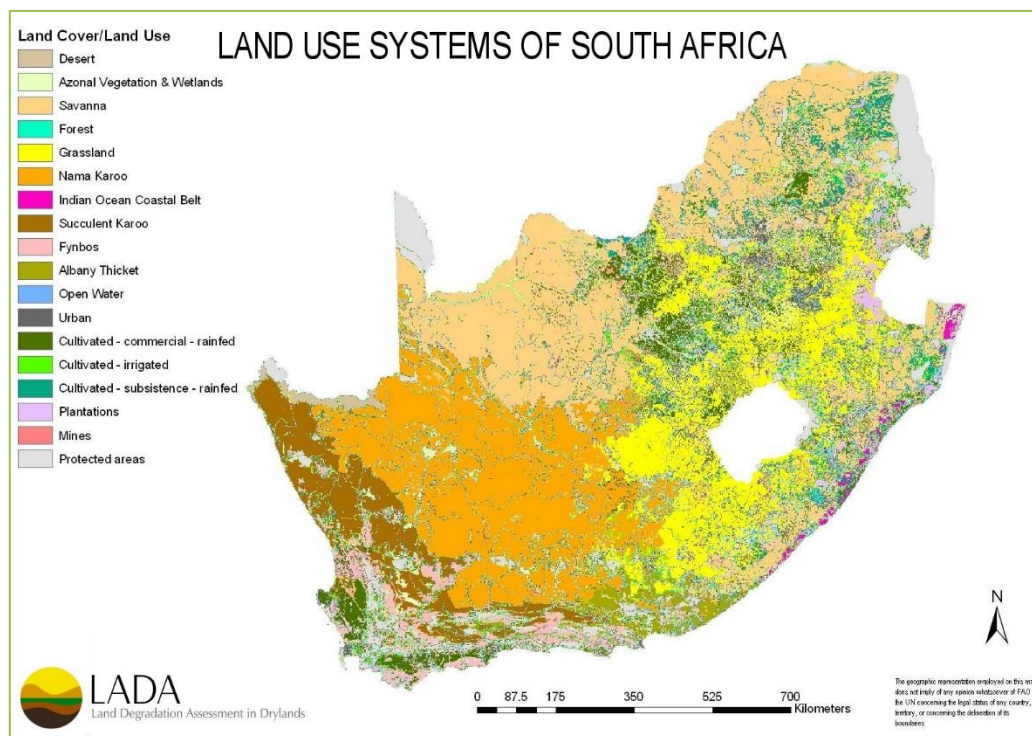


Figure 3.2 Map highlighting the major land use systems of South Africa (FAO, 2010).

The study area is deemed representative of the central grassland biome (Figure 3.3, dark green area). According to the classification by Acocks (1988), the area falls within the Dry *Themeda-Cymbopogon* veld type with *Themeda triandra* (red grass) the dominating species (Figure 3.4). If rangelands are in a good condition, almost 50% of the composition is *T. triandra* (Table 3.1). It was also the biggest component of the experimental plots at the Sydenham Experimental Farm of the University of the Free State and was thus considered to be climax plots (Fouché, 1992). It is a good indicator of a rangeland in a good condition but declines in large quantities when it is under-

utilised or overgrazed (a decrease species) (van der Westhuizen *et al.*, 2001; Wiegand *et al.*, 2004). The *Themeda-Cymbopogon* veld type is considered a sweet veld and provides palatable forage throughout the growing season (Palmer & Ainslie, 2006b).

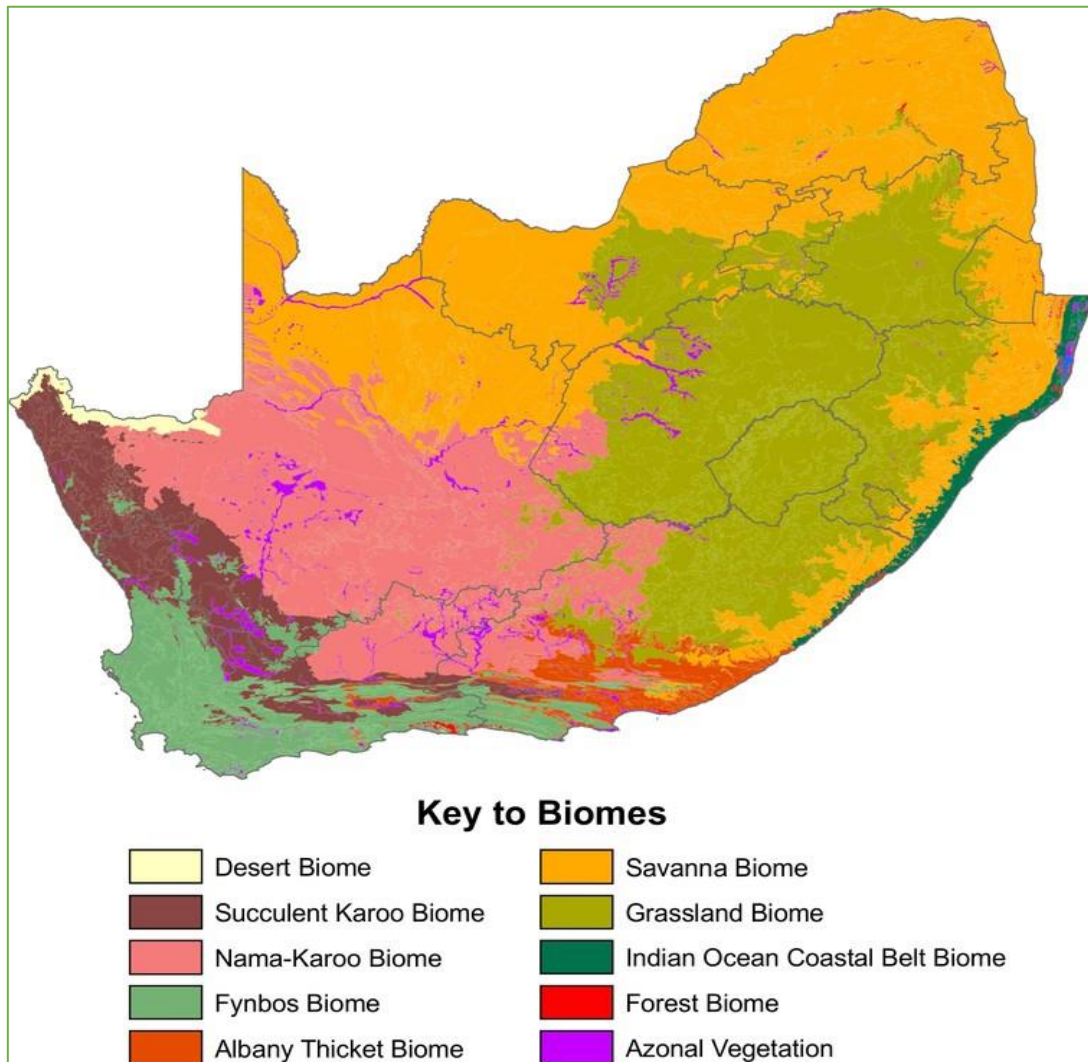


Figure 3.3 Biomes of South Africa (Mucina & Rutherford, 2006).



Figure 3.4 The seed heads of *Themeda triandra* (red grass) (Siyabonga Africa, 2016).

According to Mucina and Rutherford (2006) the area is classified as Gh (Figure 3.5) or Dry Highveld Grassland Bioregion. Although this area is endangered, it is hardly protected and conserved. A large portion (40%) of the area has been converted for crop production and urban development. The grasslands that grow on the shallow gravelly soils and also on the low-lying clayey soils are susceptible to karoo-bush encroachment when overgrazing occurs (Mucina & Rutherford, 2006).

Table 3.1 Botanical composition of the experimental plots at Sydenham Experimental Farm, Bloemfontein, when the rangeland is in a good condition (adapted from Fouché, 1992)

SPECIES	SYDENHAM (GOOD)
<i>Digitaria eriantha</i>	12.49
<i>Nenax microphylla</i>	0.31
<i>Panicum stapfianum</i>	0.29
<i>Sporobolus fimbriatus</i>	9.85
<i>Themeda triandra</i>	45.34
Total highly desirable	68.28
<i>Cymbopogon pospischilii</i>	3.08
<i>Digitaria argyrograpta</i>	1.96
<i>Eragrostis chloromelas</i>	13.70
<i>Eragrostis lehmanniana</i>	6.22
<i>Helichrysum dregeanum</i>	2.62
Total desirable	27.58
<i>Triraphis andropogonoides</i>	3.07
Total less desirable	3.07
<i>Tragus koelerioides</i>	1.07
Total undesirable	1.07
Rangeland condition (%)	97.67
Rangeland condition score	889.00

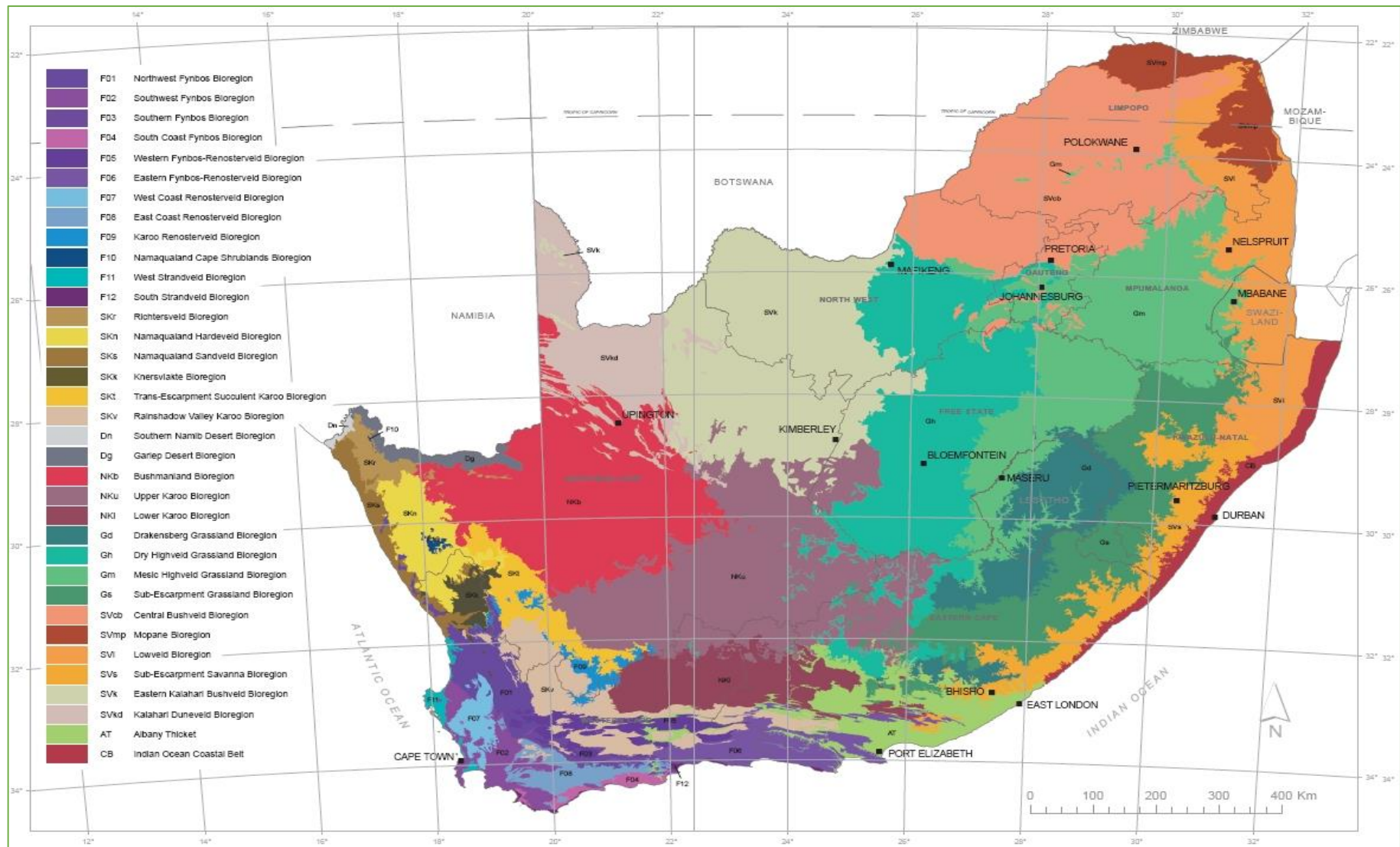


Figure 3.5 Vegetation map of South Africa (Mucina & Rutherford, 2006).

3.1.2 Climatological Description

The area lies in the summer rainfall region with an annual average rainfall of 569.7 mm for the period July 1980 to June 2010. From the climate data presented in Table 3.2, it is evident that almost 87% of the total rainfall occurred during the active growing season, October to April. The summer months of January, February and March are the wettest with the majority of the annual rainfall occurring during those months. June, July and August are the drier months with the least rainfall occurring during these winter months. The annual averages for climate data were calculated for the growing season, July to June (Fouché, 1992).

In contrast to the average annual rainfall, the average annual temperature is of relative less agricultural worth (Fouché, 1992). Extreme temperatures play a greater role as it has an inhibiting influence on the rangeland production. With regards to the maximum temperatures, December, January and February are considered the hottest months (Table 3.2). It has a larger inhibiting influence on the rangeland production during these months when below normal rainfall occurs. Minimum temperatures in the spring have a great effect on the commencement of the growing period and the growth rate. Winters are cold with sub-zero average minimum temperatures in June and July (Table 3.2).

The total amount of sunshine hours is not a limiting factor for optimal plant growth in the Central Grassland region. There was a difference of 65 hours between the months with the highest and lowest total sunshine hours (Table 3.2). The longest day occurs during December, while the shortest day occurs during June. It has been proposed that the large standard deviation during the summer months can be due to the higher amount of rainfall days (Fouché, 1992).

The prevailing wind direction is northwest to northeast (Figure 3.6) with a maximum speed during the afternoons (Snyman, 1982). These winds are prominent in spring and early summer, which is also the windiest time of the year (especially October), while autumn is the calmest season. A diurnal cycle is observed with the wind blowing from the north east during the morning and veering through northwest to become west or south-

Table 3.2 Climate data for Bloemfontein International Airport for the period 1980/81 – 2009/2010 (SAWS, 2013)

	July	August	September	October	November	December	January	February	March	April	May	June	Year
Ave. Rainfall (mm)	5.9	16.7	23.0	51.1	70.0	64.1	89.0	101.7	75.5	43.9	17.9	10.9	569.7
Ave. number of rain days	1	3	4	8	9	9	11	11	10	7	4	3	80
Highest Rainfall (mm) (Year)	37.2 (1983)	53.5 (1981)	45.7 (1987)	92.0 (1993)	69.5 (2006)	97.2 (2006)	101.5 (1994)	142.2 (1988)	72.0 (2003)	44.6 (1988)	32.2 (1984)	20.0 (1991)	186.8 (1988)
Ave. Max. Temp. (°C)	17.8	20.5	24.3	26.5	28.1	30.3	30.8	29.5	27.5	24.1	20.8	17.6	24.8
Ave. Min. Temp. (°C)	-2.2	0.7	5.1	9.4	11.6	13.6	15.2	14.7	12.1	7.5	2.3	-1.5	7.4
Ave. Temp. (°C)	7.8	10.6	14.6	18.0	19.9	22.0	23.0	22.2	19.8	15.8	11.6	8.1	16.1
Total sunshine hours	272.7	284.7	275.2	283.1	289.3	312.2	291.9	248.1	259.8	250.7	262.6	247.1	3277.4
Ave. Sunshine hours	8.8	9.2	9.2	9.1	9.7	10.1	9.4	8.8	8.4	8.4	8.5	8.2	9.0

west in the late afternoon. Although strong winds occur periodically, approximately 90% of the winds had a speed of less than 24 km.h⁻¹ (Van den Berg, 1972). However, winds do not have a limiting effect on the productivity of the rangeland (Fouché, 1992).

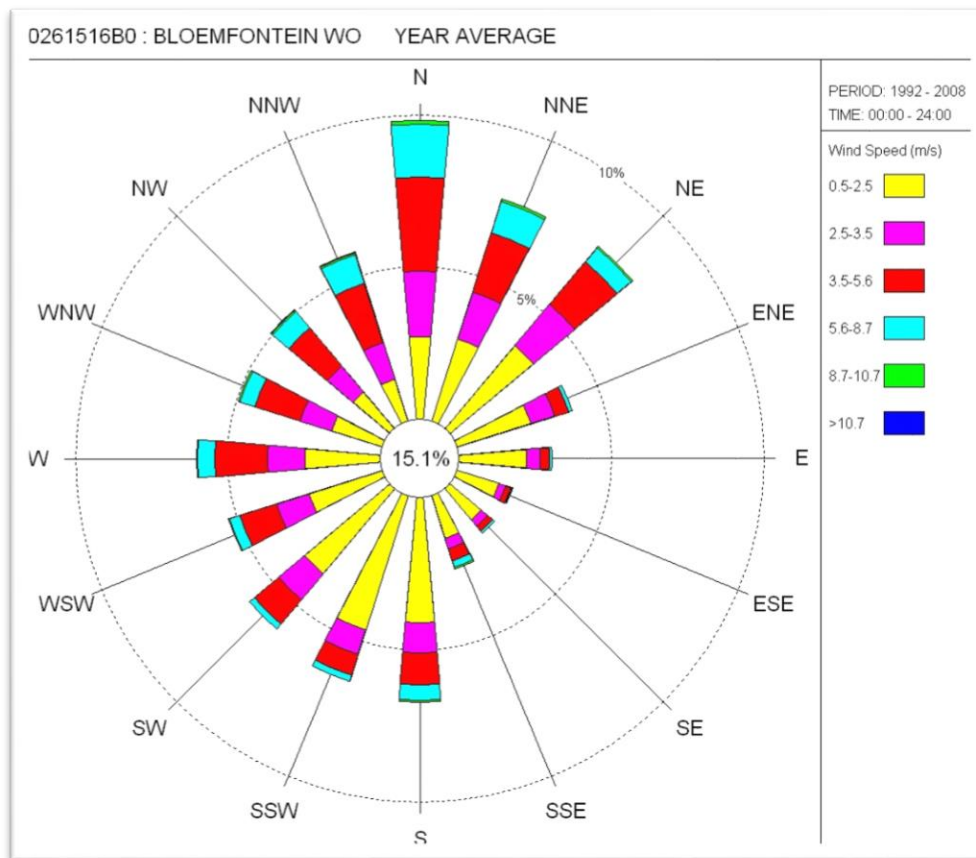


Figure 3.6 Annual wind rose for Bloemfontein Airport (SAWS, 2013).

3.2 Data Sources

3.2.1 Rangeland Production Data

The historically observed rangeland production data that was used for the validation of the PUTU VELD model was obtained from the Sydenham Experimental Farm for the period 1980/81 – 2009/10 (Snyman, 2013¹) (henceforth referred to as Sydenham). Sydenham is located at 26°12' E and 29°13' S, approximately 12 km south of Bloemfontein at an altitude of about 1 420 m above mean sea level (Figure 3.7). The measured data was collected during a water run-off trial held on the farm. The grass was cut at a 60 mm level once a year during April just before the first frost was experienced (Snyman, 2013¹). As the trial was conducted on three different rangeland

¹ Prof H.A. Snyman, personal communication, Professor at Department for Animal-, Wildlife- and Grassland Sciences, University of the Free State, September 2013.

conditions, it was suggested that the data from the good rangeland conditions be used for this study (Fouché, 2013²). Data from this trial was originally used to calibrate PUTU VELD (Section 2.2.2)

3.2.2 Historically Observed Climate Data

Although long term rainfall (30 years) was also obtained from the Sydenham Experimental Farm, most of the historical climate data was sourced from nearby weather stations. The historical climate data (1980/81 – 2009/10) for Bloemfontein International Airport was obtained from the South African Weather Service (SAWS), located at 29°6'10.8" S, 26°17'52.8" E, 1371 m, ± 15 km NE of Sydenham (Figure 3.7). This data set consisted of daily rainfall (mm), minimum and maximum temperatures (°C), and sunshine hours (h). The reference evaporation ETo (mm), was calculated at a daily timescale using the Hargreaves-Samani method (Hargreaves & Samani, 1985; Samani, 2000; Moeletsi *et al.*, 2013). The daily average temperature (°C) was also calculated. The soil moisture data (i.e. soil water content) was calculated within the PUTU VELD model from the climate data provided (refer to Section 3.3.1.3). There were gaps in the data which were patched with data from a SAWS station in the city (29°6'46.8" S, 26°12'21.6" E, 1419 m) and from the weather station located on the campus of the University of the Free State (UFS) (29°6'20.88" S, 26°11'6" E, 1417 m). The sunshine hours data was estimated using a *Microsoft Excel* "WTON" program (Snyder, 2012). Remaining gaps in the temperature were patched using information about the urban heat island for the area, comparable to a standard linear regression approach (not shown) (Snyman & Steyn, 2011).

3.2.3 Future Simulated Climate Data

The Global Climate Model (GCM) data for the historical (1980/81 – 2009/10) and future simulations (2010/11 – 2098/99) was obtained from the Climate System Analysis Group (CSAG) of the University of Cape Town, South Africa (AgMIP, 2013). The data that was obtained was generated by the team working on the Agricultural Model Intercomparison and Improvement Project (AgMIP). The AgMIP project aims to link the climate, crop, and economic modelling communities with groundbreaking information technology to produce improved crop and economic models and the next

² Dr. H.J. Fouché, personal communication, Agricultural Research Council, Animal Production, Bloemfontein, September 2013.

generation of climate impact projections for the agricultural sector (Hillel & Rosenzweig, 2013). Two RCPs was chosen for the study, namely RCP 4.5 (intermediate scenario) and RCP 8.5 (worst case scenario) as described in Section 2.3. The emission projectories were chosen because the RCP 4.5 (an intermediate stabilization pathway) represents an emission projectory accounting for certain mitigation strategies, while RCP 8.5 (a high emission scenario) will highlight the possible adaptations required. Five GCMs were chosen for the study as highlighted in Table 3.3.

Daily rainfall (mm) and minimum and maximum temperatures ($^{\circ}\text{C}$) was acquired from AgMIP for the nearest grid point located at $26^{\circ}7'44.4''$ E and $29^{\circ}12'21.6''$ S (altitude of 1371 m) (AgMIP, 2013), which is about 7 km WNW of Sydenham (Figure 3.7). The sunshine hours were estimated by converting the solar radiation data from AgMIP ($\text{MJ}\cdot\text{m}^{-2}\cdot\text{d}^{-1}$) to hours using the *Microsoft Excel* “WTON” program (Snyder, 2012). As with the historical data, the reference evaporation (mm) was calculated using the Hargreaves-Samani method (Section 3.2.2) and the average temperature ($^{\circ}\text{C}$) was also calculated. In order to compare the results, the GCM data was divided into four periods: a base period of 30 years (for validation; 1980/81 – 2009/10); and three future periods: 2010/11 – 2039/40; 2040/41 – 2069/70; 2070/71 – 2098/99, of 30, 30 and 29 years, respectively.

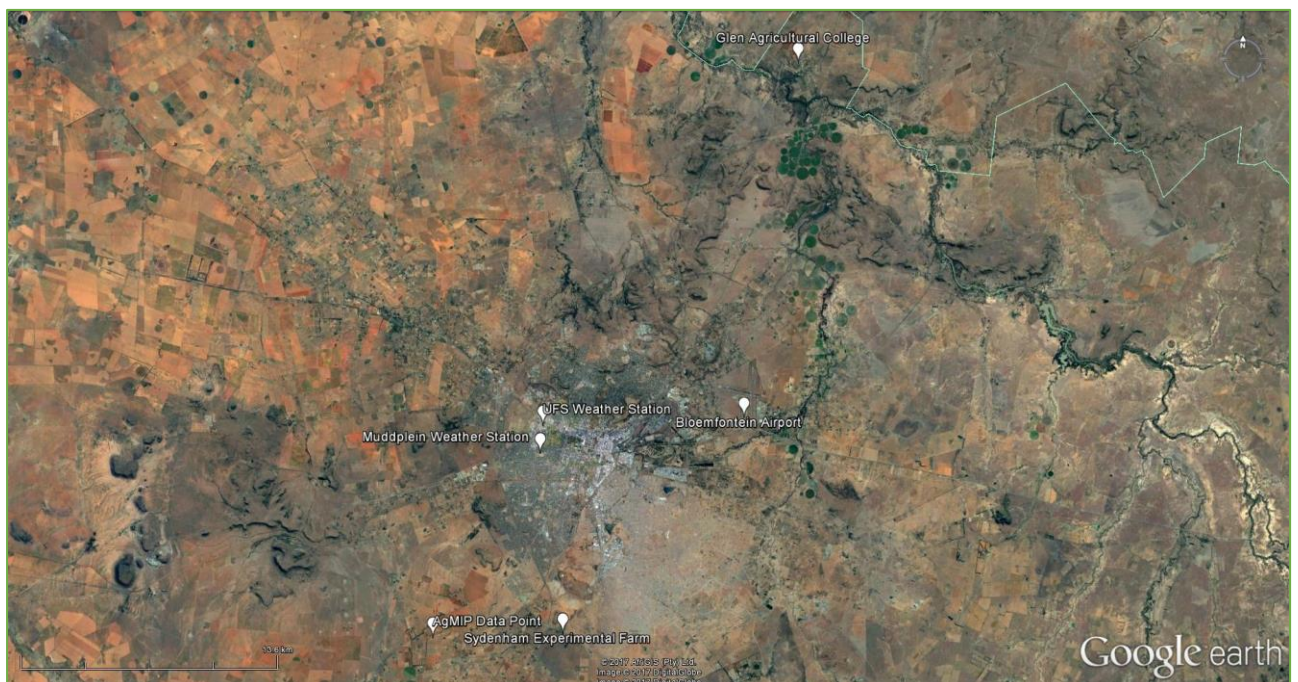


Figure 3.7 Google Earth image showing location of the data points in and around Bloemfontein (Google Earth, 2017).

Table 3.3 Information about the global climate models used

GLOBAL CLIMATE MODEL	FULL NAME	DEVELOPER(S)	DESCRIPTION	RESOLUTION (Lat° x Long°)
CCSM4	Community Climate System Model 4.0	University Corporation for Atmospheric Research (UCAR) & National Center for Atmospheric Research (NCAR), USA.	(Shields <i>et al.</i> , 2011; PCIC, 2014; CESM, 2016)	1.2 x 0.9 ~ (130 km x 100 km)
GFDL-ESM2M	Geophysical Fluid Dynamics Laboratory – Earth System Model 2M	National Oceanic and Atmospheric Administration, USA.	(Dunne <i>et al.</i> , 2013; GFDL, 2016)	2.5 x 2.0 ~ (275 km x 220 km)
HadGEM2-ES	Hadley Centre Global Environmental Model 2 – Earth System	Met Office Hadley Centre, UK.	(Collins <i>et al.</i> , 2008; Jones <i>et al.</i> , 2011; Martin <i>et al.</i> , 2011)	1.9 x 1.2 ~ (210 km x 130 km)
MIROC5	Model for Interdisciplinary Research on Climate 5.0	Centre for Climate System Research (CCSR), University of Tokyo, National Institute for Environmental Studies (NIES) & Japan Agency for Marine – Earth Science and Technology (JAMSTEC), Japan.	(Watanabe <i>et al.</i> , 2010)	1.4 x 1.4 ~ (155 km x 155 km)
MPI-ESM-MR	Max-Planck Institute – Earth System Model – MR	Max Planck Institute for Meteorology, Germany.	(Giorgetta <i>et al.</i> , 2013; MPI, 2016)	1.9 x 1.9 ~ (210 km x 210 km)

3.3 PUTU VELD Model

The PUTU VELD model, like the other PUTU models (Section 2.2.2), is a dynamic, deterministic model and is also physically and biologically orientated. The PUTU VELD model is an improved version of the PUTU 2 model (De Jager, Opperman & Booyesen,

1980; cited by Fouché, 1992). It simulates the growth and development of climax grasses. The meteorological simulation was kept but the single layered soil profile adjusted to a two-layered version. Furthermore, where the PUTU 2 worked for a single plant basis, PUTU VELD calculated the production per unit area as well as taking into account the basal cover (Fouché, 1992).

The model simulates on a daily basis beginning on 1 July (with $j = 1$) and ending on 30 June (with $j = 365$). The model also takes into account the leap years. For the radiant flux density, the day of the growing season is expressed in Julian days (JDA) (Booyesen, 1983). The weather input variables are the daily total rainfall (mm), minimum and maximum temperatures ($^{\circ}\text{C}$), reference evapotranspiration (mm) and sunshine duration (h). Appendix A contains the code for the model with Appendix B explaining each of the variables used therein. Appendix C offers a simplified explanation of the various sections of the code. An example of the format for the input files for the soil and plant variables can be found in Appendix D and for the climate data in Appendix E.

The outputs of the PUTU VELD model are (Fouché, 1992): the dry matter production ($\text{kg}\cdot\text{ha}^{-1}$) reached on a certain date; the maximum dry matter production (DMPmax) ($\text{kg}\cdot\text{ha}^{-1}$) and the date that it occurs (Dtp); the number of moisture stress days (MSD); the reserves ($\text{kg}\cdot\text{ha}^{-1}$) on 1 July; and the residual production on 1 July (from which LSU can be calculated).

3.3.1 The Operations of the PUTU VELD Model

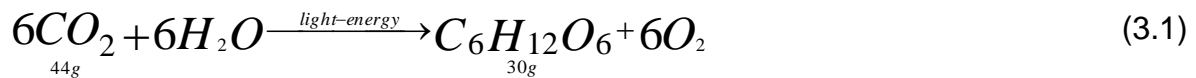
PUTU VELD (or PUTU 11 as it was originally called) was described in detail by Booyesen (1983) and to a lesser extent by Fouché (1992). However, since both of these documents are only available in Afrikaans it was deemed necessary to translate the most important sections pertaining to the model's operation into English. This will facilitate future referencing with due acknowledgement to Booyesen (1983). As far as possible, parameter names were kept similar to the model code presented in Appendix A.

Before embarking on a lengthy description of PUTU VELD, it should be noted that the connection between yield, basal cover and rangeland condition has not yet been identified in a way that can be mathematically formulated. For the objectives of this

study, the function BCFUNC conveys the relationship between yield, basal cover and rangeland condition simulated. It was originally envisaged that it be substituted with a more suitable relationship later when it becomes available. In light of the preceding, it was decided to start simulations with a theoretical hypothetical basal cover of 100%. At the end of an iteration interval, all output data will be translated to the applicable basal cover using BCFUNC. BCFUNC can accommodate basal covers of between 8 – 12% which occur commonly in the central Free State.

3.3.1.1 Plant Physiological Parameters and their initial values

A grass leaf has the ability to absorb about $2 \text{ mg}\cdot\text{m}^{-2}\cdot\text{s}^{-1}$ CO_2 under conditions where solar radiation $> 300 \text{ W}\cdot\text{m}^{-2}$ at the specified diffusion resistance of the stomata. The photochemical equivalent (FE) can be defined as the mass of CO_2 that is absorbed during photosynthesis per unit light energy that is captured during the process. It is found that 440 kJ of energy is captured during the assimilation of one molecule of CO_2 and that this process requires 2200 kJ of light energy. The chemical reaction for carbon assimilation is:



Carbon dioxide (with a molar mass of 44 g) plus water gives you carbohydrate (with a molar mass of 30 g) plus oxygen. The process is helped along with a catalyst of light energy of 2200 kJ. The relationship between the molar masses of carbohydrates and CO_2 is thus:

$$\frac{30}{44} = 0.68$$

Therefore, CO_2 to carbohydrate conversion factor (COM) is equal to 0.68 in PUTU VELD. Following the definition, the photochemical equivalent is then:

$$FE = \frac{44g}{440kJ} = 100\mu\text{g}\cdot\text{J}^{-1} \quad (3.2)$$

The conversion efficiency of light in this reaction is thus $440 \text{ kJ} / 2200 \text{ kJ}$, or 20%. If it has been observed that solar radiation is composed of about 50% photosynthetic active radiation (PAR), then it is clear that maximum conversion efficiency of solar energy during the photosynthesis process, EFFMAX, is about 10%. In PUTU VELD the value of EFFMAX is equal to 12%.

Photorespiration usually occurs in C₃-plants and the process can be divided into two parts, namely construction respiration and maintenance respiration. The maintenance respiration constant (C30) indicates the fraction of total plant biomass (CLIVE) which respire during the night at a temperature of 30°C. This fraction is, however, very temperature sensitive especially in C₃-plants. The necessary temperature relationship has been included in the program.

$$MAIN = (C30 \times (0.44 + 0.0019 \times TNITE + 0.001 \times TNITE^2)) \times CLIVE \quad (3.3)$$

where: MAIN = Carbohydrate loss due to night respiration (kg CHO.ha⁻¹.d⁻¹)

TNITE = average night time temperature (°C).

CONS is the construction respiration constant and implies that 50% of the dry matter gain is used for construction respiration. This whole process is thoroughly discussed by Kaiser (1976).

The normal heat needed by the plant (HUCRIT) in terms of heat units (degree days) has been calculated to be 250 degree days. The critical minimum (HUCRMN) (the lowest it can be decreased to as a result of water stress during the vegetative growth stage) has been calculated to be 225 degree days. This was found after numerous simulations and correlations were done with observed episodes during 1980/81 season at Glen (Booyesen, 1983). The minimum temperature for heat unit accumulation (BO) is assumed to be 12°C.

The heat units (degree days) needed during the vegetative growth stage are accumulated after the live component of the leaves have reached a stipulated minimum mass (BLT) of 2900 kg.ha⁻¹. As mentioned previously, this value is relative to a hypothetical 100% basal cover. This value was determined from numerous simulations of the vegetative growth stage where comparisons were done between the tendency of the growth curve simulated and the observed response in the rangeland at Glen (1980/81). Furthermore, leaf mass (BLM) is used as a criterion for the shift from the vegetative to the reproductive growth stage. When BLM has reached a mass of 4600 kg.ha⁻¹ (100% basal cover), the trigger mechanism starts working.

The value for the specific leaf area index (SPL) is taken as 500 kg.ha⁻¹. The maximum temperature of the previous day (TMXPD) is only needed at the beginning of the

season. The maximum temperature of the last day of the previous season is naturally not available and thus has to be estimated.

3.3.1.2 Inputs and Initial Values

The inputs to the model can be divided into two groups. The first group includes information about the initial values for soil water, retention characteristics of the specified soil, effective root depth, dry matter production, yield from the previous season and information about the cutting dates. The second group includes the climate data. All inputs are read in by the program from the data file. One of the advantages of the preceding is that the model doesn't have to be changed when moving from one soil type to another or from one climate region to another.

Certain physiological constants should not vary from one season to the next but there is to a certain degree a variation from one climax grass to the next. For this reason, the constants are directly coded into the main program. The length of the growing season ($JMAX = 365$) is for a full growth year namely beginning on 1 July (this is different from most agronomical crops) with the iteration interval equal to 1 day. The initial growth stage ($GRSTGE = 1$) is the vegetative growth stage or growth stage 1.

3.3.1.2.1 Meteorological Observations

The climate data for the whole season is read in all at once. This data is compiled from standard observations at weather stations which are collected on a daily basis. The data from SAWS (historically observed) and AgMIP (simulated future) were used (Sections 3.2.2 and 3.2.3). Only five basic elements are used, namely daily maximum and minimum temperature, total daily rainfall, sunshine duration and evaporation. Of these named elements, rainfall is most essential (Section 2.1.1.3), while less accurate results can be obtained for the other elements by estimations or simulated values.

3.3.1.2.2 Initial Values of the Different Plant Parts

The basal cover (BCOVER) is calculated using the wheel-point method (Mentis, 1981) and was averaged at 10% for the area under study. The standing phytomass at the end of the previous season's yield (PRVISC) is the mass per hectare up to a cutting height of 60 mm above ground. Furthermore, there was provision made for four arbitrary cutting dates during the season and all cutting dates (CUT) are indicated as the j-th day of the season.

The assumption is made that the yield carried over from the previous year (PRVISC) contributes to 25% of the total biomass from the previous year. The total biomass (C) is then calculated at the beginning of the relevant simulation as (line 371 in Appendix A):

$$C = PRVISC \times \frac{100}{25} \times \frac{100}{BCOVER} \quad (3.4)$$

The initial masses for the different plant parts are thus calculated as a percentage of the total biomass as indicated in Table 3.4 (lines 373 – 382 in Appendix A).

Table 3.4 The percentage distribution of total biomass (C) of the different plant parts at the beginning of the simulation (adopted from Booyesen, 1983)

Plant Part	Symbol	Percentage
Dead leaves	BD	3
Live leaves	BL	0
Dead culm	CD	2
Live culm	CL	0
Dead stubble	SD	30
Live stubble	SL	0
Dead roots	RD	1
Live roots	RL	64
Dead seed	GD	0
Live seed	GL	0
	Total	100

The following assumptions are made for plant reserves (RES). At the beginning of the season, the reserves have settled in the roots, culm and stubble. During the season, these reserves are utilized and when new reserves are made, they are stored in the living plant parts. As the living components die, these reserves are relocated to the plant parts that act as storage organs to be utilized during the next season. The amount of usable plant reserves is a function of the previous year's maximum production at the beginning of the season.

3.3.1.3 The Soil Water Balance

The water balance subroutine is discussed first as the available soil water is one of the environmental inhibiting factors for photosynthesis. The start of water stress is investigated in this subroutine. The soil profile was initially a single layered profile but as a result of a delay in the start growth which had repercussions, the profile is now divided into two layers. The first layer is 100 mm deep and only in this layer is the water level tested at the beginning of the year to see if it has an adequate supply of water to initiate plant growth. As soon as the initial growth starts and the first layer is depleted, then only does the plant use the soil water from the second layer. The first layer is always replenished first and only when it is saturated does the second layer get replenished through percolation. When the second layer is saturated, deep percolation will occur out of the profile and the profile as a whole will be at field water capacity. The profile information is supplied by the user as with the single layer profile and the program will further divide the soil so that the first layer is 100 mm deep. These calculations are found in Appendix A, lines 592 – 598.

3.3.1.3.1 Calculation of the Soil Water Potential

The retention curves as used by the model are described on a volumetric basis for the specific soil which is used for the study. Field water capacity (FC), water holding capacity at 10 kPa (WHC1), water holding capacity at 22 kPa (WHC2), 148 kPa (WHC3) and permanent wilting point (PWP), the water holding capacity at 1500 kPa (WHC4) and the initial water holding capacity (WHC) at the beginning of the season must be read into the program. The maximum depth to which the plant roots (SDP) can penetrate the soil is also needed. Mainly this study worked with the Shorrocks series, of the Hutton form. Values for WHC1 to WHC4 were respectively 41.00, 36.91, 28.61 and 19.68%. The value of WHC is calculated as 7.32% with the start of the first growth season and the initial values for the other seasons taken to be the end value of the previous season.

Water potential can be described as the negative pressure (suction force) that is exerted by a plant (or the soil) so that the water is in equilibrium when a certain point is reached. For the simulation of the general retention curves of any soil, three individual exponential relationships are used, for each of the three segments. These range from 2440 to 148, 148 to 22 and 22 to 10 kPa, respectively. The general

equation for the determination of the soil water potential (GWP) inside a given segment is given by:

$$GWP = GWPST \times EXP(ARGU) \times (-100) \quad (3.5)$$

where: GWPST = the soil water potential at WHC2, WHC3 or WHC4 (divided by 100) depending on which segment is applicable; and

$$ARGU = -1 \times AI \times (WJ - WST) \quad (3.5a)$$

where: WJ = Soil water content on a given day (%);
WST = WHC2, WHC3 or WHC4 depending on the segment used, and the constant

$$AI = \frac{(LOG(GWP_b) - LOG(GWP_o))}{(WHC_b - WHC_o)} \quad (3.5b)$$

where: GWP_b = Soil water potential at the top border of the applicable segment;
GWP_o = Soil water potential at the bottom border of the applicable segment;
WHC_b = Soil water content at the top border of the applicable segment;
and
WHC_o = Soil water content at the bottom border of the applicable segment.

GWP_b, GWP_o, WHC_b, and WHC_o are equal to the suitable values of WHC1, WHC2, etc. The algorithm for this is found in Appendix A from lines 284 – 292 and 458 – 480 and the graphical representation of it can be found in Figure 3.8.

3.3.1.3.2 Radiation Relationships

An estimation of the available incoming radiation is needed for the determination of evapotranspiration. The solar constant is defined as the mean of the incoming solar radiation that strikes a unit surface of the outer atmosphere of the Earth perpendicularly and has a value of 1.35 kW.m⁻² (Shirley, 2005). The daily total that is available at the upper reaches of the atmosphere (on a horizontal surface) varies with the time of the year and the relation is described in the following equation:

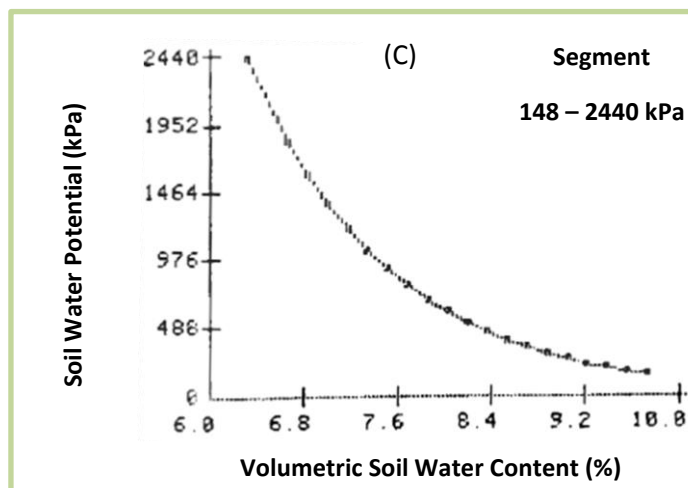
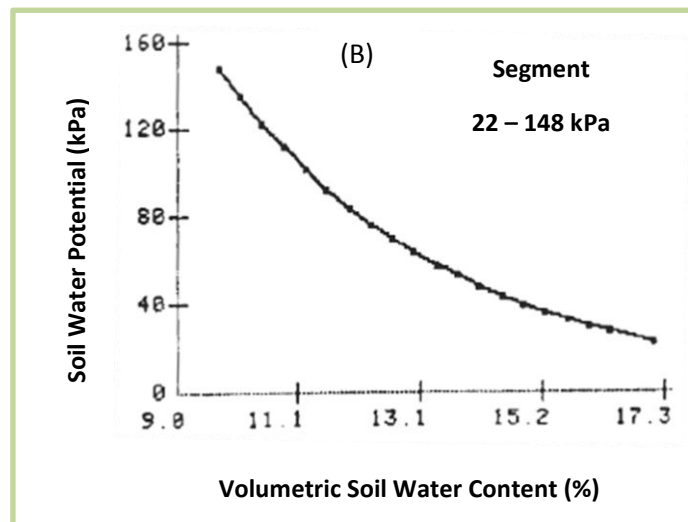
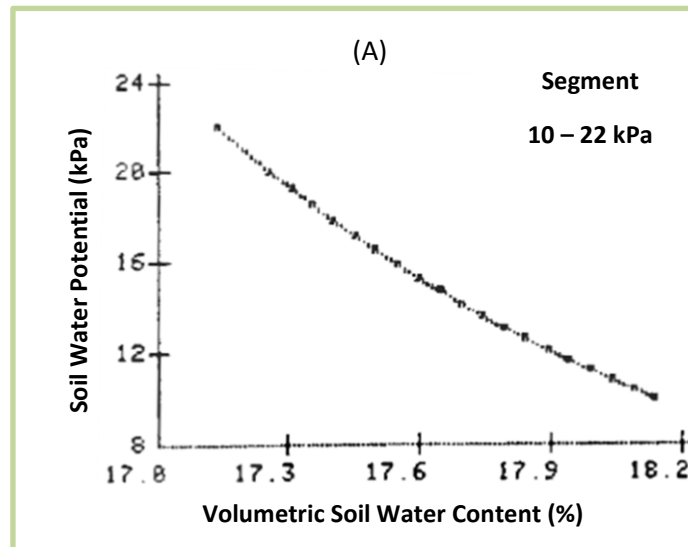


Figure 3.8 The different segments of the soil water retention curve for the total profile of a Sherock soil series of the Hutton form at Sydenham (Booyesen, 1983).

$$S = (30.85 \times 12.65 \times \cos\left(\frac{j+10}{365}\right) \times 360 \times 0.01745) \times 10^6 \quad (3.6)$$

where: S = Solar radiant flux density on a horizontal surface at the upper part of the atmosphere ($\text{J.m}^{-2}.\text{d}^{-1}$); and
 j = Julian day.

A value of 0.01745 ($= \frac{\pi}{180^\circ}$) is used to calculate the angle of S in radians. Eq. 3.6 has application on the current study. To ensure the accuracy of the PUTU VELD model at all locations, the equation suggested by Robinson (1966) must rather be used.

The daily radiant flux density at the surface available to the plant community is given by:

$$RFD = S \times \left(ALPHA + BETHA \times \left(\frac{Nw}{Nm} \right) \right) \quad (3.7)$$

where: RFD = Daily radiant flux density ($\text{J.m}^{-2}.\text{d}^{-1}$);
 Nw = Actual daylight length (h);
 Nm = Maximum possible daylight length (h);
 $ALPHA$ = Fraction of net radiation conducted into the soil; and
 $BETHA$ = Atmosphere permeability.

Approximately 21% ($ALPHA$) of S reaches the ground surface under cloudy conditions. The value of $ALPHA$ varies between 10 – 29% (Selirio & King, 1974; cited by Booyesen, 1983). Values for $BETHA$ of between 0.5 – 0.76 have been reported (Reid, 1981; cited by Booyesen, 1983). Considering that only sunshine duration is available on a spread-out observation network, it was decided to apply Eq.3.7 with values of 0.21 and 0.71 for $ALPHA$ and $BETHA$, respectively. When less than 50% of DAYFRC (fraction of daily possible sunshine duration) is available then $ALPHA$ and $BETHA$ are 0.29 and 0.5, respectively. The mean hourly radiant flux density for the specific day ($RFDM$) is given by:

$$RFDM = \frac{RFD}{(Nm \times 3600)} \quad (3.8)$$

The algorithm for Eq. 3.6 – 3.8 can be found in Appendix A, lines 490 – 506 and its graphical representation can be found in Figure 3.9.

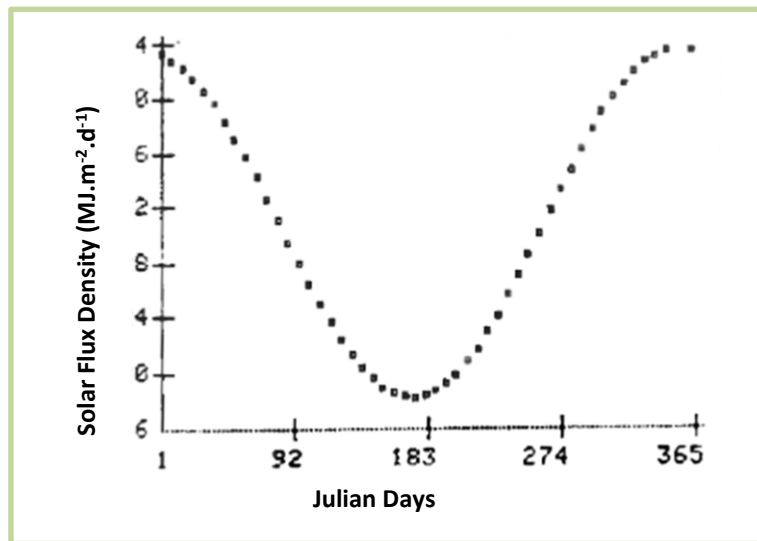


Figure 3.9 Daily variation in solar radiant flux at the outermost limits of the atmosphere above Bloemfontein (Booyesen, 1983).

3.3.1.3.3 Evapotranspiration

Potential evapotranspiration only occurs when there is no shortage of soil water. The energy balance equation at a surface is thus:

$$RN = LE + H + G \quad (3.9)$$

where: RN = Net radiation flux density ($W.m^{-2}$);
 LE = Latent heat flux density ($W.m^{-2}$);
 G = Soil heat flux density ($W.m^{-2}$); and
 If H is the energy flux density ($W.m^{-2}$) available to evaporate water or to heat the atmosphere at the surface be defined, then:

$$H = RN - G \quad (3.10)$$

Slayter and McIlroy (1961) and Monteith (1965) explained evaporation using the following equation:

$$LE = \left(\frac{s \times H}{s + \gamma} \right) + \left(\frac{\rho \times Cp}{RA} \right) \times (Dz - Do) \quad (3.11)$$

where: s = Slope of the saturation vapour pressure / temperature – curve ($mb.^{\circ}C^{-1}$);
 γ = Psychrometric constant ($0.66 mb.^{\circ}C^{-1}$);
 ρ = Density of air ($kg.m^{-3}$);

C_p = Specific heat of air ($J.kg^{-1}.^{\circ}C^{-1}$);

D_z & D_o = Wet bulb temperature slope at a height of z and at the surface, respectively ($^{\circ}C$); and

RA = Aerodynamic resistant against diffusion of evaporation between the surface and height z ($s.m^{-1}$).

If the air above the surface is saturated, then D_o is equal to nil and thus potential latent heat flux density is defined as:

$$LPE = \left(\frac{s \times H}{s + \gamma} \right) + \left(\frac{\rho \times C_p}{RA} \right) \times D_z \quad (3.12)$$

where: LPE = Potential latent heat flux density ($W.m^{-2}$).

If the air is also saturated at a height z , then D_z will also be equal to nil and thus the equilibrium latent heat flux density is defined as:

$$LEE = \left(\frac{s \times H}{s + \gamma} \right) \quad (3.13)$$

where: LEE = equilibrium latent heat flux density ($W.m^{-2}$).

This value can be calculated using insufficient weather data. It is used as a description for atmospheric evaporation demand.

Priestley & Taylor (1972) applied Eq. 3.13 for the calculation of LPE :

$$LPE = \alpha \times LEE, \quad \text{or} \quad LPE = \alpha \frac{s \times H}{s + \gamma} \quad (3.14)$$

The mean value for the constant of proportionality, α , was 1.26, but this constant was adapted further for South African conditions by Meyer *et al.* (1979). They deduce the following relationship:

$$\alpha = 1.28 + (0.08 \times (T_x - 20)) \quad (3.15)$$

where: T_x = Daily maximum temperature ($^{\circ}C$).

Eq. 3.15 has the specification built in that $\alpha = 1.28$ for $T_x < 20^{\circ}C$.

In Appendix A lines 509 and 511, α is equal to PECONS.

Schulze (1974) determined the following relation between temperature and $\frac{s}{s + \gamma}$:

$$GS = 0.4019914 + (0.01725101 \times T) - (0.0001485 \times T^2) \quad (3.16)$$

where: $GS = \text{The value of } \frac{s}{s + \gamma} \text{ at a temperature } T; \text{ and}$
 $T = \text{Mean air temperature } (^\circ\text{C}).$

The graphical representation of Eq.3.16 is found in Figure 3.10 and the algorithm is in Appendix A, line 485.

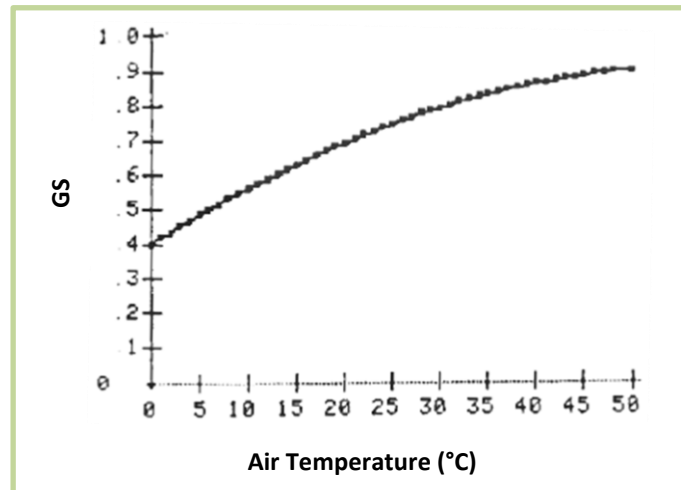


Figure 3.10 Graph of $GS \left(\frac{s}{s + \gamma} \right)$ as a function of air temperature (Booyesen, 1983).

Even though it was previously used with irrigated wheat, it can, according to Hellmann (1976), be accepted that RN is approximately equal to $0.64 \times RFDM$. If it is further accepted that G is equal to $0.1 \times RN$ then equilibrium evapotranspiration (EE) can be calculated through the following steps:

$$\text{Set } H = RN - G$$

Motram (1976) found that on planted pastures $RN = 0.5 \times RFDM$.

Therefore:
$$H = 0.5 - (0.1 \times 0.5 \times RFDM) = 0.45 \times RFDM \quad (3.17)$$

The equilibrium evapotranspiration can thus be determined by Eq. 3.18 (Appendix A, line 513):

$$EE = 0.63 \times \left(\frac{GS \times RFDM}{2450 \times 1000} \right) \quad (3.18)$$

The numerical values of 2450 and 1000 ensure that EE can be calculated in $\text{mm} \cdot \text{s}^{-1}$.

The potential evaporation (PE) can then be written as:

$$PE = \alpha \times EE \quad (3.19)$$

The graphical presentation of the influence of temperature and radiation on PE is indicated in Figure 3.11 and the algorithm is found in Appendix A, line 508 – 516.

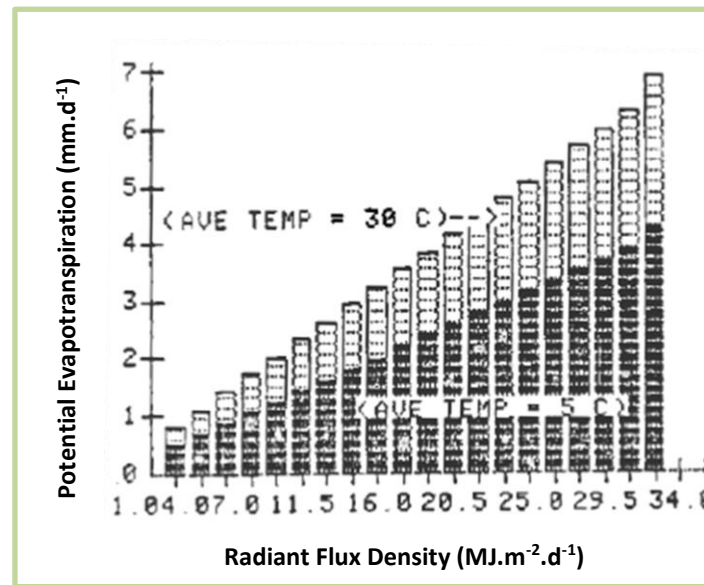


Figure 3.11 Influence of temperature and radiant flux density upon computed potential evapotranspiration (Booyen, 1983).

3.3.1.3.4 Hydraulic Conductance and Leaf Water Potential

The water flow rate is defined as the volume of water that flows past a point in the system per unit time. The hydraulic conductance (HYCON) of a crop is defined as the water flow rate through the crop per unit difference in water potential between the leaves (Ψ_b) and the soil (Ψ_g) (De Jager *et al.*, 1982). If it is assumed that for full plant coverage the water flow rate is equal to the potential evapotranspiration rate, PE, then the involved control function is:

$$PE = HYCON \times (\Psi_g - \Psi_b) \quad (3.20)$$

$$PE = HYCON \times \Delta\Psi \quad (3.21)$$

where: HYCON = Hydraulic conductance ($\text{g.m}^{-2}.\text{s}^{-1}.\text{kPa}^{-1}$) of the vegetation;
 Ψ_g = Water potential (in kPa) of the soil; and
 Ψ_b = Water potential (in kPa) of the leaves.

The hypothesis that HYCON is a constant, is accepted. Through the test and hit method in respect to the simulations of the grassland behavior during the 1980/81 season at Glen, the value of $HYCON = 0.006 (\text{g.m}^{-2}.\text{s}^{-1}.\text{kPa}^{-1})$ was attained. From Eq. 3.20 and 3.21, the leaf water potential (LWP) can be calculated by:

$$LWP = \Psi_b = \Psi_g - \left(\frac{PE}{HYCON} \right) \quad (3.22)$$

where: LWP = Ψ_b = Leaf water potential (kPa).

If the leaf water potential becomes excessively large, but less than a certain critical value, the turgor pressure decreases, wilting occurs, the stomata close and the resistance against evaporation diffusion becomes unending immense. The critical leaf water potential (WPC) where these conditions occur vary from crop to crop. For example, for maize, sunflower and potatoes, respective values of -1100 kPa, -1400 kPa and -1100 kPa, have been reported. Depending on the root development climax grass species can develop excessively high suction power and in accordance with Van Niekerk & Opperman (1982) the critical value of -1800 kPa is employed by PUTU VELD. This value is decreased by 15 kPa per water stress day until a minimum of -3000 kPa is reached.

The hydraulics limitations factor (FW) that describes the effect of the plant-water relations on water flow through the plant and thus photosynthetic rate, can then be defined as follows (De Jager *et al.*, 1982):

$$FW = \frac{1}{(1+A)} \quad (3.23)$$

where: FW = Hydraulic limiting factor (%); and
A (the exponent of the coefficient) is defined by:

$$A = EXP(COEF) \quad (3.23a)$$

where: COEF can be one of the following three options (Eq. 3.23b – 3.23d) depending on a set of conditions that must first be met (Appendix A, lines 543 – 555):

$$COEF = 0.005 \times (WPC - LWP) \quad (3.23b)$$

$$COEF = \frac{WPC}{100} \quad (3.23c)$$

$$COEF = \frac{WPC}{-100} \quad (3.23d)$$

FW is the direct relationship to the break of potential photosynthetic rate that is allowed through prevailing conditions in the soil-plant-atmosphere continuum. The graphical presentation of Eq. 3.23 is found in Figure 3.12 and the algorithm for Eq. 3.22 and 3.23 is indicated in Appendix A, lines 539 – 555.

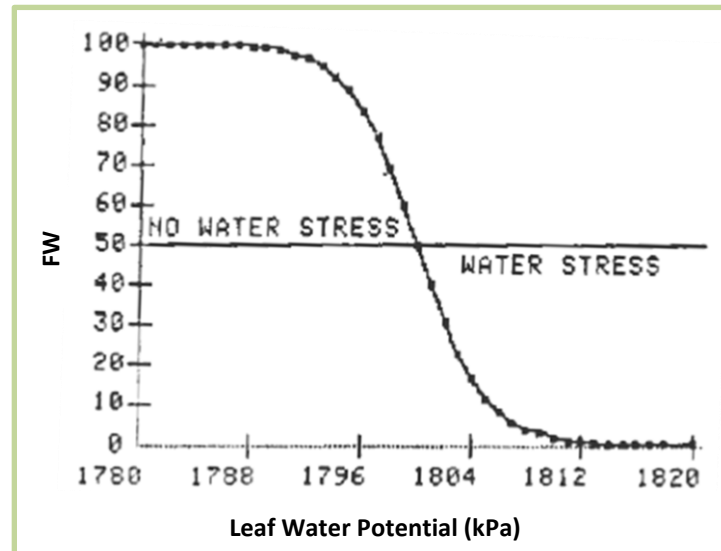


Figure 3.12 Dependence of the hydraulic limiting factor (FW) upon leaf water potential (Booyesen, 1983).

3.3.1.3.5 Soil Water Withdrawal

Actual potential soil water withdrawal (APE) is a function of the range of the plant coverage at the relevant stage. To be able to quantify it the following assumptions of the original PUTU 2 were taken:

- (i) The minimum value of APE is 10% of PE;
- (ii) APE is equal to PE when the leaf area index (AL) is greater than three; and
- (iii) The increase in APE will be directly proportional to the increase in AL.

Say that B is the crop evaporation factor defined as:

$$B = \frac{APE}{PE} \quad (3.24)$$

then the defining equation for B in the range of $0.1 \leq B \leq 1.0$ is as follows:

$$B = 0.1 + \frac{AL}{3} \times 0.9 \quad (3.25)$$

where: AL = The leaf area index for 100% basal coverage.

The algorithm for Eq. 3.25 is indicated in Appendix A, lines 527 – 537.

The primary resource of soil water refill is rainfall. It is further accepted that rainfall values of 5 mm.d⁻¹ or less do not contribute to soil water replenishment. The evaporation rate out of the soil with rainfall quantities greater than 5 mm.d⁻¹ is governed by an exponential function (FG) (De Jager *et al.*, 1982) and is defined as:

$$FG = EXP\left(-0.5 \times (CNT \times (j + 1))\right) \quad (3.26)$$

where: FG = Soil water evaporation factor; and
 CNT = Count of the number of days (j) after a rainfall occurrence of more than 5 mm.d⁻¹.

Soil water withdrawal will be done by evaporation from a bare soil surface (SLVAP) and by transpiration (TRANS) from a vegetation covered surface. De Jager *et al.* (1982) developed the necessary theory. Briefly:

$$SLVAP = (1 - B) \times FG \times LPE \quad (3.27)$$

and (see Eq. 3.23)

$$TRANS = B \times FW \times LPE \quad (3.28)$$

The actual evapotranspiration (APE) and thus the total demand for soil water is then:

$$APE = SLVAP + TRANS \quad (3.29)$$

The algorithm of Eqs. 3.26 to 3.29 is indicated in Appendix A, lines 566 to 590. The graphical presentation of Eq. 3.26 is shown in Figure 3.13.

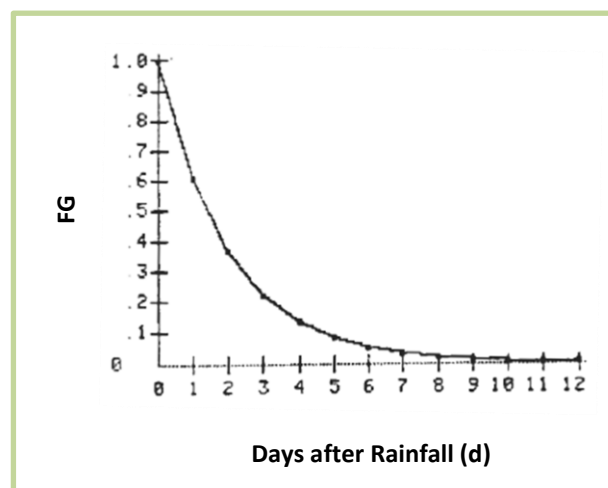


Figure 3.13 Decrease in soil water evaporation rate factor (FG) with time following a rainfall event of greater than 5 mm.d⁻¹ (Booyesen, 1983).

The water loss from the soil occurs first out of the top layer. Only when the water content (SLWAT1) therein is less than the evaporation demand does water get drawn out of the second level (TRANS2). Soil water evaporation can only occur out of the top layer.

3.3.1.3.6 Soil Water Replenishment and Drainage

The top layer is replenished through rainfall until the soil water content exceeds the field water capacity (FC1). All excess water percolates (DRAIN1) down to the lower level and replenishes it. Just as with the top layer, percolation will occur out of the lower layer (DRAIN2) when the soil water content exceeds the field water capacity (FC2) of the current soil level. The algorithm for this estimate is found in Appendix A, lines 592 – 649.

3.3.1.4 Influence of Environmental Driving Forces on Production

3.3.1.4.1 Calculation of Leaf Area

PUTU VELD calculates for each day the standing, living leaf mass (BL). From here the daily AL can be determined from the specific leaf area ratio (SPL):

$$AL = \frac{BL}{SPL} \quad (3.30)$$

The work of Van Niekerk *et al.* (1982; cited by Booysen, 1983) shows that a constant SPL value of 50 kg.ha⁻¹ is reliable.

3.3.1.4.2 Environmental Limiting Factors

The main elements that influence photosynthesis are solar radiation, temperature and water. The various relationships between the elements and photosynthesis is described in the paragraphs below.

According to Stapper (1980) it is accepted that at a given growth stage the efficiency with which absorbed solar radiation for photosynthesis is utilized becomes a constant value. If the efficiency and the amount of absorbed solar radiation is known, then the photosynthetic rate can be determined. The environmental limiting factor for solar radiation (FI) is thus equal to the absorption factor of the crop foliage. A similar exponential function as used by Kaiser (1976) is utilized here:

$$FI = (1 - EXP(-0.7 \times AL \times BCFUNC)) \times 100 \quad (3.31)$$

where: FI = Percentage of solar radiation that is absorbed by the foliage; and
BCFUNC = The ratio of the prevailing basal cover to 100% basal cover.

The graphical presentation is found in Figure 3.14, and the algorithm is indicated in Appendix A, line 691. The arrangement of the leaves in the foliage only affects FI slightly. A difference of about 10% is noted in the radiation usage between planophile and erectofile type foliage.

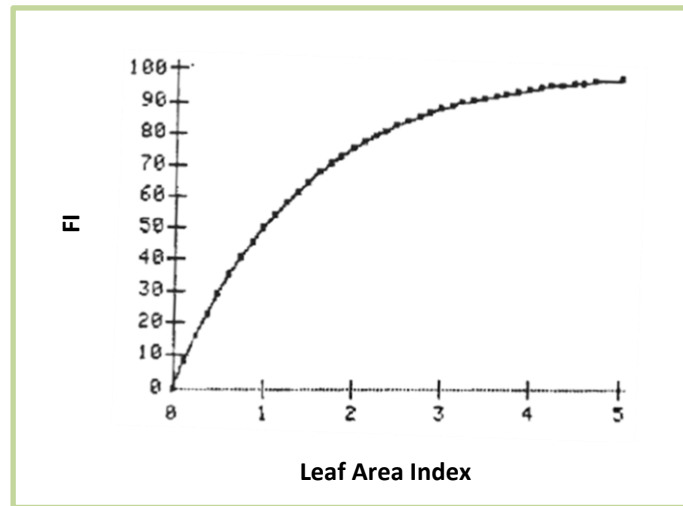


Figure 3.14 Dependence of the radiation limiting factor (FI) upon leaf area index at a 10% basal cover (Booyesen, 1983).

A change in temperature affects the rate of daylight respiration and therefore the net CO₂-exchange of the leaves. The percentage of the optimal rate of photosynthesis which is allowed through the prevailing temperature (FT) after motivation from work with *Paspalum dilatatum* (see De Jager *et al.*, 1982) can thus be defined as follows:

$$FT = 100 \times EXP \left(-\frac{(T-T_{opt})^2}{360} \right) \quad (3.32)$$

where: FT = Portion of the optimal net CO₂-exchange rate of the grass (%);
T = Mean daily temperature (°C); and
T_{opt} = Optimal growth temperature of climax grass (37°C).

From Eq. 3.32 it is thus clear that temperature can have a strong effect on the growth pattern of a crop during the season, especially at the beginning of the growth season when an increase in photosynthetic rate is paired with an increase in leaf area. With reference to Section 3.3.1.1 where the base temperature (BO) for the determination of heat units is given, FT is then set as nil for temperatures below a BO equal to 12°C.

The graphical presentation of Eq. 3.32 is indicated in Figure 3.15 and the algorithm is in lines 694 – 693 of Appendix A.

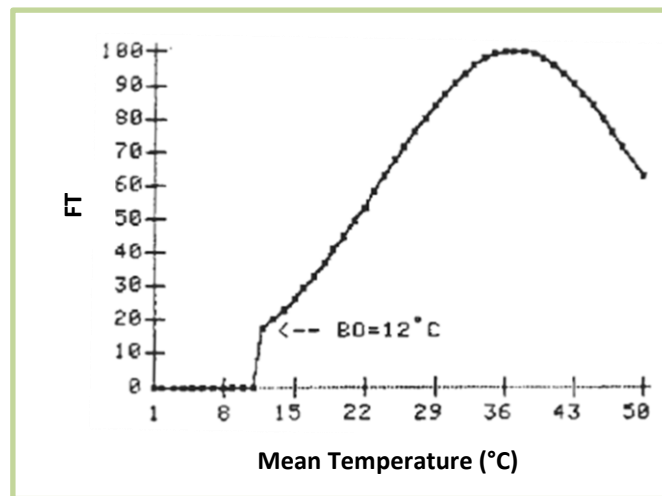


Figure 3.15 Variation of the temperature limiting factor (FT) with temperature (Booyesen, 1983).

The critical leaf water potential is attributed to plant water stress; thus, FW from Section 3.3.1.3.4 is used. The assumption is made that a decrease in photosynthesis has a direct relation to a decrease in the transpiration rate. Therefore Eq. 3.23 is used to determine FW.

The combined effect of the separate environmental driving forces on the photosynthesis process can now be summarized in one overall environmental limiting factor (F). The fundamental law of mutual constraint is accepted and F can now be determined as:

$$F = \left(\frac{FI}{100}\right) \times \left(\frac{FT}{100}\right) \times \left(\frac{FW}{100}\right) \times 100 \quad (3.33)$$

where: F = The overall environmental limiting factor (%).

The algorithm for Eq. 3.33 is found in Appendix A, line 754.

3.3.1.4.3 Photosynthetic Efficiency

The maximum efficiency of photosynthesis (EFFMAX), as discussed in Section 3.3.1.1, is by approximation equal to 12%. As a result of the effect of shade caused by leaves in the foliage and the change in living green material, EFFMAX will change during the growing season. The efficiency with which photosynthesis occurs (EFF) is determined with help of Eqs. 3.23, 3.31, 3.32 and 3.33, namely:

$$EFF = \frac{F \times EFFMAX}{100} \quad (3.34)$$

The photosynthetic rate (P) is determined by:

- (i) The absorbed radiant flux density (RFDM) ($\text{MJ.m}^{-1}.\text{d}^{-1}$);
- (ii) Converting the radiant flux density and the recorded CO_2 by multiplying them with the solar radiation conversion efficiency EFF and FE, so that:

$$P = \left(\frac{EFF}{100}\right) \times FE \times RFDM \quad (3.35)$$

The algorithm of the above two equations (3.34 and 3.35) are found in Appendix A, lines 758 and 767, respectively. The daily photosynthesis is the value from Eq. 3.35 multiplied with the number of seconds in the current day (Appendix A, line 768).

3.3.1.4.4 Assimilation, Respiration and Net Production of Dry Material

COM is the factor for the conversion of carbon dioxide to carbohydrates (Section 3.3.1.1). The rate of carbohydrate assimilation (ASSIM) is then:

$$ASSIM = P \times COM \quad (3.36)$$

Before the value of ASSIM can be seen as the daily dry matter gain, respiration must first be deducted from it. Plants can be divided into two groups according to their respiration characteristics. C_3 -plants are photorespires while C_4 -plants only respire at night. The respiration can be divided further into two types, namely maintenance respiration which stands in relation with living dry material and evenly changes with the total dry mass of the plant, and construction respiration which stands in relation with the development of new material and an evenly changing relationship with the previous day's photosynthesis rate (Chen *et al.*, 2005; Martin *et al.*, 2009; Bange *et al.*, 2016) material production per day, thus:

$$ASSIM = COM \times P \times (1 - CONS) \quad (3.37)$$

The fraction of the living dry material that is needed for maintenance respiration (MAINF) stands in a narrow relation with temperature. McCree (1974) calculated it for clover as:

$$MAIN = C30 \times (0.044 + (0.0019 \times TNITE) + (0.001 \times TNITE^2)) \times CLIVE \quad (3.38)$$

where: TNITE = The average night-time temperature in $^{\circ}\text{C}$ for day j given by

$$TNITE = \left(\frac{TMXPD + AMN(j)}{4} \right) \quad (3.39)$$

where: AMN(j) = The minimum temperature for day j (°C);
 TMXPD = The maximum temperature for the previous day (°C);
 CLIVE = The mass of living dry material (kg.ha⁻¹);
 MAIN = Carbohydrate loss due to night respiration (kg CHO.ha⁻¹.d⁻¹);
 MAINF = The fraction of CLIVE that is needed for maintenance respiration; and
 C30 = The fraction of the living dry material that is lost in the form of respiration at a temperature of 30°C.

The breakdown of carbohydrates occurs within the living components of the plant. It is done in the translocation subroutine after ASSIM is first sent to the reserve pool. The algorithm for the above is found in Appendix A, lines 770 – 786.

3.3.1.5 Phenology and Growth Functions

There are five distinct growth stages namely, the vegetative-, reproductive-, seed-, seed-fall-, and dormant growth stage. The daily produced dry material is translocated to the different plant parts by mass flow changes (Figure 3.16). In this section, the mechanisms that is used to transition from one growth stage to the next is discussed. These mechanisms are mostly set by using literature studies and field observations.

Translocation rate is regulated through the relationship between the mass of a given plant part and the mass of the whole plant. Furniss (1981; cited by Booyesen, 1983) proposed that there is a desired part/whole mass relationship for each growth stage. The main plant parts that are dealt with are the leaves, culms, roots and stubbles. Furniss (1981; cited by Booyesen, 1983) also suggested that there is a maximum translocation rate for each growth stage. PUTU VELD is therefore refined by incorporating these principles. It is achieved with help from the assumptions that translocation in a given plant and given growth stage is equal to a maximum rate multiplied with a factor that changes exponentially with the relative desired part/whole mass relationship change. This function is shown in Appendix A, lines 1107 – 1172. The exponential relationship is shown in Figure 3.17. It is accepted that all

translocation stops when water stress occurs. How the flow mass in the plant is addressed in PUTU VELD will be discussed fully in Section 3.3.1.6.

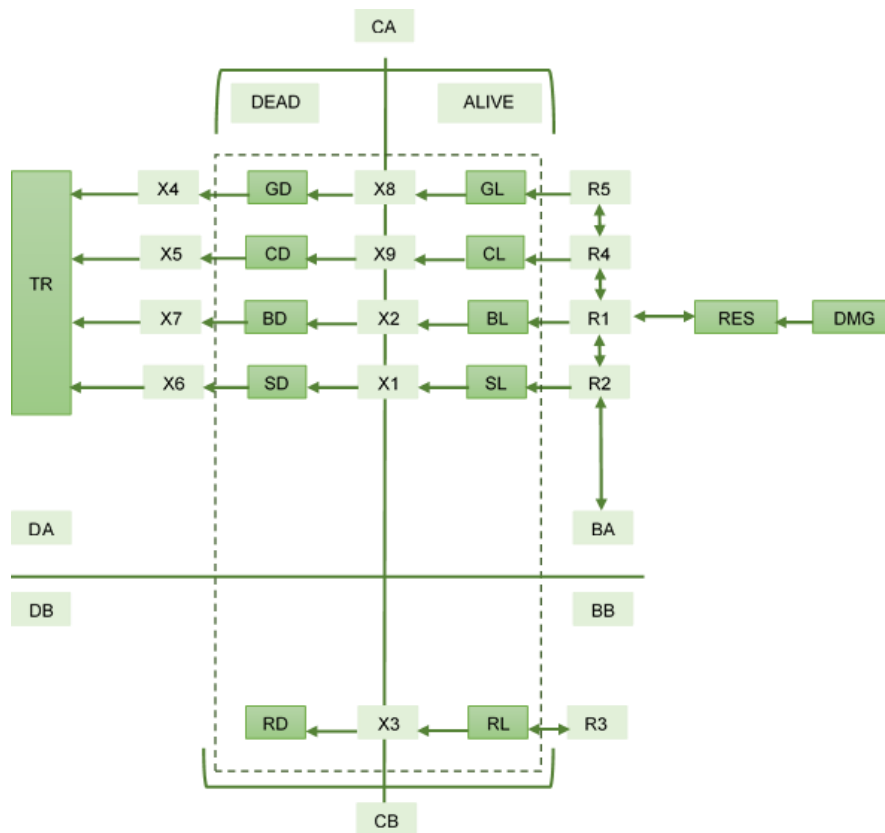


Figure 3.16 Diagrammatic representation of translocation and mass flow inside the plant as seen in the PUTU VELD model (Booyesen, 1983). DMG = The days dry matter gain ($\text{kg CHO}\cdot\text{ha}^{-1}\cdot\text{d}^{-1}$); GD = Grain dead; GL = Grain living; CD = Culm dead; CL = Culm living; BD = Leaves dead; BL = Leaves living; SD = Stubble dead; SL = Stubble living; RD = Roots dead; RL = Roots living; TR = Trash dead; RES = Carbohydrate reserves; DA = Above ground dead; BA = Above ground living; DB = Below ground dead; BB = Root biomass; CA = Above ground standing crop; CB = Below ground standing crop; R_n = Translocated masses; X_n = Mass flow variables.

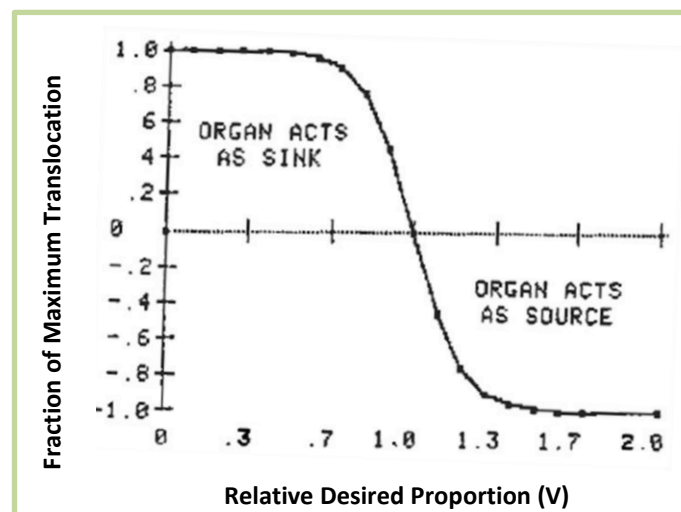


Figure 3.17 Relationship between translocation rate multiplier and the relative desired proportion decrement (Booyesen, 1983).

3.3.1.5.1 Vegetative Growth Stage

This growth stage is the initial growth stage and the following assumptions are made:

- a) The heat demand that must be met for the shift to the next growth stage (HUCRIT) is 250 degree days;
- b) The maximum and minimum daily mean temperature between which heat units are accumulated is respectively 30°C and 12°C;
- c) When water stress occurs during this growth stage, the heat demand will thus decrease with the number of heat units equal to:

$$-3 \times \left(\frac{100 - FW}{100} \right) \quad (3.40)$$

This implies that the heat demand will decrease proportionally to the extent of the water stress that is encountered. The minimum heat demand (HUCRMN) that is allowed is however 25 degree days;

- d) In fact, in (c) is it assumed to have a minimum leaf mass at 100% basal cover (BLM) of 4600 kg.ha⁻¹ which must be disposed of during the growth stage before moving on to the reproductive growth stage;
- e) Further, heat accumulation will not commence before the living leaf mass of the plant has reached a minimum mass (BLT) of 2900 kg.ha⁻¹ (at 100% basal cover);
- f) The daily growth rate factor of the leaves (BCON) during the vegetative growth stage is assumed to be 37 kg.ha⁻¹.d⁻¹.°C⁻¹ but for the period where BLM is smaller than BLT the growth rate is only 20% of BCON;
- g) If the above requirements have not yet been met by the 258th day of the growth season (16 March) then the plant will absolutely proceed to the dormant growth stage with the first frost occurrence;
- h) The daily increase in leaf mass (DBL) is given by:

$$DBL = BCON \times (TGROW - BO) \quad (3.41)$$

where: TGROW is the daily mean air temperature provided that $BO \leq TGROW \leq 30^\circ\text{C}$. If $TGROW < BO$ then $TGROW = BO$; and

- i) The dying off rate for the stubble, leaves and roots is 0.1 during this stage.

3.3.1.5.2 Reproductive Growth Stage

When the shift to the reproductive growth stage occurs, the following desired part/whole mass fractions (DPRO_x, where x stands for seed, culms, leaves, stubble or roots) for the stage is laid: seed = 0.0; culms = 0.125; leaves = 0.125; stubble = 0.25 and roots = 0.5 (lines 900 – 904 in Appendix A). The following assumptions apply for this growth stage:

- a) The minimum length of this growth stage (MKOUNT) is accepted as 25 days;
- b) The minimum mass of the living culms (CL), which must be met before the shift occurs to the seed forming growth stage, is 25% of the mass of the living leaves (BL);
- c) If the above mentioned have not yet been met before the 258th day of the growth season, then the first occurrence of frost becomes the absolute shift mechanism from the reproductive to the dormant growth stage; and
- d) The dying off rate of living to dead material during the growth season stays the same as for the vegetative growth stage.

3.3.1.5.3 Seed Formation Growth Stage

When the shift to the seed formation growth stage occurs the following desired part/whole mass fractions are laid: seed = 0.003; culms = 0.1; leaves = 0.1; stubble = 0.347 and roots = 0.45 (lines 916 – 920 in Appendix A). The assumptions that apply for this growth stage is as follows:

- a) The length of this growth stage (MKOUNT) is 50 days;
- b) If frost occurs after the 258th day of growth season, then shift occurs absolutely to the reproductive growth stage;
- c) Dying off of living plant material occurs at the culms, leaves, stubble and roots and also in the case of seeds after the 20th day of the seed formation. This implies that a certain amount of the dead seeds or dried out seeds are ready to be flung from the plant at the end of the growth season;
- d) The dying off rate is thus seen as follows: seed after the 20th day of the growth stage = 15% per day, culms = 0.1% per day, leaves = 0.2% per day, stubble = 0.2% per day and leaves = 0.3% per day; and
- e) Dead plant material is cast from the plant during the growth season at the following rates: leaves = 0.1% per day and stubble = 0.1% per day.

3.3.1.5.4 Seed-Fall Growth Stage

When the shift occurs to the seed-fall growth stage the following part/whole mass relationships are laid: seeds = 0.0; culms = 0.08; leaves = 0.08; stubbles = 0.26 and roots = 0.58 (lines 980 – 984 in Appendix A). The following assumptions apply here:

- a) The only mechanism for the shift to the dormant growth stage is the first occurrence of frost;
- b) The rate at which seed death occurs is:

$$X4 = (GLO - (GD + GL)) \times 0.3 \quad (3.42)$$

where: $X4$ = Dying off rate of living to dead seed ($\text{kg} \cdot \text{ha}^{-1} \cdot \text{d}^{-1}$);
 GLO = Maximum mass that seeds reach during the current growth stage ($\text{kg} \cdot \text{ha}^{-1}$);
 GD = Dead seed mass ($\text{kg} \cdot \text{ha}^{-1}$); and
 GL = Living seed mass ($\text{kg} \cdot \text{ha}^{-1}$).

Eq. 3.42 (line 1002 in Appendix A) implies that 3% of the left over (standing) seeds die off per day. This rate is only maintained as long as there are still living seeds available. Culms die off at a rate of 0.5% per day, leaves at 1% per day, stubble at 0.2% per day and roots at 0.3% per day;

- c) The rate at which plant material falls from the seeds, culms, leaves and stubble per day is 50%, 5%, 0.5% and 0.5%, respectively; and
- d) The desired relationships as described under the reproductive growth stage stays unchanged when the shift to the dormant growth stage occurs in preparation for the following season.

3.3.1.5.5 Dormant Growth Stage

This growth stage will persist until the end of the growth season or until the above ground material is removed by one or another utilization practice. The following assumptions apply during this season:

- a) The dying off rates during the season for the seeds, culms, leaves and stubble per day is 50%, 25%, 20% and 2%, respectively; and
- b) The rate at which the plant material falls off the plant for seeds equal 50% of the remaining GD per day; culms equal 0.5% of the remaining CD per day; leaves equal 0.5% of the remaining BD per day and stubble equals 0.3% of the remaining SD per day.

During all of the growth stages, tests are done to check for the possible removal of above ground material caused by cutting of rangeland. If this is the case then the following assumptions are made:

- a) It will be attempted to shift again to the vegetative growth stage if the weather conditions allow it. If not, the growth stage will anyhow be determined by going through the shift mechanisms of the consecutive growth stage;
- b) The critical value for the leaf water potential (WPC) will be restored to -1800 kPa;
- c) The efficiency factor for photosynthesis (Q) will be decreased to 0.75;
- d) The heat demand of the plant will be cut by 20%; and
- e) The values of BLM and BLT will be decreased by 60%.

3.3.1.6 Translocation in the Plant

The mechanisms for translocation are subject to the assumptions as discussed in Section 3.3.1.2.2 (Initial values) and are as follows:

- a) The daily dry material gain (ASSIM) is theoretically first awarded to the plant reserves as a whole and then the plant reserves are distributed to the different plant parts depending on the mass flow variables; and
- b) The values that the mass flow variables will adopt is a function of the growth stage (GRSTGE), the desired mass relationships (DPRO_x), the maximum growth rates (AGR_x, where *x* stands for leaves, culms, seed, roots or stubble) and the actual translocation rates (TLR_x, where *x* stands for leaves, culms, seed, roots or stubble) (see Section 3.3.1.5).

The coding of the above-mentioned parameters is indicated in the following sections.

3.3.1.6.1 Maximum Growth Rates and Actual Translocation Rates

The maximum growth rate (AGR_x) for each plant part during each growth stage is included in the program as a constant value and indicated in Table 3.5 (lines 1130 – 1153 in Appendix A).

To describe the procedure, the example of translocation from the culms will be discussed. The relevant parameters are AGRC and DPROC for maximum translocation rate and desired culm mass to total biomass relationship, respectively. TRLC is the actual translocation rate in the culm and CL and CD are the living and

dead masses, respectively. VC is the relationship of the prevailing part mass to total biomass, and is defined as:

$$VC = \frac{\left(\frac{CL + CD}{C}\right)}{DPROC} \quad (3.43)$$

Table 3.5 Maximum growth rate for each plant part during each growth stage. Where an AGR- value is not specified for a certain growth stage, the value is taken as nil. G, C, B, S and R stands for seeds, culms, leaves, stubbles and roots respectively. DBL stands for leaf mass change demand. All values are consistent with a basal cover of 100% (Booyesen, 1983)

Growth Stage		Maximum Growth Rate (kg.ha ⁻¹ .d ⁻¹ .°C ⁻¹)
Vegetative	AGRB	DBL
	AGRR = 0.15 x DBL	0.15 x DBL
Reproductive	AGRC	420
	AGRB	520
	AGRS	810
	AGRR	1250
Seed Formation	AGRG	50
	AGRS	810
	AGRR	1250
Seed Fall	AGRS	810
	AGRR	1250

The quantitative $1 - VC$ or $DPROC - \frac{(CL + CD)}{C}$ is the relative difference between the prevailing and desired relationship. Therefore, the actual translocation rate will be given by:

$$TLRC = \left(\frac{2.0}{1 + EXP(-10 \times (1 - VC))} \right) - 1 \quad (3.44)$$

The graphical presentation of Eq. 3.44 is found in Figure 3.18, presented at the end of Section 3.3 due to its length, while its coding can be found in Appendix A, line 1169.

3.3.1.6.2 The Mass Flow Variables

The mass flow variables are the mass carbohydrate that is either received or removed from a given plant part per hectare per day. The values that these variables take on are:

- a) Dependent on the degree of plant water stress (FW/100); and

b) The presence of sufficient plant reserves (RES).

In the case of the culms, the mass flow variable (with units of $\text{kg}\cdot\text{ha}^{-1}\cdot\text{d}^{-1}\cdot^{\circ}\text{C}^{-1}$) will be given by:

$$R4 = TLRC \times AGRC \times \frac{FW}{100} \quad (3.45)$$

If the available plant reserve is more than the estimated demand (sum of all the R-values), then the actual translocation of plant material to the different plant parts will occur. At a lack of enough sufficient translocatable material the mass flow variable becomes nil and only the dying off rates and rates of plant material falloff will be maintained.

3.3.1.6.3 Mass Balance of the Different Plant Parts

The retention of mass in each plant part is maintained by the general equation (only for culms shown):

$$CL = CL + R4 - X9 - \left(\frac{CL}{CLIVE} \times RESP \right) \quad (3.46)$$

where: $CLIVE$ = total living biomass ($\text{kg}\cdot\text{ha}^{-1}$); and

$\left(\frac{CL}{CLIVE} \times RESP \right)$ = the fraction of maintenance respiration that is due to the specific plant part.

The mass balance for the dead components of the plant part is given by (only for culms shown):

$$CD = CD + X9 - X5 \quad (3.47)$$

where: $X9$ = dying off rate ($\text{kg}\cdot\text{ha}^{-1}\cdot\text{d}^{-1}$); and

$X5$ = rate of falling off of dead material ($\text{kg}\cdot\text{ha}^{-1}\cdot\text{d}^{-1}$).

3.3.1.6.4 Plant Reserves

Because the plant reserves are contained in the stubble part of the plant, the estimate of the stubble mass differs somewhat from the general equations 3.39 and 3.40. The changes on plant reserve mass per day (DRES) is equal to the difference between the mass of the dry material produced ($ASSIM = DMG$; line 785 in Appendix A) and the algebraic sum of the mass flow variables (the R-values). This quantity forms part of the living stubble mass. In the case of the stubble we can write:

$$SL = SL - X1 - \left(\frac{SL}{CLIVE} \times RESP \right) + DRES \quad (3.48)$$

where: $DRES = ASSIM - R1 - R2 - R3 - R4 - R5 \quad (3.49)$

and the R-values can be negative or positive.

The estimate of the plant reserves (RES) as a separate entity (Appendix A, line 1209) is thus maximum to have a quantitative value for plant reserves at any given time period, however it is still seen as an integral part of the stubble mass.

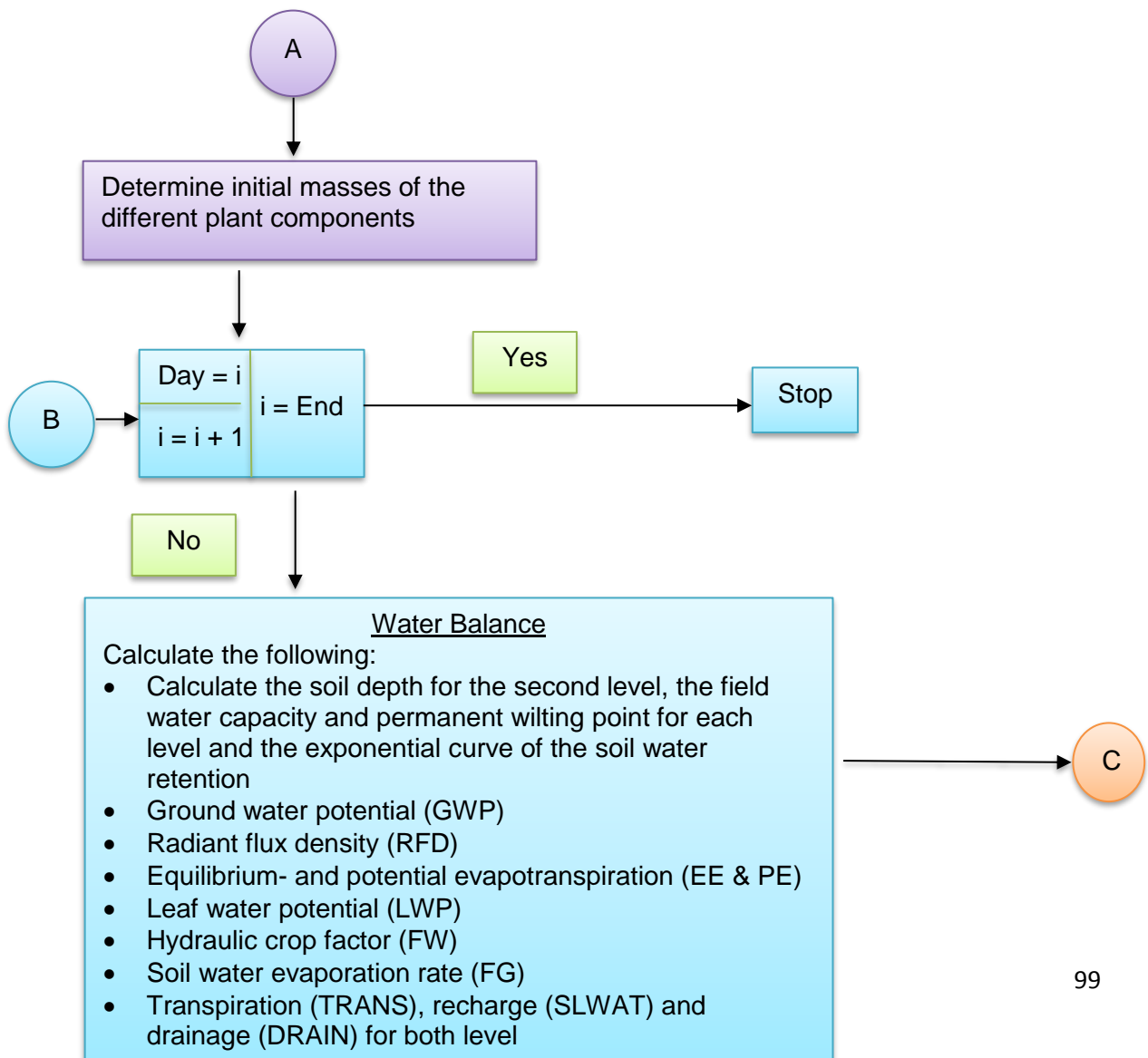
3.3.1.7 Iteration and Output

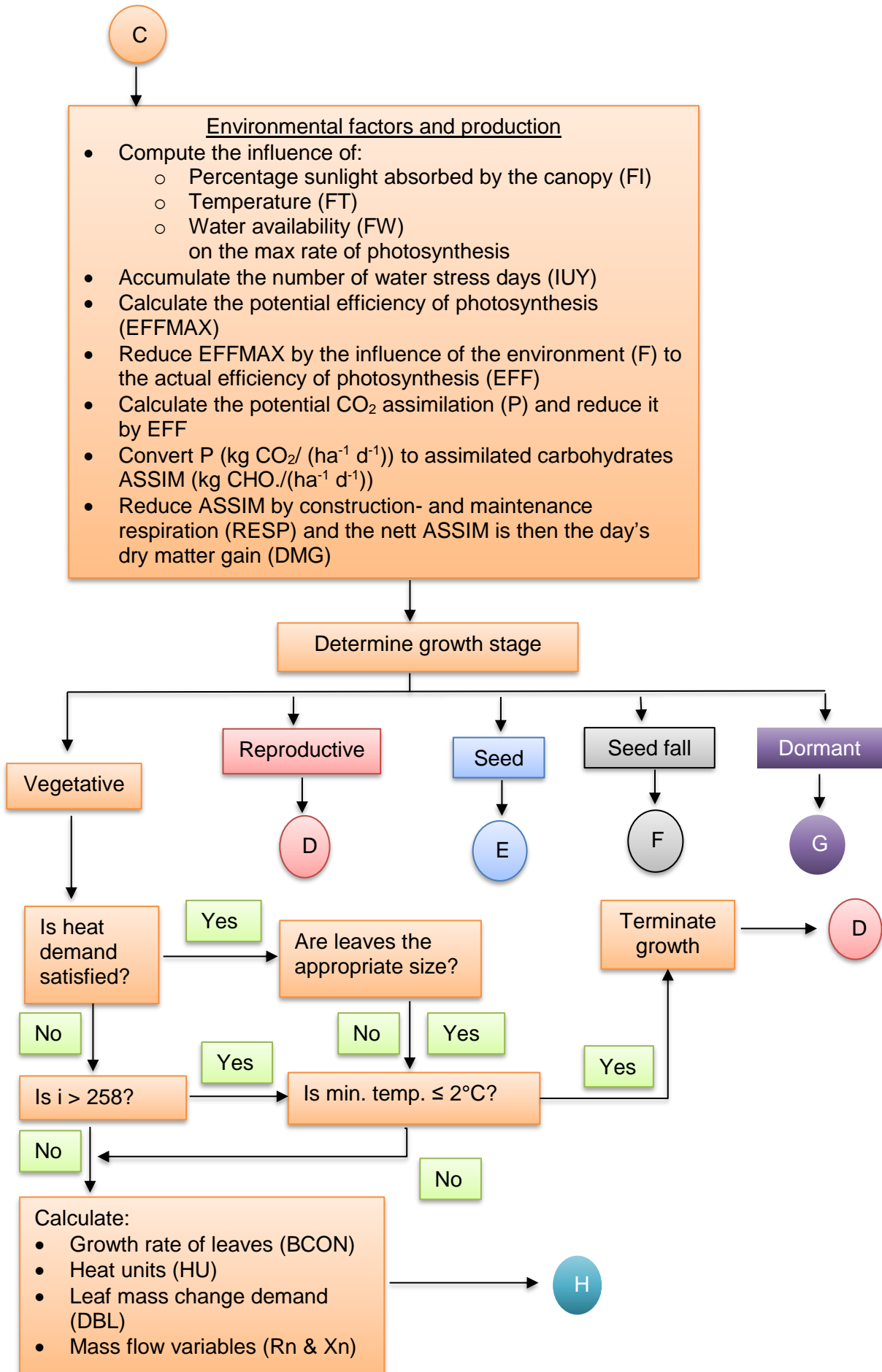
The model simulates on a daily basis beginning on 1 July with day $j = 1$ and ending on 30 June when $j = 365$. The program also takes into consideration leap years. For the determination of radiant flux density, the day of the growth season is expressed in Julian days (JDA). The output data can be presented in any selected interval by choosing the desired interval (ITERM). All plant mass information is presented as the mass per unit area against the prevailing basal cover at the specific time period. All the climate data is presented as the mean daily value over the iteration interval, ITERM. The algorithm for the preparation of data for output is found in Appendix A, lines 1278 to 1369. Lines 715 to 735 contain the algorithm for the determination of the beginning and end dates of water stress periods as well as the number of days over which the period extends. For the calculation of the former it is accepted that water stress starts when the hydraulic limiting factor (FW) drops below 50% at an average daily temperature higher than 15°C.

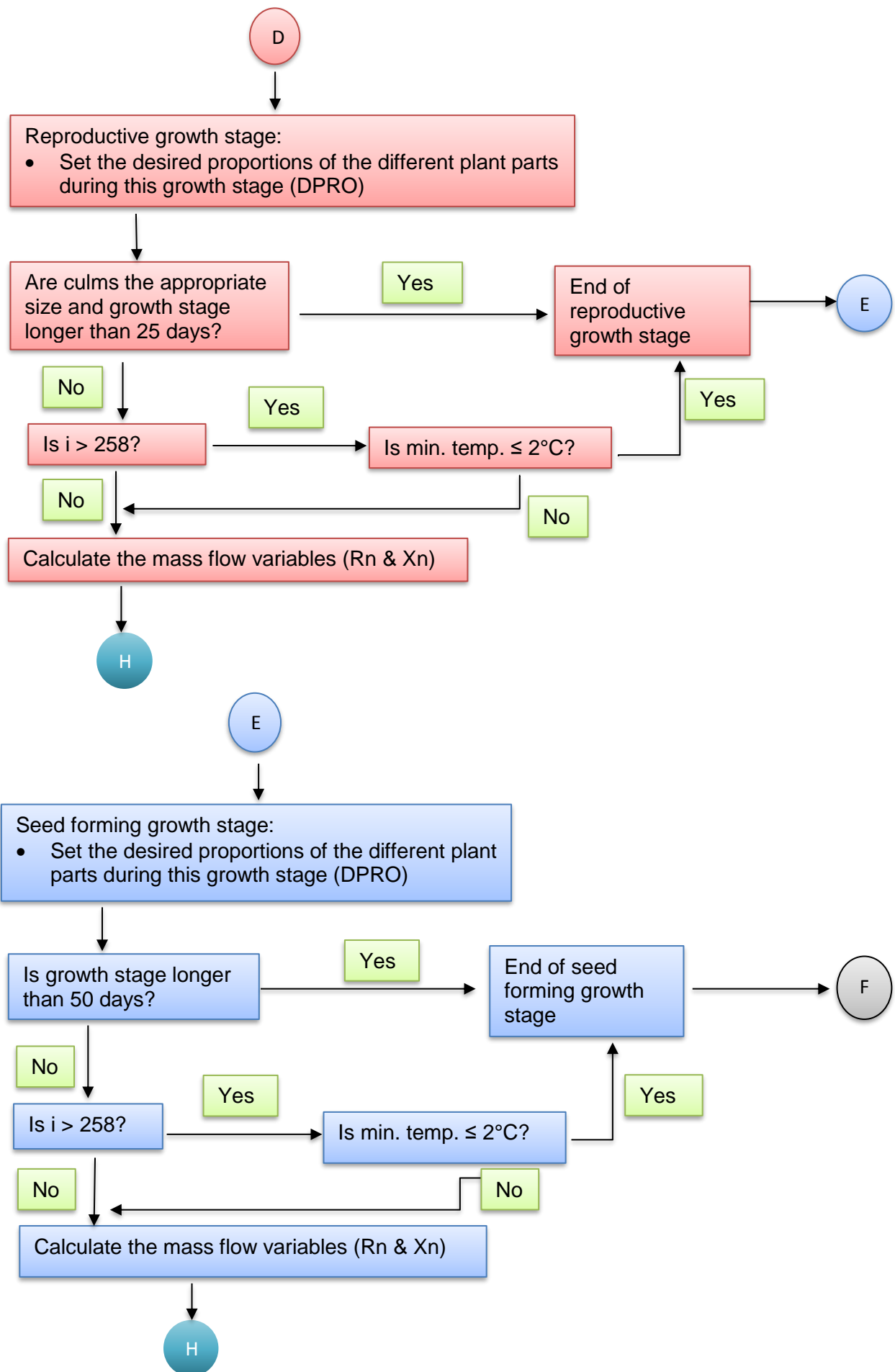
Lastly, there is an option in the model regarding the carryover of soil water from one season to the next. The algorithm for this is found from lines 633 to 649 in Appendix A and three options are possible. Firstly, no soil water can be carried over and the initial value for the season must be specified as a new initial value. Secondly, the end value of the previous season can be carried over to the next subsequent season, and thirdly there can be compensated for soil water evaporation during the winter by allowing 0.3 mm.d⁻¹ soil water withdrawal as a result of soil water evaporation (used in PUTU VELD, Appendix A lines 651 – 655).

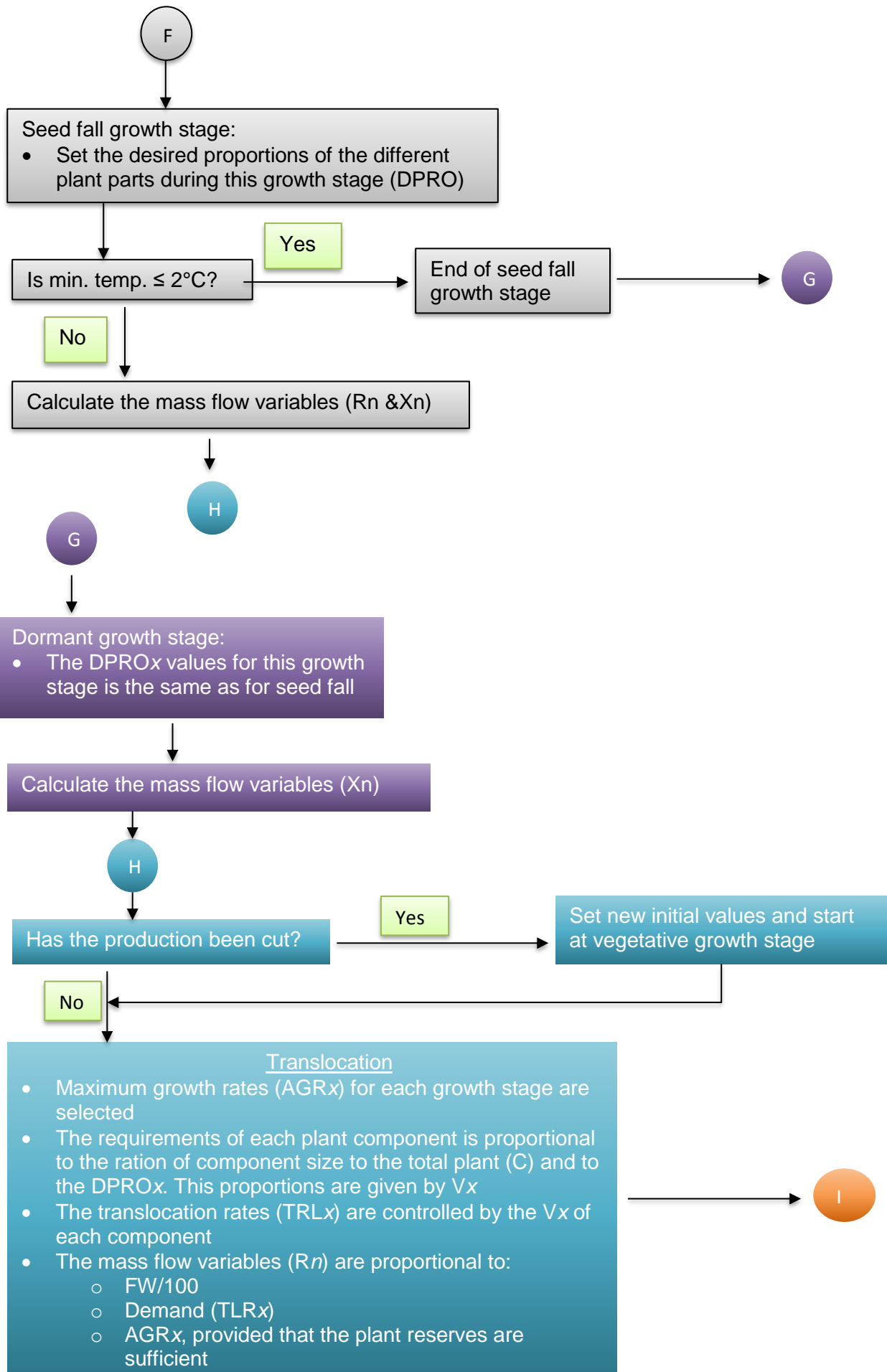
To get a clearer picture of the PUTU VELD model one should consult Figure 3.18 which illustrates in a simple manner the process that the model follows. Figure 3.18 is

divided into sections just like in the code of the model. Section A (purple background, black font) deals with the determination of the initial masses of the different plant components (line 361 in Appendix A). Section B (light blue background, black font) contains the start of the simulations per day of the growth season as well as the water balance (line 393 in Appendix A). Section C (orange background, black font) contains the environmental factors and production (line 685 in Appendix A). Section D (red background, black font) denotes the start of the productive stage (growth stage 2) (line 909 in Appendix A). Section E (darker blue background, black font) represents the start of the seed stage (growth stage 3) (line 948 in Appendix A). Section F (grey background, black font) marks the start of the seed fall stage (growth stage 4) (line 989 in Appendix A). Section G (darker purple background, white font) represents the dormant stage (growth stage 5) (line 1024 in Appendix A). Section H (blue background, white font) contains the calculation of the mass flow variables as well as translocation (line 1174 in Appendix A). Finally, Section I (orange background, white font) tests for the availability of the reserves (line 1189 in Appendix A).









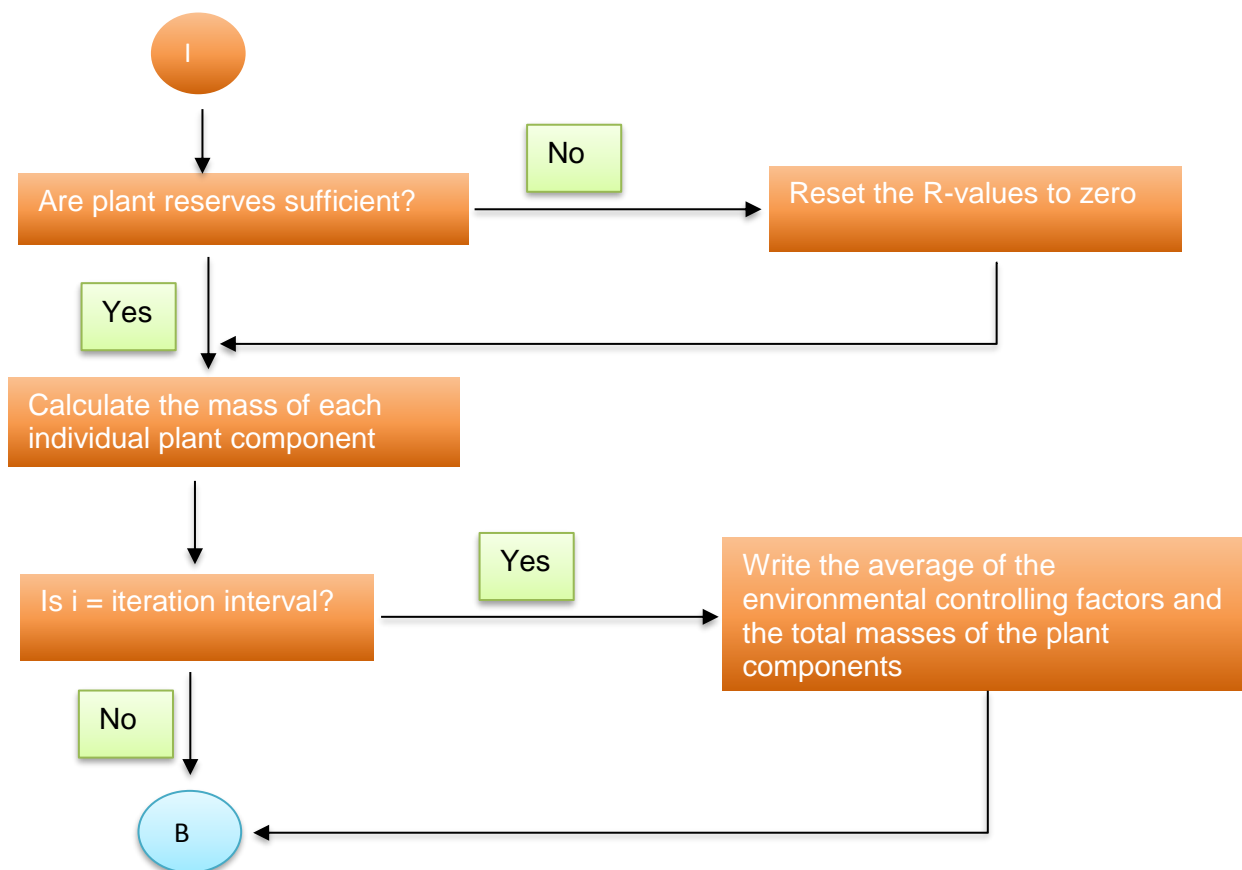


Figure 3.18 Detailed Forrester diagram explaining the PUTU VELD model (adapted from Booyesen, 1983).

3.4 Assumptions

There are certain conditions that needs to be taken into account before the output data is analysed and conclusions are made. Fire is a frequent and recurring driver of change and disturbance in rangelands (Section 2.1.4). It plays an important ecological role and influences vegetation structure and dynamics, species composition, habitat values and ecosystem functioning. Fire can be seen as an advantage (removing old biomass or unwanted grass species) or a disadvantage (destroying biomass used as feed for animal production, seen as a negative impact for the next 12 to 18 months) (Sabiiti *et al.*, 1992; Snyman, 2003a; Snyman, 2004a; Snyman, 2004b; Snyman, 2006; van Etten, 2017). To simulate fire occurrences temperature, relative humidity, wind speed and fuel wetness is needed as input (Teague *et al.*, 2008) of which only temperature is used as input for PUTU VELD. For these reasons, the PUTU VELD model does not simulate fire and therefore we assume that no fire incidences occurred during the simulation time periods.

Species composition of rangeland can change due to climatic factors, fire occurrence or the utilisation of the rangeland. When conditions are optimal there will be more climax grasses and when they are poor the rangeland will be dominated by increaser species (Smet & Ward, 2009). Animal grazing has a detrimental effect on species composition when not managed properly and continuous grazing can change a rangeland from climax to an increaser rangeland which is mostly unpalatable for the animals (Smet & Ward, 2009). In the real world, this can be controlled with the correct management practices and mitigation steps (van der Westhuizen *et al.*, 2001; Landsberg *et al.*, 2003; Snyman *et al.*, 2013; Zarekia *et al.* 2013; Jawuoro *et al.*, 2017). As the PUTU VELD model is developed for a climax veld of *Themeda-Cymbopogon* no other species is used in the model as the simulations would become very complex and it was for this reason that it was assumed that the species composition of the rangeland did not change.

Bush encroachment has a damaging effect on rangeland production as it leads to reduced grass biomass production which in turn leads to a decrease in animal productivity (Kraaij & Ward, 2006; O'Connor *et al.*, 2014; Kgosikoma *et al.*, 2012). It also has a negative economic impact (Mugasi *et al.*, 2000) and reduces the carrying capacity of a rangeland (Wiegand *et al.*, 2006). The increase in bush encroachment is an indication that the rangelands are being degraded (Oba *et al.*, 2000). The Sydenham Experimental Farm noted no bush encroachment during the monitoring period of the rangeland (Snyman, 2013). Therefore, PUTU VELD does not take into account bush encroachment and it was assumed that there was no bush encroachment during the future simulation periods as well.

Livestock need to feed but grazing rangelands at the wrong time can be detrimental to the biomass production of the rangeland and cause a decline in biomass in subsequent years (Liu *et al.*, 2016). Grazing can be a complex scenario to model and most RP models take into account that the rangeland was cut and not grazed (Cingolani *et al.*, 2005). The Sydenham Experimental Farm was not grazed during the period that the rangeland was monitored and was only cut once during each growth season (Snyman, 2013) to obtain the dry matter production that was used in the validation of the PUTU VELD model. For this reason, it was assumed that the DMP in the PUTU VELD model was not grazed but cut once during each growth season.

Global climate models (GCMs) (Section 3.2.2) are complex models that are based on the general principles of thermodynamics and fluid dynamics and simulate the conditions of the atmosphere (Stute *et al.*, 2001; Bader *et al.*, 2008). An advantage of GCMs is their aptitude to perform multiple simulations trials using different greenhouse gas emission scenarios while a disadvantage is that, although computer power continues to increase precipitously, GCMs currently do not resolve smaller-scale climate features (Bader *et al.*, 2008; Lupo & Kinimonth, 2017). There is however extensive confidence in GCMs to provide credible quantitative estimates of future climate change (Randall *et al.*, 2007). It was therefore assumed that the GCMs used in this study gave a good representation of the future state of the climate and that the use of various ensemble members would decrease the uncertainty and provide a better, average picture of the atmospheric conditions.

3.5 Analysis of PUTU VELD Output Data

The PUTU VELD output data was analyzed using various validation statistics and cumulative distribution functions as described below.

3.5.1 Validation of the PUTU VELD model

The most critical step in modelling is the process of validation. According to Loomis *et al.* (1979) verification and validation is distinguished from each other through the fact that the former is the process by which the model is investigated to determine to which degree it can handle the data as was initially intended (Klemmer *et al.*, 2011). Validation is the test of the results from the program against experimental determined results. Deviations from the reality usually testify of a model with errors or comprehensive assumptions of basic processes that actually require drastic investigation and rectification. The verification of the model was performed by Booysen (1983) and Fouché (1992) and will not be discussed further. Previous studies on model validation suggest the use of numerous statistics to validate production models (e.g. Brisson *et al.*, 2004; Ruiz-Ramon & Mínguez, 2006; Moulton *et al.*, 2009; McNider *et al.*, 2015). The various proposed statistics to be used will be discussed in detail below. PUTU VELD was previously validated by Fouché (1992) for a relatively short period.

For the interest of this study, PUTU VELD was tested against a set of performance measures using simulated production data using SAWS and AgMIP climate data and

observed production data from Sydenham Experimental Farm (Section 3.2). The performance measures included mean absolute error (MAE), root mean square error (RMSE), index of agreement (d), correlation coefficient (r) and coefficient of determination (R^2), which allow comparative assessment of the RP model performance at a particular data point (Brisson *et al.*, 2004; Ruiz-Ramon & Mínguez, 2006; Moulton *et al.*, 2009; Ahmed & Hassan, 2011; McNider *et al.*, 2015).

3.5.1.1 Mean Absolute Error (MAE)

The MAE is a simple measure of the accuracy of a simulation model. Simply put, it is the mean of the absolute errors. An absolute error is the absolute value of the difference between the simulated production value and the observed production value (Mayer & Butler, 1993). It is calculated by:

$$MAE = n^{-1} \sum_{i=1}^n |P_i - O_i| \quad (3.50)$$

where: n = The number of observations;
 P_i = The simulated (predictand) production yields; and
 O_i = The measured (observed) production yields.

The MAE can tell us how big of an error we can expect from the simulation on average. We can also compare MAE and RMSE to determine whether the forecast contains large but infrequent errors. The larger the difference between MAE and RMSE, the more inconsistent the error size (Wood, 2012).

3.5.1.2 Root Mean Square Error (RMSE)

The RMSE has been used as a standard statistical metric of model performance in air quality, climate and meteorology research studies (Chai & Draxler, 2014). Willmott *et al.* (1985), van der Burgt *et al.* (2006) and Bitri *et al.* (2014) describe the RMSE as a measure of the overall deviation between the observed and simulated production values, specifically, a mock indicator of the absolute model uncertainty. It is calculated as:

$$RMSE = \left[\sum_{i=1}^n \frac{(P_i - O_i)^2}{n} \right]^{0.5} \quad (3.51)$$

It attains the same units of the variable being simulated, and hence the closer the value is to 0, the better the model simulation performance (Bitri *et al.*, 2014).

3.5.1.3 Index of agreement (d)

The index of agreement (d) was used to measure the degree to which the RP model's predictions were error free (Willmott *et al.*, 1985; Willmott *et al.*, 2011). The statistic assesses the sum of squared deviations between simulated and observed data, relative to the sum of squared absolute deviations from the mean for both simulated and observed data. Therefore, it measures the simulation error on variation in observations and simulation results (van der Burgt *et al.*, 2006). It was calculated as:

$$d = 1 - \frac{\sum_{i=1}^n (P_i - O_i)^2}{\sum_{i=1}^n (|P_i - \bar{O}| + |O_i - \bar{O}|)^2} \quad (3.52)$$

where: \bar{O} = The mean of the measured productions yields.

The index of agreement varies between 0 (complete disagreement) and 1 (complete agreement between the measured and simulated production yields).

3.5.1.4 Correlation Coefficient (r)

The linear correlation coefficient (r) is a measure of the direction and strength of a linear relationship between the simulated and measured production yields (Lane, 2016; Weisstein, 2016). It can be calculated by:

$$r = \frac{n \sum P_i O_i - (\sum P_i)(\sum O_i)}{\sqrt{n(\sum P_i^2) - (\sum P_i)^2} \sqrt{n(\sum O_i^2) - (\sum O_i)^2}} \quad (3.53)$$

The value of r is such that $-1 \leq r \leq +1$. The negative and positive signs are used to denote a negative or positive linear correlation, respectively. For a negative correlation, P_i increases while O_i decreases. For a positive correlation, P_i increases when O_i increases.

3.5.1.5 Coefficient of Determination (R^2)

The coefficient of determination (R^2) is used to analyse to what extent variability in one variable can be explained by a difference in a second variable and is calculated using the following equation:

$$R^2 = \frac{SSR}{SST} = 1 - \frac{SSE}{SST} \quad (3.54)$$

where: SSR = The regression sum of squares;

SST = The total sum of squared deviations of the predicted values around their mean; and

SSE = The sum of squared differences between the residuals/errors and their means.

R^2 can be explained as that portion of the variation of the predictand (proportional to SST) that is “described” or “accounted for” by the regression (SSR) (Mendenhall & Sincich, 2003; Wilks, 2006). For a perfect fit, $SSR = SST$ and $SSE = 0$, so that $R^2 = 1$. For an extremely poor fit, $SSR = 0$ and $SSE = SST$, so that $R^2 = 0$ (Wilks, 2006).

3.5.2 Cumulative Distribution Function (CDF)

The cumulative distribution function (CDF) ($D_{(x)}$) is used to determine the probability that a random observation (X) that is taken from the data being used will be less than or equal to a certain value (x) (Weisstein, 2017). It can also be used to determine the probability that an observation will be greater than a certain value, or between two values (Minitab, 2017; Weisstein, 2017). The CDF is related to a discrete probability ($P_{(x)}$) and is calculated by:

$$D_{(x)} = P(X \leq x) \quad (3.55)$$

CDFs was also used to interpret any differences between simulated RP for the historical base and future periods.

3.6 Seasonal Prediction of Maximum Dry Matter Production

The value of being able to predict DMPmax for the forthcoming season cannot be denied. An indication of how the following growth season will be, can help guide the implementation of mitigation steps to minimize the loss or maximize the gains. ENSO (Section 2.4) was shown to be one of the most dominant large-scale climate modes to affect Southern Africa’s rainfall variability over the summer rainfall region (Ambrosino *et al.*, 2011). For example, Landman *et al.* (2001), and Moeletsi *et al.* (2011) used the state of ENSO to predict streamflow and rainfall characteristics for maize yields, respectively, in South Africa. For this reason, the correlation between the 3-month running mean of Niño 3.4 anomalies and standardized DMPmax was investigated. Since El Niño or La Niño have historically developed during the austral autumn months and reached its peak intensity in mid-summer (IRI, 2017). Thus, in order to be useful

as a potential predictor for DMPmax, the current year's 3-month running mean of Niño 3.4 anomalies could only be considered from March onwards (i.e. March-April-May or MAM).

It is preferred that the date of occurrence of DMPmax (Dtp) occurs anytime from March as it will result in a higher DMP. Dtp early in the growing season means that there wasn't enough time for a larger DMP to occur so production might be poor. The optimal period for Dtp to occur is between day of growth season 244 (1 March) and 304 (30 April). A Dtp that occurs later than this results in a risk of cold temperature (chilling and freezing) damage. This implied that only the 3-month running mean of Niño 3.4 anomalies up to February (i.e. DJF) can be considered as potential predictors in order to facilitate an adequate lead time. Therefore, the potential predictors for the unfolding season's DMPmax were the 3-month running mean of Niño 3.4 anomalies for the following seasons: MAM, AMJ, MJJ, JJA, JAS, ASO, SON, OND, NDJ, and DJF.

3.7 Process Description

For the sake of clarity, a summary of the process that was followed from data acquisition to data analysis is included here:

1) Data collection

a) Historical climate data:

- i) Obtained data from SAWS for the base period: 1980/81 – 2009/10 for Bloemfontein Airport and Bloemfontein City
 - Daily minimum and maximum temperature, rainfall and sunshine hours
- ii) Patched using data from stations at Bloemfontein city and University of the Free State
- iii) Calculate ET, using Hargreaves-Samani method
- iv) Structure the data into the correct format for RPM

b) Future simulated climate data:

- i) Obtain GCM data from AgMIP project
 - 1 base period: 1980/81 – 2009/10 and 3 future periods: 2010/11 – 2039/40 2040/41 – 2069/70; and 2070/71 – 2098/99
 - 2 RCP scenarios: 4.5 W.m⁻² and 8.5 W.m⁻²

- 5 GCMs: CCSM4, GFDL-ESM2M, HadGEM2-ES, MIROC5 and MPI-ESM-ER
 - Daily minimum and maximum temperature, rainfall and solar radiation
- ii) Convert solar radiation ($\text{MJ.m}^{-2}.\text{d}^{-1}$) to sunshine hours using WTON *Microsoft excel* program
 - iii) Calculate ET using Hargreaves-Samani method
 - iv) Structure the data into the correct format for RPM
- c) Historical rangeland production data:
- Obtain observed rangeland production data from Sydenham Experimental Farm for the base period: 1980/81 – 2009/10
- 2) Obtain working version of the RPM
 - a) Rewrote the QBasic version of PUTU 11 into FORTRAN 95
 - b) Restructured the code so that there are no more subroutines
 - c) Fixed minor errors with respect to translocation
 - d) RPM now called PUTU VELD to clarify its purpose
 - 3) Validate PUTU VELD for historical base period
 - a) Run PUTU VELD using observed SAWS climate data
 - b) Compare the results to the data obtained from Sydenham
 - c) Standardise the DMPmax and find the correlation between the 3-month running mean of Niño 3.4 anomalies and standardized DMPmax
 - d) Run PUTU VELD using historical modelled AgMIP climate data
 - e) Compare the results to those obtained from the simulation with SAWS climate data (compare simulated data with simulated data)
 - f) Analyse the results
 - 4) Run PUTU VELD for AgMIP climate data for the future periods
 - a) 2 RCPs and 5 GCMs
 - b) Compare the 3 periods (2010/11 – 2039/40; 2040/41 – 2069/70; and 2070/71 – 2098/99) with each other as well as against the base period
 - c) Analyse the results

The results and discussion will follow the same outline as the process description presented in the Methodology (Section 3.7). Where findings were presented graphically, care was taken to depict the actually observed (Section 4.1) or base period data (Section 4.3) in black in order to facilitate the interpretation and comparison thereof.

4.1 Validation of the PUTU VELD Model

The initial validation of PUTU VELD (originally referred to as PUTU 11; Section 3.3) was done by Fouché (1992) (henceforth known as PV-Fouché) for a nine-year period (1980/81 – 1988/89) using historically observed climate data from Glen Agricultural College against measured rangeland production (RP) from Sydenham Experimental Farm (henceforth referred to as Sydenham). It should be noted that Sydenham is located ± 30 km south south west of Glen. For comparison, a validation was performed by feeding PUTU VELD with SAWS climate data from the nearby Bloemfontein airport for the same nine-year time period, and extending it for the complete 30-year base period (1980/81 – 2009/10) (henceforth known as PV-SAWS). The validation statistics for simulations using the GCM derived climate data from AgMIP (henceforth known as PV-AgMIP) was also calculated. Simulated maximum dry matter production (DMPmax) was compared against the measured RP for Sydenham (Section 3.2.1). The results are shown in Table 4.1. The time series presented in Figure 4.1 provides a visual comparison between the PUTU VELD simulated RPs for the shorter nine-year period (PV-Fouché) and the longer 30-year base period (PV-SAWS) against the measured RP from Sydenham. It should be noted that PUTU VELD contains only minor modifications to the initial masses for the different plant parts (Table 3.4) as these were erroneous in PUTU 11 as used by Booysen (1983) and Fouche (1992).

The original 9-year validation of PUTU 11 showed very good results (e.g. $R^2 = 0.92$, RMSE = 239.26, $d = 0.98$). However, neither the QBasic model version published in Fouché (1992), nor the earlier FORTRAN version of Booysen (1983) or the later QBasic versions obtained from Swiegelaar (2014³) managed to duplicate these

³ Miss E. Swiegelaar, personal communication, Agricultural Research Council, Animal Production, Bloemfontein, September 2014.

results, even when using the same climate data from Glen. The closest match (as represented by the values in brackets in Table 4.1) was obtained by the slightly modified PUTU VELD version used in this study (e.g. $R^2 = 0.78$, $RMSE = 509.48$, $d = 0.91$). Comparing the two shorter 9-year period data sets (PV-Fouché and PV-SAWS, Figure 4.1), one can see that they followed the same trend in four of the nine years. This discrepancy could be attributed to the different sources of historically observed climate data as highlighted above.

Table 4.1 Validation statistics for the original nine years (1980/81 – 1988/89) and the extended 30-year base period (1980/81 – 2009/10) (n = number of years, Min. Prod. = minimum dry matter production, Max. Prod. = maximum dry matter production, MAE = mean absolute error, RMSE = root mean square error, d = index of agreement, r = correlation coefficient and R^2 = coefficient of determination; * indicates value obtained using PUTU VELD and climate data from Glen)

	PV-Fouché	PV-SAWS	PV-SAWS	PV-AgMIP
n	9	9	30	30
Min. Prod.	350.00 (256.96)*	466.83	466.83	261.38
Max. Prod.	2300.00 (3272.48)*	2327.77	4082.75	2711.57
MAE	596.98 (336.58)*	381.52	610.30	588.91
RMSE	239.26 (509.48)*	624.44	895.12	743.83
d	0.98 (0.91)*	0.80	0.69	0.72
r	0.96 (0.88)*	0.65	0.53	0.58
R^2	0.92 (0.78)*	0.42	0.28	0.34

The biggest setback came when PUTU VELD was validated over the extended base period (e.g. $R^2 = 0.28$, $RMSE = 895.12$, $d = 0.69$), indicating severe issues with the model's robustness. This problem could have arisen from a failure to use an independent data set when calibrating and validating the model. Such issues with "overfitting" were highlighted by Wilks (2006). The best positive aspect of the PV-SAWS 30-year run was the fair positive correlation ($r = 0.53$) with the Sydenham

RP (Table 4.1). Unfortunately, PV-SAWS seemed to show a lag in its response and only followed the same trend as Sydenham for a few of the years.

In terms of the index of agreement, the PV-SAWS was the furthest from 1 which means that there was less agreement between the simulated RP data and the measured RP data. The two long time period data sets (Sydenham and PV-SAWS) followed the same tendency (direction of change) for about half of the years. The variance in the PV-SAWS, as depicted by a standard deviation of 989.59 kg.ha⁻¹, was considerably higher than that measured at Sydenham (i.e. 692.24 kg.ha⁻¹). For certain time periods there also seemed to be a lag between PV-SAWS and Sydenham (e.g. 1985/86 and 2006/07). However, simply applying a +1 or -1 year lag yielded poorer results (i.e. R² = 0.10 and 0.06, respectively). It seemed that the seasons when PUTU VELD faired exceptionally poor was characterized by highly variable rainfall (e.g. 1985/86 was very dry and 2000/01 was very wet). It may be speculated that the model's soil water section could be at fault. Due to the fact that PUTU VELD is used in the industry (Manley, 2012⁴), it was hoped that another amended version yielding better results would still come forward. Unfortunately, this was never the case and due to time constraints alternative biophysical rangeland production models could not be considered.

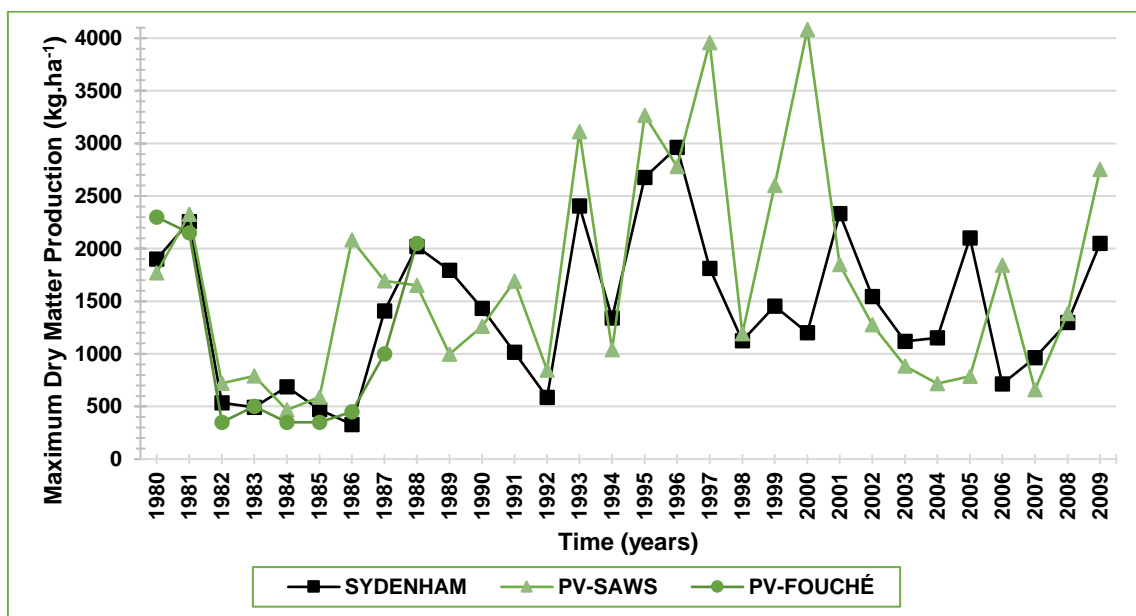


Figure 4.1 Time series comparison between simulated rangeland production data from PV-Fouché, PV-SAWS and the measured rangeland production data from Sydenham Experimental Farm.

⁴ Mr. C. Manley, personal communication, Systems Developer at SANTAM Agriculture, Bloemfontein, April 2012.

4.2 Simulated Rangeland Production during the Historical Base Period (1980/81 – 2009/10)

In light of the model validation, the results of this study should be interpreted and extrapolated with caution and should only be understood in light of this report.

4.2.1 Maximum Dry Matter Production

To clarify for the discussions that follows PV-SAWS DMPmax denotes the maximum dry matter production (biomass) for every growing season (one value for each year) as simulated by PUTU VELD using observed climate data from SAWS. In turn, PV-AgMIP DMPmax represents similar values obtained from PUTU VELD simulations using the GCM derived climate data from AgMIP. A comparison between PV-SAWS DMPmax and PV-AgMIP DMPmax (Figure 4.2) shows a reasonably good correlation with a R^2 of 0.53. A perfect fit was not expected (nor required) as the GCMs are not able to predict day-to-day weather accurately but rather the long-term averages and variability (Kirtman *et al.*, 2013). In light of the above, a R^2 of 0.53 is fairly good and implies that the AgMIP data can be used for future simulations.

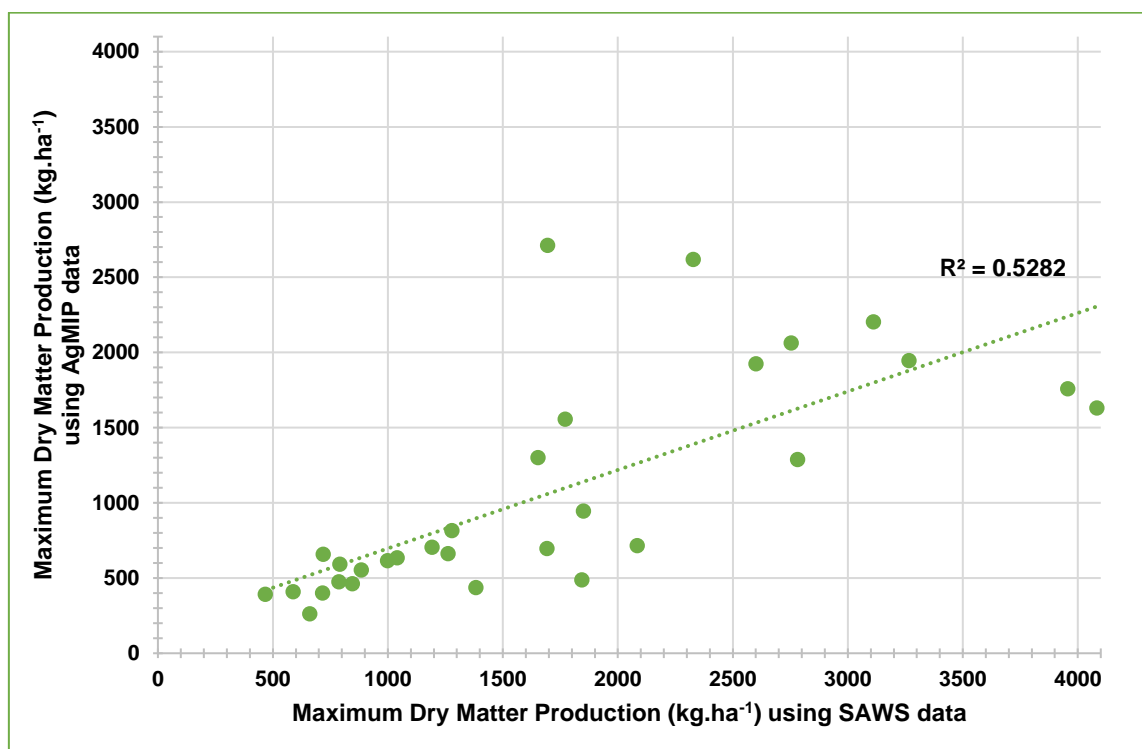


Figure 4.2 Scatterplot of the PUTU VELD simulated maximum dry matter production in Bloemfontein over the historical base period (1980/81 – 2009/10) using observed climate data (PV-SAWS) and GCM-derived climate data (PV-AgMIP).

The CDFs in Figure 4.3 show that PV-AgMIP fell below PV-SAWS, implying that DMPmax will normally be under-forecasted for future time periods. For example, the 33.3rd and 66.6th percentiles corresponded to PV-SAWS DMPmax values of 998.52 kg.ha⁻¹ and 1850.27 kg.ha⁻¹, respectively, while these respective values were 592.25 kg.ha⁻¹ and 1299.39 kg.ha⁻¹ for PV-AgMIP. It is suspected that the AgMIP GCMs do not adequately account for the extreme weather events such as major floods and droughts. During the wettest 3-year period (1986/87 – 1988/89) the total rainfall was 2183.9 mm. PV-SAWS and PV-AgMIP overestimated the accumulated DMPmax at 5431.48 and 4726.97 kg.ha⁻¹, respectively, when compared to the measured accumulated DMPmax from Sydenham (3756.52 kg.ha⁻¹). During the driest 3-year period (1983/84 – 1985/86) the total rainfall was 1136.9 mm. PV-SAWS overestimated (1846.34 kg.ha⁻¹) while PV-AgMIP underestimated (1391.72 kg.ha⁻¹) the accumulated DMPmax when compared to the measured accumulated DMPmax from Sydenham (1649.72 kg.ha⁻¹).

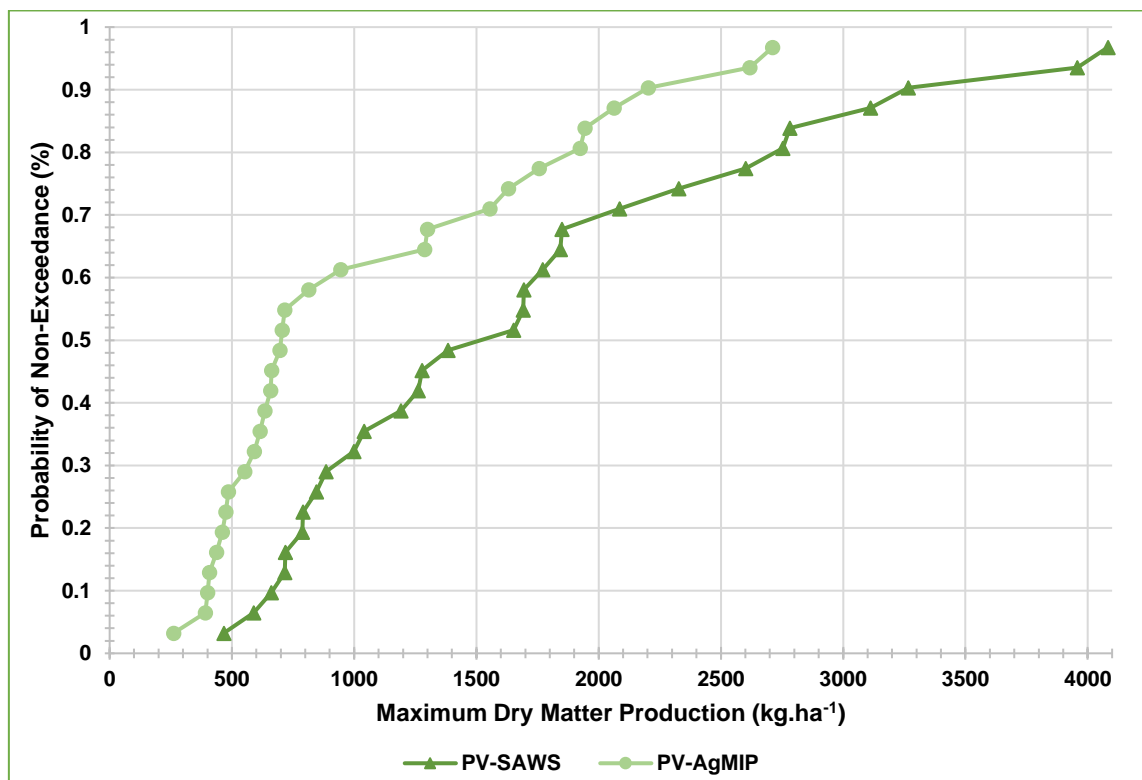


Figure 4.3 Cumulative distribution functions of the PUTU VELD simulated maximum dry matter production in Bloemfontein over the historical base period (1980/81 – 2009/10) using observed climate data (PV-SAWS) and GCM-derived climate data (PV-AgMIP).

The time series presented in Figure 4.4 clearly depicts the concomitant series of PV-SAWS and PV-AgMIP DMPmax. Regression analysis revealed a weak positive trend in PV-SAWS DMPmax in contrast to a weak negative trend in PV-AgMIP DMPmax (simple linear regression equations are provided at the bottom of Figure 4.4). As was expected, the smaller variance in the GCM-derived climate data (AgMIP) resulted in a relatively smoother PV-AgMIP DMPmax when compared to the PV-SAWS DMPmax. This is particularly evident during 1995/1996 – 1997/98 (Figure 4.4). Although PV-AgMIP generally underestimated the DMPmax (Figure 4.5) it was still decided to run the PUTU VELD model for the future time periods. There was a 46% difference between the accumulated DMPmax for PV-SAWS (51083.39 kg.ha⁻¹) and PV-AgMIP (31907.17 kg.ha⁻¹) over the 30-year base period. It is interesting to note that the PV-AgMIP DMPmax simulation fared much better during those highly variable seasons highlighted in Section 4.1 (i.e. 1985/86 and 2000/01). There is, however, no scientific reason why PV-AgMIP DMPmax should be closer to the Sydenham measured RP than the PV-SAWS DMPmax for these seasons.

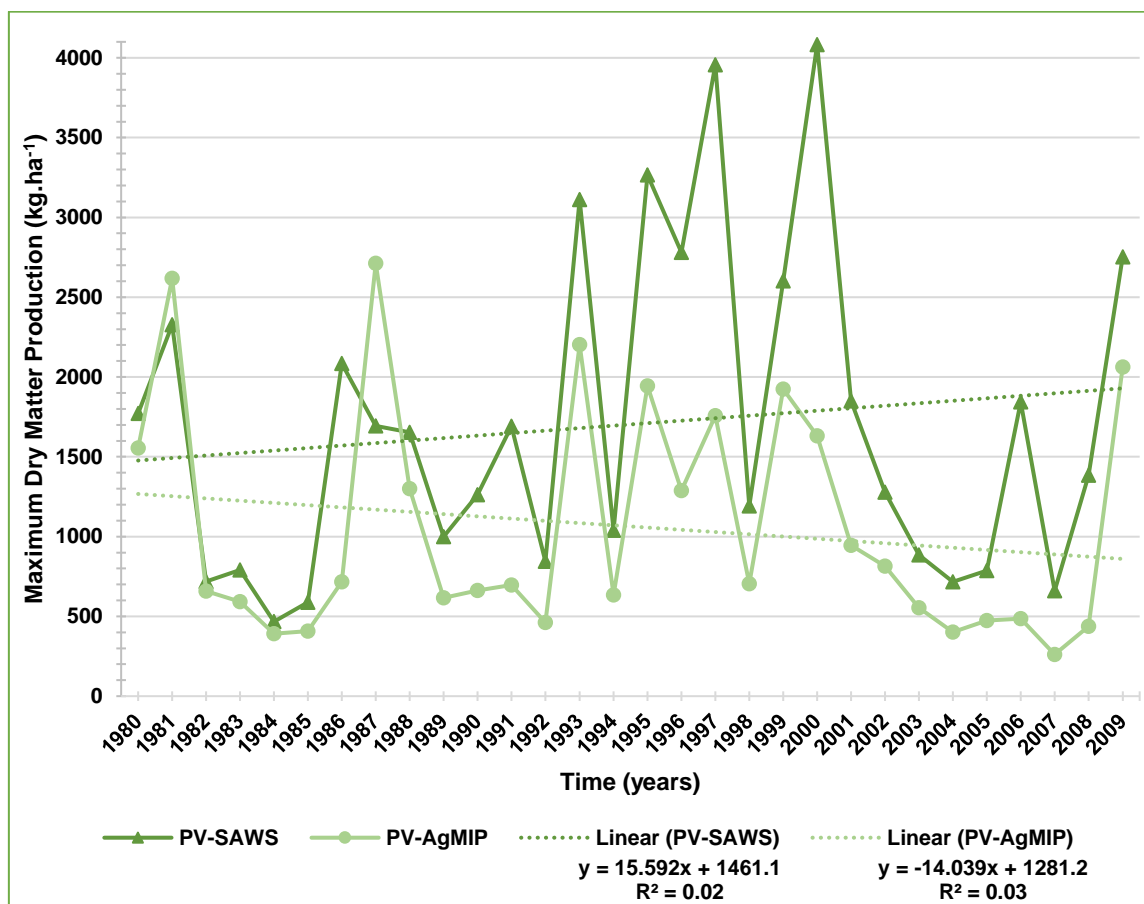


Figure 4.4 Time series comparison of PUTU VELD simulated maximum dry matter production in Bloemfontein using observed climate data (PV-SAWS) and GCM-derived climate data (PV-AgMIP).

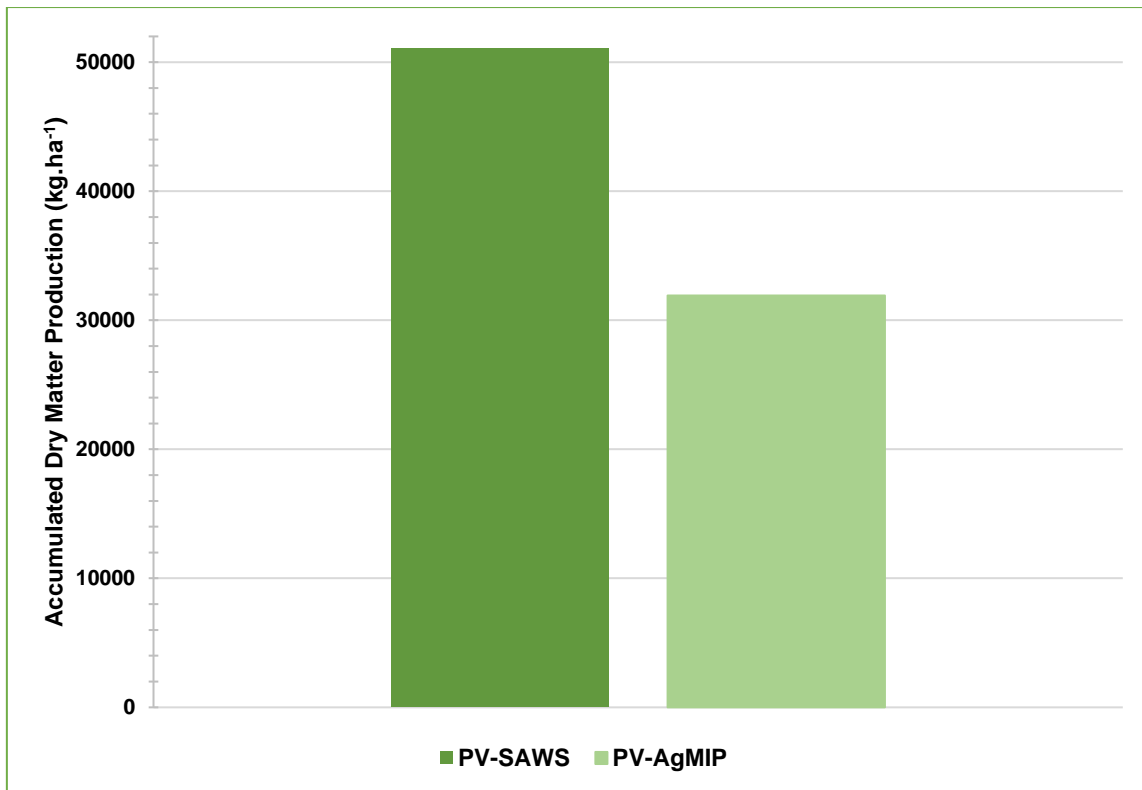


Figure 4.5 Accumulated maximum dry matter production in Bloemfontein for the historical base period (1980/81 – 2009/10) using observed climate data (PV-SAWS) and GCM-derived climate data (PV-AgMIP).

4.2.2 Date of Occurrence of Maximum Dry Matter Production

The day of the growth season that the DMPmax occurs (Dtp) is a good indication of ability to produce an adequate amount of DMP for livestock consumption. As mentioned in Section 3.5, the optimal period for Dtp to occur falls between day of growth season 244 (1 March) and 304 (30 April). The date on which Dtp occurs can be attributed to various weather factors. For example, a drought occurring middle of the season (summer months) or floods occurring during the rainy season (summer months) may result in the Dtp not occurring during the optimal period. The basic growth pattern of a grass plant is illustrated in Figure 4.6 where the top dotted line, representing a slowdown in seed formation, corresponds to DMPmax in Figure 4.7.

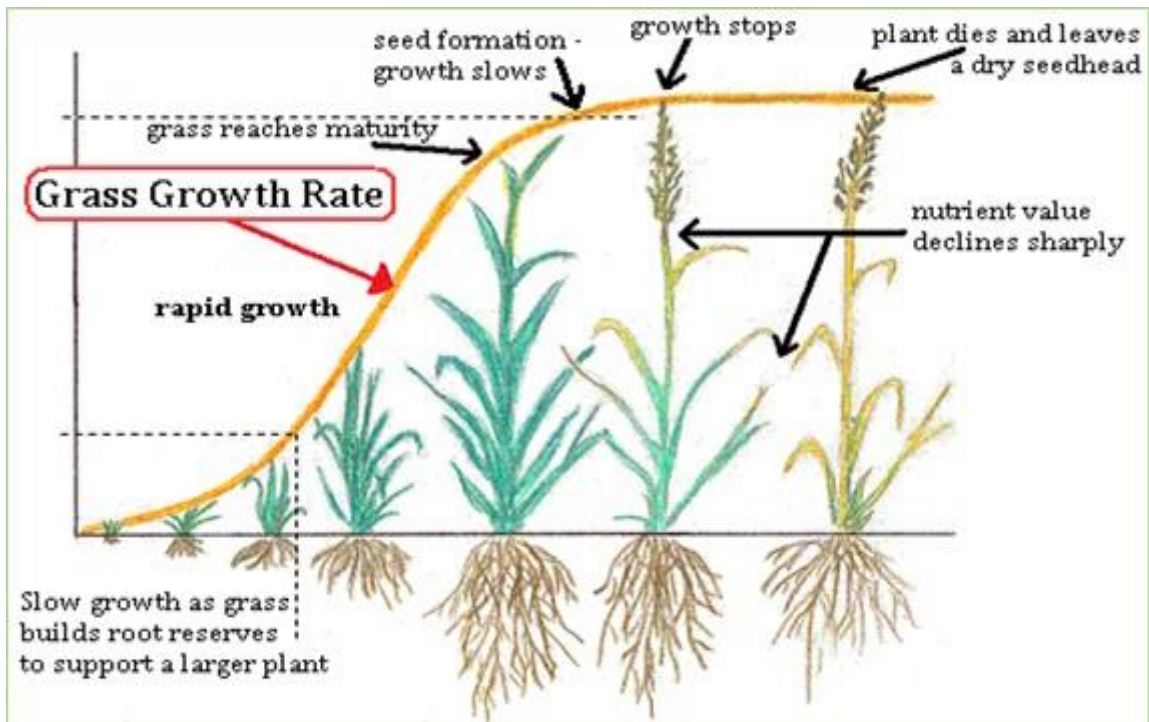


Figure 4.6 Basic growth curve of a grass plant (Grass Fed Solutions, 2016).

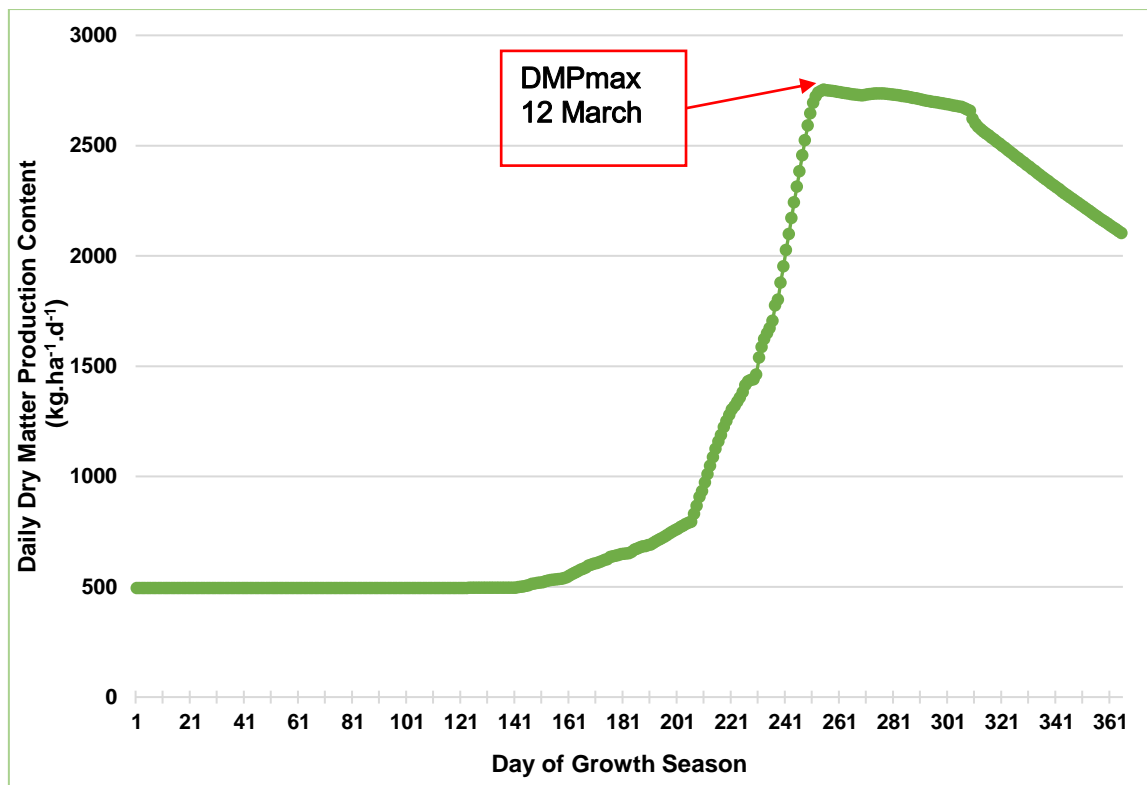


Figure 4.7 Daily dry matter production simulated by PUTU VELD for Bloemfontein during a typical growing season (2009/10).

Figure 4.8 shows that 83% of both the PV-SAWS Dtp and PV-AgMIP Dtp for the base period occurred during the optimal period of day 244 – 304. Historically speaking, there was a 94% probability that Dtp occurred after day 244 and an 84% probability that Dtp fell before day 304 for PV-SAWS. For PV-AgMIP there was an 80% probability that Dtp would not exceed day 304, while Dtp falling before day 244 was highly unlikely. Generally, the probability of Dtp occurring in the optimal period was high. In Figure 4.9 it can be seen that the Dtp for PV-SAWS and PV-AgMIP followed a similar weak negative trend, implying a tendency for Dtp to occur slightly earlier in the season with time. PV-SAWS Dtp exhibited a higher variance.

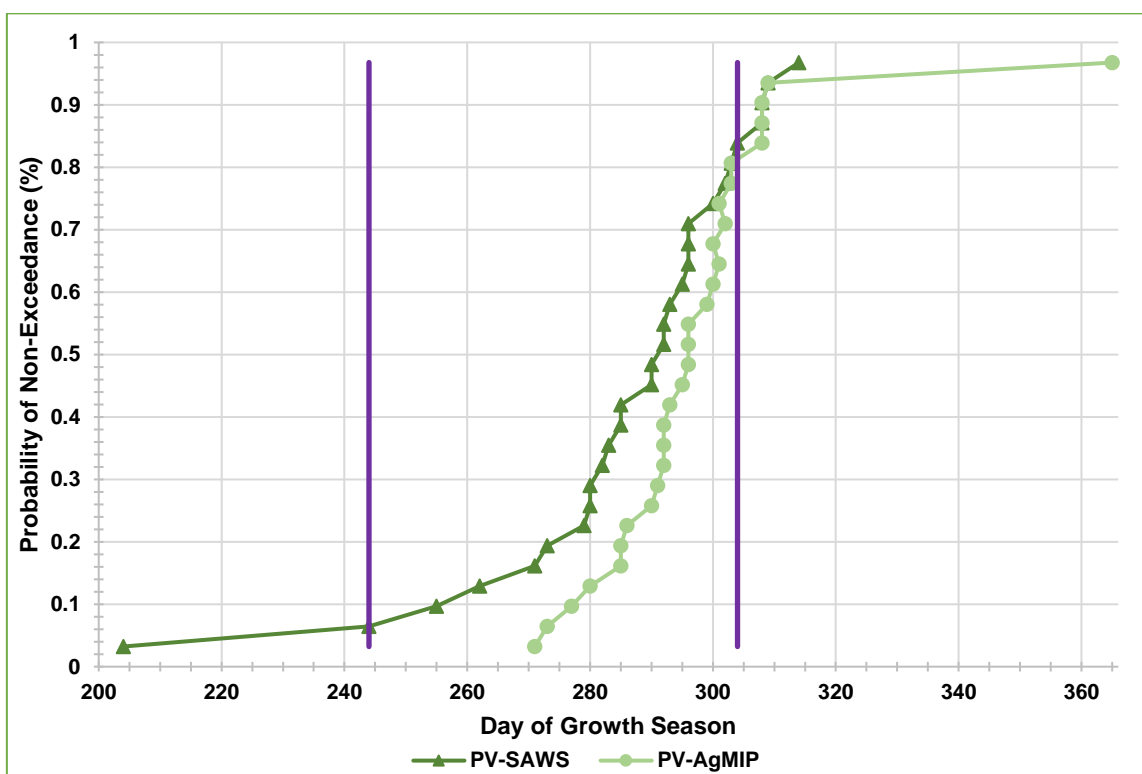


Figure 4.8 Cumulative distribution functions of the PUTU VELD simulated date (Dtp) on which maximum dry matter production occurred in Bloemfontein for the base period (1980/81 – 2009/10) using observed climate data (PV-SAWS) and GCM-derived climate data (PV-AgMIP). The two vertical lines demarcate the optimal period (244 – 304) for Dtp to occur.

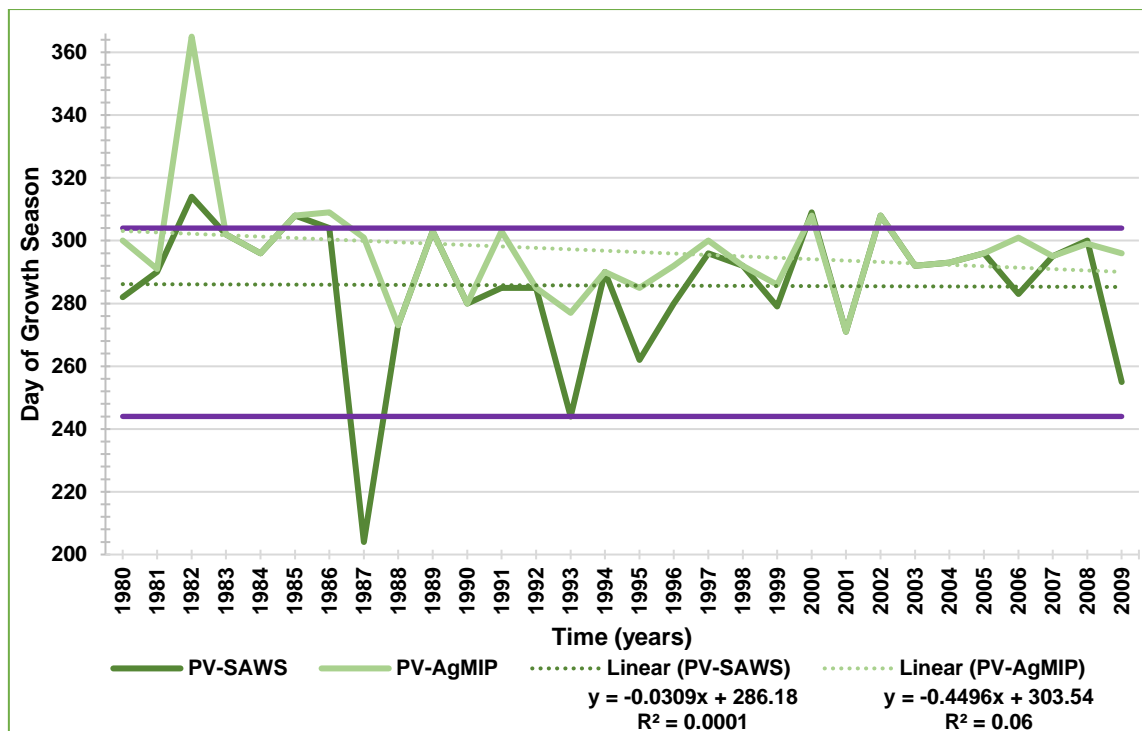


Figure 4.9 Time series comparison for the date (Dtp) on which maximum dry matter production occur in Bloemfontein for the base period (1980/81 – 2009/10) using observed climate data (PV-SAWS) and GCM-derived climate data (AgMIP). The two horizontal purple lines demarcate the optimal period (244 – 304) for Dtp to occur.

4.2.3 Number of Moisture Stress Days

A moisture stress day (MSD) is accepted in this context to start when the hydraulic limiting factor (FW) drops below 50% at an average daily temperature higher than 15°C (Section 3.3.1.3.4). A good result will be a low MSD total which means that there was an adequate supply of water for the plant to utilize in the process of photosynthesis and that no wilting occurred. Figure 4.10 clearly shows that there was a lower number of MSD for PV-SAWS than for PV-AgMIP. This probably also translated to the lower DMPmax observed in PV-AgMIP (Section 4.2.1). There was a 64% probability that the MSD would not exceed 200 for PV-SAWS when compared to PV-AgMIP's 58%. Figure 4.11 shows a good match between PV-SAWS MSD and PV-AgMIP MSD, while neither revealed a strong linear trend. Both responded similarly during the driest 3-year period (1983/84 – 1985/86) when the most MSD occurred and wettest 3-year period (1986/87 – 1988/89) when the least MSD occurred.

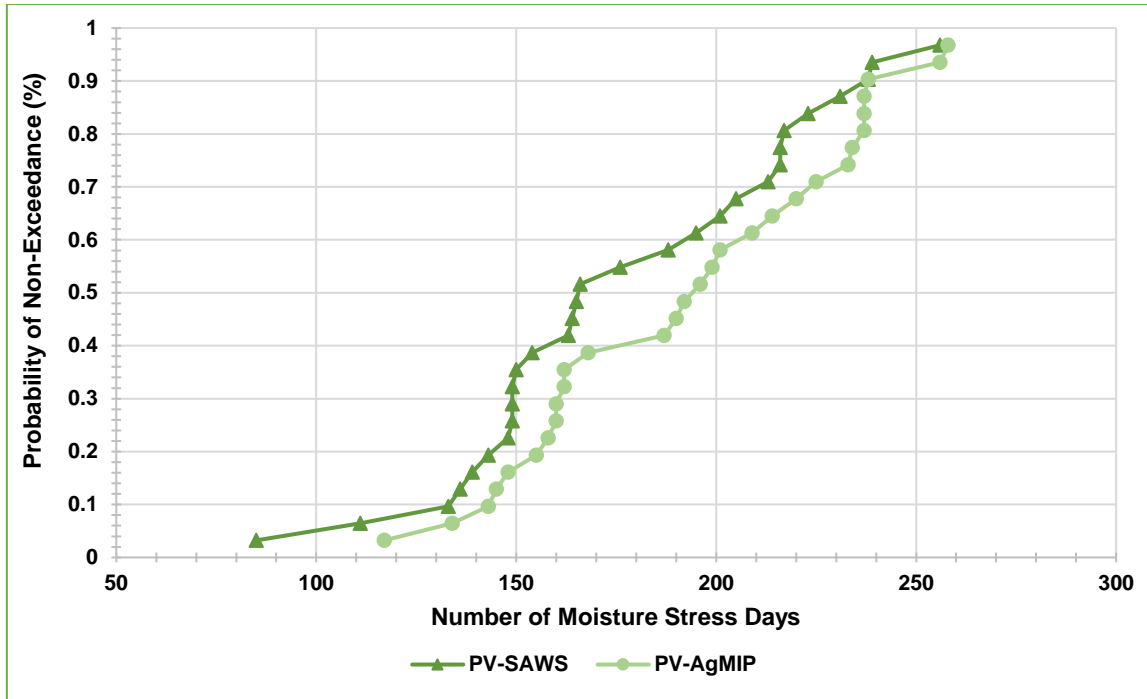


Figure 4.10 Cumulative distribution functions of the PUTU VELD simulated number of moisture stress days (MSD) in Bloemfontein for the base period (1980/81 – 2009/10) using observed climate data (PV-SAWS) and GCM-derived climate data (PV-AgMIP).

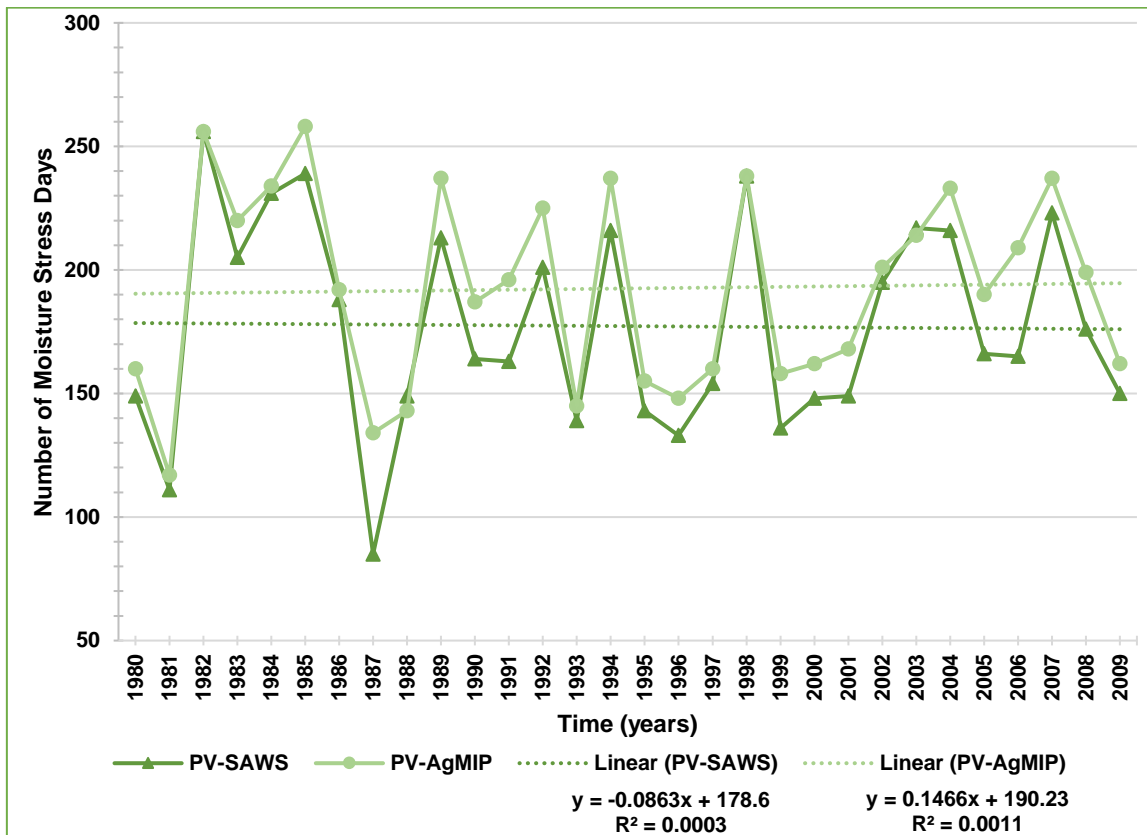


Figure 4.11 Time series of the PUTU VELD simulated number of moisture stress days in Bloemfontein for the base period (1980/81 – 2009/10) using observed climate data (PV-SAWS) and GCM-derived climate data (PV-AgMIP).

4.2.4 Seasonal Prediction of Maximum Dry Matter Production

Table 4.2 summarizes the results of using all possible combinations of the preceding 3-month running means of the Niño 3.4 anomalies as predictors of PV-SAWS DMPmax (Section 3.6). It can be seen that July-August-September (JAS) yielded the best result as about 17.5% of the variation in PV-SAWS DMPmax could be explained by JAS Niño 3.4, offering a short yet sufficient forecast lead time. Unfortunately, the prediction-potential of using Niño 3.4 anomalies were fairly low. This compared well with Moeletsi *et al.* (2011) in that they also had low correlations between ENSO and the onset of the rainfall season in the Free State. Landman *et al.* (2011), however, found a good correlation between ENSO and streamflow. For comparable reasons, the use of 3-month running means of the Niño 3.4 anomalies as predictors of Sydenham DMP was investigated but this yielded poorer results. The correlation between JAS Niño 3.4 and PV-SAWS DMPmax is presented in Figure 4.12. The positive slope in the simple linear regression equation presented in Figure 4.12 implied that lower Niño 3.4 values (generally denoting La Niña conditions) would result in higher DMPmax in Bloemfontein.

Table 4.2 Summary of coefficient of determination obtained using various combinations of the Niño 3.4 anomalies as predictor of measured standardized maximum dry matter production and simulated standardized maximum dry matter production using historical climate data in Bloemfontein during the base period (1980/81 – 2009/10)

3-Month Niño 3.4 Anomalies	R ²	R ²
	Sydenham	PV-SAWS
March-April-May (MAM)	0.0238	0.0115
April-May-June (AMJ)	0.0225	0.0517
May-June-July (MJJ)	0.0143	0.1034
June-July-August (JJA)	0.0114	0.1465
July-August-September (JAS)	0.0160	0.1745
August-September-October (ASO)	0.0192	0.1619
September-October-November (SON)	0.0209	0.1383
October-November-December (OND)	0.0233	0.1005
November-December-January (NDJ)	0.0227	0.0734
December-January-February (DJF)	0.0222	0.0507

The outlier point in Figure 4.12 occurred in the 1987/88 growth season when the ENSO conditions was a moderate/strong El Niño.

However, removing this point resulted in a R^2 of 0.0461 which is lower than the current R^2 of 0.1745.

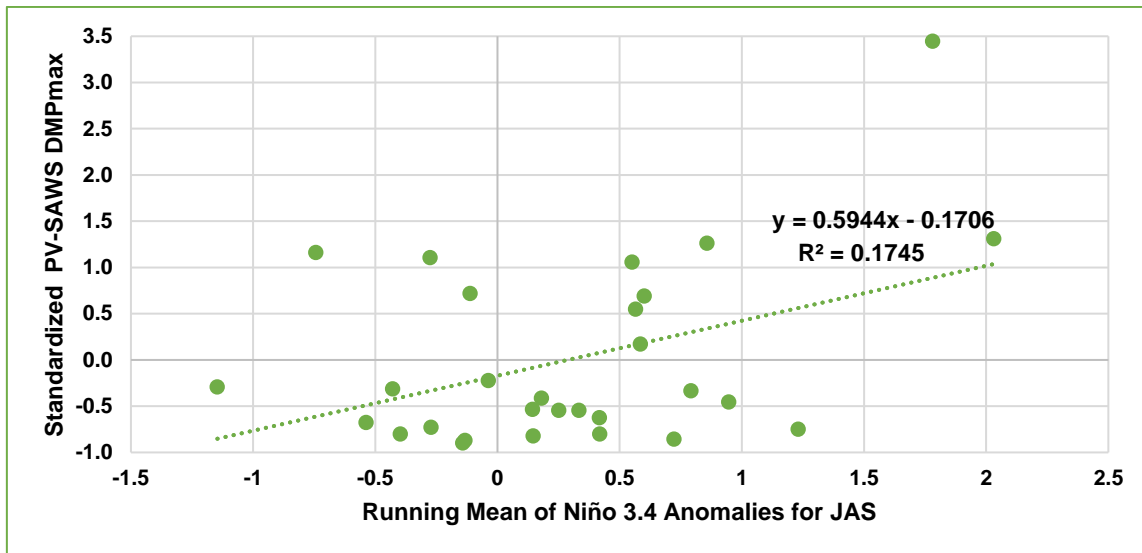


Figure 4.12 Scatterplot showing the correlation between the 3-month Niño 3.4 anomalies for July-August-September (JAS) and simulated standardized maximum dry matter production using historical climate data using historical climate data (PV-SAWS DMPmax) for Bloemfontein during the base period (1980/81 – 2009/10).

4.3 Simulated Future Rangeland Production

The discussion will focus on the following three time-periods:

- 2010/11 – 2039/40 (30 years) – current period (P1);
- 2040/41 – 2069/70 (30 years) – near future (P2); and
- 2070/71 – 2098/99 (29 years) – distant future (P3).

The discussions on the results for PV-AgMIP DMPmax, Dtp and MSD will focus on a comparison between the various periods under the two RCPs (i.e. RCP 4.5 and 8.5) and five GCMs used (Section 3.2.3). Results will also be compared against those obtained from PV-AgMIP for the historical base period (1980/81 – 2009/10).

4.3.1 Maximum Dry Matter Production

Figure 4.13 and 4.14 provide comparisons of DMPmax between the various GCMs and time periods under RCP 4.5 and 8.5, respectively. With respect to the spreads of the five GCMs, GFDL-ESM2M (orange lines) lay mostly to the far left of the base period (black line) while HadGEM2-ES (grey lines) lay mostly to the far right of the

base period. CCSM4 (blue lines), MIROC5 (yellow lines) and MPI-ESM-ER (green lines) straddled the base period (Figure 4.13 and 4.14). The bigger differences of the GFDL-ESM2M and HadGEM2-ES can be attributed to their climate data since the former estimated less rain while the latter estimated more rain to occur during the current, near future, and distant future periods. The differences can be more clearly noted in Table 4.3 where the 33.3rd and 66.6th percentiles of the various GCMs for the different time periods for both RCP 4.5 and 8.5 are tabulated.

Table 4.3 The 33.3rd and 66.6th percentiles for simulated dry matter production for Bloemfontein for 10 ensemble members (five GCMs and 2 RCPs) for each simulated time period

		Maximum Dry Matter Production (kg.ha ⁻¹)			
		RCP 4.5		RCP 8.5	
Time Period	GCM	33.3 rd	66.6 th	33.3 rd	66.6 th
Current Period	CCSM4	455	1200	685	1695
	GFDL-ESM2M	420	870	450	903
	HadGEM2-ES	810	2060	690	1600
	MIROC5	453	2005	525	1351
	MPI-ESM-MR	570	1275	570	1300
Near Future	CCSM4	440	1040	660	1500
	GFDL-ESM2M	300	525	384	600
	HadGEM2-ES	1000	2150	855	1770
	MIROC5	510	960	526	1053
	MPI-ESM-MR	420	815	525	960
Distant Future	CCSM4	580	1153	987	2188
	GFDL-ESM2M	241	536	267	603
	HadGEM2-ES	957	2097	811	1844
	MIROC5	653	1275	602	1514
	MPI-ESM-MR	415	651	649	1659
Base Period		600.00	1300.00		

Under RCP 4.5 (Figure 4.13) when comparing the current period and the distant future to the base period for the 33.3rd percentile the differences are noted as a reduction for the current period of 145 and 180 kg.ha⁻¹ for CCSM4 and GFDL-ESM2M, respectively, and an increase of 210 kg.ha⁻¹ for HadGEM2-ES when compared to the base period.

For the distant future there was a reduction of 20 and 359 kg.ha⁻¹ for CCSM4 and GFDL-ESM2M, respectively, and an increase of 357 kg.ha⁻¹ for HadGEM2-ES when compared to the base period.

Under RCP 8.5 (Figure 4.14) when comparing the near future and the distant future to the base period for the 66.6th percentile, the differences are noted as a reduction for the near future of 247 and 700 kg.ha⁻¹ for MIROC5 and GFDL-ESM2M, respectively, and an increase of 470 kg.ha⁻¹ for HadGEM2-ES when compared to the base period. For the distant future there was a reduction of 697 kg.ha⁻¹ for GFDL-ESM2M, respectively, and an increase of 214 and 544 kg.ha⁻¹ for MIROC5 and HadGEM2-ES when compared to the base period.

Figure 4.15 shows that the ensemble means for the different time periods under RCP 4.5 was not considerably different from each other when considering lower probabilities of non-exceedance (e.g. 33.3%), while larger changes were expected for higher probabilities (e.g. 66.6%). For example, there was a 66.6% probability that the DMPmax would not exceed 1300 kg.ha⁻¹ for the base period as compared to 1350, 1030 and 1030 kg.ha⁻¹ for the current, near future and distant future periods, respectively (Table 4.4). In terms of production differences, the latter translated to 270 kg.ha⁻¹ (near future and distant future) reductions in the corresponding DMPmax and an increase of 50 kg.ha⁻¹ for the current period.

It can be seen that for the 33.3rd percentile there was considerably smaller differences between the various time periods under both emission scenarios as compared to the 66.6th percentile. The relatively small differences under RCP 4.5 are generally indicative of an intermediate emission scenario (Section 2.3.4 Table 2.2).

Figure 4.16 shows that the differences between the various ensemble means for the time periods under RCP 8.5 were larger than under RCP 4.5. For example, there was a 66.6% probability that the DMPmax would not exceed 1300 kg.ha⁻¹ for the base period as compared to 1240 kg.ha⁻¹ for the near future period. There was a 34% probability that DMPmax would exceed 1300 kg.ha⁻¹ for the base period as compared to 1475 and 1417 kg.ha⁻¹ for the current and distant future periods, respectively (Figure 4.16, Table 4.4). In terms of production differences, the latter translated to a 60 kg.ha⁻¹ (near future) reductions in the corresponding DMPmax and an increase of 175 kg.ha⁻¹ (current) and 117 kg.ha⁻¹ (distant future). The larger difference between

the base period and distant future DMPmax (72 kg.ha⁻¹) for the 33.3rd percentile is indicative of a worse-case emission scenario (Section 2.3.4 Table 2.2).

For clarification, the DMPmax values corresponding to the 33.3rd and 66.6th percentiles in Figure 4.15 and 4.16 are summarized in Table 4.4.

Table 4.4 Ensemble-average 33.3rd and 66.6th percentiles of the PUTU VELD simulated maximum dry matter production for Bloemfontein for each of the time periods and emission scenario

	Maximum Dry Matter Production (kg.ha ⁻¹)			
	RCP 4.5		RCP 8.5	
Time Periods	33.3 rd	66.6 th	33.3 rd	66.6 th
Current Period	570	1330	605	1475
Near Future	565	1030	560	1240
Distant Future	560	1030	673	1417
Base Period	600	1300		

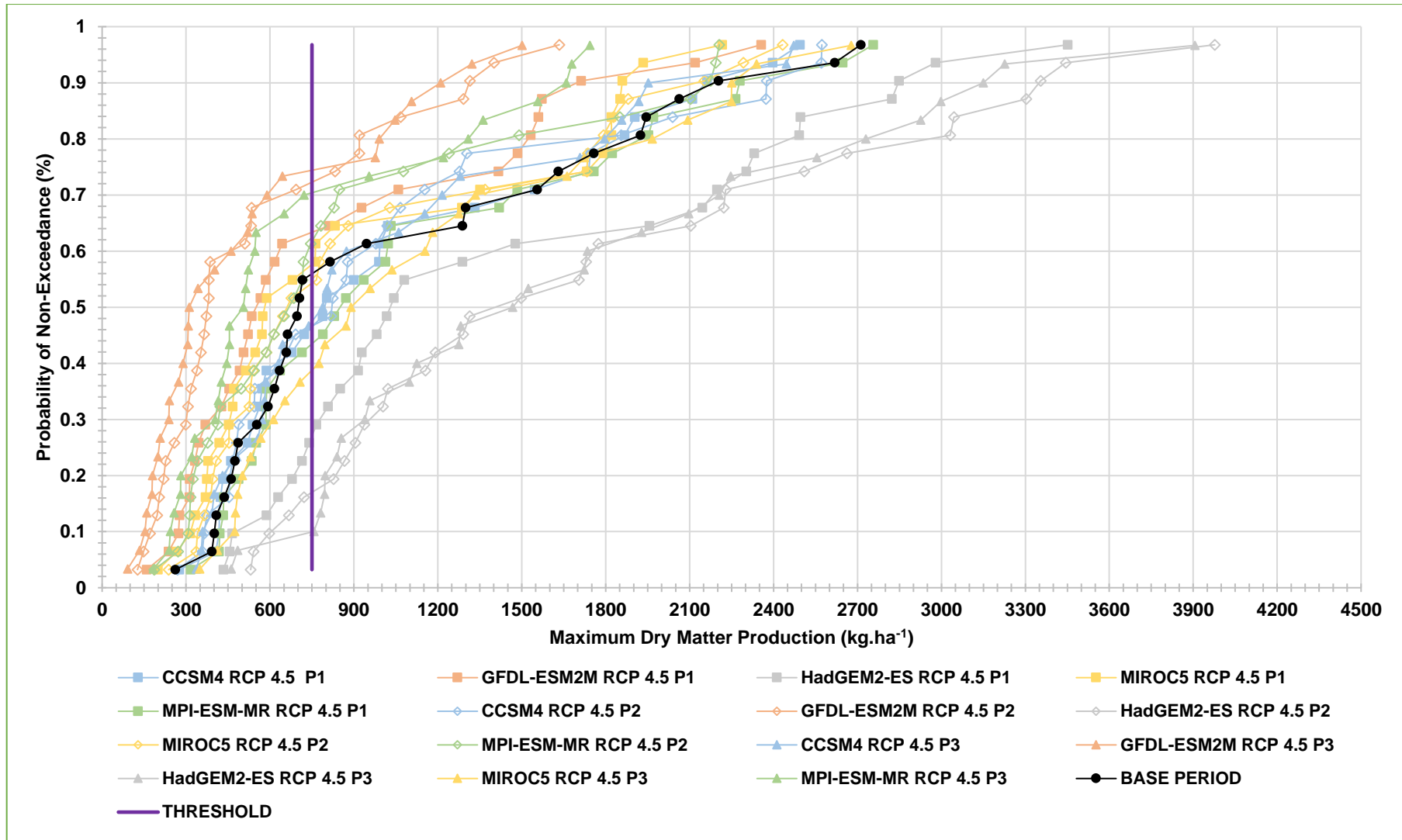


Figure 4.13 Cumulative distribution functions of simulated dry matter production in Bloemfontein for each GCM and time period under RCP 4.5. The purple vertical line represents a threshold of 750 kg.ha⁻¹ which equates to the norm grazing capacity for the Free State of 6 ha.LSU⁻¹. P1 = current period; P2 = near future; and P3 = distant future.

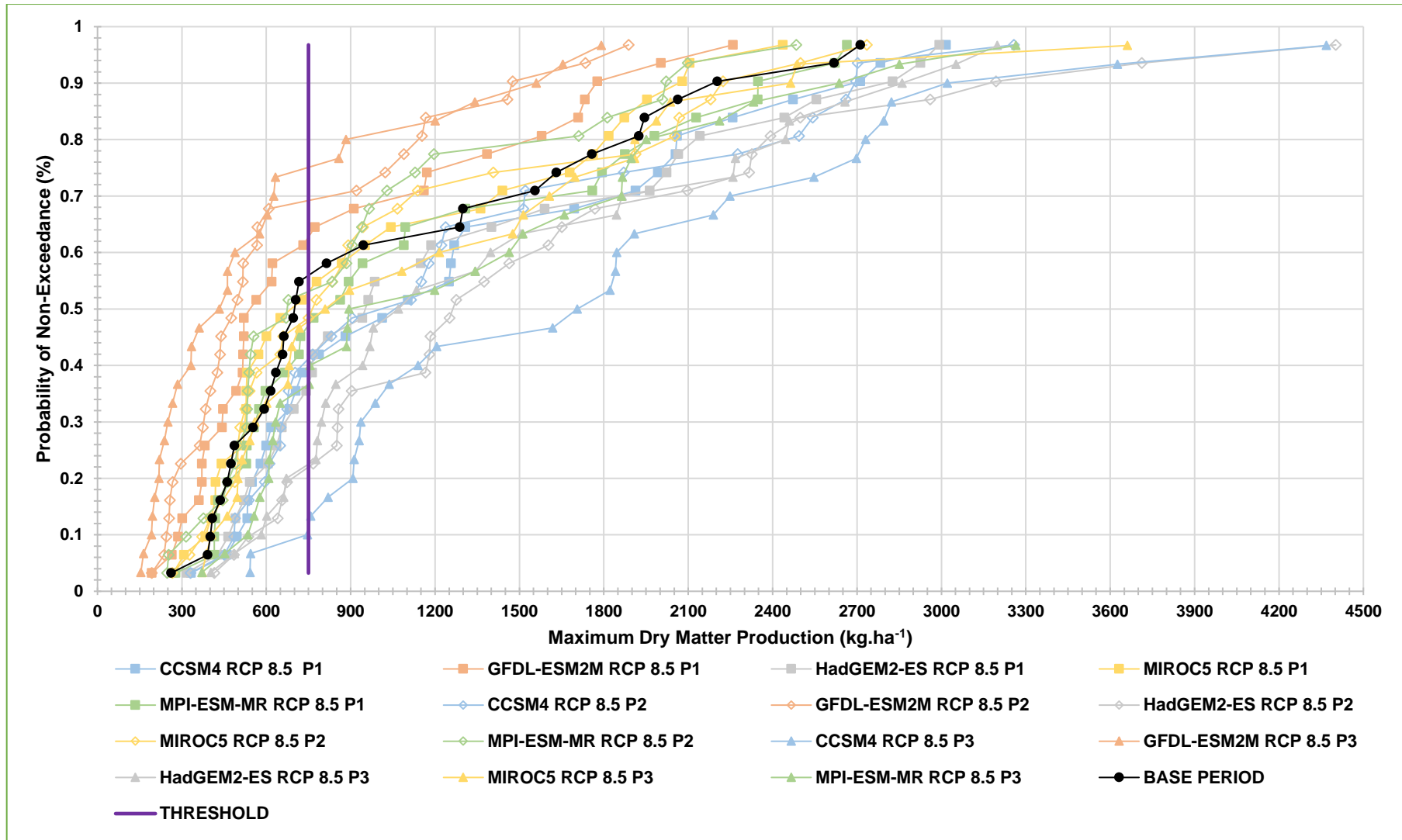


Figure 4.14 Cumulative distribution functions of simulated dry matter production in Bloemfontein for each GCM and time period under RCP 8.5. The purple vertical line represents a threshold of 750 kg.ha⁻¹ which equates to the norm grazing capacity for the Free State of 6 ha.LSU⁻¹. P1 = current period; P2 = near future; and P3 = distant future.

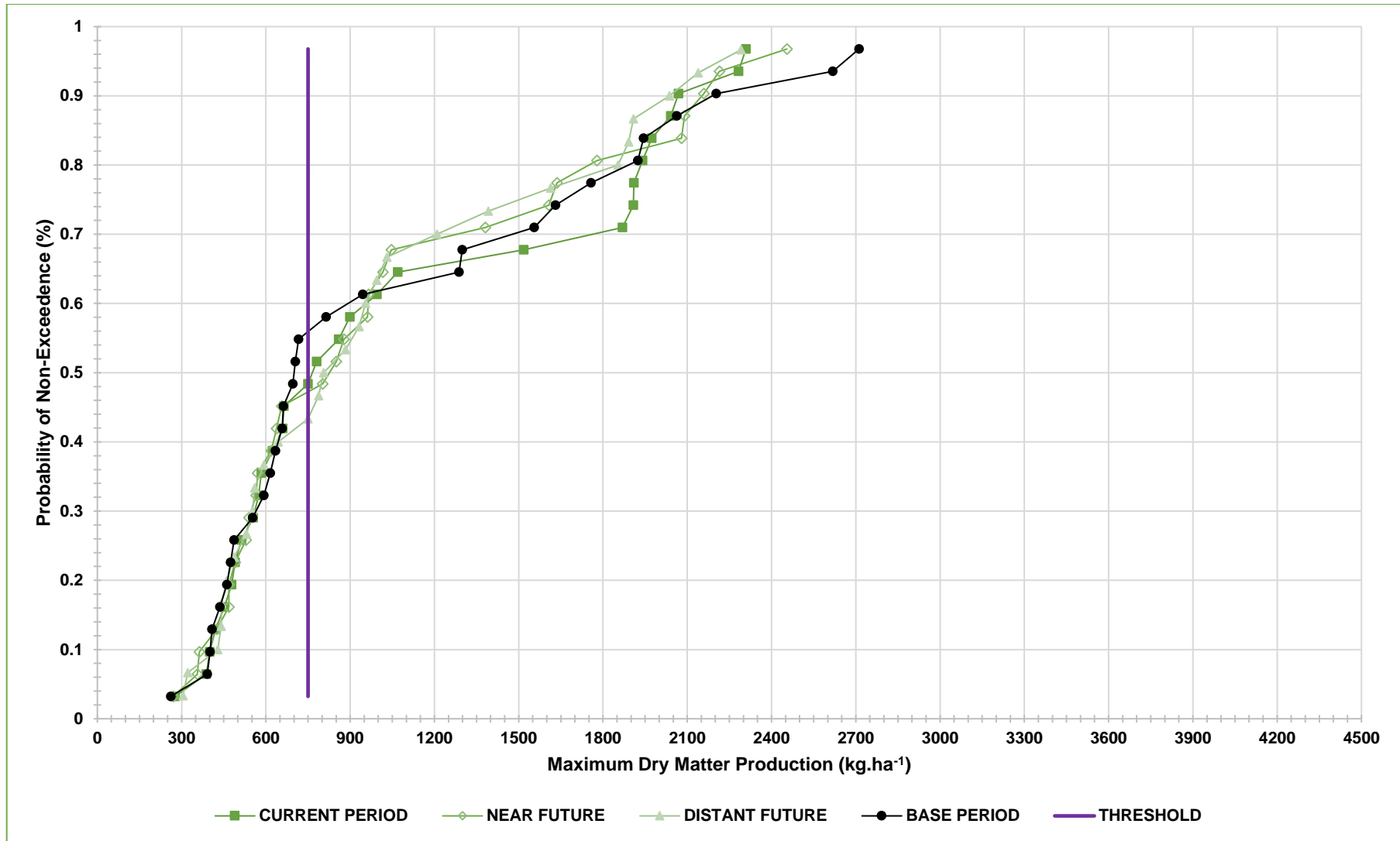


Figure 4.15 Cumulative distribution functions of ensemble-averaged simulated maximum dry matter production in Bloemfontein for each time period under RCP 4.5. The vertical line represents a threshold of 750 kg.ha⁻¹ which equates to the norm grazing capacity for the Free State of 6 ha.LSU⁻¹.

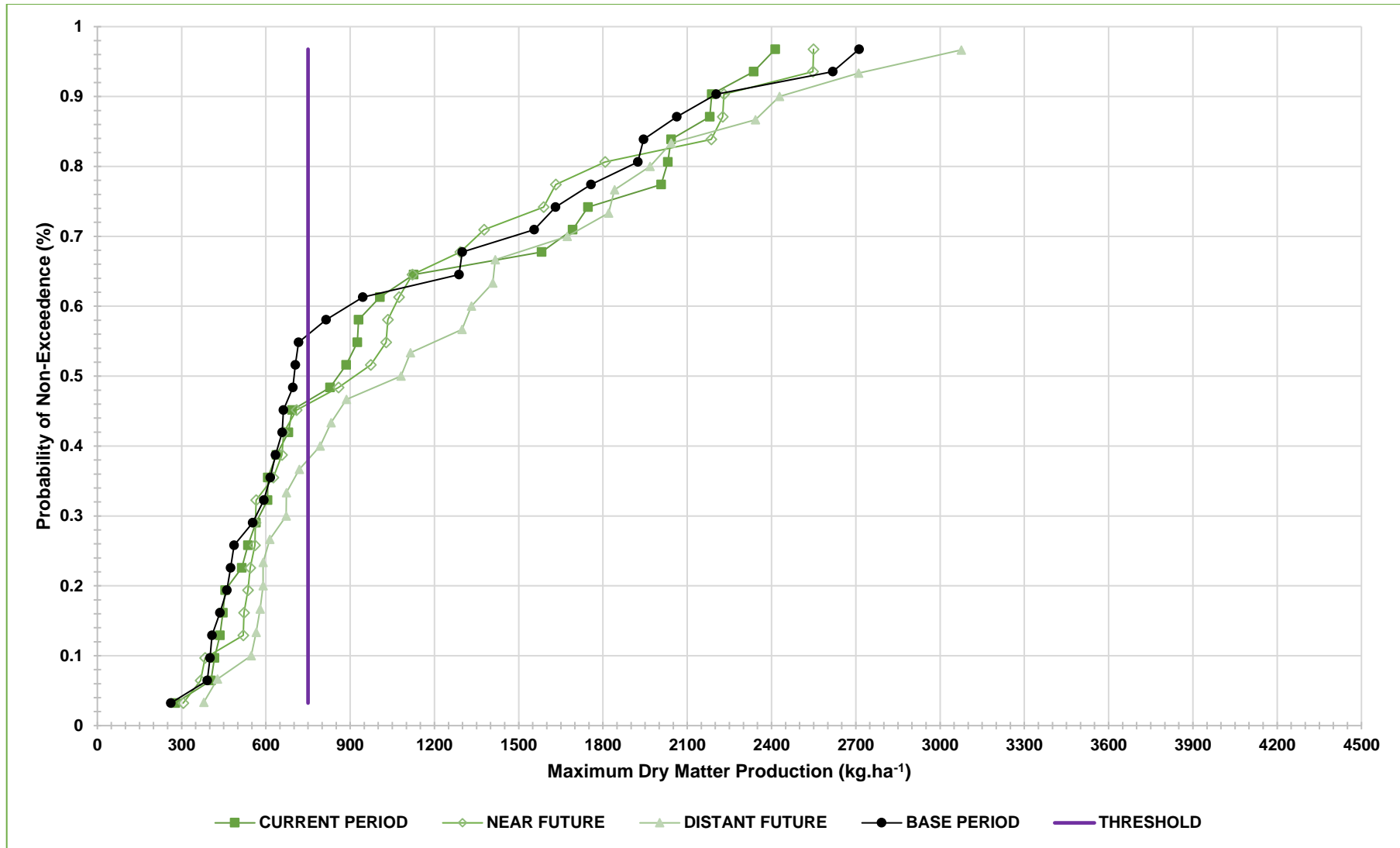


Figure 4.16 Cumulative distribution functions of ensemble-averaged simulated maximum dry matter production in Bloemfontein for each time period under RCP 8.5. The vertical line represents a threshold of 750 kg.ha⁻¹ which equates to the norm grazing capacity for the Free State of 6 ha.LSU⁻¹.

When looking at the DMPmax accumulated (Figure 4.17) one can see that there were considerable differences between the various ensemble members. Overall, runs utilizing GFDL-ESM2M estimated lower and those using HadGEM2-ES higher DMPmax when compared to the base period. The average RCP 8.5 had a slightly higher accumulated DMPmax than the average RCP 4.5 but both were in a similar range of DMPmax to that of the base period (Figure 4.17). Interestingly HadGEM2-ES was the only GCM to produce a decrease in accumulated DMPmax from RCP 4.5 to 8.5. There were marked differences between the different time periods with consecutive decreases in DMPmax shown under CCSM4 RCP 4.5, both GFDL-ESM2M RCP 4.5 and 8.5, and MPI-ESM-MR RCP 4.5, while consecutive increases were found for CCSM4 RCP 8.5 and both MIROC5 RCP 4.5 and 8.5. Both HadGEM2-ES RCP 4.5 and 8.5 and MPI-ESM-MR RCP 8.5 had no discernable trends between the time periods. Six ensemble members predicted an increase in accumulated DMPmax in the distant future (relative to the base period), while four showed a relative decrease.

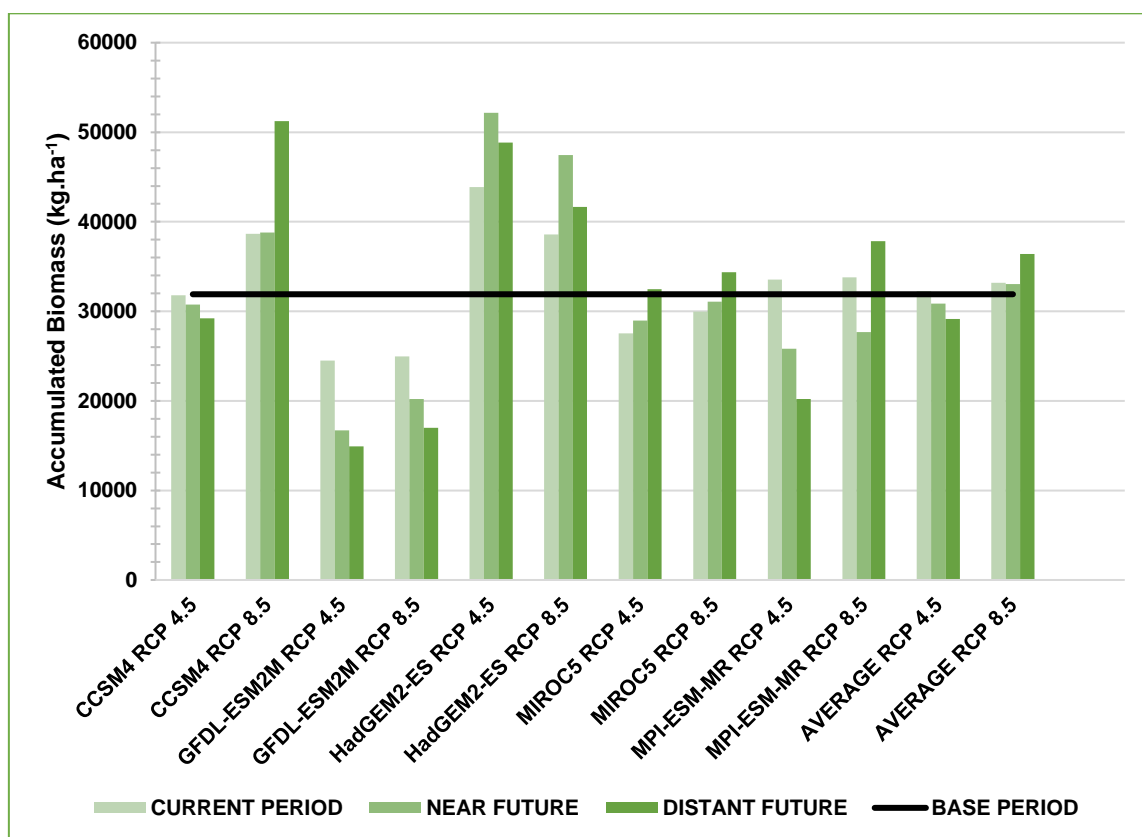


Figure 4.17 Accumulated PUTU VELD simulated maximum dry matter production (DMPmax) for Bloemfontein for 10 ensemble members (five GCMs and two RCPs). The averaged RCP 4.5 and RCP 8.5 values are also included, along with those for the base period (black horizontal line).

As mentioned in Section 1.1 the grazing capacity (GC) signifies the true number of animals that an area of land can sustain for a time period of a year. In the Free State, the general GC is 6 ha.LSU⁻¹. This equates to an average of 750 kg.ha⁻¹ DMP to nourish one animal for a year. The higher the numeral of GC, the more area of land is needed per animal for sufficient feeding and the less animals can be carried on a certain area of land. There was a 56% probability that the DMPmax would not exceed the 750 kg.ha⁻¹ threshold during the base period, while this probability of non-exceedance decreased to 43% under RCP 4.5 (Figure 4.15) and 37% under RCP 8.5 (Figure 4.16) for the distant future. When looking at the average GC (Figure 4.18) one can see that there were also notable differences between the various ensemble members. Thus, GFDL-ESM2M had a higher numeral for GC than HadGEM2-ES, although both were higher than the base period (solid line) but HadGEM2-ES was less than the norm (dashed line). With the exception of CCSM4 RCP 4.5, all ensemble members predicted a future increase in the numeral for GC over that of the base period, meaning that the rangeland will no longer sustain the same number of animals during future periods. Four ensemble members predicted a lower numeral for GC than the norm of 6 ha.LSU⁻¹ during any of the simulation periods. This means that under these scenarios the rangeland will be able to sustain more animals than the norm. Unfortunately, the majority of the ensemble members pointed to the opposite.

On average, RCP 8.5 had a slightly lower average GC than RCP 4.5 for the near and distant future periods but both were higher than the base period and the norm. There were marked differences between the different time periods with consecutive decreases in GC shown under CCSM4 RCP 4.5, and both MIROC5 RCP 4.5 and 8.5 and consecutive increases for both GFDL-ESM2M RCP 4.5 and 8.5, and MPI-ESM-MR RCP 4.5. CCSM4 RCP 8.5, both HadGEM2-ES RCP 4.5 and 8.5. MPI-ESM-MR RCP 8.5 had no discernable trends between the time periods. These patterns of increasing and decreasing GC all correspond to Figure 4.17 where, in most cases, when DMPmax increased the GC decreased and vice versa.

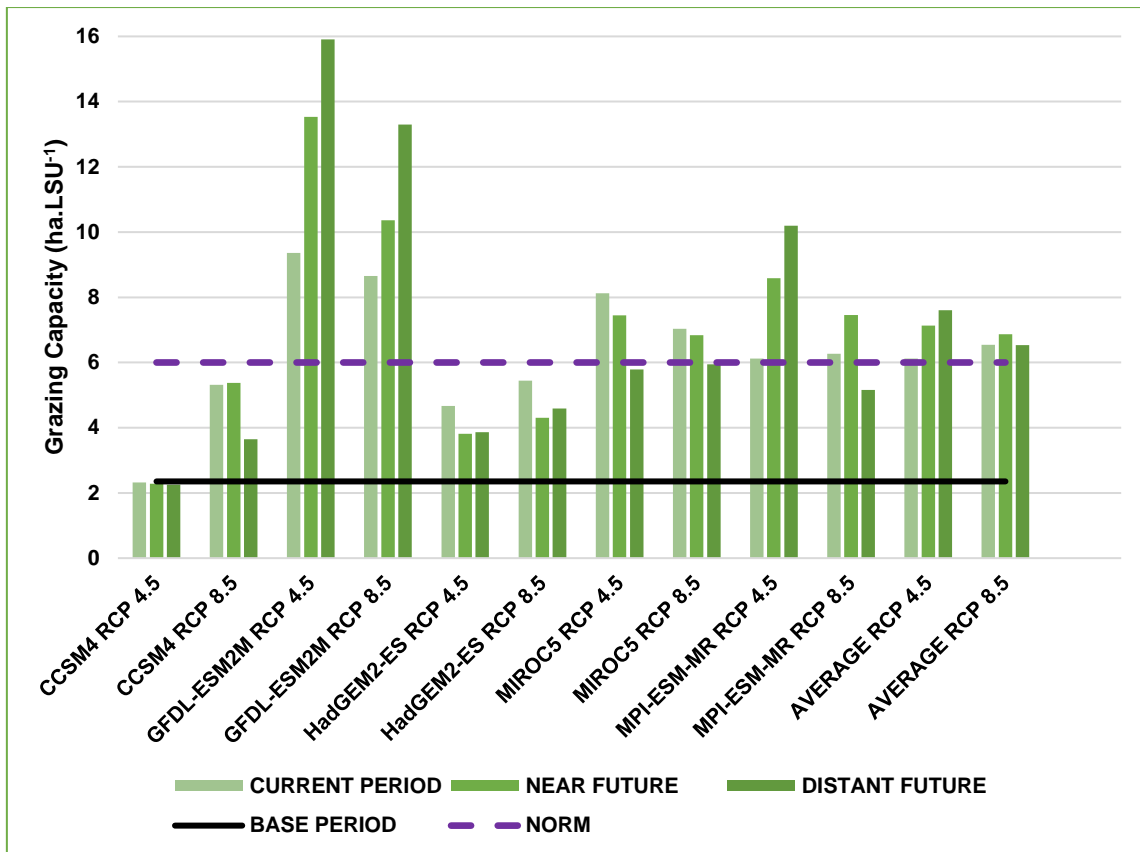


Figure 4.18 Average grazing capacity for Bloemfontein for 10 ensemble members (five GCMs and two RCPs) and the averaged RCP 4.5 and RCP 8.5 values, compared to the base period (black solid line) and the norm (purple dashed line).

4.3.2 Date of Occurrence of Maximum Dry Matter Production

Figure 4.19 and 4.20 are comparisons of Dtp between the various GCMs and time periods under RCP 4.5 and 8.5, respectively. With respect to the ensemble spread, the CDFs for the current period generally lay to the left of the base period under both RCP 4.5 and 8.5 for all five GCMs. For each GCM the distant future CDFs lay the furthest right. This means that more Dtps fell within the optimal period for the current period (80% MPI-ESM-ER) than for the distant future (26.7% MPI-ESM-ER). The differences can be more clearly noted in Table 4.5 where the 33.3rd and 66.6th percentiles of the various GCMs for the different time periods under both RCP 4.5 and 8.5 are summarized.

Table 4.5 The 33.3rd and 66.6th percentiles for date of occurrence of maximum dry matter production in Bloemfontein for 10 ensemble members (five GCMs and 2 RCPs) for each time period

		Date of Occurrence of Maximum Dry Matter Production			
		RCP 4.5		RCP 8.5	
Time Period	GCM	33.3 rd	66.6 th	33.3 rd	66.6 th
Current Period	CCSM4	291	300	284	299
	GFDL-ESM2M	293	300	292	300
	HadGEM2-ES	285	300	291	303
	MIROC5	293	301	291	300
	MPI-ESM-MR	285	299	291	300
Near Future	CCSM4	291	307	298	317
	GFDL-ESM2M	296	304	301	317
	HadGEM2-ES	293	307	298	315
	MIROC5	297	311	298	316
	MPI-ESM-MR	301	317	309	325
Distant Future	CCSM4	299	310	303	325
	GFDL-ESM2M	296	310	309	328
	HadGEM2-ES	297	316	308	332
	MIROC5	298	316	323	329
	MPI-ESM-MR	303	325	317	337
Base Period		293	301		

Under RCP 4.5 (Figure 4.19), when comparing the current period and the distant future to the base period for the 33.3rd percentile, the differences are noted as a shift to the left for the current period of 8 and 2 days for HadGEM2-ES and CCSM4, respectively, and no shift for MIROC5 when compared to the base period (Table 4.5). For the distant future, there was a shift to the right of 4, 6 and 5 days for HadGEM2-ES, CCSM4 and MIROC5, respectively (Table 4.5).

Under RCP 8.5 (Figure 4.20), when comparing the near future and the distant future to the base period for the 66.6th percentile, the differences are noted as a shift to the right for the near future of 16, 14 and 24 days for GFDL-ESM2M, HadGEM2-ES and MPI-ESM-ER, respectively, as well as for the distant future of 27, 31, 36 days for GFDL-ESM2M, HadGEM2-ES and MPI-ESM-ER, respectively, when compared to the

base period (Table 4.5). Under RCP 4.5, 55.1% of the GCMs Dtps fell in the optimal period compared to 49.4% under RCP 8.5.

Figure 4.21 and 4.22 shows that the ensemble means for the different time periods under RCP 4.5 and 8.5, respectively, were considerably different from each other with somewhat larger changes observed for higher probabilities of non-exceedance (e.g. 66.6%). For example, under RCP 4.5, there was a 66.6% probability that the Dtp would not exceed day 301 for the base period and current period when compared to day 310 and 315 for the near future and distant future, respectively (Figure 4.21; Table 4.6). Thus, 16.7%, 26.7%, 46.7% and 62.1% of the years in the base period, current period, near future and distant future, respectively, saw the Dtp falling outside the optimal period.

Under RCP 8.5, there was a 66% probability that the Dtp would not exceed day 301 for the base period and current period when compared to 316 and 330 for the near future and distant future, respectively (Figure 4.22; Table 4.5). Thus, 16.7%, 23.3%, 60.0% and 66.7% of the years in the base period, current period, near future and distant future, respectively, had Dtp falling outside the optimal period. Generally, larger changes were observed under RCP 8.5 in comparison to RCP 4.5. It is noted that under both emission scenarios there was a larger shift in Dtp from the current period to the distant future and that this shift was more prominent under RCP 8.5 (Figure 4.22) than under RCP 4.5 (Figure 4.21). The shift from the base period to current period was not that pronounced with small differences for both RCP 4.5 and 8.5.

Table 4.6 Ensemble-averaged 33.3rd and 66.6th percentiles for the date of occurrence of maximum dry matter production in Bloemfontein for each of the time periods and emission scenarios

Time Periods	Date of Occurrence of Maximum Dry Matter Production			
	RCP 4.5		RCP 8.5	
	33.3 rd	66.6 th	33.3 rd	66.6 th
Current Period	285	301	289	301
Near Future	303	310	298	316
Distant Future	302	315	315	330
Base Period	293	301		

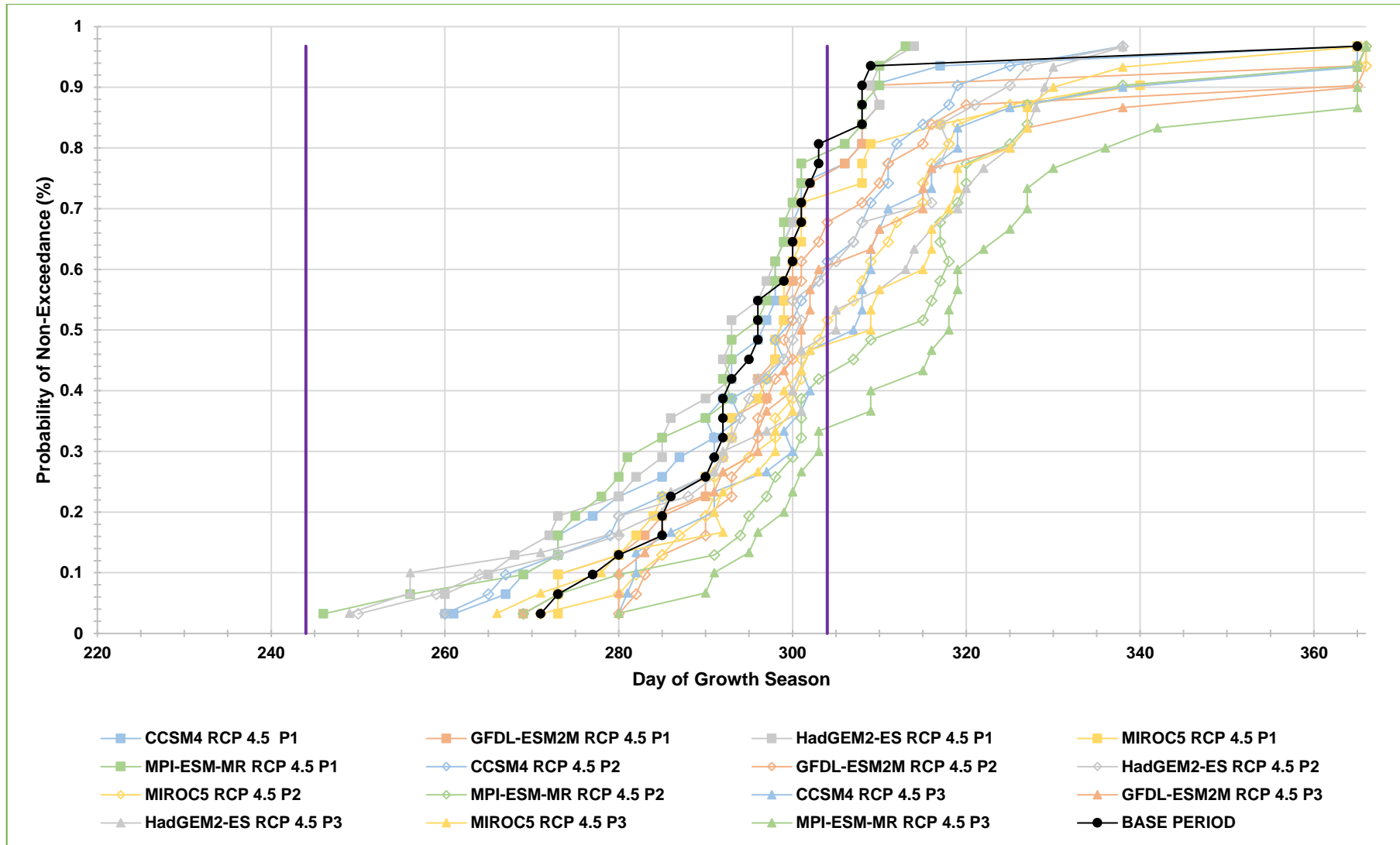


Figure 4.19 Cumulative distribution functions of date of occurrence of maximum dry matter production (Dtp) in Bloemfontein for each GCM and time period under RCP 4.5. The two vertical lines demarcate the optimal period (244 – 304) for Dtp to occur. P1 = current period; P2 = near future; and P3 = distant future.

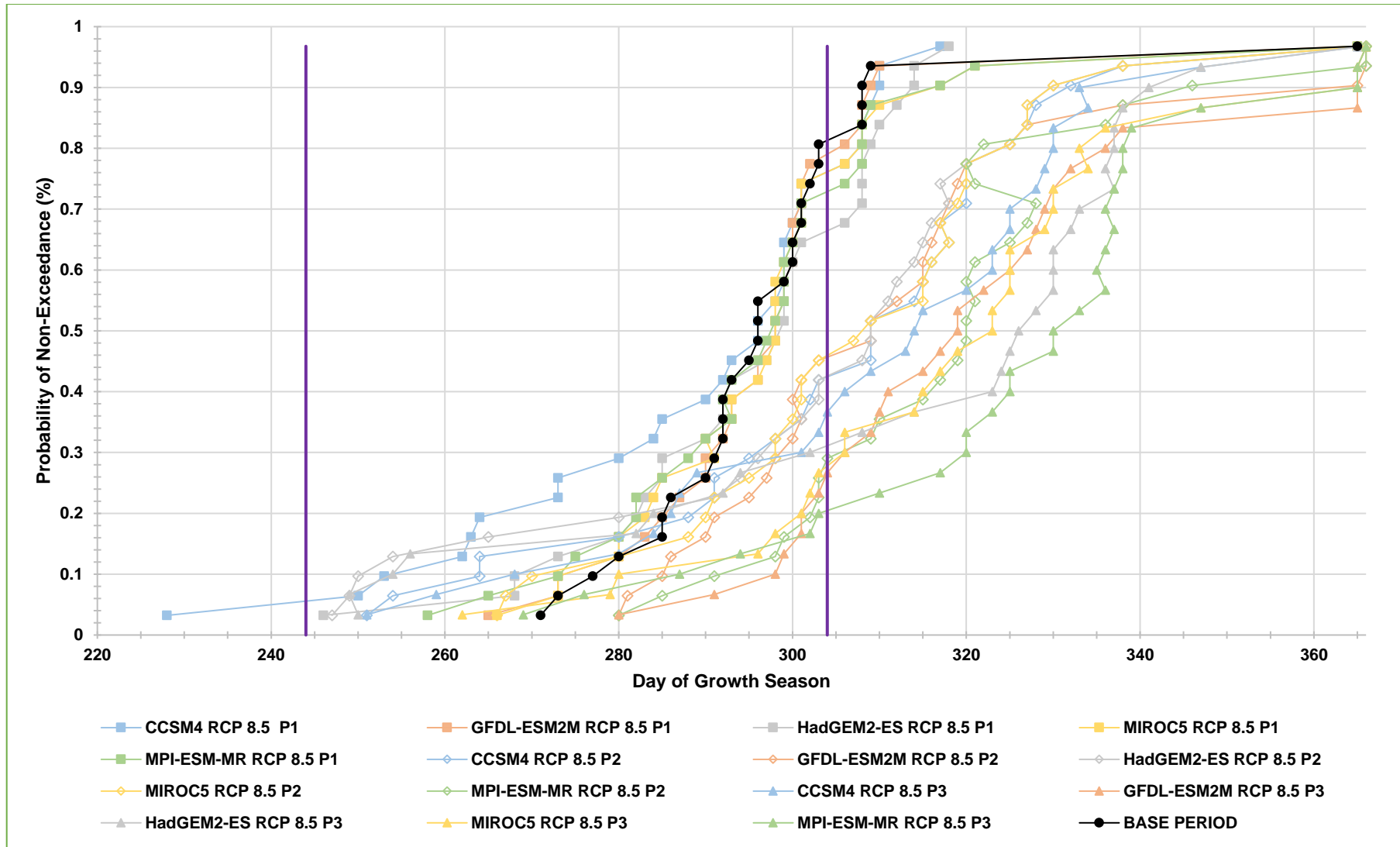


Figure 4.20 Cumulative distribution functions of date of occurrence of maximum dry matter production (Dtp) in Bloemfontein for each GCM and time period under RCP 8.5. The two vertical lines demarcate the optimal period (244 – 304) for Dtp to occur. P1 = current period; P2 = near future; and P3 = distant future.

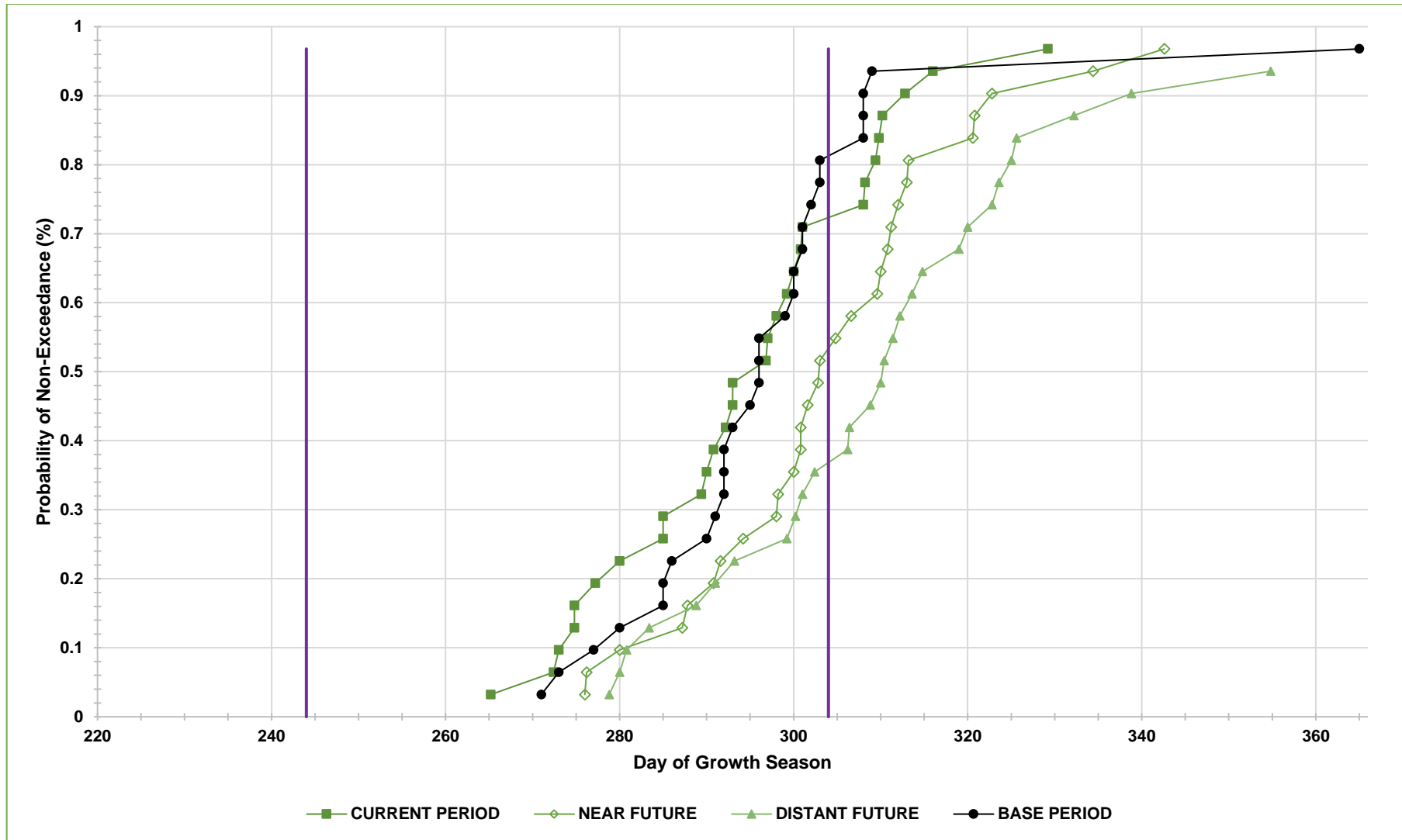


Figure 4.21 Cumulative distribution functions of ensemble-averaged date of occurrence of maximum dry matter production (Dtp) in Bloemfontein for each time period under RCP 4.5. The two vertical lines demarcate the optimal period (244 – 304) for Dtp to occur.

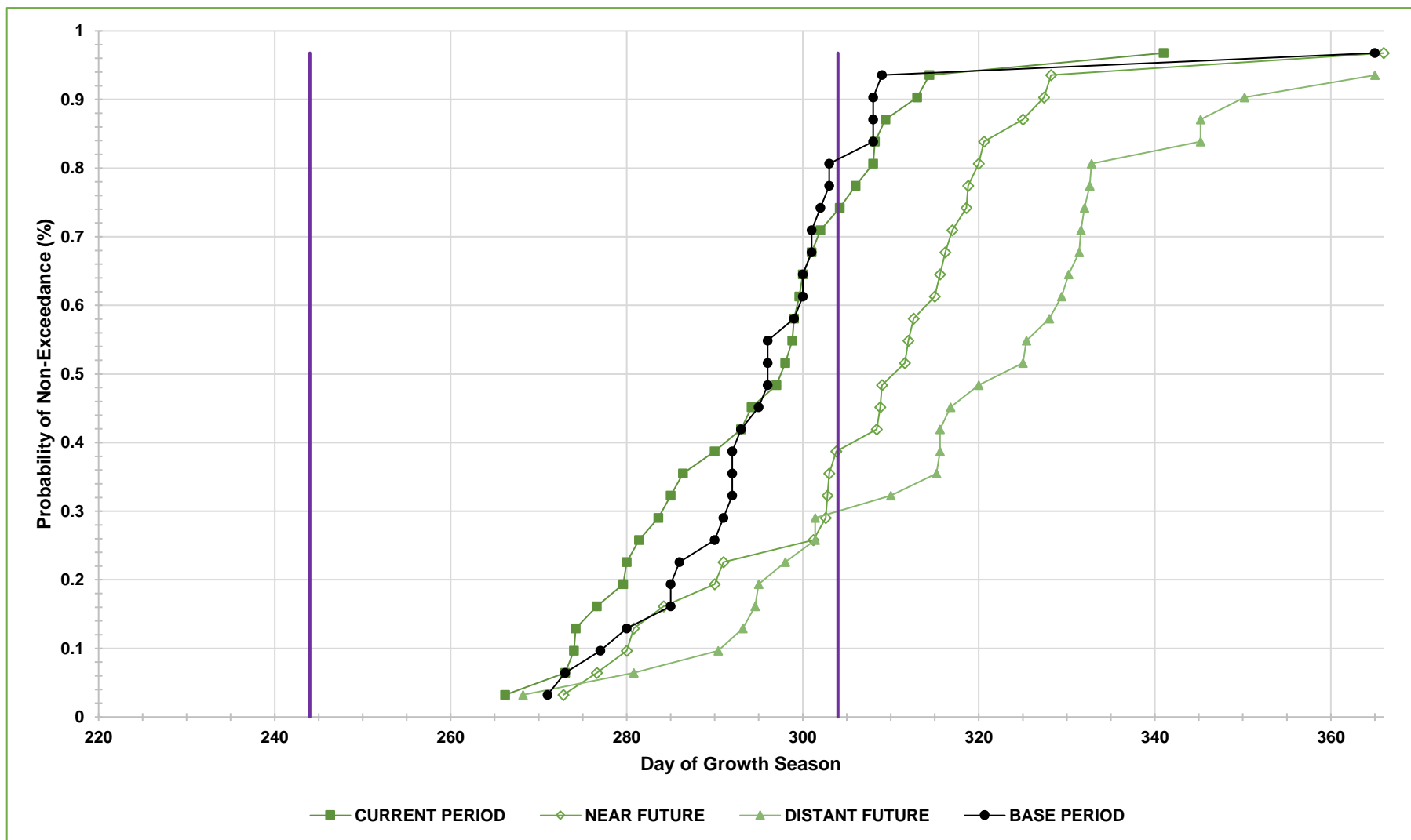


Figure 4.22 Cumulative distribution functions of ensemble-averaged date of occurrence of maximum dry matter production (Dtp) in Bloemfontein for each time period under RCP 8.5. The two vertical lines demarcate the optimal period (244 – 304) for Dtp to occur.

4.3.3 Number of Moisture Stress Days

Figure 4.23 and 4.24 provide comparisons of MSD between the various GCMs and time periods under RCP 4.5 and 8.5, respectively. Generally, the CDFs of all the ensemble members for the three time periods (denoted P1, P2 and P3 in these figures) and the two emission scenarios lay to the right of the base period, indicating a future increase in MSD. Under both emission scenarios, larger increases in MSD were found for the distant future period. The differences between the two emission scenarios are summarized for each time period in Table 4.7 with respect to the 33.3rd and 66.6th percentiles.

Under RCP 4.5 (Figure 4.23; Table 4.7), a comparison between the current period and the base period for the 33.3rd percentile, revealed an increase of 9, 17 and 19 days for CCSM4, MPI-ESM-MR and HadGEM2-ES, respectively. For the distant future, there was also an increase of 44, 58 and 74 days for CCSM4, HadGEM2-ES and MPI-ESM-MR, respectively (Table 4.7), when compared to the base period. When comparing the near future to the base period for the 66.6th percentile under RCP 8.5 (Figure 4.24; Table 4.7), an increase of 40, 34 and 40 days was observed for CCSM4, MIROC5 and HadGEM2-ES, respectively. For the distant future, there was also an increase of 55, 69 and 94 days for CCSM4, MIROC5 and HadGEM2-ES, respectively (Table 4.7), when compared to the base period. It is good to note that although more MSD were observed under RCP 8.5, higher DMPmax were expected during the distant future time period. According to the ensemble averages under RCP 4.5 (Figure 4.15) there's no big changes from base to distant future, and under RCP 8.5 (Figure 4.16) there is a slight increase in DMPmax from base to distant future.

As expected from the foregoing discussion, the CDFs of the ensemble means for all time periods fell to the right of the base period's CDF under both RCP 4.5 and 8.5 (Figures 4.25 and 4.26). The MSD-values corresponding to the 33.3rd and 66.6th probability of non-exceedance are summarized in Table 4.8. Again, the most striking conclusion is a clear increase in MSD for future periods (relative to the historical base period), while slightly bigger increases were indicated under the RCP 8.5 scenario.

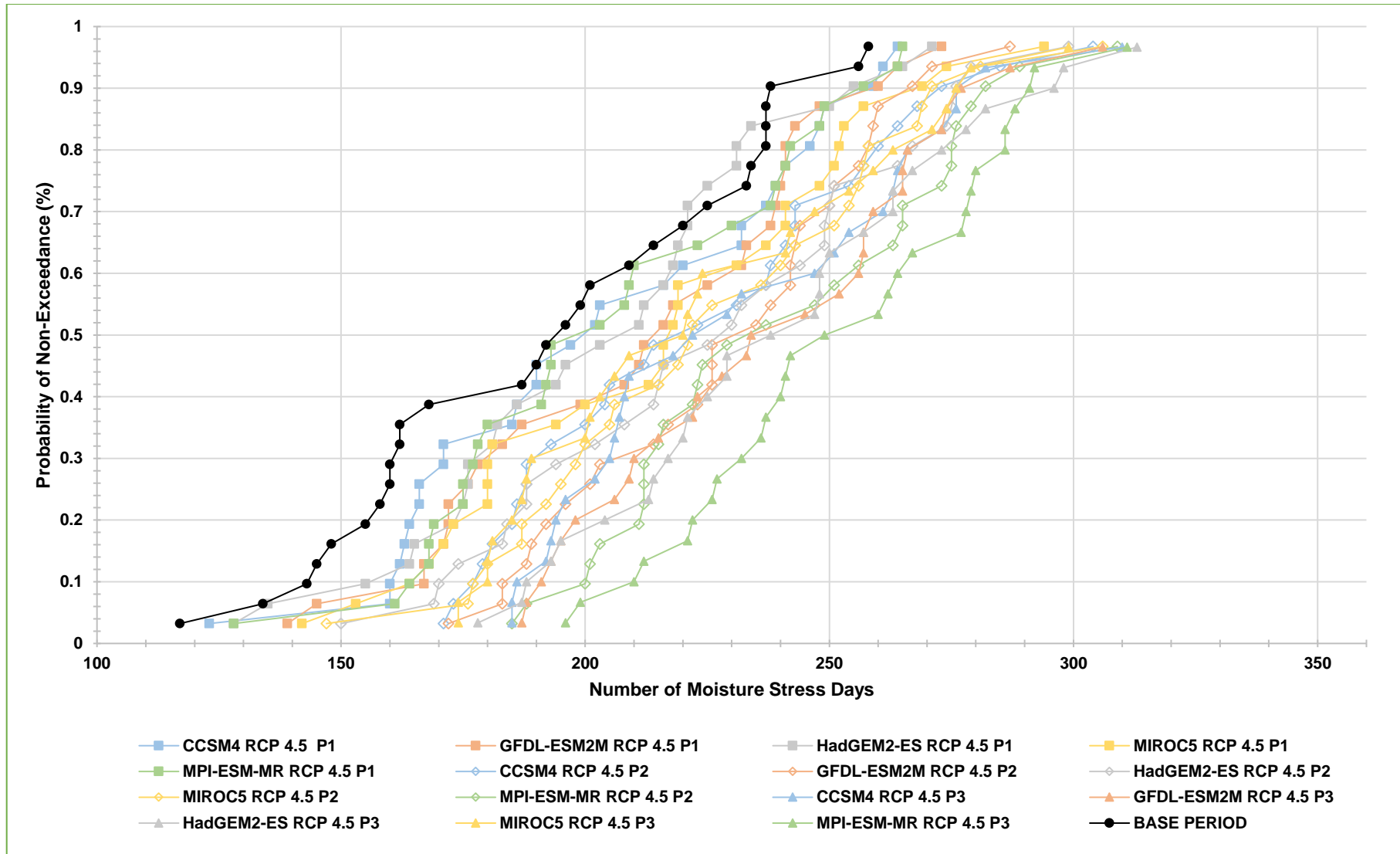


Figure 4.23 Cumulative distribution functions of the number of moisture stress days in Bloemfontein for each GCM and time period under RCP 4.5. P1 = current period; P2 = near future; and P3 = distant future.

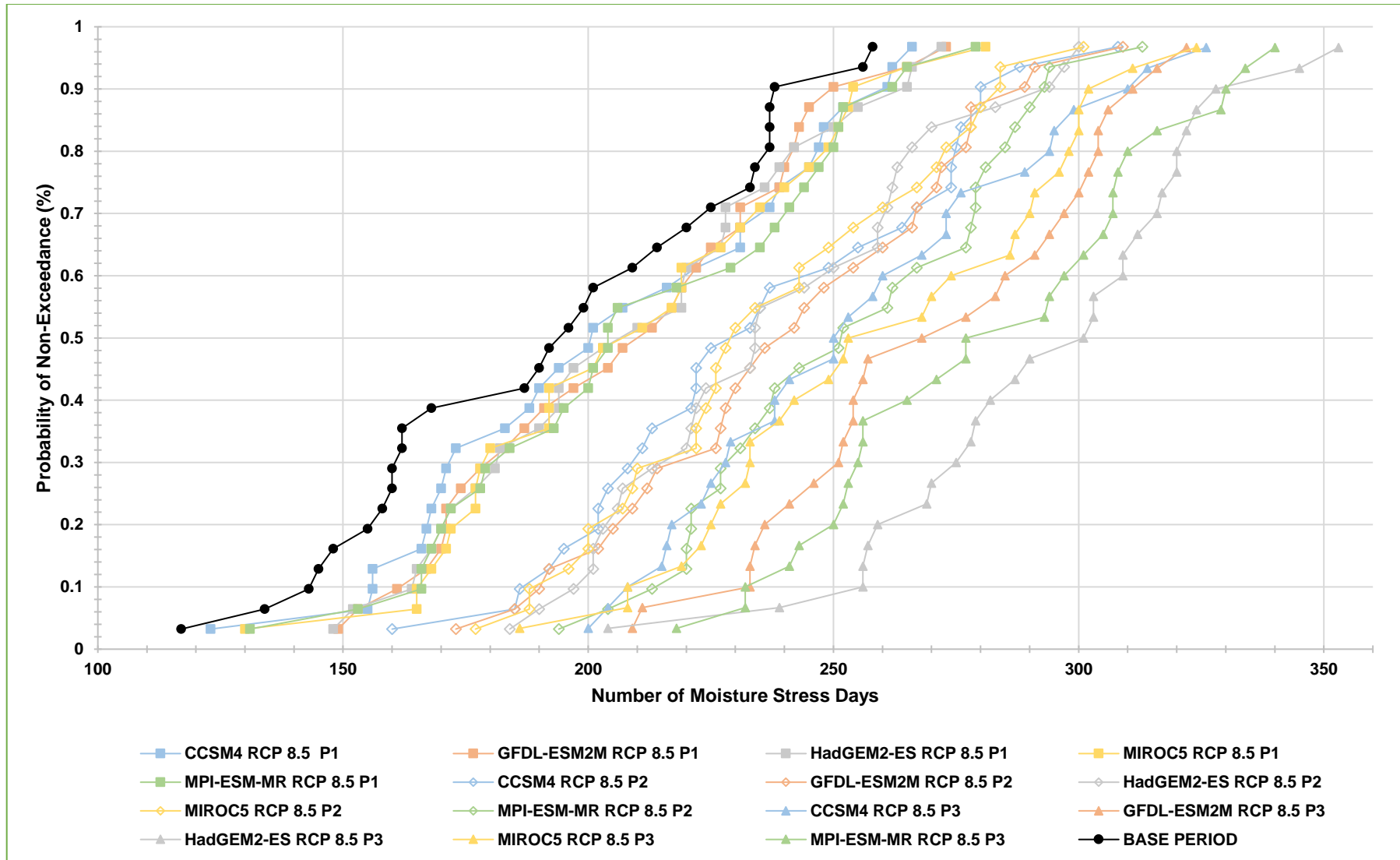


Figure 4.24 Cumulative distribution functions of the number of moisture stress days in Bloemfontein for each GCM and time period under RCP 8.5. P1 = current period; P2 = near future; and P3 = distant future.

Table 4.7 The 33.3rd and 66.6th percentiles for number of moisture stress days in Bloemfontein for the various GCMs and time periods under both RCP 4.5 and 8.5

		Number of Moisture Stress Days			
		RCP 4.5		RCP 8.5	
Time Period	GCM	33.3 rd	66.6 th	33.3 rd	66.6 th
Current Period	CCSM4	171	231	175	229
	GFDL-ESM2M	182	235	183	225
	HadGEM2-ES	181	219	183	226
	MIROC5	181	239	183	225
	MPI-ESM-MR	179	227	186	235
Near Future	CCSM4	192	241	211	258
	GFDL-ESM2M	214	242	225	262
	HadGEM2-ES	201	249	219	258
	MIROC5	200	249	221	252
	MPI-ESM-MR	215	264	231	275
Distant Future	CCSM4	206	254	229	273
	GFDL-ESM2M	215	257	252	294
	HadGEM2-ES	220	257	278	312
	MIROC5	200	242	233	287
	MPI-ESM-MR	236	277	256	305
Base Period		162	218		

The differences under RCP 4.5 can be attributed to the characteristics of the emission scenario where mitigation schemes are implemented and the benefits are noticed during the later time periods (Section 2.3.4). The larger differences under RCP 8.5 can be accredited to the characteristics of the emission scenario where no mitigation schemes are implemented and the detriments are perceived during the later time periods (Section 2.3.4).

Table 4.8 Ensemble-averaged 33.3rd and 66.6th percentiles for the number of moisture stress days in Bloemfontein for each of the time periods and emission scenarios

	Number of Moisture Stress Days			
	RCP 4.5		RCP 8.5	
Time Periods	33.3 rd	66.6 th	33.3 rd	66.6 th
Current Period	177	229	178	232
Near Future	203	244	214	248
Distant Future	212	259	247	293
Base Period	162	218		

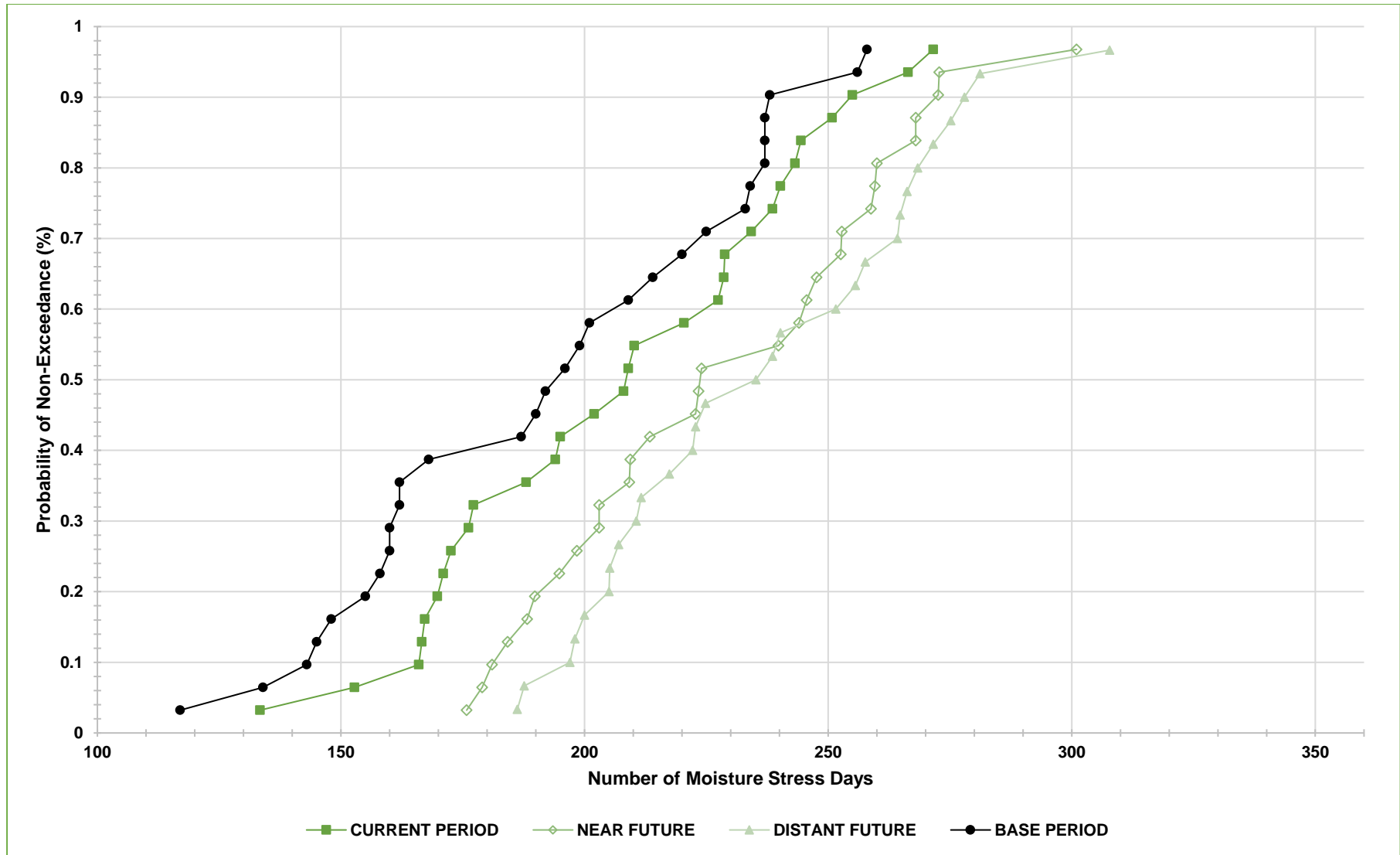


Figure 4.25 Cumulative distribution functions of ensemble-averaged number of moisture stress days in Bloemfontein for each time period under RCP 4.5.

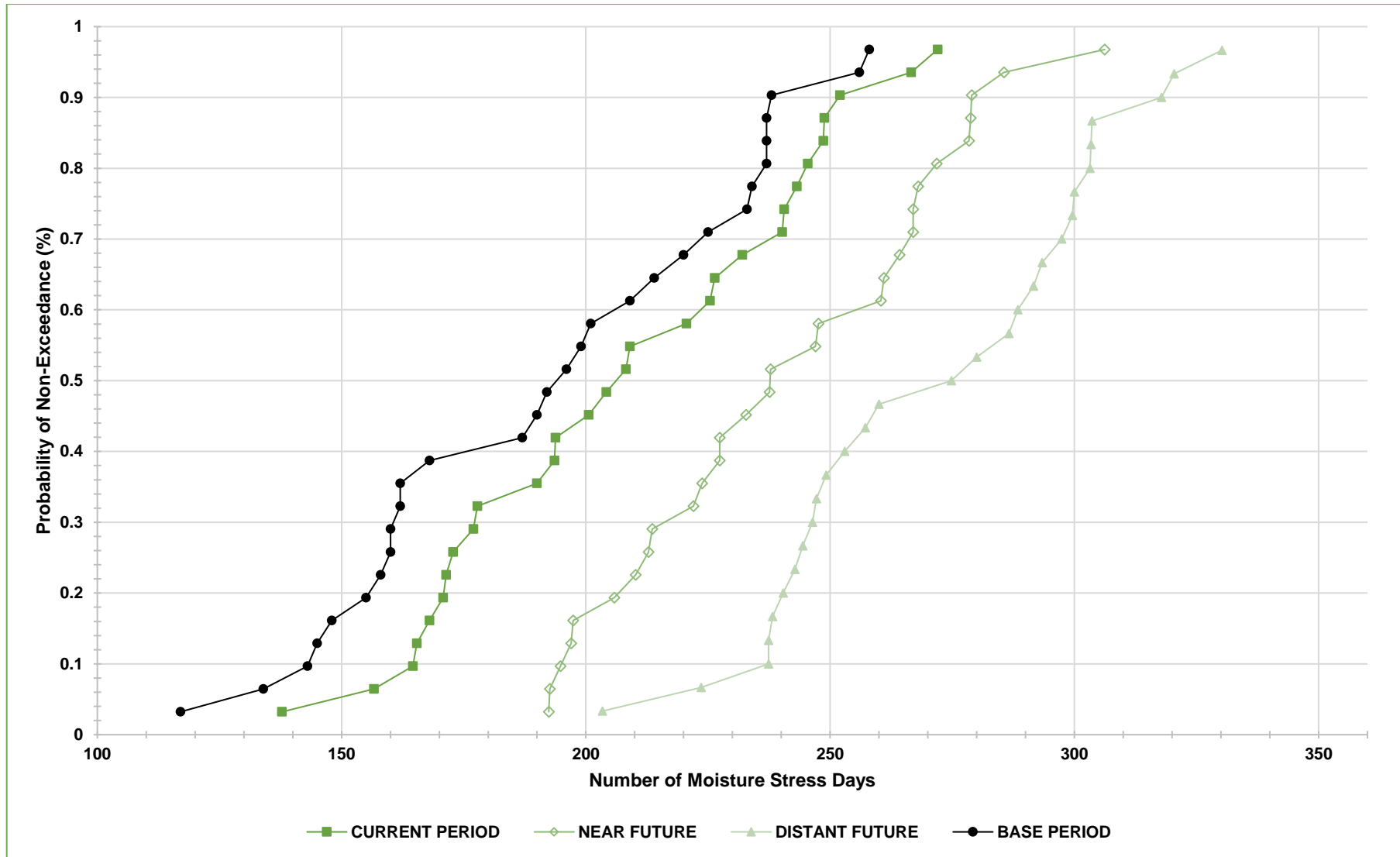


Figure 4.26 Cumulative distribution functions of ensemble-averaged number of moisture stress days in Bloemfontein for each time period under RCP 8.5.

Grasslands provide various natural resources for man but the only real potential it has for food production is as a feed source for animal production (Fogel & Manuel, 1980; cited by Fouché, 1992). Rangeland is an animal farmer's most precious resource and the cheapest resource if it is in a good condition. A considerable 91% of South Africa is defined as arid or semi-arid where land degradation (compounded by climate change) can lead to desertification and the subsequent irreparable loss of productive land (Gbetibouo & Ringler, 2009).

South Africa's annual population growth rate is higher than the global rate (Worldometers, 2016), and is estimated to reach 82 million by the year 2035 (Goldblatt, 2015). In order to feed the ever-increasing population, better rangeland management practices are needed together with food imports which need to double. The increase in food prices is a big burden for the poor population, who already spend a third of their income on food compared to the small amount of the wealthier population's salary. Food security is not only about food prices and availability, but it is also an unemployment issue. All farmers need to employ the use of sustainable farming as it is about meeting the needs of South Africans today and in the future.

Agriculture is one of the most vulnerable sectors against climate variability and change. Climate variability is one of the main causes for variable crop yields (IPCC, 2007; Polley *et al.*, 2013). Phenomenon like ENSO can have a large effect on the global average surface temperatures and rainfall distribution (WMO, 2014). ENSO can be monitored by using indices like the Niño 3.4 or Oceanic Niño Index (NOAA, 2016b).

A change in rainfall and variability is very likely to lead to a global drop in cover and productivity in grasslands in response to the observed drying trend of about 8 mm.yr⁻¹ since 1970 (IPCC, 2007). The upside to an elevated atmospheric carbon dioxide (CO₂) is an increase in plant growth and a reduction of the negative effects of drying in warmer climates due to an increase in water use efficiency (Polley *et al.*, 2013).

It is expected that over South Africa, the temperatures will increase by 4°C, mainly over the northern and central interior regions during the distant future while the coastal regions will experience the least amount of warming (Stevens *et al.*, 2015). It has also been predicted that winter and autumn will warm the most compared to summer and spring. Predictions show a reduction of rainfall over Limpopo and south-western Cape with a moderate to strong increase over the central interior regions extending to the south-east coast. These increases in rainfall are projected to occur during summer and spring. GCMs have the ability to simulate important aspects of the current climate and agree with the prediction of significant warming under greenhouse gases. GCMs are becoming more proficient in their capability to represent more biological and physical processes and their interactions (IPCC, 2007).

Biophysical production models are excellent tools for prediction crop performance and thus provide exceptional information for planning and management assessments over both the long and short term (Singels *et al.*, 2010). The use of crop models to investigate the potential impacts of climate change and variability provides a direct link between models, Agrometeorology and the concerns of the society (Murthy, 2004; Rauff & Bello, 2015). A plethora of crop models are used, incorporating different approaches and levels of complexity and highlighting different aspects of the soil-plant-atmosphere system (e.g. PUTU VELD) (Singels *et al.*, 2010).

5.1 Validation of PUTU VELD

With regards to the validation of PUTU VELD, comparing the two short period data sets (PV-Fouché and PV-SAWS, Figure 4.1), it was noted that four of the nine years they followed the same trend (when one increased so did the other, and vice versa). The biggest setback came when PUTU VELD was verified over the extended base period, indicating severe concerns with the model's robustness. The best positive aspect of the PV-SAWS 30-year run was the fair positive correlation ($r = 0.53$) with the Sydenham RP (Table 4.1; Figure 4.1). Unfortunately, PV-SAWS seemed to show a lag in its response and only followed the same trend as Sydenham for a few of the years. It is suspected that overfitting is to blame (i.e. failing to use an independent data set to validate the model).

5.2 Maximum Dry Matter Production

In light of the model validation, the results of this study should be interpreted and extrapolated with caution and should only be understood in light of this report. The comparison between historical PV-SAWS DMPmax and historical PV-AgMIP DMPmax (Figure 4.2) showed a fairly good correlation with a R^2 of 0.53 and implies that the AgMIP data can be used for future simulations. The CDFs (Figure 4.3) showed that PV-AgMIP underestimated DMPmax when compared to PV-SAWS. It was suspected that the AgMIP GCMs do not adequately account for the extreme weather events such as major floods and droughts. During the wettest 3-year period (1986/87 – 1988/89) PV-SAWS and PV-AgMIP overestimated the accumulated DMPmax, when compared to the measured accumulated DMPmax from Sydenham, while during the driest 3-year period (1983/84 – 1985/86) PV-SAWS overestimated and PV-AgMIP underestimated the accumulated DMPmax. There was a weak positive trend in PV-SAWS DMPmax in contrast to a weak negative trend in PV-AgMIP DMPmax (Figure 4.4). As was expected, the smaller variance in the GCM-derived climate data (AgMIP) resulted in a relatively smoother PV-AgMIP DMPmax when compared to the PV-SAWS DMPmax. A weak positive trend in Sydenham DMP was found for the base period.

Simulated rangeland for the future time periods showed reductions of DMPmax for three GCMs under RCP 4.5 (Figure 4.13; Table 4.3) when comparing the current period to the base period for the lower percentiles, and increases for two GCMs. The distant future showed reductions of DMPmax for two GCMs, and increases for three GCMs when compared to the base period. Under RCP 8.5 (Figure 4.14; Table 4.3) when comparing the near future to the base period for the higher percentiles there was reductions for three GCMs, and increases for two GCMs when compared to the base period. The distant future showed a reduction for one GCM, and increases for four GCMs when compared to the base period. The higher percentile ensembled-averages showed a reduction in DMPmax for the near future and increases for the current and distant future periods under RCP 8.5 (Figure 4.16; Table 4.4). Six ensemble members predicted an increase in accumulated DMPmax in the distant future (relative to the base period), while four showed a relative decrease. The average RCP 4.5 and 8.5 had slightly lower accumulated DMPmax although it was in a

similar range to the base period (Figure 4.17). HadGEM2-ES was the only GCM to produce a decrease in accumulated DMPmax from RCP 4.5 to 8.5.

5.3 Date of Occurrence of Maximum Dry Matter Production

Both the historical PV-SAWS Dtp and historical PV-AgMIP Dtp occurred 83% of the time during the optimal period (Figure 4.8). The Dtp for PV-SAWS and PV-AgMIP follow a similar weak negative trend (Figure 4.9), implying a tendency for Dtp to occur slightly earlier in the season with time. PV-SAWS Dtp exhibited a higher variance than PV-AgMIP Dtp.

For each GCM the Dtp for the distant future occurred later in the growth season. This means that more Dtps fell in the optimal period for the current period than for the distant future (Figure 4.19; Table 4.5). On average, under RCP 4.5 and RCP 8.5 an increasing amount of the years from the base period to the current period to the near future to the distant future had Dtp falling outside the optimal period with larger increases noted under RCP 8.5 (Figure 4.21 and 4.22 Table 4.6).

5.4 Number of Moisture Stress Days

There was a lower number of historical PV-SAWS MSD than for historical PV-AgMIP MSD (Figure 4.10). Both PV-SAWS MSD and PV-AgMIP MSD revealed weak linear trends (Figure 4.11). During the driest 3-year period (1983/84 – 1985/86) the highest amount of MSD occurred and during the wettest 3-year period (1986/87 – 1988/89) the least amount of MSD occurred.

Under both emission scenarios, larger increases in MSD were found for the distant future period. Larger increases in MSD from the current period to the distant future was found under RCP 8.5 than for RCP 4.5 for all ensemble members. Although more MSD is observed under RCP 8.5, higher DMPmax was expected during the distant future time period (Figure 4.15 and 4.16). The CDFs of all the ensemble members for the three periods and the two emission scenarios showed a clear future increase in MSD (Figure 4.23 and 4.24; Table 4.7). The ensemble means for all time periods also showed increases in MSD under RCP 4.5 (Figures 4.25) and RCP 8.5 (Figure 4.26). The most noticeable observation is that of a marked increase in MSD for future periods (relative to the historical base period), while slightly bigger

increases were shown under the RCP 8.5 scenario (Table 4.8). These differences for MSD under RCP 4.5 and 8.5 can be ascribed to the characteristics of the emission scenarios where for the RCP 4.5 mitigation schemes are implemented and the benefits are noticed during the later time periods and for RCP 8.5 no mitigation schemes are implemented and the detriments are perceived during the later time periods (Section 2.3.4).

5.5 Seasonal Prediction of Maximum Dry Matter Production

It was shown that July-August-September (JAS) yielded the best result, as about 17.5% (Table 4.2) of the variation in PV-SAWS DMPmax could be explained by JAS Niño 3.4, offering a relatively short yet sufficient forecast lead time. The positive slope in the simple linear regression equation presented in Figure 4.12 implied that lower Niño 3.4 values (generally denoting La Niña conditions) would result in higher DMPmax in Bloemfontein.

As a final point it was noted that for the whole future simulation period (2010/11 – 2098/99): under RCP 4.5 the averaged DMPmax showed a general negative trend which means that DMPmax would be decreasing over time while under RCP 8.5 the averaged DMPmax showed a general positive trend of increasing DMPmax over time. There was a general positive trend for GC under both RCP 4.5 and 8.5 meaning that over time more land is needed per animal for sustainable farming. Both RCP 4.5 and RCP 8.5 Dtp showed a general positive trend although it was noted that RCP 8.5 had a further shift later in the growing season than RCP 4.5. And lastly, there was a general positive trend for MSD under RCP 4.5 and 8.5 with RCP 8.5 increasing more over time than RCP 4.5.

5.6 Recommendations

If the results presented in this study are to be believed, there are certain recommendations that can be made to farmers to ensure a sustainable farming system. Livestock farmers should ensure that rangeland improvement techniques (e.g. rotational grazing) are well understood and well managed in order to avoid environmental damage and long-term decreases in production. The rangeland should be monitored and thus managed for any changes in its condition and health by ensuring appropriate rest periods after relevant

grazing and/or fire events. Trampled and eroded rangeland should be rehabilitated in a timely manner in order to ensure no loss of grazing area. Livestock farmers should also ensure that the stocking rate is within the rangeland's grazing capacity and that good rotational grazing practices are used. Livestock farmers can also consult weather reports and heed to the severe weather early warning in order to minimize the loss of livestock due to extreme weather events such as cold snaps, heat waves, and flood or drought conditions. Consultation of the seasonal forecasts can be advantageous to farmers as this will give them a good lead time as to whether very dry or very wet conditions are expected in the following season. Thus, knowing if it will be a El Niño or a La Niña season will ensure that livestock farmers adapt their management strategies for the coming seasons as to minimise (maximise) the loss (gain) of stock (less or more feed available according to the relevant climate season) or revenue. As pointed out earlier, consulting the Niño 3.4 index during the months of July, August and September could be beneficial.

If autumns and winters do become warmer (Section 2.3.2), it is an indication that the growth season can become longer and more RP can be produced. Livestock farmers will be able to reap the benefits as there could be more feed available for the livestock, and farmers could have a greater store of feed for use during the drought years. The change in the rainfall patterns could mean that with an increase in rainfall during the active growing months, plants could experience less moisture stress resulting in more RP. Farmers need to adapt their management practices in order to get the most out of the wetter years and be able to store enough feed for the drier years as climate variability is unlikely to decrease in future. A change in climate can facilitate a change in vegetation where farmers need to adapt the GC and SR according to the new carrying capacity of the rangeland. The numbers of the different types of animals might also need to be adjusted from grazers to more browsers in order that all of the RP is utilised. During warmer, drier seasons, farmers can include more heat tolerant breeds of animals and ensure that there is enough feed during this period. The time and duration of grazing can be managed and adjusted in order to ensure that the livestock get enough feed but also that the rangeland is not overgrazed and degraded. During hot seasons, farmers can plant trees in order to provide shade for livestock and adequate water supply is needed to keep animals from dying from heat stroke. Extra feed and nutrients can

be supplied during the seasons where the rangeland is not able to provide enough food for the livestock.

It is highly recommended that further work should focus on recalibrating PUTU VELD or identifying alternative rangeland models to be used by industry role-players. Although crop models based largely on the Penman-Monteith equation still have some favour and a role to play, recent advances in light use efficiency models have provided greater insight into ecosystem functions and should be investigated. It is also suggested, that if possible, that daily CO₂ be added as an input in PUTU VELD in order to estimate more accurately the seasonal DMP as it is in the real world.

REFERENCES

- ACOCKS, J.P.H., 1988. Veld types of South Africa. *Mem. Bot. Surv. S. Afr.* No. 40, Government Printer, Pretoria. pp 128.
- AGMIP, 2013. Climate data supplied by The Agricultural Model Intercomparison and Improvement Project. Climate databank. Cape Town: CSAG.
- AHMED, M. & HASSAN, F-U., 2011. APSIM and DSSAT models as decision support tools. *Proceedings of the 19th International Congress on Modelling and Simulation, 12 – 16 December 2011, Perth, Australia.* pp 1174 – 1180.
- AINSWORTH, E.A. & LONG, S.P., 2005. What have we learnt from 15 years of free-air CO₂ enrichment (FACE)? A meta-analytic review of the responses of photosynthesis, canopy properties and plant production to rising CO₂. *New Phytol.* 165: 351 – 372.
- AMBROSINO, C., CHANDLER, R.E. & TODD, M.C., 2011. Southern Africa Monthly Rainfall Variability: An Analysis Based on Generalised Linear Models. *Bull. Amer. Meteor.* 24: 4600 – 4617.
- AMERICAN CHEMICAL SOCIETY (ACS), 2015. Radiative Forcing. [Online]. Retrieved from <http://www.acs.org/content/acs/en/climatescience/atmosphericwarming/radiativeforcing.html> (Accessed 4/08/2015).
- AMERMAN, C.R., 1976. Water flow in soils: A generalised steady-state, two-dimensional porous media flow model. U.S. Sept. of Agr., ARS-NC-30.
- ARVE, L.E., TORRE, S., OLSEN, J.E. & TANINO, K.K., 2011. Stomatal Response to Drought Stress and Air Humidity. In: A. Shanker (ed.). *Abiotic Stress in Plants – Mechanisms and Adaptations.* [Online]. Retrieved from <https://www.intechopen.com/books/abiotic-stress-in-plants-mechanisms-and-adaptations/stomatal-responses-to-drought-stress-and-air-humidity> (Accessed 22/11/2017).
- ARVIDSSON, J., 1999. Nutrient uptake and growth of barley as affected by soil compaction. *Plant Soil* 208: 9 – 19.
- AYDINALP, C. & CRESSER, M.S., 2008. The Effect of Global Climate Change on Agriculture. *Am. Eurasian J. Agric. Environ. Sci.* 3: 672 – 676.
- BADE, D.H., CONRAD, B.E. & HOLT, E.C., 1985. Temperature and Water Stress Effects on Growth of Tropical Grasses. *J. Range Manage.* 38: 321 – 324.
- BADER, D.C., COVEY, C., GUTOWSKI, W.J., HELD, I.M., KUNKEL, K.E., MILLER, R.L., TOKMAKIAN, R.T. & ZHANG, M.H., 2008. Climate Models: An Assessment of Strengths and Limitations. A Report by the U.S. Climate Change Science Program and the Subcommittee on Global Change Research. Washington D.C., USA. pp 124.

- BAIER, W., 1977. Crop-weather models and their use in yield assessments. Tech. Note No. 151, World Meteorological Organization, WMO-No 458, Geneva, Switzerland.
- BAIER, W., 1979. Note on the Terminology of Crop-Weather Models. *Agric. Meteorol.* 20: 137 – 145.
- BAKER, B.B., HANSON, J.D., BOURDON, R.M. & ECKERT, J.B., 1993. The potential effects of climate change on ecosystem processes and cattle production on U.S. rangelands. *Clim. Change* 25: 97 – 117.
- BANGE, M.P., BAKER, J.T., BAUER, P.J., BROUGHTON, K.J., CONSTABLE, G.A., LUO, Q., OOSTERHUIS, D.M., OSANAI, Y., PAYTON, P., TISSUE, D.T., REDDY, K.R. & SINGH, B.K., 2016. Climate Change and Cotton Production in Modern Farming Systems. CABI, United Kingdom and United States of America. pp 45.
- BARFIELD, B.J. & NORMAN, J.M., 1983. Potential for plant environment modification. *Agr. Water Manage.* 7: 73 – 88.
- BENHIN, J.K.A., 2006. Climate change and South African Agriculture. CEEPA Discussion Paper No. 21. Centre for Environmental Economics and Policy in Africa, University of Pretoria.
- BENNETT, L.T., JUDD, T.S. & ADAMS, M.A., 2002. Growth and nutrient content of perennial grasslands following burning in semi-arid, sub-tropical Australia. *Plant Ecol.* 164: 185 – 199.
- BITRI, M., GRAZHDANI, S. & AHMETI, A., 2014. Validation of the AquaCrop Model for Full and Deficit Irrigated Potato Production in Environmental Condition of Korça Zone, South-eastern Albania. *Int. J. Innov. Res. Sci. Eng. Technol.* 3: 12013 – 12020.
- BJØRNÆS, C., 2013. A guide to Representative Concentration Pathways. [Online]. Retrieved from <https://www.sei-international.org/mediamanager/documents/A-guide-to-RCPs.pdf> (Accessed 31/07/2013).
- BOND, W.J. & MIDGLEY, G.F., 2012. Carbon dioxide and the uneasy interactions of trees and savannah grasses. *Philos. T. Roy. Soc. B.* 367: 601 – 612.
- BOOTE, K.J., JONES, J.W. & PICKERING, N.B., 1996. Potential Uses and Limitations of Crop Models. *Agron. J.* 88: 704 – 716.
- BOOYSEN, J., 1983. *Twee metodes vir die kwantitatiewe simulering van groeitoestande van klimaksgras*. M.Sc. Agric. Thesis, University of the Orange Free State, Bloemfontein.
- BOSCH, O.H., 1978. *Die gebruik van biomassa gegewens vir die berekening van produksie*. Ongepubliseerde gegewens, Dept. Landbou en Visserye, Middelburg K.P.
- BOSCH, O.J.H. & VAN RENSBERG, F.P.J., 1987. Ecological status of species on grazing gradients on the shallow soils of the western grassland biome in South Africa. *J. Grassl. Soc. South Afr.* 4: 143 – 147.

- BOVAL, M. & DIXON, R.M., 2012. The importance of grasslands for animal production and other functions: a review on management and methodological progress in the tropics. *Animal* 6: 748 – 762.
- BRANDT, L., 2014. Agriculture Outlook 2015. ABSA AgriConnect report.
- BRISSON, N., BUSSIÈRE, F., OZIER-LAFONTAINE, H., TOURNEBIZE, R. & SINOQUET, H., 2004. Adaption of the crop model STICS to intercropping. Theoretical basis and parameterisation. *Agronomie* 24: 409 – 421.
- BROWN, P.W., 1995. The water relations of range plants: adaptation to water deficits. In: D.J. Bedunah & R.E. Sosebee (eds.). *Wildland plants: physiological ecology and developmental morphology*. Soc. Range Manage., Denver, Colorado pp 291 – 414.
- BROWN, R.W., 1977. Water Relations of Range Plants. In: R.E. Sosebee (ed.). *Rangeland Plant Physiology*. Society for Range Management, Colorado. pp 97.
- CADMAN, M., PETERSEN, C., DRIVER, A., SEKHRAN, N., MAZE, K. & MUNZHEDZI, S., 2010. Biodiversity for Development: South Africa's landscape approach to conserving biodiversity and promoting ecosystem resilience. South African National Biodiversity Institute, Pretoria.
- CAMERON, K.C., DI, H.J. & MOIR, J.L., 2013. Nitrogen losses from the soil/plant system: a review. *Ann. Appl. Biol.* 162: 145 – 173.
- CAMPILLO, C., FORTES, R. & PRIETO, M.H., 2012. Solar Radiation Effect on Crop Production. In: E.B. Babatunde (ed.). *Solar Radiation*. [Online]. Retrieved from [http://cdn.intechopen.com/pdfs/33351/InTech-Solar_radiation_effect_on_crop / production.pdf](http://cdn.intechopen.com/pdfs/33351/InTech-Solar_radiation_effect_on_crop_production.pdf) (Accessed 20/11/2017).
- CARLSON, D.H. & THUROW, T.L., 1992. SPUR-91: Workbook and user guide, Publication MP-1743. Texas A & M University. Department of Rangeland Ecology and Management in cooperation with USDA Soil Conservation Service, College Station, TX.
- CHAI, T. & DRAXLER, R.R., 2014. Root mean square error (RMSE) or mean absolute error (MAE)? – Arguments against avoiding RMSE in the literature. *Geosci. Model Dev.* 7: 1247 – 1250.
- CHEN, H., QUALL, R. & BLANK, R.R., 2005. Effects of soil flooding on photosynthesis, carbohydrate partitioning and nutrient uptake in the invasive exotic *Lepidium latifolium*. *Aquat. Bot.* 82: 250 – 268.
- CHRISTIAAN, K.R., FREER, M., DONNELLY, J.R., DAVIDSON, J.L. & ARMSTRONG, J.S., 1978. Simulation of grazing systems. Centre for agricultural publishing and documentation, Wageningen, The Netherlands. pp 115.
- CIAIS, P.H., REICHSTEIN, M., VIOVY, N., GRANIER, A., OGÉE, J., ALLARD, V., AUBINET, M., BUCHMANN, N., BERNHOFER, C.H.R., CARRARA, A., CHEVALLIER, F., DE NOBLET, N., FRIEND, A.D., FRIEDLINGSTEIN, P., GRÜNWARD, T., HEINESCH,

- B., KERONEN, P., KNOHL, A., KRINNER, G., LOUSTAU, D., MANCA, G., MATTEUCCI, G., MIGLIETTA, F., OURCIVAL, J.M., PAPAIE, D., PILEGAARD, K., RAMBAL, S., SEUFERT, G., SOUSSANA, J.F., SANZ, M.J., SCHULZE E.D., VESALA, T. & VALENTINI, R., 2005. Europe-wide reduction in primary productivity caused by the heat and drought in 2003. *Nature* 437: 529 – 553.
- CINGOLANI, A.M., NOY-MEIR, I. & DÍAZ, S., 2005. Grazing effects on rangeland diversity: a synthesis of contemporary models. *Ecol. Appl.* 15: 757 – 773.
- CLARKE, L.E., EDMONDS, J.A., JACOBY, H.D., PITCHER, H., REILLY, J.M. & RICHEL, R., 2007. Scenarios of Greenhouse Gas Emissions and Atmospheric Concentrations. Sub-report 2.1A of Synthesis and Assessment Product 2.1 by the U.S. Climate Change Science Program and the Subcommittee on Global Change Research. Department of Energy, Office of Biological Environmental Research, Washington, DC., USA. pp 154.
- COHN, A.S., VANWEY, L.K., SPERA, S.A. & MUSTARD, J.F., 2016. Cropping frequency and area response to climate variability can exceed yield response. *Nat. Clim. Change* 6: 601 – 604.
- COMMUNITY EARTH SYSTEM MODEL (CESM), 2016. CCSM4.0 Public Release. [Online]. Retrieved from <http://www.cesm.ucar.edu/models/ccsm4.0/> (Accessed 3/10/2016).
- COLLINS, W.J., BELLOUIN, N., DOUTRIAUX-BOUCHER, M., GEDNEY, N., HINTON, T., JONES, C.D., LIDDICOAT, S., MARTIN, G., O'CONNOR, F., RAE, J., SENIOR, C., TOTTERDELL, I., WOODWARD, S., REICHLER, T. & KIM, J., 2008. Evaluation of the HadGEM2 model. Met Office Hadley Centre Technical Note no. HCTN 74. UK.
- CORSON, M.S., SKINNER, R.H. & ROTZ, C.A., 2006. Modification of the SPUR rangeland model to simulate species composition and pasture productivity in humid temperate regions. *Agric. Syst.* 87: 169 – 191.
- DANCKWERTS, J.E. & TAINTON, N.M., 1996. Range management: Optimisation forage production and quality. *Bull. Grassland Soc. S. Africa.* 7: 36 – 42.
- DE BRUIN, J.N., 1980. *Modellering*. Ongepubliceerde gegewens, Tecknikon, Bloemfontein.
- DE JAGER, J.M., 1974. Putu a dynamic seasonal maize crop growth model. Canadian C.I.B.P. Res. Rep. pp 306 – 320.
- DE JAGER, J.M., 1976. The environmental potential for maize production during the 1974/75 season at Bethlehem. *Crop. Prod.* 5: 9 – 13.
- DE JAGER, J.M., 1992. The PUTU Decision Support System. Monograph of the Department of Agrometeorology, University of the Orange Free State, Bloemfontein. pp 95.
- DE JAGER, J.M., 1997. Research on a computerized weather-based irrigation water management system. Report to the Water Research Commission by Department of Agrometeorology UOFS. Report No. K5/581/0/97.

- DE JAGER, J.M., BOTHA, A.P. & VAN VUUREN, C.J.J., 1981. Effective rainfall and the assessment of potential wheat yields in shallow soil. *Crop. Prod.* 10: 51 – 56.
- DE JAGER, J.M., HOFFMAN, J.E., VAN EDEN, F., PRETORIUS, J., MARAIS, J., ERASMUS, J.F., COWLEY, B.S. & MOTTRAM., 1983a. Preliminary validation of the PUTU maize crop growth model in different parts of South Africa. *Crop. Prod.* 2: 3 – 6.
- DE JAGER, J.M., MOTTRAM, R. & KENNEDY, J.A., 2001. Research on a computerized weather-based irrigation water management system. WRC Report 581/01/01. Pretoria. pp 256.
- DE JAGER, J.M., POTGIETER, A.B. & VAN DEN BERG, W.J., 1998. Framework for forecasting the extent and severity of drought in maize in the Free State province of South Africa. *Agr. Syst.* 5: 351 – 365.
- DE JAGER, J.M., VAN ZYL, W.H., BRISTOW, K.L. & VAN ROOYEN, A., 1982. *Besproeiingskedulering van koring in die besproeiingsgebied van die Vrystaatstreek*. Report from the Water Research Commission, Pretoria. pp 125.
- DE JAGER, J.M., VAN ZYL, W.H., KELBE, B.E. & SINGELS, A., 1983b. Research on the weather service for scheduling the irrigation of winter wheat in the OFS. Final report by the Department of Agrometeorology of the University of the Free State to the Water Research Commission. WRC Report No. 117/1/87.
- DE JONG, R. & CAMERON, D.R., 1979. Computer simulation model for predicting soil water content profiles. *Soil Sci.* 1: 41 – 48.
- DEPARTMENT OF ENVIRONMENTAL AFFAIRS (DEA), 2013a. Long-Term Adaptation Scenarios Flagship Research Program (LTAS) for South Africa: Climate Trends and Scenarios for South Africa. Pretoria, South Africa.
- DEPARTMENT OF ENVIRONMENTAL AFFAIRS (DEA), 2013b. Long-Term Adaptation Scenarios Flagship Research Program (LTAS) for South Africa: Climate Change Implications for the Agriculture and Forestry Sectors in South Africa. Pretoria, South Africa.
- DE WIT, C.T. & GOUDRIAAN, J., 1978. Simulation of ecological processes. Centre for agricultural publishing and documentation, 2nd Rev. Ed., Wageningen, The Netherlands. pp. 180.
- DUNNE, J.P., JOHN, J.G., SHEVLIKOVA, E., STOUFFER, R.J., KRASTING, J.P., MALYSHEV, S.L., MILLY, P.G.D., SENTMAN, L.T., ADCROFT, A.J., COOKE, W., DUNNE, K.A., GRIFFIES, S., HALLBERG, R.W., HARRISON, M.J., LEVY, H., WITTENBERG, A.T., PHILLIPS, P.J. & ZADEH, N., 2013. GFDL's ESM2M Global Coupled Climate – Carbon Earth System Models. Part II: Carbon System Formulation and Baseline Simulation Characteristics. *J. Climate* 6: 2247 – 2267.

- DU PISANI, A.L., 1979. *Agroklimaat, Dataverwerking en Gewasmodellering*. Studiebesoekverslag aan die V.S.A., N.I.G & B., Dept. Landbou en Visserye, Pretoria.
- DU PISANI, L.G., 1992. *Simulasiestudies met Cenchrus ciliaris L. cv. Molopo*. Ph.D. Thesis, University of the Free State, Bloemfontein.
- DURAND, W. & DU TOIT, A.S., 2000. A preliminary study on the maize production potential for a number of localities in the Molopo and Ditsebotla districts using CERES-maize. Report to the Land and Agricultural Bank of South Africa, compiled by the ARC-Grain Crops Institute, Potchefstroom, South Africa. pp 19.
- DU TOIT, A.S., PRINSLOO, M.A., DURAND, W. & KIKER, G., 2000. Vulnerability of maize production to climate change and adaptation assessment in South Africa. In: G. Kiker (ed.). *Climate Change Impacts in Southern Africa*. Report to the National Climate Change Committee, Department of Environmental Affairs and Tourism, Pretoria, South Africa. pp 92.
- EDWARDS, D., 1984. Fire regimes in the biomes of South Africa. In: P. deV Booyesen & N.M. Tainton (eds.). *Ecological effects of fire in South Africa ecosystems*. Ecological Studies No. 48. Springer-Verlag, Berlin, Heidelberg, New York, Tokyo. pp 19 – 37.
- EVERSON, C.S., 1999. Veld burning in different vegetation types: Grassveld. In: N.M. Tainton (ed.). *Veld management in South Africa*. University of Natal Press, Pietermaritzburg. pp 218 – 228.
- FELLER, U. & VASEVA, I.I., 2014. Extreme climate events: impacts of drought and high temperature on physiological processes in agronomically important plants. *Front. Environ. Sci.* 2: 1 – 17.
- FERRARO, D.O. & OESTERHELD, M., 2002. Effect of defoliation on grass growth. A quantitative review. *OIKOS* 98: 125 – 133.
- FISH, L., 2012. *Themeda triandra*. South African National Biodiversity Institute. [Online]. Retrieved from <http://www.plantzafrica.com/planttuv/themedatri.htm> (Accessed 07/06/2012).
- FOOD AND AGRICULTURE ORGANIZATION OF THE UNITED NATIONS (FAO), 2010. Land Degradation Assessment in Dryland: Land use systems of South Africa. [Online]. Retrieved from <http://www.fao.org/nr/lada/indexf4ac.html?option=com/content&view=article&id=156&Itemid=200026&lang=en> (Accessed 14/08/2017).
- FOUCHÉ, H.J., 1984. *Ondersoek na die gebruik van die PUTU 11 simulasiemodel en PALMER-INDEKS vir die karakterisering van droogtetoestande*. M.Sc. Agric. Thesis, University of the Orange Free State, Bloemfontein.

- FOUCHÉ, H.J., 1992. *Simulering van die produksiepotensiaal van veld en die kwantifisering van droogte in die Sentrale Oranje-Vrystaat*. Ph.D. Thesis, University of the Orange Free State, Bloemfontein.
- FOURCAUD, T., ZHANG, X., STOKES, A., LAMBERS, H. & KÖRNER, C., 2008. Plant Growth Modelling and Applications: The Increasing Importance of Plant Architecture in Growth Models. *Ann. Bot.* 101: 1053 – 1063.
- FOY, J.K., TEAGUE, W.R. & HANSON, J.D., 1999. Evaluation of the upgraded SPUR model (SPUR2.4). *Ecol. Modell.* 118: 149 – 165.
- FREER, M., DAVIDSON, J.L., ARMSTRONG, J.S. & DONNELLY, J.R., 1970. Simulation of summer grazing. *Proceedings of the 11th International Grassland Congress, Surfers Paradise*. pp 913-917.
- FUJINO, J., NAIR, R., KAINUMA, M., MASUI, T. & MATSUOKA, Y., 2006. Multi-gas Mitigation Analysis on Stabilization Scenarios Using Aim Global Model. *Energ. J.* 27: 343 – 354.
- FYN, R.W.S., 2003. Determinants of community composition and diversity in KwaZulu-Natal mesic grasslands: evidence from long-term experiments and pot and plot competition experiments. PhD Thesis, University of KwaZulu Natal, Pietermaritzburg.
- FYN, R.W.S., HAYNES, R.J. & O'CONNOR, T.G., 2003. Burning causes long-term changes in soil organic matter content of a South African grassland. *Soil Biol. Biochem.* 35: 677 – 687.
- GBETIBOUO, G.A. & RINGLER, C., 2009. Mapping South African farming sector vulnerability to climate change and variability. A subnational assessment. IFPRI discussion paper 885. International Food Policy Research Institute (IFPRI).
- GEOPHYSICAL FLUID DYNAMICS LABORATORY (GFDL), 2016. Earth System Models. [Online]. Retrieved from <https://www.gfdl.noaa.gov/earth-system-model/> (Accessed 3/10/2016).
- GERÇEK, S. & OKANT, M., 2010. Evaluation of CERES-maize simulation model results with measured data using water pillow irrigation under semi-arid climatic conditions. *Afr. J. Agric. Res.* 5: 606 – 613.
- GIORGETTA, M.A., JUNGCLAUS, J., REICK, C.H., LEGUTKE, S., BADER, J., BÖTTINGER, M., BROVKIN, V., CRUEGER, T., ESCH, M., FIEG, K., GLUSHAK, K., GAYLER, V., HAAK, H., HOLLWEG, H-D., ILYINA, T., KINNE, S., KORNBLUEH, L., MATEI, D., MAURITSEN, T., MIKOLAJEWICZ, H., MUELLER, W., NOTZ, D., PITHAN, F., RADDATZ, T., RAST, S., REDLER, R., ROECKNER, E., SCHMIDT, H., SCHNUR, R., SEGSCHEIDER, J., SIX, K.D., STOCKHAUSE, M., TIMMRECK, C., WEGNER, J., WIDMANN, H., WIENERS, K-H., CLAUSSEN, M., MAROTZKE, J. & STEVENS, B., 2013. Climate and carbon cycle changes from 1850 to 2100 in

MPI-ESM simulations for the Coupled Model Intercomparison Project phase 5. *J. Adv. Model. Earth Syst.* 23: 6312 – 6335.

GOLDBLATT, A., 2015. AGRICULTURE: FACTS & TRENDS: South Africa. WWF-SA.

GOOGLE EARTH. V 7.1.7.2600 (1/12/2017). Bloemfontein and surrounding area, South Africa. 29°10'28.12" S, 26°13'00.39" W, Eye alt 79.66 km. Landsat 2014. [Online]. Retrieved from <http://www.earth.google.com> (Accessed 01/12/2017).

GOUDRIAAN, J., 1977. Crop Micrometeorology: A simulation study. Centre for agricultural publications and documentation, Wageningen, The Netherlands. pp 257.

GRASS FED SOLUTIONS, 2016. The Daily Pasture Rotation. [Online]. Retrieved from http://www.grass-fed-solutions.com/pasture-rotation.html#at_pco=smlre-1.0&at_si=58491004e95219df&at_ab=per-2&at_pos=2&at_tot=4 (Accessed 27/06/2016).

GRASSLAND PROGRAMME., 2012. Grasslands: Living in a working landscape. [Online]. Retrieved from <http://www.eiatoolkit.ewt.org.za/documents/biodiversity/grassl-1.pdf> (Accessed 12/06/2012).

HANAOKA, T.R., KAWASE, M., KAINUMA, Y., MATSUOKA, H. & OKA, K., 2006. Greenhouse gas emissions scenarios database and regional mitigation analysis. NIES, Tsukuba.

HARDY, M.B. & MENTIS, M.T., 1986. Grazing dynamics in sour grassveld. *S. Afr. J. Sci.* 82: 566 – 572.

HARGREAVES, G.H. & SAMANI, Z.A., 1985. Reference Crop Evapotranspiration from Temperature. *Appl. Eng. Agric.* 1: 96 – 99.

HASANUZZAMAN, M., NAHAR, K. & FUJITA, M., 2013. Extreme Temperature Responses, Oxidative Stress and Antioxidant Defence in Plants. In: K. Vahdati (ed.). *Abiotic Stress – Plant Responses and Applications in Agriculture*. [Online]. Retrieved from <https://www.intechopen.com/books/abiotic-stress-plant-responses-and-applications-in-agriculture/extreme-temperature-responses-oxidative-stress-and-antioxidant-defense-in-plants> (Accessed 20/11/2017).

HATCH, G.P., 1999. The management of different types of veld: Sweet grassveld. In: N.M. Tainton (ed.). *Veld management in South Africa*. University of Natal Press, Pietermaritzburg. pp 289 – 293.

HAVERKORT, A.J., FRANKE, A.C., STEYN, J.M., PRONK, A.A., CALDIZ, D.O. & KOOMAN, P.L., 2015. A Robust Potato Model: LINTUL-POTATO-DSS. *Potato Res.* 58: 313 – 327.

HELLMANN, D.B., 1976. The study of water use in wheat in relation to environment and yield, on the Makatini Flats, using lysimeters and neutron probes. M.Sc. Thesis, University of Natal, Pietermaritzburg.

- HIJIOKA, T., MATSUOKA, Y., NISHIMOTO, H., MASUI, T. & KAINUMA, M., 2008. Global GHG emission scenarios under GHG concentration stabilization targets. *J. Glob. Environ. Eng.* 13: 97 – 108.
- HILLEL, D. & ROSENZWEIG, C. (ed.), 2013. Handbook of climate change and agroecosystems: global and regional aspects and implications. London, Imperial College Press. pp 301.
- HIRZEL, J. & MATUS, I., 2013. Effect of soil depth and increasing fertilisation rate on yield and its components of two durum wheat varieties. *Chilean J. Agric. Res.* 73: 55 – 59.
- HOELL, A., FUNK, C., ZINKE, J. & HARRISON, L., 2017. Modulation of the Southern Africa precipitation response to the El Niño Southern Oscillation by the subtropical Indian Ocean Dipole. *Clim. Dynam.* 48: 2529 – 2540.
- HOLMES, W., 1989. Grass: its production and utilisation. 2nd ed. Blackwell Sci. Publ., Oxford. pp 7 – 42.
- HUNT, H.W., TRLICA, M.J., REDENTE, E.F., MOORE, J.C., DETLING, J.K., KITTEL, T.G.F., WALTER, D.E., FOWLER, M.C., KLEIN, D.A., ELLIOT, E.T. & WALTER, L.E.F., 1991. Simulation model for the effects of climate change on temperate grassland ecosystems. *Ecol. Modell.* 53: 205 – 246.
- HURT, C.R., HARDY, M.B. & TAINTON, N.M., 1993. Identification of key grass species under grazing in the Highland sourveld of Natal. *Afr. J. Range & For. Sci.* 10: 96 – 102.
- INNIS, G.S., 1978. Grassland simulation model. Ecological Studies, Springer-Verlag, New York, Heidelberg, Berlin.
- INTERGOVERNMENTAL PANEL ON CLIMATE CHANGE (IPCC), 2007. The Physical Science Basis, Contribution of Working Group 1 to the Fourth Assessment Report of the Intergovernmental Panel on Climate Change. IN: S. Solomon, D. Qin, M. Manning, Z. Chen, M. Marquis, K.B. Averyt, M. Tignor & H.L. Miller (eds.). *Climate Change 2007*. Cambridge University Press, Cambridge. pp 1-18.
- INTERNATIONAL RESEARCH INSTITUTE FOR CLIMATE AND SOCIETY (IRI), 2016. What is ENSO? [Online]. Retrieved from https://iridl.ldeo.columbia.edu/maproom/ENSO/ENSO_Info.html (Accessed 5/12/2016).
- INTERNATIONAL RESEARCH INSTITUTE FOR CLIMATE AND SOCIETY (IRI), 2017. IRI ENSO Forecast. [Online]. Retrieved from <https://iri.columbia.edu/our-expertise/climate/forecasts/enso/current/> (Accessed 15/11/2017).
- JALOTA, S.K., SINGH, S., CHAHAL, G.B.S., RAY, S.S., PANIGRAPHY, S., SINGH, B. & SINGH, K.B., 2010. Soil texture, climate and management effects on plant growth,

grain yield and water use by rainfed maize-wheat cropping system: Field and simulation study. *Agr. Water Manage.* 97: 83 – 90.

- JAWUORO, S.O., KOECH, O.K., KARUKU, G.N. & MBAU, J.S., 2017. Plant species composition and diversity depending on piospheres and seasonality in the southern rangelands of Kenya. *Ecological Processes* 6:16 – 24.
- JENSEN, M.E., WRIGHT, J.L. & PRATT, B.J., 1971. Estimating soil moisture depletion from climate, crop and soil data. *Transac. ASAE.* 14: 954 – 958.
- JOHNSON, D.A., 1980. Improvement of perennial herbaceous plants for drought-stressed western rangelands. In: N.C. Turner & P.J. Kramer (eds.). *Adaptations of plants to water and temperature stress.* John Wiley & Sons, New York: pp 419 – 433.
- JONES, C. D., HUGHES, J. K., BELLOUIN, N., HARDIMAN, S. C., JONES, G. S., KNIGHT, J., LIDDICOAT, S., O'CONNOR, F. M., ANDRES, R. J., BELL, C., BOO, K.-O., BOZZO, A., BUTCHART, N., CADULE, P., CORBIN, K. D., DOUTRIAUX-BOUCHER, M., FRIEDLINSTEIN, P., GORNALL, J., GRAY, L., HALLORAN, P. R., HURTT, G., INGRAM, W. J., LAMARQUE, J.-F., LAW, R. M., MEINSHAUSEN, M., OSPREY, S., PALIN, E. J., PARSONS CHINI, L., RADDATZ, T., SANDERSON, M. G., SELLAR, A. A., SCHURER, A., VALDES, P., WOOD, N., WOODWARD, S., YOSHIOKA, M. & ZERROUKAT, M., 2011. The HadGEM2-ES implementation of CMIP5 centennial simulations. *Geosci. Model Dev.* 4: 543 – 570.
- JONES, J.W., COLWICK, R.F. & THREADGILL, E.D., 1972. A simulation Environmental model of temperature, evaporation, rainfall and soil moisture. *Transac. ASAE.* 15: 366 – 372.
- JONES, J.W., HOOGENBOOM, G., PORTER, C., BOOTE, K.J., BATCHELOR, W.D., HUNT, L.A., WILKENS, P.W., SINGH, U., GUSMAN, A.J. & RITCHIE, J.T., 2003. The DSSAT cropping system model. *Eur. J. Agron.* 18: 235 – 265.
- KAISER, H.W., 1976. Maize crop growth and development related to solar radiation. Ph.D. Thesis, University of Natal, Pietermaritzburg.
- KEATING, B.A., CARBERRY, P.S., HAMMER, G.L., PROBERT, M.E., ROBERTSON, M.J., HOLZWORTH, D., HUTH, N.I., HARGREAVES, J.N.G., MEINKE, H., HOCHMAN, Z., MCLEAN, G., VERBURG, K., SNOW, V., DIMES, J.P., SILBURN, M., WANG, E., BROWN, S., BRISTOW, K.L., ASSENG, S., CHAPMAN, S., MCCOWN, R.L., FREEBAIRN, D.M. & SMITH, C.J., 2003. Overview of APSIM, a model designed for farming systems simulations. *Eur. J. Agron.* 18: 267 – 288.
- KGOSIKOMA, O.E., HARVIE, B.A. & MOJEREMANE, W., 2012. Bush encroachment in relation to rangeland management systems and environmental conditions in Kalahari ecosystems of Botswana. *Afr. J. Agric. Res.* 7: 2312 – 2319.
- KIDD, P.S. & PROCTOR, J., 2001. Why plants grow poorly on very acid soils: are ecologists missing the obvious? *J. Exp. Biol.* 52: 791 – 799.

- KIKER, G.A., 2015. South African county study on Climate Change: Synthesis report for the vulnerability and adaptation assessment section. University of Natal. [Online]. Retrieved from https://unfccc.int/files/meetings/seminar/application/pdf/sem_sups_south_africa.pdf (Accessed 28/07/2015).
- KIMBALL, B.A., KOBAYASHI, K. & BIND, M., 2002. Responses of Agricultural Crops to Free-Air CO₂ Enrichment. *Adv. Agron.* 77: 293 – 368.
- KIRTMAN, B., POWER, S.B., ADEDOYIN, J.A., BOER, G.J., BOJARIU, R., CAMILLONI, I., DOBLAS-REYES, F.J., FIORE, A.M., KIMOTO, M., MEEHL, G.A., PRATHER, M., SARR, A., SCHÄR, C., SUTTON, R., VAN OLDENBORGH, G.J., VECCHI, G. & WANG, H.J., 2013. Near-term Climate Change: Projections and Predictability. In: T.F. Stocker, D. Qin, G.-K. Plattner, M. Tignor, S.K. Allen, J. Boschung, A. Nauels, Y. Xia, V. Bex & P.M. Midgley (eds.). *Climate Change 2013: The Physical Science Basis. Contribution of Working Group I to the Fifth Assessment Report of the Intergovernmental Panel on Climate Change*. Cambridge: Cambridge University Press.
- KLEMMER, J., LAUER, J., FORMANSKI, V., FONTAINE, R., KILIAN, P., SINSEL, S., ERBES, A. & ZÄPF, J., 2011. Definition and Application of a Standard Verification and Validation Process for Dynamic Vehicle Simulation Models. *SAE Int. J. Mater. Manuf.* 4: 743 – 758.
- KÖCKY, M., 2008. Effects of simulated daily precipitation patterns on annual plant populations depend on life stages and climatic region. *BMC Ecol.* 8: 1 - 23.
- KOEVOETS, I.T., VANEMA, J.H., ELZENGA, J.T.M. & TESTERINK, C., 2016. Roots Withstanding their Environment: Exploiting Root System Architecture Responses to Abiotic Stress to Improve Crop Tolerance. *Front. Plant Sci.* 7: 1 – 19.
- KOOMAN, P.L. & HAVERKORT, A.J., 1994. Modelling development and growth of the potato crop influenced by temperature and day length: LINTUL-POTATO. In: A.J. Haverkort & D.K.L. MacKerron (eds.). *Ecology and modelling of potato crops under conditions limiting growth*. Kluwer Academic Publishers, Dordrecht. pp 41 – 60.
- KRAAIJ, T. & WARD, D., 2006. Effects of rain, nitrogen, fire and grazing on tree recruitment and early survival in bush-encroachment savanna, South Africa. *Plant Ecol.* 186: 235 – 246.
- KRASENSKY, J. & JONAK, C., 2012. Drought, salt and temperature stress-induced metabolic rearrangements and regulatory networks. *J. Exp. Bot.* 63: 1593 – 1608.
- LANDMAN, W.A., MASON, S., TYSON, P.D. & TENNANT, W., 2001. Statistical Downscaling of GCM Simulations to Streamflow. *J. Hydrol.* 252: 221 – 236.
- LANDSBERG, J., JAMES, C.D., MORTON, S.R., MÜLLER, W.J. & STOL, J., 2003. Abundance of composition of plant species along grazing gradients in Australian rangelands. *J. Appl. Ecol.* 40: 1008 – 1024.

- LANE, D.M., SCOTT, D., HEBL, M., GUERRA, R., OSHERSON, D. & ZIMMER, H., 2016. Introduction to Statistics. [Online]. Retrieved from http://onlinestatbook.com/Online_Statistics_Education.pdf (Accessed 10/10/2016).
- LEGHARI, S.J., WAHOCHO, N.A., LAGHARI, G.M., LAGHARI, A.H., BHABHAN, G.M., TALPUR, K.H., BHUTTO, T.A., WAHOCHO, S.A. & LASHARI, A.A., 2016. Role of Nitrogen for Plant Growth and Development: A review. *J. Environ. Biol.* 10: 209 – 218.
- LETEY, J. & VAUGHAN, P., 2013. Soil type, crop and irrigation technique affect nitrogen leaching to groundwater. *Calif. Agr.* 67: 231 – 241.
- LI, S., KANG, S., ZHANG, L., ZHANG, J., DU, T., TONG, L. & DING, R., 2016. Evaluation of six potential evapotranspiration models for estimating crop potential and actual evapotranspiration in arid regions. *J. Hydrol.* 543: 450 – 461.
- LIU, H., ZANG, R. & CHEN, H.Y.H., 2016. Effects of grazing on photosynthetic features and soil respiration of rangelands in the Tianshan Mountains of Northwest China. *Sci. Rep.* 6: 30087 – 30095.
- LIU, Z., CHENG, R., XIAO, W., GUO, Q. & WANG, N., 2014. Effects of Off-Season Flooding on Growth, Photosynthesis, Carbohydrate Partitioning, and Nutrient Uptake in *Distylium chinense*. *PLoS One* 9: 1 – 9.
- LOOMIS, R.S., RABBINGE, R. & NG, E., 1979. Explanatory models of crop physiology. Research paper, University of Davis, California.
- LUPO, A. & KINIMONTH, W., 2017. Global Climate Models and Their Limitations. [Online]. Retrieved from http://weather.missouri.edu/gcc/09-09-13_%20Chapter%201%20Models.pdf (Accessed 17/11/2017).
- MACASKILL, C., 2013. Agriculture in the Provinces. In: Department of Agriculture, Forestry and Fisheries (eds.). The Agri Handbook of South Africa 2013 – 2014. Pretoria: RainbowSA Publishing (Pty) Ltd. pp 34.
- MACHADO, R.M.A. & SERRALHEIRO, R.P., 2017. Soil Salinity: Effect on Vegetable Crop Growth. Management Practices to Prevent and Mitigate Soil Salinization. *Horticulturae* 3: 1 – 13.
- MACKELLAR, N., NEW, M. & JACK, C., 2014. Observed and modelled trends in rainfall and temperature for South Africa: 1960 – 2010. *S. Afr. J. Sci.* 110: 1 – 13.
- MAGNUSSON, P.S., CHRISTENSSON, M., ESKILSON, J., FORSGREN, D., HALLBERG, G., HOGBERG, J., LARSSON, F., MOESTEDT, A. & WERNER, B., 2002. Simics: A full system simulation platform. *Computer* 35: 50 – 58.
- MAKKINK, G.F. & VAN HEEMST, H.D.J., 1975. Simulation of the water balance of arable land and pastures. Centre for agricultural publishing and documentation, Wageningen, The Netherlands. pp 87.

- MARICLE, B.R., WHITE, S.J., MERAZ, A., MAFORO, N.G., BIGGS, T.N., MARTIN, N.M. & CAUDLE, K.L., 2014. Effects of Ethanol Toxicity on Enzyme Activity in Anaerobic Respiration in Plants. *Trans. Kans. Acad. Sci.* 117: 237 – 244.
- MARIMUTHU, S. & SURENDRAN, U., 2015. Effect of nutrients and plant growth regulators on growth and yield of black gram in sandy loam soils of Cauvery new delta zone, India. *Cogent Food Agric.* 1: 1 – 8.
- MARTIN, G.M., BELLOUIN, N., COLLINS, W.J., CULVERWELL, I.D., HALLORAN, P. R., HARDIMAN, S.C., HINTON, T.J., JONES, C.D., MCDONALD, R.E., MCLAREN, A.J., O'CONNOR, F.M., ROBERTS, M.J., RODRIGUEZ, J.M., WOODWARD, S., BEST, M.J., BROOKS, M.E., BROWN, A.R., BUTCHART, N., DEARDEN, C., DERBYSHIRE, S.H., DHARSSI, I., DOUTRIAUX-BOUCHER, M., EDWARDS, J.M., FALLOON, P.D., GEDNEY, N., GRAY, L.J., HEWITT, H.T., HOBSON, M., HUDDLESTON, M.R., HUGHES, J., INESON, S., INGRAM, W.J., JAMES, P.M., JOHNS, T.C., JOHNSON, C.E., JONES, A., JONES, C.P., JOSHI, M.M., KEEN, A.B., LIDDICOAT, S., LOCK, A.P., MAIDENS, A.V., MANNERS, J.C., MILTON, S.F., RAE, J.G.L., RIDLEY, J.K., SELLAR, A., SENIOR, C.A., TOTTERDELL, I.J., VERHOEF, A., VIDALE, P.L. & WILTSHIRE, A., 2011. The HadGEM2 family of Met Office Unified Model climate configuration. *Geosci. Model Dev.* 4: 723 – 757.
- MARTIN, S.A., SANTOS, M.P., PEÇANHA, A.L., POMMER, C., COMPOSTRINI, E., VIANA, A.P., FAÇANHA, A.R. & SMITH, R.B., 2009. Photosynthesis and cell respiration modulated by water deficit in grapevine (*Vitis vinifera* L.) cv. Cabernet Sauvignon. *Braz. J. Plant Physiol.* 21: 95 – 102.
- MAX-PLANCK-INSTITUT FÜR METEOROLOGIE (MPI), 2016. New Earth system model of Max Planck Institute for Meteorology. [Online]. Retrieved from <http://www.mpimet.mpg.de/en/science/models/mpi-esm.html> (Accessed 3/10/2016).
- MAYER, D.G. & BUTLER, D.G., 1993. Statistical validation. *Ecol. Model.* 68: 21 – 32.
- MCCREE, K.J., 1974. Equations for the rate of dark respiration of White Clover and Grain Sorghum, as constants of dry weight, photosynthetic rate and temperature. *Crop. Sci.* 14: 509-514.
- MCDONALD, M., 2012. Grassland Biome. South African National Biodiversity Institute. [Online]. Retrieved from <http://www.plantzafrica.com/vegetation/grassland.htm> (Accessed 11/06/2012).
- MCKEON, G.M., STONE, G.S., SYKTUS, J.I., CARTER, J.O., FLOOD, N.R., AHRENS, D.G., BRUGET, D.N., CHILCOTT, C.R., COBON, D.H., COWLEY, R.A., CRIMP, S.J., FRASER, G.W., HOWDEN, S.M., JOHNSTON, P.W., RYAN, J.G., STOKES, C.J. & DAY, K.A., 2009. Climate change impacts on northern Australian rangeland livestock carrying capacity: a review of issues. *Rangeland J.* 31: 1 – 29.
- MCNIDER, R.T., HANDYSIDE, C., DOTY, K., ELLENBURG, W.L., CRUISE, J.F., CHRISTY, J.R., MOSS, D., SHARDA, V. & HOOGENBOOM, G., 2015. An integrated crop and

hydrologic modeling system to estimate hydrologic impacts of crop irrigation demands. *Environ. Modell. Softw.* 72: 341 – 355.

- MEISSNER, H.H., HOFMEYR, H.S., VAN RENSBURG, W.J.J. & PIENAAR, J.P., 1983. *Klassifikasie van vee vir sinvolle beraming van vervangingswaardes in terme van 'n biologiese-gedefinieerde Grootvee-eenheid*. Technical report No 175. Department of Agriculture, Pretoria.
- MENDENHALL, W. & SINCICH, T.L., 2003. *A Second Course in Statistics: Regression Analysis*. 6th ed. Texas: Prentice Hall.
- MENTIS, M.T., 1981. Evaluation of the wheel-point and step-point methods of veld condition assessment. *Proceedings of the Grassland Society of southern Africa* 16: 89 – 94.
- MENTIS, M.T. & BIGALKE, R.C., 1979. Some effects of fire on two grasslands francolins in the Natal Drakensberg. *S. Afr. J. Wildl. Res.* 9: 1 – 8.
- MENTIS, M.T. & TAINTON, N.M., 1984. The effects of fire on forage production and quality. In: P.deV. Booysen & N.M. Tainton (eds.). *Ecological effects of fire in South African ecosystems*. Ecological Studies No. 48. Springer-Verlag, Berlin, Heidelberg, New York, Tokyo. pp 245 – 254.
- MEYER, W.S., WALKER, S. & GREEN, G.C., 1979. The prediction of water use by spring wheat in South Africa. *Crop Prod.* 8: 185-191.
- MINAR, N., BURKHARTY, R., LANGTONZ, C. & ASKENAZIX, M., 1996. The Swarm Simulation System: A Toolkit for Building Multi-agent Simulations. [Online]. Retrieved from <http://cobweb.cs.uga.edu/~maria/pads/papers/swarm-MinarEtAl96.pdf> (Accessed 21/11/2017).
- MINITAB, 2017. Overview for Cumulative Distribution Function (CDF). [Online]. Retrieved from <http://support.minitab.com/en-us/minitab-express/1/help-and-how-to/basic-statistics/probability-distributions/how-to/cumulative-distribution-function-cdf/before-you-start/overview/> (Accessed 17/11/2017).
- MITSUI, S. & UEDA, M., 1963. Cation Exchange Capacity of Crop Roots and Ion Uptake. *Soil Sci. Plant Nutr.* 9: 1 – 6.
- MOELETSI, M.E., WALKER, S. & LANDMAN, W.A., 2011. ENSO and Implications on Rainfall Characteristics with Reference to Maize Production in the Free State Province of South Africa. *Phys. Chem. Earth, Pt. A/B/C* 36: 715 – 726.
- MOELETSI, M.E., WALKER, S. & HAMANDAWANA, H., 2013. Comparison of the Hargreaves and Samani equation and the Thornthwaite equation for estimating dekadal evapotranspiration in the Free State Province, South Africa. *Phys. Chem. Earth* 66: 4 – 15.
- MOHAWESH, O.E., 2011. Evaluation of evapotranspiration models for estimating daily reference evapotranspiration in arid and semi-arid environments. *Plant Soil Environ.* 57: 145 – 152.

- MOHTAR, R.H., ZHAI, T. & CHEN, X., 2000. A world wide web-based grazing simulation model (GRASIM). *Comput. Electron. Agr.* 29: 243 – 250.
- MONTEITH, J.L., 1965. Evaporation and Environment. *19th Symp. Soc. Exptl. Biol.* pp 205 – 234.
- MOORE, A.D., DONNELLY, J.R. & FREER, M., 1997. GRAZPLAN: decisions support systems for Australian grazing enterprises. III. Pasture growth and soil moisture submodels, and the GrassGro DSS. *Agric. Syst.* 55: 535 – 582.
- MOPIPI, K., 2012. The roles of competition, disturbance and nutrients on species composition light interception and biomass production in South African semi-arid savanna. PhD Thesis, University of KwaZulu Natal, Pietermaritzburg.
- MORGAN, J.A., PATAKI, D.E., KORNER, C., CLARK, H., DEL GROSSO, S.J., GRÜNZWEIG, J.M., KNAPP, A.K., MOSIER, A.R., NEWTON, P.C., NIKLAUS, P.A., NIPPERT, J.B., NOWAK, R.S., PARTON, W.J., POLLEY, H.W. & SHAW, M.R., 2004. Water relations in grassland and desert ecosystems exposed to elevated atmospheric CO₂. *Oecologia* 140: 11 – 15.
- MORGAN, J.W., 1999. Defining grassland fire events and the response of perennial plants to annual fire in temperate grasslands of south-eastern Australia. *Plant Ecol.* 144: 127 – 144.
- MORRIS, C.D., TANTON, N.M. & HARDY, M.B., 1992. Plant species dynamics in the Southern Tall Grassveld under grazing, resting and fire. *J. Grassld Soc. Sth. Afr.* 9: 90 – 95.
- MOSS, R.H., BABIKER, M., BRINKMAN, S., CALVO, E., CARTER, T.R., EMONDS, J., ELGIZOULI, I., EMORI, S., ERDA, L., HIBBARD, K.A., JONES, R., KAINUMA, M., KELLEHER, J., LAMARQUE, J.F., MANNING, M.R., MATTHEWS, B., MEEHL, J., MEYER, L., MITCHELL, J.F.B., NAKICENOVIC, N., O'NEILL, B., PICHS, R., RIAHI, K., ROSE, S.K., RUNCU, P., STOUFFER, R.J., VAN VUUREN, D.P., WEYANT, J.P., WILBANKS, T.J., VAN YPERSELE, J.P. & ZUREK, M., 2008. Towards New Scenarios for Analysis of Emissions, Climate Change, Impacts, and Response Strategies. Intergovernmental Panel on Climate Change, Geneva. pp 132.
- MOSS, R.H., EDMONDS, J.A., HIBBARD, K.A., MANNING, M.R., ROSE, S.K., VAN VUUREN, D.P., CARTER, T.R., EMORI, S., KAINUMA, M., KRAM, T., MEEHL, G.A., MITCHELL, J.F.B., NAKICENOVIC, N., RIAHI, K., SMITH, S.J., STOUFFER, R.J., THOMSON, A.M., WEYANT, J.P. & WILBANKS, T.J., 2010. The next generation of scenarios for climate change research and assessment. *Nature* 463: 747 – 756.
- MOTRAM, R., 1976. Measurement of evapotranspiration from *Lolium multiflorum* and *Paspalum dilatatum* and its dependents upon the climate variables. M.Sc. Thesis, University of Natal, Pietermaritzburg.

- MOULT, N.G., LECLER, N.L., SMITHERS, J.C. & CLARK, D.J., 2009. A Catchment-scale irrigation systems model for sugarcane. Part 1: Model development. *Water SA*. 35: 21 – 28.
- MUCINA, L. & RUTHERFORD, M.C., 2006. Vegetation Map: Gh5 Bloemfontein Dry Grassland. CD-ROM. Pretoria: SANBI.
- MUGASI, S.K., SABIITI, E.N. & TAYEBWA, B.M., 2000. The economic implications of bush encroachment on livestock farming in rangelands of Uganda. *Afri. J. Range For. Sci.* 17: 64 – 69.
- MUNIANDY, J.M., YUSOP, A. & ASKARI, M., 2016. Evaluation of reference evapotranspiration models and determination of crop coefficient for *Momordica chatantia* and *Capsicum annuum*. *Agr. Water Manage.* 169: 77 – 89.
- MURTHY, V.K.R., 2002. Basic Principles of Agricultural Meteorology. Book Syndicate Publishers, Koti, Hyderabad.
- MURTHY, V.R.K., 2004. Crop growth modeling and its applications in agricultural meteorology. In: M.V.K. Sivakumar, P.S. Roy, K. Harmsen, & S.K. Saha. *Satellite Remote Sensing and GIS Applications in Agricultural Meteorology. Proceedings of the Training Workshop 7 – 11 July 2003, Dehra Dun, India*. WMO, Geneva, Switzerland. pp 235 – 261.
- MYBURGH, P.A., VAN ZYL, J.L. & CONRADIE, W.J., 1996. Effect of Soil Depth on Growth and Water Consumption of Young *Vitis vinifera* L. cv. Pinot noir. *S. Afr. J. Enol. Vitic.* 17: 53 – 62.
- NATIONAL AERONAUTICS AND SPACE ADMINISTRATION (NASA), 2017a. Climate Change: Vital Signs of the Planet. [Online]. Retrieved from <https://climate.nasa.gov/news/916/for-first-time-earths-single-day-co2-tops-400-ppm/> (Accessed 20/05/2017).
- NATIONAL AERONAUTICS AND SPACE ADMINISTRATION (NASA), 2017b. Climate Change: Vital Signs of the Planet – Global Temperature. [Online]. Retrieved from <https://climate.nasa.gov/vital-signs/global-temperature/> (Accessed 3/06/2017).
- NATIONAL OCEANIC & ATMOSPHERIC ADMINISTRATION (NOAA), 2016a. El Niño Southern Oscillation (ENSO). [Online]. Retrieved from <http://www.esrl.noaa.gov/psd/enso/> (Accessed 5/12/2016).
- NATIONAL OCEANIC & ATMOSPHERIC ADMINISTRATION (NOAA), 2016b. Equatorial Pacific Sea Surface Temperatures. [Online]. Retrieved from <https://www.ncdc.noaa.gov/teleconnections/enso/indicators/sst.php> (Accessed 5/12/2016).
- NATIONAL OCEANIC & ATMOSPHERIC ADMINISTRATION (NOAA), 2017. State of the Climate: Global Climate Report for Annual 2016. [Online]. Retrieved from <https://www.ncdc.noaa.gov/sotc/global/201613> (Accessed 3/06/2017).

- NOWAK, R.S., ELLSWORTH, D.S. & SMITH, S.D., 2004. Functional responses of plants to elevated atmospheric CO₂ – do photosynthetic & productivity data from FACE experiments support early predictions. *New Phytol.* 162: 253 – 280.
- NUMERICAL TERRADYNAMIC SIMULATION GROUP (NTSG), 2017. MODIS GPP/NPP Project (MOD 17). [Online]. Retrieved from <http://www.ntsg.umd.edu/project/modis/mod17.php> (Accessed 28/11/2017).
- OBA, G., POST, E., SYVERTSEN, P.O. & STENSETH, N.C., 2000. Bush cover and range conditions assessments in relation to landscape and grazing in southern Ethiopia. *Landscape Ecol.* 15: 535 – 546.
- O'CONNOR, T.G., PUTTICK, J.R. & HOFFMAN, M.T., 2014. Bush encroachment in southern Africa: changes and causes. *Afri. J. Range For. Sci.* 31: 67 – 88.
- OLESEN, J.E. & BINDI, M., 2002. Consequences of climate change for European agricultural productivity, land use and policy. *Eur. J. Agron.* 16: 239 – 262.
- OPPERMAN, D.P.J. & HUMAN, J.J., 1976. *Die invloed van ontblaring en vogstremming op die groeikragtigheid van Themeda triandra Forsk. onder gekontroleerde toestande. Proc. Grassld Soc. Sth. Afr.* 12: 65 – 71.
- ORMEÑO, E. & FERNANDEZ, C., 2012. Effects of Soil Nutrient on Production and Diversity of Volatile Terpenoids from Plants. *Curr. Bioact. Compd.* 8: 71 – 79.
- PACIFIC CLIMATE IMPACTS CONSORTIUM (PCIC), 2014. Statistically Downscaled Climate Scenarios. [Online]. Retrieved from <https://www.pacificclimate.org/data/statistically-downscaled-climate-scenarios> (Accessed 3/10/2016).
- PALMER, A.R. & AINSLIE, A., 2006a. Country Pasture/Forage Resource Profiles South Africa. Prepared by Palmer and Ainslie in May 2002, livestock data updated by S.G. Reynolds in August 2006. [Online]. Retrieved from <http://www.fao.org/ag/AGP/agpc/doc/Counprof/southafrica/southafrica2.htm> (Accessed 28/07/2015).
- PALMER, A.R. & AINSLIE, A., 2006b. Arid rangeland production systems of Southern Africa. *Sécheresse* 17: 98 – 104.
- PALMER, A.R., KILLER, F.J., AVIS, A.M. & TONGWAY, D., 2001. Defining function in rangelands of the Peddie District, Eastern Cape, using Landscape Function Analysis. *Afr. J. Range For. Sci.* 18: 53 – 58.
- PALMER, A.R., SAMUELS, I., CUPIDO, C., FINCA, A., KANGOMBE, W.F., YANUSA, I.A.M., VETTER, S. & MAPAURE, I., 2016. Aboveground biomass production of a semi-arid southern African Savanna: towards a new model. *Afr. J. Range For. Sci.* 33: 43 – 51.
- PASSIOURA, J.B., 1991. Soil Structure and plant growth. *Aust. Soil. Res.* 29: 717 – 728.

- PELTON, W.L., KING, K.M. & TANNER, C.B., 1960. An evaluation of the Thornthwaite and mean air temperature methods of determining potential evapotranspiration. *Agron. J.* 52: 387-395.
- PEREIRA, A.B., VILLA NOVA, N.A., RAMOS, V.J. & PEREIRA, A.R., 2008. Potato potential yield based on climatic elements and cultivar characteristics. *Bragantia, Campinas* 67: 327 – 334.
- PIERCE, L.J., 1958. Estimating seasonal and short-term fluctuations in evapotranspiration from meadow crops. *Bull. Am. Met. Soc.* 39: 73-75.
- POLLEY, H.W., BRISKE, D.D., MORGAN, J.A., WOLTER, K., BAILEY, D.W. & BROWN, J.R., 2013. Climate Change and North American Rangelands: Trends, Projections, and Implications. *Rangeland Ecol. Manag.* 66: 493 – 511.
- POORTER, H., ANTEN, N.P.R. & MARCELIS, L.F.M., 2013. Physiological mechanisms in plant growth models: do we need a supra-cellular systems biology approach. *Plant Cell Environ.* 36: 1673 – 1690.
- PRIESTLEY, C.H.B. & TAYLOR, R.J., 1972. An assessment of surface heat flux and evaporation using large-scale parameters. *Mon. Weather Rev.* 100: 81-92.
- PRINSLOO, M.A., DU TOIT, A.S. & DURAND, W., 1998. System modelling of maize production potential on rehabilitated open cast coal mine soils in Mpumalanga. Contract research report. ARC-ISCW, Pretoria. pp 34.
- PRINZENBERG, A.E., BARBIER, H., SALT, D.E., STICH, B. & REYMOND, M., 2010. Relationships between Growth, Growth Response to Nutrient Supply, and Ion Content Using a Recombinant Inbred Line Population in Arabidopsis. *Plant Physiol.* 154: 1361 – 1371.
- RAITT, G.R., 2005. *Themeda triandra* resnosterveld in the Heidelberg district. MSc. Thesis, University of Stellenbosch, Stellenbosch.
- RANA, B., 2016. South Africa Tourism: Map of South Africa. [Online]. Retrieved from <http://southafricatourism1.blogspot.co.za/> (Accessed 10/10/2016).
- RANDALL, D.A., WOOD, R.A., BONY, S., COLMAN, R., FICHEFET, T., FYFE, J., KATTSOV, V., PITMAN, A., SHUKLA, J., SRINIVASAN, J., STOUFFER, R.J., SUMI, A. & TAYLOR, K.E., 2007. Climate Models and Their Evaluation. In: S. Solomon, D. Qin, M. Manning, Z. Chen, M. Marquis, K.B. Averyt, M. Tignor, & H.L. Miller (eds.). *Climate Change 2007: The Physical Science Basis. Contribution of Working Group I to the Fourth Assessment Report of the Intergovernmental Panel on Climate Change*. Cambridge University Press, Cambridge, United Kingdom and New York, NY, USA.
- RAUFF, K.O. & BELLO, R., 2015. A Review of Crop Growth Simulation Models as Tools for Agricultural Meteorology. *A. S.* 6: 1098 – 1105.

- REIDSMA, P., EWERT, F., LANSINK, A.O. & LEEMANS, R., 2010. Adaptation to climate change and climate variability in European agriculture. *Eur. J. Agron.* 32: 91 – 102.
- REILLY, J., TUBIELLO, F.N., MCCARL, B., ABLER, D., DARWIN, R., FUGLIE, K., HOLLINGER, S., IZAURRALDE, C., JAGTAP, S., JONES, J., MEARN, L., OJIMA, D., PAUL, E., PAUSTIAN, K., RIHA, S., ROSENBERG, N. & ROSENZWEIG, C., 2003. U.S. Agriculture and Climate Change: New Results. *Clim. Change* 57: 43 – 79.
- RETHMAN, N.F.G. & BOOYSEN, P.DEV., 1968. The influence of time on defoliation on the vigour of a tall grassveld sward in the next season. *Proceedings of the Annual Congresses of the Grassland Society of Southern Africa* 3: 91 – 94.
- RIAHI, K., GRÜBLER, A. & NAKICENOVIC, N., 2007. Scenarios of long-term socio-economic and environmental development under climate stabilization. *Technol. Forecast Soc. Chang.* 74: 887 – 935.
- RILEY, W.J., ORTIZ-MONASTERIO, I. & MATSON, P.A., 2001. Nitrogen leaching and soil nitrate, nitrite, and ammonium levels under irrigated wheat in Northern Mexico. *Nutr. Cycl. Agroecosys.* 61: 223 – 236.
- ROBINSON, N., 1966. Solar radiation. Elsevier, Amsterdam.
- RODRIGUEZ, A., 2017. The Effects of Ground Temperature on Grass. [Online]. Retrieved from <http://homeguides.sfgate.com/effects-ground-temperature-grass-69755.html> (Accessed 20/11/2017).
- ROGELJ, J., MEINSHAUSEN, M. & KNUTTI, R., 2012. Global warming under old and new scenarios using IPCC climate sensitivity range estimates. *Nat. Clim. Change* 2: 248 – 253.
- ROTZ, C.A., SATTER, L.D., MERTENS, D.R. & MUCK, R.E., 1999. Feeding strategy, nitrogen cycling and profitability of dairy farms. *J. Dairy Sci.* 82: 2841 – 2855.
- ROWE, J.H., TOPPING, J.F., LIU, J. & LINDSEY, K., 2016. Abscisic acid regulates root growth under osmotic stress conditions via an interacting hormonal network with cytokinin, ethylene and auxin. *New Phytol.* 211: 225 – 239.
- RUIZ-RAMON, M. & MÍNGUEZ, M.I., 2006. ALAMEDA, a Structural-Functional Model for Faba Bean Crops: Morphological Parameterization and Verification. *Ann. Bot-London.* 97: 377 – 388.
- RUNNING, S., NEMANI, R.R., HEINSCH, F.A., ZHAO, M., REEVES, M. & HASHIMOTO, H., 2004. A continuous satellite-derived measure of global terrestrial primary production. *BioScience* 54: 547 – 560.
- SABIITI, E.N., WAMARA, J.B., OGEN-ODOI, A.A. & WEIN, R.W., 1992. The Role of Fire in Pasture and Rangeland Management. *Normadic People* 31: 107 – 110.

- SAIDI, D., 2012. Importance and Role of Cation Exchange Capacity on the Physical Properties of the Cheliff Saline Soils (Algeria). *Procedia Eng.* 33: 435 – 449.
- SAMANI, Z.A., 2000. Estimating Solar Radiation and Evapotranspiration using Minimum Climatological Data (Hargreaves-Samani equation). *J. Irrig. Drain-ASCE.* 126: 265 – 267.
- SAWS, 2013. Climate data supplied by South African Weather Service. Climate databank. Pretoria: SAWS.
- SAXTON, K.E., JOHNSON, H.P. & SHAW, R.H., 1974. Modeling evapotranspiration and soil moisture. *Transac. ASAE.* 17: 673-677.
- SCHAUMBERGER, A., KOWARIK, A. & BADER, R., 2010. Estimation of forage production in Austria. Final report of Eurostat Grant 2008, Topic 4.07, Wien and Gumpenstein, Austria.
- SCHULZE, R.E., 1974. Catchment evapotranspiration in the Natal Drakensberg. Ph.D. Thesis, University of Natal, Pietermaritzburg.
- SCHULZE, R.E., KIKER, G.A. & KUNZ, R.P., 1993. Global climate change and agricultural productivity in southern Africa: Thought for food and food for thought. *Global Environ. Chang.* 3: 330 – 349.
- SCOTT, J.D., 1947. Veld management in South Africa. *Bull. Dept. Agric. S. Afr.* No. 278.
- SCRIPPS INSTITUTE OF OCEANOGRAPHY, 2017. The Keeling Curve. [Online]. Retrieved from <https://scripps.ucsd.edu/programs/keelingcurve/> (Accessed 21/11/2017).
- SELIRIO, I.S. & BROWN, D.M., 1979. Soil Moisture-based simulation of forage yield. *Agric. Met.* 28: 99-114.
- SHAWCROFT, R.W., LEMON, E.R., ALLEN, L.H., STEWART, D.W. & JENSEN, S.E., 1974. The soil-plant-atmosphere model and some of its predictions. *Agric. Met.* 14: 287 – 307.
- SHI, H., WANG, B., YANG, P., LI, Y. & MIAO, F., 2016. Differences in Sugar Accumulation and Mobilization between Sequential and Non-Sequential Senescence Wheat Cultivars under Natural and Drought Conditions. *PLoS One* 11: 1 – 17.
- SHIELDS, C.A., BAILEY, D.A., DANABASOGLU, G., JOCHUM, M., KIEHL, J.T., LEVIS, S. & PARK, S., 2011. The Low Resolution CCSM4. Revised submission to Journal of Climate, CCSM4 Special Collection.
- SHIRLEY, J.H., 2005. Solar Constant. In: J.E. Oliver (ed.). *Encyclopedia of World Climatology.* Springer, The Netherlands. pp 666 – 667.
- SHRIVASTAVA, P. & KUMAR, R., 2015. Soil salinity: A serious environmental issue and plant growth promoting bacteria as one of the tools for its alleviation. *Saudi J. Biol. Sci.* 22: 123 – 131.

- SINCLAIR, T.R. & SELIGMAN, N.G., 1996. Crop Modelling: From Infancy to Maturity. *Agron. J.* 88: 698 – 704.
- SINGELS, A., ANNANDALE, J.G., DE JAGER, J.M., SCHULZE, R.E., INMAN-BAMBER, N.G., DURAND, W., VAN RENSBURG, L.D., VAN HEERDEN, P.S., CROSBY, C.T., GREEN, G.C. & STEYN, J.M., 2010. Modelling crop growth and crop water relations in South Africa: Past achievements and lessons for the future. *S. Afr. J. Plant Soil* 27: 46 – 65.
- SINGELS, A. & DE JAGER, J.M., 1991a. Refinement and validation of the PUTU wheat crop growth model. 1. Phenology. *S. Afr. J. Plant Soil* 8: 59 – 66.
- SINGELS, A. & DE JAGER, J.M., 1991b. Refinement and validation of the PUTU wheat crop growth model. 2. Leaf area expansion. *S. Afr. J. Plant Soil* 8: 67 – 72.
- SINGELS, A. & DE JAGER, J.M., 1991c. Refinement and validation of the PUTU wheat crop growth model. 3. Grain growth. *S. Afr. J. Plant Soil* 8: 73 – 77.
- SIYABONGA AFRICA, 2016. Kruger Park: Red Grass. [Online]. Retrieved from http://www.krugerpark.co.za/africa_red_grass.html (Accessed 2/12/2016).
- SKIRVAN, S.M. & MORAN, M.S., 2003. Rangeland Ecological and Physical Modeling in a Spatial Context. *Proceedings from the 1st Interagency Conference on Research in the Watersheds, October 2003, Arizona, USA.*
- SLAYTER, R.O. & MCILROY, I.C., 1961. Practical Micrometeorology. CSIRO, Melbourne, Australia.
- SMET, M. & WARD, D., 2009. A comparison of the effects of different rangeland management systems on plant species composition, diversity and vegetation structure in a semi-arid savanna. *Afri. J. Range For. Sci.* 22: 59 – 71.
- SMIT, G.N., 2009. Calculation of grazing capacity and browse capacity for game species. [Online]. Retrieved from <http://www.wildliferanching.com/content/grazing-capacity-game> (Accessed 10/10/2016).
- SMITH, S.J. & WIGLEY, T.M.L., 2006. Multi-gas forcing stabilization with minicam. *Energ. J.* 27: 373 – 392.
- SNYDER, R.L., 2012. WTON *Excel* application for converting Rs ($W.m^{-2}.d^{-1}$) to number of sunshine hours (n). Atmospheric Science, Davis, CA, USA.
- SNYMAN, H.A., 1982. *Die hidrologiese siklus en waterverbruiksdoeltreffendheid van veld in verskillende suksessiestadia in die Sentrale Oranje-Vrystaat.* M.Sc. Agric. Thesis, University of the Free State, Bloemfontein.
- SNYMAN, H.A., 1989. *Evapotranspirasie en waterverbruiksdoeltreffendheid van verskillende grasspesies in die sentrale Oranje-Vrystaat.* Tydskrif. Weidingvern. *S. Afr.* 6: 146 – 151.

- SNYMAN, H.A., 1998. Dynamics and sustainable utilization of rangeland ecosystems in arid and semi-arid climates of southern Africa. *J. Arid Environ.* 39: 645 – 666.
- SNYMAN, H.A., 2002. Fire and the dynamics of a semi-arid grassland: Influence on soil characteristics. *Afri. J. Range For. Sci.* 19: 137 – 145.
- SNYMAN, H.A., 2003a. Fire and the dynamics of semi-arid grassland: influence of plant survival, productivity and water-use efficiency. *Afri. J. Range For. Sci.* 20: 29 – 39.
- SNYMAN, H.A., 2003b. Short-term response of rangeland following an unplanned fire in terms of soil characteristics in a semi-arid climate of South Africa. *J. Arid Environ.* 55: 160 – 180.
- SNYMAN, H.A., 2004a. Short-term response in productivity following an unplanned fire in a semi-arid rangeland of South Africa. *J. Arid Environ.* 56: 465 – 485.
- SNYMAN, H.A., 2004b. Estimating the short-term impact of fire on rangeland productivity in a semi-arid climate of South Africa. *J. Arid Environ.* 59: 685 – 697.
- SNYMAN, H.A., 2006. Short-term response of burnt grassland to defoliation in a semi-arid climate of South Africa. *Afri. J. Range For. Sci.* 23: 1 – 11.
- SNYMAN, H.A., 2009a. Root studies on grass species in a semi-arid South Africa along a degradation gradient. *Agr. Ecosyst. Environ.* 130: 100 – 108.
- SNYMAN, H.A., 2009b. Root studies on grass species in a semi-arid South Africa along a soil-water gradient. *Agr. Ecosyst. Environ.* 131: 247 – 254.
- SNYMAN, 2013. Rangeland production data supplied by Prof. H.A. Snyman. Personal rangeland production databank. Bloemfontein: University of the Free State.
- SNYMAN, H.A. & FOUCHÉ, H.J., 1991. Production and water-use efficiency of semi-arid grasslands of South Africa as affected by veld conditions and rainfall. *Water SA* 17: 263 – 268.
- SNYMAN, H.A. & FOUCHÉ, H.J., 1993. Estimating seasonal herbage production of a semi-arid grassland base on veld condition, rainfall and evapotranspiration. *Afri. J. Range For. Sci.* 10: 21 – 24.
- SNYMAN, H.A., INGRAM, L.J. & KIRKMAN, K.P., 2013. *Themeda triandra*: a keystone grass species. *Afri. J. Range For. Sci.* 30: 99 – 125.
- SNYMAN, H.A. & OPPERMAN, D.P.J., 1983. *Die invloed van vog en ontblaringsbehandelings in hidrologiese eenhede op natuurlike veld in die Sentrale Oranje-Vrystaat. Proc. Grassld Soc. Sth. Afr.* 18: 124 – 130.
- SNYMAN, P.E. & STEYN, A.S., 2011. Monitoring the 2D Bloemfontein urban heat island. *Proceedings of the 27th annual conference of the South African Society for Atmospheric Sciences, 22 - 23 September, Hartbeespoort, South Africa.* p 61-62.

- SOUSA, C.A.F. & SODEK, L., 2002. The metabolic response of plants to oxygen deficiency. *Braz. J. Plant Physiol.* 14: 83 – 94.
- SOUSSANA, J-F., MAIRE, V., GROSS, N., BACHELET, B., PAGÈS, L., MARTIN, R., HILL, D. & WIRTH, C., 2012. GEMINI: A grassland model simulating the role of plant traits for community dynamics and ecosystem functioning. Parameterization and evaluation. *Ecol. Modell.* 231: 134 – 145.
- SOUTH AFRICAN NATIONAL BIODIVERSITY INSTITUTE (SANBI), 2013. Climate Change and Biodiversity: Climate and Impacts Factsheet Series, Factsheet 7 of 7. [Online]. Retrieved from <http://www.sanbi.org/sites/default/files/ocuments/documents/ltas-factsheetclimate-change-and-biodiversity-sector2013.pdf> (Accessed 28/07/2015).
- STAPPER, M., 1980. A dynamic growth and development model for maize (*Zea maize*). Program and model documentation No. 80-2.
- SPITTERS, C.J.T., 1990. Crop growth models: their usefulness and limitations. *Acta Hortic.* 267: 349 – 368.
- SPITTERS, C.J.T. & SCHAPENDONK, A.H.C.M., 1990. Evaluation of breeding strategies for drought tolerance in potato by means of crop growth simulation. *Plant Soil.* 123: 193 – 203.
- STENSETH, N.C., OTTERSEN, G., HURREL, J.W., MYSTERUD, A., LIMA, M., CHAN, K-S., YOCCOZ, N.G. & ÅDLANDSVIK, B., 2003. Studying climate effects on ecology through the use of climate indices: the North Atlantic Oscillation, El Niño Southern Oscillation and beyond. *P. Roy. Soc. B. – Biol. Sci.* 270: 2087 – 2096.
- STEVENS, N., BOND, W., HOFFMAN, T. & MIDGLEY, G., 2015. Change is in the Air: Ecological trends and their drivers in South Africa. South African Environmental Observation Network (SAEON). Pretoria. pp 5.
- STICHLER, C., 2002. Grass growth and development. [Online]. Retrieved from http://counties.agrilife.org/kerr/files/2011/09/grass-growth-and-development_3.pdf (Accessed 28/02/2017).
- STÖCKLE, C.O., DONATELLI, M. & NELSON, R., 2003. CropSyst, a cropping systems simulation models. *Eur. J. Agron.* 18: 289 – 307.
- STUTE, M., CLEMENT, A. & LOHMANN, G., 2001. Global climate models: Past, present, and future. *Proc. Natl. Acad. Sci. U.S.A.* 98: 10529 – 10530.
- SWEMMER, A.M. & KNAPP, A.K., 2008. Defoliation synchronizes aboveground growth of co-occurring C4 grass species. *Ecology* 89: 2860 – 2867.
- TAINTON, N.M., 1999a. The ecology of the main grazing lands of South Africa: The grassland biome. In: N.M. Tainton (ed.). *Veld management in South Africa*. University of Natal Press, Pietermaritzburg. pp 23 – 33.

- TAINTON, N.M., 1999b. The ecology of the main grazing lands of South Africa: Production characteristics of the main grazing lands of South Africa. In: N.M. Tainton (ed.). *Veld management in South Africa*. University of Natal Press, Pietermaritzburg. pp 46 – 50.
- TAINTON, N.M., 1999c. Veld condition assessment. In: N.M. Tainton (ed.). *Veld management in South Africa*. University of Natal Press, Pietermaritzburg. pp 194 – 195.
- TAINTON, N.M., 1999d. Veld burning. In: N.M. Tainton (ed.). *Veld management in South Africa*. University of Natal Press, Pietermaritzburg. pp 217 – 218.
- TAINTON, N.M., GROVES, R.H. & NASH, R., 1977. Time of mowing and burning: Short term effects on production and tiller development. *Proc. Grassld Soc. Sth. Afr.* 12: 59 – 64.
- TAINTON, N.M. & HARDY, M.B., 1999. Introduction to the concepts of development of vegetation. In: N.M. Tainton (ed.). *Veld management in South Africa*. University of Natal Press, Pietermaritzburg. pp 1 – 22.
- TAINTON, N.M. & MENTIS, M.T., 1984. Fire in grassland. In: P. de V. Booyesen & N.M. Tainton (eds.). *Ecological effects of fire in South African ecosystems*. Springer-Verlag, Berlin. pp 115 – 197.
- TAJER, A., 2016. What's the function of Nitrogen (N) in plants? [Online]. Retrieved from <https://www.greenwaybiotech.com/blogs/news/whats-the-function-of-nitrogen-n-in-plants> (Accessed 23/11/2017).
- TARDIEU, F., 2013. Plant response to environmental conditions: assessing potential production, water demand, and negative effects of water deficit. *Front. Physiol.* 4: 1 – 11.
- TEAGUE, W.R. & DANCKWERTS, J.E., 1989. The concept of vegetation change and veld condition. In: J.E. Danckwerts & W.R. Teague (eds.). *Veld management in the Eastern Cape*. Dept. Agric. & Water Supply, Eastern Cape Region.
- TEAGUE, W.R., GRANT, W.E., KREUTER, U.P., DIAZ-SOLIS, H., DUBE, S., KOTHMANN, M.M., PINCHAK, W.E. & ANSLEY, R.J., 2008. An ecological economic simulation model for assessing fire and grazing management effects on mesquite rangelands in Texas. *Ecol. Econ.* 64: 611 – 624.
- THORVALDSSON, G., TREMBLAY, G.F. & KUNELIUS, H.T., 2007. The effects of growth temperature on digestibility and fibre concentration of seven temperate grass species. *Acta Agr. Scand. B – S. P.* 57: 322 – 328.
- TOL. R.S., 2002. Estimates of the Damage Costs of Climate Change. Part 1: Benchmark Estimates. *Environ. Resour. Econ.* 21: 47 – 73.

- TRNKA, M., EITZINGER, J., GRUSZCZYNSKI, G., BUCHGRABER, K., RESCH, R. & SCHAUMBERGER, A., 2006. A simple statistical model for predicting herbage production from permanent grassland. *Grass Forage Sci.* 61: 253 – 271.
- TROLLOPE, W.S.W., 1999. Veld burning: Fire behaviour. In: N.M. Tainton (ed.). *Veld management in South Africa*. University of Natal Press, Pietermaritzburg. pp 218 – 228.
- TROLLOPE, W.S.W., TROLLOPE, L.A. & BOSCH, O.J.H., 1990. Veld and Pasture management terminology in southern Africa. *J. Grassld Soc. Sth. Afr.* 7: 52 – 61.
- TUBIELLO, F.N., DONATELLI, M., ROSENZWEIG, C. & STOCKLE, C.O., 2002a. Effects of climate change and elevated CO₂ on cropping systems: model predictions at two Italian locations. *Eur. J. Agron.* 13: 179 – 189.
- TUBIELLO, F.N., ROSENZWEIG, C., GOLDBERG, R., JAGTAP, S. & JONES, J.W., 2002b. Effects of climate change on US crop production: simulation results using two different GCM scenarios. Part 1: Wheat, potato, maize, and citrus. *Climate Res.* 20: 259 – 270.
- TUBIELLO, F.N., SOUSSANA, J-F. & HOWDEN, S.M., 2007. Crop and pasture response to climate change. *Proc. Natl. Acad. Sci. U.S.A.* 104: 19686 – 19690.
- UCHIDA, R., 2002. Essential Nutrients for Plant Growth: Nutrient Functions and Deficiency Symptoms. In: J.A. Silva & R. Uchida (eds.). *Plant Nutrient Management in Hawaii's Soils, Approaches for Tropical and Subtropical Agriculture*. College of Tropical Agriculture and Human Resources, University of Hawaii at Manoa, Hawaii. pp 24.
- UNITED NATIONS (UN), 2004. Long-range world population projection (1950 – 2300). Based on the 2002 revision. United Nations, New York.
- VALLVERDÚ, J., 2014. What are Simulations? An Epistemological Approach. *Proc. Technol.* 13: 6 – 15.
- VAN DEN BERG, J.A., 1972. *Die invloed van seisoensbeweiding op Cymbopogon-Themeda veld*. M.Sc. Agric. Thesis, University of the Orange Free State, Bloemfontein.
- VAN DER BURGT, G.J.H.M., OOMEN, G.J.M., HABETS, N.S.J. & ROSSING, W.A.H., 2006. The NDICEA Model, a tool to improve nitrogen use efficiency in cropping systems. *Nutr. Cycl. Agroecosys.* 74: 275 – 294.
- VAN DER WESTHUIZEN, H.C., SNYMAN, H.J., VAN RENSBURG, W.L.J. & POTGIETER, J.H.J., 2001. The quantification of grazing capacity from grazing – and production values for forage species in semi-arid grasslands of southern Africa. *Afr. J. Range Forage Sci.* 18: 43 – 52.
- VAN ETTEN, E.J.B., 2017. Fire in Rangelands and its Role in Management. [Online]. Retrieved from <https://www.eolss.net/sample-chapters/C10/E5-35-19.pdf> (Accessed 17/11/2017).

- VAN KEULEN, H., 1975. Simulation of water use and herbage growth in arid regions. Centre for agricultural publishing and documentation, Wageningen, The Netherlands. pp 184.
- VAN NIEKERK, G. & OPPERMAN, D.P.J., 1982. *Onderzoek van plantwaterverhoudinge in natuurlike weiveld*. UOVS. Navorsingsverslag. pp 2.
- VAN VUUREN, D.P., DEN ELZEN, M.G.J., LUCAS, P.L., EICKHOUT, B., STRENGERS, B.J., VAN RUIJVEN, B., WONINK, S. & VAN HOUDT, R., 2007. Stabilizing greenhouse gas concentrations at low levels: an assessment of reduction strategies and costs. *Clim. Change* 81: 119 – 159.
- VAN VUUREN, D.P., EDMONDS, J., KAINUMA, M., RIAHI, K., THOMSON, A., HIBBARD, K., HURTT, G.C., KRAM, T., KREY, V., LAMARQUE, J-F., MASUI, T., MEINSHAUSEN, M., NAKICENOVIC, N., SMITH, S.J. & ROSE, S.K., 2011. The representative concentration pathways: an overview. *Clim. Change* 109: 5 – 31.
- VAN VUUREN, D.P., EICKHOUT, B., LUCAS, P.L. & DEN ELZEN, M.G.J., 2006. Long-term multi-gas scenarios to stabilize radiative forcing – exploring costs and benefits within an integrated assessment framework. *Energ. J.* 27: 201 – 233.
- VOLENEC, J.J. & NELSON, C.J., 2003. Environmental Aspects of Forage Management. In: R.F. Barnes, C.J. Nelson, M. Collins & K.J. Moore (eds.). *Forages Volume 1: An Introduction to Grassland Agriculture*. Blackwell Publishing, Iowa. pp 99.
- WATANABE, M., SUZUKI, T., O'ISHI, R., KOMURO, Y., WATANABE, S., EMORI, S., TAKEMURA, T., CHIKIRA, M., OGURA, T., SEKIGUCHI, M., TAKATA, K., YAMAZAKI, D., YOKOHATA, T., NOZAWA, T., HASUMI, H., TATEBE, H. & KIMOTO, M., 2010. Improved climate simulation by MIROC5: Mean states, variability, and climate sensitivity. *J. Climate* 23: 6312 – 6335.
- WAYNE, G., 2013. The Beginner's Guide to Representative Concentration Pathways. *Skeptical Science*. pp 5 – 20.
- WEISSTEIN, E.W., 2016. Correlation Coefficient. [Online]. Retrieved from <http://mathworld.wolfram.com/CorrelationCoefficient.html> (Accessed 10/10/2016).
- WEISSTEIN, E.W., 2017. Distribution Function. [Online]. Retrieved from <http://mathworld.wolfram.com/DistributionFunction.html> (Accessed 17/11/2017).
- WIEGAND, K., SALTZ, D. & WARD, D., 2006. A patch-dynamics approach to savanna dynamics and woody plant encroachment – Insights from an arid savanna. *Perspect. Plant Ecol.* 7: 229 – 242.
- WIEGAND, T., SNYMAN, H.A., KELLNER, K. & PARUELO, J.M., 2004. Do grasslands have a memory: modelling phytomass production of a semi-arid South African grassland. *Ecosystems* 7: 243 – 258.

- WIGHT, J.R. & SKILES, J.W., 1987. SPUR: Simulation of production and utilization of rangelands. Documentation and user guide, ARS 63. U.S. Department of Agriculture, ARS.
- WILKS, D.S., 2006. Statistical methods in the Atmospheric Sciences. 2nd ed. Vol 91 of the International Geophysics Series. Paris: Academic Press.
- WILLMOTT, C.J., ACKLESON, S.G., DAVIS, R.E., FEDDEMA, J.J., KLINK, K.M., LEGATES, D.R., O'DONNELL, T. & ROWE, C.M., 1985. Statistics for the evaluation of model performance. *J. Geophys. Res.* 90: 8995 – 9005.
- WILLMOTT, C.J., ROBESON, S.M. & MATSUURA, K., 2011. A refined index of model performance. *Int. J. Climatol.* 32: 2088 – 2094.
- WILSON, A.D., TONGWAY, D.J., GRAETZ, R.D. & YOUNG, M.D., 1984. Range inventory and monitoring. In: G.N. Hamington, A.D. Wilson & M.D. Young (eds.). *Management of Australia's rangelands*. CSIRO, Melbourne.
- WISE, M., CALVIN, K., THOMSON, A., CLARKE, L., BOND-LAMBERTY, B., SANDS, R., SMITH, S.J., JANETOS, A. & EDMONDS, J., 2009. Implications of limiting CO₂ concentrations for land use and energy. *Science* 324: 1183 – 1186.
- WOLFSON, M.M. & TAINTON, N.M., 2000. The morphology and physiology of the major forage plants: Grasses. In: N.M. Tainton (ed.). *Pasture Management in South Africa*. University of Natal Press, Pietermaritzburg, South Africa. pp 7.
- WOOD, T., 2012. Using Mean Absolute Error for Forecast Accuracy. [Online]. Retrieved from <http://canworksmart.com/using-mean-absolute-error-forecast-accuracy/> (Accessed 10/10/2016).
- WORLDOMETERS, 2016. World Population. [Online]. Retrieved from <http://www.worldometers.info/world-population/> (Accessed 16/11/2016).
- WORLD METEOROLOGICAL ORGANIZATION (WMO), 2014. El Nino/Southern Oscillation. Report NO. 1145. Geneva, Switzerland.
- WORLD RAINFOREST MOVEMENT (WRM), 2016. Map of Africa. [Online]. Retrieved from <http://wrm.org.uy/browse-by-country/africa/south-africa/> (Accessed 10/10/2016).
- WU, Y., SAKAMOTO, C.M. & BOTNER, D.M., 1989. On the application of the CERES-Maize model to the North China Plain. *Agric & Forestry Meteorology* 49: 9 – 22.
- XU, C-Y. & CHEN, D., 2005. Comparison of seven models for estimation of evapotranspiration and groundwater recharge using lysimeter measurement data in Germany. *Hydrol. Process.* 19: 3717 – 3734.
- YAN, L., ZHOU, G. & ZHANG, F., 2013. Effects of Different Grazing Intensities on Grassland Production in China: A Meta-Analysis. *PloS One* 8: 1 – 9.

ZAREKIA, S., ARZANI, H., JAFARI, M., JAVADI, S.A., JAFARI, A.A. & ZANDNI ESFAHAM, E., 2013. Changes of vegetation structure and biomass in response to the livestock grazing in steppe rangelands of Iran. *J. Anim. Plant Sci.* 23: 1466 – 1472.

APPENDIX A

The FORTRAN program for the PUTU VELD model.

```
1      PROGRAM PUTU VELD
2      ! The FORTRAN version of the PUTU 11 model
3      !
4      ! *****
5      ! *      PROGRAM PUTUVELD          VERSION 3          22 JUNE 2017      *
6      ! *****
7      ! THIS PROGRAM IS BASED ON THE 1989 QUICK BASIC VERSION 2          ##
8      ! OF THE PUTU11 MODEL THAT WAS ORIGINALLY DEVELOPED BY          ##
9      ! BOOYSEN AND DE JAGER AT THE UNIVERSITY OF THE FREE          ##
10     ! STATE AND LATER USED BY HJ FOUCHE IN HIS PHD.          ##
11     ! ALTERATIONS WERE MADE IN ORDER TO ALLOW ITS FUNCTIONING          ##
12     ! IN FORTRAN, TO AUTOMATE SIMULATIONS FOR EXTENDED          ##
13     ! PERIODS, AND A GENERIC INPUT FORMAT THAT WILL ALSO          ##
14     ! HANDLE GCM DATA.          ##
15     ! FOR A DETAILED MODEL DESCRIPTION, THE USER IS REFERRED          ##
16     ! TO C ODENDAAL-ETSEBETH's M.SC. DISSERTATION.          ##
17     ! ----- ##
18
19     IMPLICIT NONE
20     REAL, DIMENSION (1:367) :: AMX, AMN, AVET, EVAP, RAIN, SUN,
21     & SLWAT, SLWAT1, SLWAT2, SLWP1, SLWP2
22     REAL, DIMENSION (1:13) :: DALEN
23     REAL, DIMENSION (1:9) :: X
24     REAL, DIMENSION (1:5) :: R
25     REAL :: A, ABSB, ABSC, ABSG, ABSR, ABSS, AE, AECVAP, AGRB, AGRC,
26     & AGRG, AGRR, AGRS, AI1, AI2, AI3, AL, ALAI, ALPHA, ARGU,
27     & ASSIM, ATEMP, AX, B, BA, BASSIM, BBD, BBL, BCD, BCFUNC,
28     & BCL, BCON, BCOVER, BD, BDBL, BDMG, BETA, BGD, BGL, BL,
29     & BLM, BLTT, BO, BP, BRD, BRES, BRESP, BRL, BSD, BSL, BTB,
30     & BTC, BTG, BTR, BTRO, BTS, C, C30, CD, CL, CLIVE, COEF,
31     & COMM, CONS, CPHA, DAYFRC, DBL, DMG, DPROB, DPROC, DPROG,
32     & DPROR, DPROS, DRAIN1, DRAIN2, DRAINP, DRES, DRN1P, EE,
33     & EFF, EFFDMG, EFFMAX, F, FC1, FC2, FE, FG, FI, FRACL, FT,
34     & FW, GD, GL, GLO, GS, GWP, GWPST, HU, HUCRIT, HUCRMN,
35     & HYCON, INFIL, IRRIG, LWP, MAIN, P, PE, PECONS, PECVAP,
36     & PNF, PO, PPROD, PPRODO, PRVISC, PWP1, PWP2, RD, RES, RESP,
37     & RFD, RFDL, RL, RUNOF, RUNPAR, SD, SDP, SDP1, SDP2, SL,
38     & SLVAP, SOLK, SPL, STRESS, SSLWP1, SSLWP2, TASSIM, TDMG,
39     & TDRAIN, TEFF, TF, TFFDMG, TFFMAX, TFI, TFT, TFW, TGROW,
40     & TLRB, TLRC, TLRG, TLRR, TLRD, TLRN, TLRP, TLRQ, TLRV, TLRW, TLRX,
41     & TPNF, TPROD, TR, TRANS1, TRANS2, TRESP, TRFD, TRUNOF, VB,
42     & VC, VG, VR, VS, VCS, WAT, WHC, WHC1, WHC2, WHC3, WHC4,
43     & WHCTEMP, WJ, WPC, WST, XX
44     INTEGER, DIMENSION (1:367) :: CNT
```

```

45     INTEGER, DIMENSION (1:13) :: DAE
46     INTEGER :: AV, BOGUS, CUT, CUT1, CUT2, CUT3, CUT4, DAG, EX,
47     &         FLAG, GRSTGE, I, IKOUNT, INDEKS, IL, IR, ITERM, ITTRE
48     INTEGER :: J, JDA, JDMAKS, JMAX, JR, LP, MKOUNT, NMNTH, NN,
49     &         STAT, TELLER, TNEXT, DSTAT, YEAR
50     CHARACTER, DIMENSION (1:5) :: STAGE*12
51     CHARACTER, DIMENSION (1:2) :: DAT*2
52     CHARACTER :: ANA*3, EXT*4
53     CHARACTER :: FILED*1000, FILEE*1000, FILEG*1000, FILEH*1000
54     CHARACTER :: GSTAGE*1000, Header1*54, Header2*54, MAAND*3, OD*1
55     CHARACTER :: FILES*1000, WEATHER*1000, LOGFILE*100
56     CHARACTER :: SOIL*1000, STATION*100
57     CHARACTER :: DIR*1000, WDIR*1000, DATAFILE*1000, ODIR*1000
58     LOGICAL :: EXIST
59
60     DALEN = (/10.5,11.1,11.9,12.8,13.6,14.0,13.8,13.1,12.3,11.4,10.7,
61     &         10.3,10.3/)
62     DAE = (/31,31,30,31,30,31,31,28,29,31,30,31,30/)
63     Header1 = "-----"
64     Header2 = "PERIODS OF MOISTURE STRESS : START : END : No DAYS : "
65     OD = "Y" !Used to indicate that output should be in daily timesteps
66
67     EXT = ".txt"
68     DIR = "/home/catherine/Desktop/DATA/" !Working directory; length = 29
69     DATAFILE = "/home/catherine/Desktop/DATA/DATA.txt"
70     SOIL = "/home/catherine/Desktop/DATA/INFOG.txt"
71     GSTAGE = "/home/catherine/Desktop/DATA/STAGE.txt"
72
73     OPEN(999,FILE=LOGFILE)
74
75     ! READ THE GROWTH STAGES
76     OPEN (4, FILE=TRIM(GSTAGE), STATUS='OLD')
77     DO I = 1,5
78         READ (4,501) STAGE(I)
79     ENDDO !End of I-loop
80
81     OPEN (15, FILE=TRIM(DATAFILE))
82     READ (15, 999, IOSTAT=DSTAT) YEAR, WDIR
83     DO WHILE (DSTAT == 0) !READING THE DATA FILE
84         IF (YEAR == 0) THEN
85             ODIR = WDIR
86
87             FILED = TRIM(ODIR)//"/OUTD"//EXT
88             FILEE = TRIM(ODIR)//"/OUTE"//EXT
89             FILEG = TRIM(ODIR)//"/OUTG"//EXT
90             FILEH = TRIM(ODIR)//"/OUTH"//EXT
91             FILES = TRIM(ODIR)//"/STATS"//EXT
92
93             INQUIRE(FILE=TRIM(FILES), EXIST=EXIST)
94             IF (EXIST) THEN

```



```

145 ! * * | | ##
146 ! * * | | ##
147 ! * * | | ##
148 ! * * * * * | * * * * * | ##
149 ! * * <-X6- * SD * <-X1-- * SL * ---R2--- | ##
150 ! * * * * * | * * * * * | ##
151 ! DA | | BA ##
152 ! ----- | ----- | ##
153 ! DB | | BB ##
154 ! | | | ##
155 ! | | | ##
156 ! | | | ##
157 ! | | | ##
158 ! * * * * * | * * * * * | ##
159 ! * RD * <-X3-- * RL * ---R3--- | ##
160 ! * * * * * | * * * * * | ##
161 ! | | | ##
162 ! | CB | | ##
163 ! | | | ##
164 ! | | | ##
165 ! | | | ##
166 ! KEY: ##
167 ! DMG = THE DAYS DRY MATTER GAIN (KG CARBOH./HA/DAY) ##
168 ! GD = SEEDS DEAD GL = SEEDS LIVING ##
169 ! CD = CULM DEAD CL = CULM LIVING ##
170 ! BD = LEAVES DEAD BL = LEAVES LIVING ##
171 ! SD = STUBBLE DEAD SL = STUBBLE LIVING ##
172 ! RD = ROOTS DEAD RL = ROOTS LIVING ##
173 ! TR = TRASH DEAD RES = CARBOHYDRATE RESERVES ##
174 ! DA = ABOVE GROUND DEAD BA = ABOVE GROUND BIOMASS ##
175 ! DB = ROOT DEAD BB = ROOT BIOMASS ##
176 ! D = DA+DB = TOTAL DEAD B = BA+BB = TOTAL BIOMASS (STANDING BIO) ##
177 ! CA = ABOVE GROUND STANDING CROP ##
178 ! CB = BELOW GROUND STANDING CROP ##
179 ! ' = STANDING CROP-SUMMATION OF ALL MASS ##
180 ! =====
181 ! VARIABLE NAME CODE UNITS ##
182 ! ===== ===== ##
183 ! BASAL COVER BCOVER (%) ##
184 ! DISIRED PROPORTION OF RELEVANT ORGAN DPRO ##
185 ! AVERAGE TEMP AVET (°C) ##
186 ! TEMP MAX AMX (°C) ##
187 ! TEMP MIN AMN (°C) ##
188 ! MEAN TEMP OF PREVIOUS DAY TMPD (°C) ##
189 ! RADIANT FLUX DENSITY RFD (W/M**2) ##
190 ! WATER POTENTIAL OF LEAF LWP (KPA) ##
191 ! LEAF AREA AL (M**2) ##
192 ! SPECIFIC LEAF AREA SPL (KG/HA) ##
193 ! ITERM PERIOD OVER WHICH MEAN DETERMINED ITERM ##
194 ! MAX CAP OF CO2-EXCHANGE PO (KG/HA/DAY) ##

```

```

195      ! BA IS PO DIVIDED BY PHOTOCHEMICAL COEF          BA          (W/M**2)  ##
196      ! PHOTOCHEMICAL EQUIVALANT                      FE          (KG/J)    ##
197      ! NUMBER OF PLANTS PER HECTARE                   ANPL                ##
198      ! CARBOHYDRATE-CO2 COEF                          COMM                ##
199      ! RANGELAND CONDITION SCORE                      VCS          (%)  ##
200      ! *****
201
202      WHCTEMP = 0.0
203      ! *****
204      ! *                      SET INITIAL STATUSES AND PARAMETERS          *
205      ! *****
206      ! READ SOIL WATER AND CUT INFO                                ##
207      ! IF CUTS ARE READ, IL = 1,15 IN DO AND PUTUINFO            ##
208
209      OPEN (1, FILE=SOIL)
210      READ (1, 501) STATION
211      READ (1, 501) DAT(1)
212      READ (1, 501) DAT(2)
213      DO IL = 1,15
214          IF (IL == 2 .AND. OD == "Y") THEN
215              WRITE (5,502) "Read the data for ", DAT(1), DAT(2), STATION
216          END IF
217          IF (IL == 2) THEN
218              WRITE (6,502) "Read the data for ", DAT(1), DAT(2), STATION
219          END IF
220          IF (IL == 3 .AND. WHCTEMP /= 0.0) THEN
221              WHC = WHCTEMP
222          END IF
223          IF (IL == 3) THEN
224              WRITE (6,519) "INITIAL SOIL MOISTURE FOR THIS SEASON IS ",
225      &              WHC
226          END IF
227      ENDDO !END OF IL-LOOP
228
229      READ (1, 503) SLWP1(1)
230      READ (1, 503) SLWP2(1)
231      READ (1, 503) WHC1
232      READ (1, 503) WHC2
233      READ (1, 503) WHC3
234      READ (1, 503) WHC4
235      READ (1, 503) SDP
236      READ (1, 503) BCOVER
237      READ (1, 504) CUT1
238      READ (1, 504) CUT2
239      READ (1, 504) CUT3
240      READ (1, 504) CUT4
241      READ (1, 504) ITERM
242      READ (1, 503) PRVISC
243      READ (1, 504) NN
244      READ (1, 504) JDMAKS

```



```

245 READ (1, 503) TPKAKS
246 READ (1, 504) GRSTGE
247 READ (1, 504) MKOUNT
248 READ (1, 504) TNEXT
249 READ (1, 503) PO
250 READ (1, 505) FE
251 READ (1, 503) COMM
252 READ (1, 503) BA
253 READ (1, 503) C30
254 READ (1, 503) CONS
255 READ (1, 503) HUCRIT
256 READ (1, 503) HUCRMN
257 READ (1, 503) BO
258 READ (1, 503) VCS
259 READ (1, 503) SPL
260 READ (1, 503) TMPD
261 READ (1, 503) WPC
262 READ (1, 504) LP
263 READ (1, 503) HYCON
264 READ (1, 503) BCON
265 READ (1, 503) RUNPAR
266 READ (1, 503) DRAINP
267 READ (1, 503) PPRODO
268 CLOSE (1)
269
270 CUT = CUT1
271 BLTT = 2900.0 !KG/HA
272 BLM = 4600.0 !KG/HA
273
274 ! COMPUTE SOIL DEPTH FOR SECOND LEVEL ##
275 SDP1 = 100.0
276 SDP2 = SDP - SDP1
277
278 ! COMPUTE FC AND PWP FOR EACH LEVEL ##
279 FC1 = WHC1 / 100.0 * SDP1
280 FC2 = WHC1 / 100.0 * SDP2
281 PWP1 = WHC4 / 100.0 * SDP1
282 PWP2 = WHC4 / 100.0 * SDP2
283
284 ! COMPUTE AI FOR THE EXPONENTIAL CURVE; GWP=M*E**AI(WJ) ##
285 AI1 = (LOG(2440.0) - LOG(148.4)) / (WHC3 - WHC4)
286 AI2 = (LOG(148.4) - LOG(22.1)) / (WHC2 - WHC3)
287 AI3 = (LOG(22.1) - LOG(10.0)) / (WHC1 - WHC2)
288
289 ! WATER CONTENT EXPRESSED IN MM/SOIL DEPTH FOR BOTH LEVELS ##
290 SLWAT(1) = (SLWP1(1) * SDP1 + SLWP2(1) * SDP2) / SDP / 100.0 * SDP
291 SLWAT1(1) = SLWP1(1) / 100.0 * SDP1
292 SLWAT2(1) = SLWP2(1) / 100.0 * SDP2
293
294 INDEKS = 1 ! INDEKS = Day of Growth Season

```

```

295     STAT = 0 ! To test for End of File
296
297     ! READING THE WEATHER DATA
298     WRITE(999,518) "READING CLIMATE DATA = "//TRIM(SOIL)
299     READ (2,506,IOSTAT=STAT) AV, MAAND, JR
300     DO WHILE (STAT == 0)
301         IF (AV == 1) THEN
302             ! TEST FOR LEAP YEAR - DEPENDS ON TWO CRITERIA:
303             ! 1) YEAR MUST BE DIVISIBLE BY 4
304             ! 2) CENTURIES MUST BE DIVISIBLE BY 400 AS WELL
305             IF ((JR/4)*4 == JR) THEN
306                 FLAG = 1
307                 IF ((JR/400)*400 == JR) THEN
308                     FLAG = 1
309                 ELSE IF ((JR/100)*100 == JR) THEN
310                     FLAG = 0
311                 END IF
312             ELSE
313                 FLAG = 0
314             END IF
315             SELECT CASE (MAAND)
316                 CASE ("JUL")
317                     TELLER = 31
318                 CASE ("AUG")
319                     TELLER = 31
320                 CASE ("SEP")
321                     TELLER = 30
322                 CASE ("OCT")
323                     TELLER = 31
324                 CASE ("NOV")
325                     TELLER = 30
326                 CASE ("DEC")
327                     TELLER = 31
328                 CASE ("JAN")
329                     TELLER = 31
330                 CASE ("FEB")
331                     IF (FLAG == 1) THEN
332                         TELLER = 29
333                     ELSE
334                         TELLER = 28
335                     END IF
336                 CASE ("MAR")
337                     TELLER = 31
338                 CASE ("APR")
339                     TELLER = 30
340                 CASE ("MAY")
341                     TELLER = 31
342                 CASE ("JUN")
343                     TELLER = 30
344             END SELECT

```

```

345         READ (2,507) ! Skipping rest of header in file
346         TR = 0.0      ! Setting Total Rain to zero
347         DO EX = 1,TELLER
348         READ (2,508) DAG, AMX(INDEKS), AMN(INDEKS), RAIN(INDEKS),
349         &           EVAP(INDEKS), SUN(INDEKS), AVET(INDEKS)
350         TR = TR + RAIN(INDEKS)
351         INDEKS = INDEKS + 1
352         END DO
353         WRITE (6,509) "Total rainfall for the month ", MAAND,
354         &           " = ", TR, " mm"
355         END IF !End of AV-if
356         READ (2,507) !Skipping a line
357         READ (2,506,IOSTAT=STAT) AV, MAAND, JR
358     END DO ! End of STAT-loop
359
360     ! *****
361     ! *   DETERMINE INITIAL MASSES OF THE DIFFERENT PLANT COMPONENTS   *
362     ! *****
363     ! C IS TOTAL PLANT MASS AT 100% BASAL COVER                        ##
364     ! ALL CALCULATIONS WILL PROCEED WITH 100% BASAL COVER            ##
365     ! ON COMPLETION BIOMASSES WILL BE MULTIPLIED BY                  ##
366     ! BCOVER*BCOVER FORMULA (BCFUNC)                                   ##
367     ! THE ASSUMPTION IS MADE THAT THE PREVIOUS PRODUCTION IS        ##
368     ! EQUAL TO 25% OF THE TOTAL BIOMASS                               ##
369
370     JMAX = INDEKS - 1
371     C = PRVISC * 100.0 / 25.0 * 100.0 / BCOVER
372     BCFUNC = BCOVER / 100.0
373     BL = 0.0      ! was 0.0 in previous version
374     BD = 0.03 * C ! was 0.01 in previous version
375     CL = 0.0      ! was 0.0 in previous version
376     CD = 0.02 * C ! was 0.01 in previous version
377     SL = 0.0      ! was 0.0 in previous version
378     SD = 0.3 * C  ! was 0.3 in previous version
379     RL = 0.64 * C ! was 0.68 in previous version
380     RD = 0.01 * C ! was 0.01 in previous version
381     GL = 0.0      ! was 0.0 in previous version
382     GD = 0.0      ! was 0.0 in previous version
383
384     ! RES IS NOW A FUNCTION OF THE PREVIOUS YEAR'S MAXIMUM PRODUCTION ##
385     RES = 20.0 * TPMAKS
386     TPMAKS = 0.0
387     CLIVE = BL + SL + RL
388     J = 1
389     WRITE (6,510) "The growth stage is ", STAGE(1), " on Julian Day ",
390     & JDA
391
392     ! *****
393     ! *   START OF SIMULATION PER DAY FOR THE GROWING SEASON   *
394     ! *****

```

```

395     IF (OD == "Y") THEN
396         WRITE (5,501) " JDA      BCL      BCD      BBL      BBD      BSL      BSD TP
397     & PPROD TPROD      BCON      AL"
398     END IF
399     DO J = 1,JMAX !START OF LONG LOOP THAT ENDS IN LINE 1357
400         NMNTH = J / 30 + 1
401         ! HERE AL = LA PER HECTARE LEAF SPL = 500 KH/HA      ##
402         AL = BL / SPL
403         IF (C /= 0.0) THEN
404             FRACL = BL / C
405         END IF
406         ! *****
407         ! *                WATER BALANCE                *
408         ! *****
409
410         ! *****
411         ! *                SUBSECTION FOR WATER            *
412         ! *****
413         ! USE CORRECT DALEN DATA STATEMENT CORRESPONDING TO      ##
414         ! RELEVANT LATITUDE                                       ##
415
416         DRAIN2 = 0.0
417         DRAIN1 = 0.0
418         TRANS2 = 0.0
419         AE = 0.0
420         ! CODE TO COMPUTE AND TABULATE CROP EVAPORATION AND      ##
421         ! WATER BALANCE OVER A PERIOD OF 365 DAYS ON A DAILY      ##
422         ! BASIS, DATA OBTAINED FROM WEATHER STATIONS            ##
423         !   DATA                FORTRAN DESIGNATION            ##
424         !   ----                -
425         !   RAINFALL              RAIN      (MM)                ##
426         !   MAX TEMP              AMX      (°C)                ##
427         !   MIN TEMP              AMN      (°C)                ##
428         !   SUNSHINE HOURS        SUN      (HOURS)            ##
429         !   EVAPORATION (CLASS-A PAN) EVAP    (MM)            ##
430         !   GROUND WATER POTENTIAL GWP      (KPA)            ##
431         !   LEAF WATER POTENTIAL  LWP      (KPA)            ##
432         !   SPEC LEAF AREA        SPL
433         !   SOIL WATER LEVEL      SLWAT    (MM/M)            ##
434         !   POT. EVAPORATION      PE      (MM)                ##
435         !   ACTUAL EVAPORATION    AE      (MM)                ##
436         !   LEAF AREA INDEKS     AL
437         !   SOIL EVAPORATION      SLVAP    (MM)            ##
438         !   TRANSPIRATION        TRANS    (MM)            ##
439         !   SOIL WATER LEVEL 1    SLWAT1   (MM)            ##
440         !   SOIL WATER LEVEL 2    SLWAT2   (MM)            ##
441         !
442         !   WATER AVAILBLE AS A % (ESTIMATED VOLUMETRICALLY)      ##
443         !   ON DAY ONE          WHC (%)            ##
444         !   AT 10 KPA          WHC1 (%) I.E. FIELD CAPACITY (FC)  ##

```

```

445      !      AT 22 KPA      WHC2 (%) READ FROM RETENTION CURVE      ##
446      !      AT 148 KPA     WHC3 (%) READ FROM RETENTION CURVE      ##
447      !      AT 2440 KPA    WHC4 (%) I.E. PERMANENT WILTING PIONT    ##
448      !      P.S. PERMANENT WILT FOR A MESOPHYTE IS 1500 KPA        ##
449      !      AND FOR A ZEROPHYTE 2400 KPA BUT THE DIFFERENCE        ##
450      !      IN % MOISTURE IS NEGLIGIBLE                             ##
451      !      SOIL DEPTH      SDP      (MM)                            ##
452      !      ATMOS TRANSMISSIVITY  0.75                               ##
453      !      -----                                                ##
454      !                                                                 ##
455      ! WJ IS THE WATER CONTENT EXPRESSED AS A %                       ##
456      ! CALCULATE GWP                                                ##
457
458      WHC = SLWAT(J) * 100.0 / SDP
459      WJ = SLWAT(J) / SDP * 100.0
460      NMNTH = J / 30 + 1
461      IF (WJ >= WHC3) THEN
462          GOTO 201
463      END IF
464      WST = WHC4
465      GWPST = 24.4
466      COEF = -1.0 * AI1
467      GOTO 203
468 201  IF (WJ >= WHC2) THEN
469          GOTO 202
470      END IF
471      WST = WHC3
472      GWPST = 1.48
473      COEF = -1.0 * AI2
474      GOTO 203
475 202  WST = WHC2
476          GWPST = 0.22
477          COEF = -1.0 * AI3
478 203  ARGU = COEF * (WJ - WST)
479          GWP = GWPST * EXP(ARGU)
480          GWP = GWP * (-100.0)
481
482      ! MEAN DAILY TEMPERATURE IS EQUAL TO THE MEAN OF THE      ##
483      ! DAILY MAXIMUM AND THE DAILY MINIMUM TEMPERATURE          ##
484      ATEMP = (AMX(J) + AMN(J)) / 2.0
485      GS = 0.4019914 + 0.01725101 * ATEMP - 0.0001485 * ATEMP**2.0
486      JDA = J + 181 !JDA = Julian Day
487      IF (J > 184) THEN
488          JDA = JDA - 365
489      END IF
490      XX = ((JDA + 10.0) / 365.0) * 360.0
491      XX = XX * 0.01745
492      ! SOLK = SOLAR CONSTANT      ##
493      SOLK = 30.85 + 12.65 * COS(XX)
494      SOLK = SOLK * 10.0**6.0

```

```

495     ALPHA = 0.21
496     BETA = 0.71
497     DAYFRC = SUN(J) / DALEN(NMNTN)
498     IF (DAYFRC > 0.5) THEN
499         ALPHA = 0.29
500     END IF
501     IF (DAYFRC > 0.5) THEN
502         BETA = 0.5
503     END IF
504     ! RFD = RADIANT FLUX DENSITY                                ##
505     RFD = SOLK * (ALPHA + BETA * DAYFRC)
506     RFDM = RFD / (DALEN(NMNTN) * 3600.0)
507
508     ! CALCULATION OF EQUILIBRIUM EVAPORATION                    ##
509     PECONS = 1.28
510     IF (AMX(J) >= 20.0) THEN
511         PECONS = 1.28 + 0.08 * (AMX(J) - 20.0)
512     END IF
513     EE = (((GS * 0.63 * RFD) / 2450.0) / 1000.0)
514
515     ! CALCULATION OF POTENTIAL EVAPORATION                      ##
516     PE = PECONS * EE
517
518     ! EXPRESS THE RATIO OF POTENTIAL EVAP TO PAN EVAP          ##
519     IF (EVAP(J) == 0.0) THEN
520         EVAP(J) = 1.0
521     END IF
522     PECVAP = PE / EVAP(J)
523     IF (PECVAP > 1.5) THEN
524         PECVAP = 1.5
525     END IF
526
527     ! 0.1 PLANT COVERAGE IS 10% THROUGHOUT THE YEAR.          ##
528     ! AL/3 * 0.9 WHEN AL = 3 THE REMAINING GROUND WILL BE COVERED ##
529     ! GRASS NEVER ALLOW (0.1 + AL/3 * 0.9) TO BECOME GREATER   ##
530     ! THAN ONE, WHEN THIS HAPPENS (AL GREATER THAN 3) ASSUME AE = PE ##
531     B = (0.1 + ((AL * BCFUNC) / 3.0) * 0.9)
532     IF (B >= 1.0) THEN
533         B = 1.0
534     END IF
535     IF (B <= 0.0) THEN
536         B = 0.0
537     END IF
538
539     ! CALCULATION OF LEAF WATER POTENTIAL                        ##
540     LWP = PE / HYCON
541     LWP = GWP - LWP
542
543     ! CALCULATE THE LIMITATION OF WATER AVAILABILITY ON        ##
544     ! PHOTOSYNTHETIC EFFICIENCY                                ##

```

```

545     COEF = 0.005 * (WPC - LWP)
546     IF (COEF <= (WPC / (-100.0))) THEN
547         GOTO 204
548     END IF
549     COEF = WPC / (-100.0)
550 204   IF (COEF >= WPC / 100.0) THEN
551         GOTO 205
552     END IF
553     COEF = WPC / 100.0
554 205   A = EXP(COEF)
555         FW = 1.0 / (1.0 + A)
556
557     ! EVAPORATE RAINFALL 3,0 MM OR LESS AS PART OF ACTUAL EVAP      ##
558     IF (RAIN(J) <= 3.0) THEN
559         PE = PE - RAIN(J)
560         RAIN(J) = 0.0
561     END IF
562     IF (PE <= 0.0) THEN
563         PE = 0.0
564     END IF
565
566     ! IF RAINFALL EXCEED 5,0 MM THEN EVAP ACCORDING TO EQ.      ##
567     IF (RAIN(J) > 5.0) THEN
568         CNT(J) = -2
569     END IF
570     CNT(J + 1) = CNT(J) + 1
571     FG = EXP(-0.5 * CNT(J))
572     IF (FG >= 1.0) THEN
573         FG = 1.0
574     END IF
575
576     ! CALCULATE RUNOFF      ##
577     RUNOF = 0.0
578     IRRIG = 0.0
579     INFIL = (RAIN(J) + IRRIG) / 1000.0
580     IF (INFIL <= 0.2 * RUNPAR) THEN
581         RUNOF = 0.0
582     ELSE
583         RUNOF = (INFIL - 0.2 * RUNPAR)**2.0 / (INFIL + 0.8 * RUNPAR)
584     END IF
585     INFIL = (INFIL - RUNOF) * 1000.0
586     TRUNOF = TRUNOF + RUNOF
587
588     ! CALCULATE SOIL EVAPORATION      (SLVAP)      ##
589     SLVAP = (1.0 - B) * FG * PE
590     TRANS1 = B * FW * PE
591
592     ! SLVAP CAN ONLY OCCUR FROM THE FIRST LEVEL IF WATER IS AVAILABLE      ##
593     IF (SLVAP <= SLWAT1(J) - PWP1) THEN
594         GOTO 206

```

```

595     ELSE
596         SLVAP = SLWAT1(J) - PWP1
597     END IF
598 206   SLWAT1(J) = SLWAT1(J) - SLVAP
599
600     ! RECHARGE OF LEVEL 1 COMES FROM RAIN(J) AND THAT OF LEVEL 2      ##
601     ! FROM DRAINAGE OF LEVEL 1 WHEN IT HAS REACHED FC                ##
602     SLWAT1(J) = SLWAT1(J) + RAIN(J) + IRRIG - TRANS1
603     IF (SLWAT1(J) >= FC1) THEN
604         GOTO 207
605     END IF
606     IF (SLWAT1(J) >= PWP1) THEN
607         GOTO 208
608     END IF
609
610     ! TRANSPIRATION, HOWEVER, CAN OCCUR FROM BOTH LEVELS AND IF      ##
611     ! WATER IS NOT AVAILABLE IN LEVEL 1 THE REST WILL BE DRAWN      ##
612     ! FROM LEVEL 2                                                  ##
613     SLWAT1(J) = PWP1
614     TRANS2 = TRANS1 - (SLWAT1(J) - PWP1)
615     TRANS1 = 0.0
616     GOTO 208
617 207   DRN1P = 1.0
618     DRAIN1 = (SLWAT1(J) - FC1) * DRN1P
619     IF (DRAIN1 <= 0.0) THEN
620         DRAIN1 = 0.0
621     END IF
622     SLWAT1(J) = SLWAT1(J) - DRAIN1
623
624     ! CALCULATE WATER CONTENT OF LEVEL 2                              ##
625 208   SLWAT2(J) = SLWAT2(J) + DRAIN1 - TRANS2
626
627     ! EXPRESS THE RATIO OF ACTUAL EVAP TO PAN EVAP                  ##
628     AECVAP = AE / EVAP(J)
629     IF (AECVAP > 1.5) THEN
630         AECVAP = 1.5
631     END IF
632
633     ! IF SLWAT2 EXCEEDS FC2 DRAIN THE AMOUNT GREATER THAN FC2      ##
634     IF (SLWAT2(J) <= FC2) THEN
635         GOTO 210
636     END IF
637     DRAIN2 = DRAINP * (SLWAT2(J) - FC2)
638     IF (DRAIN2 <= 0.0) THEN
639         DRAIN2 = 0.0
640     END IF
641     SLWAT2(J) = SLWAT2(J) - DRAIN2
642
643     ! IF SLWAT2 GETS LOWER THAN PWP2, SLWAT2 IS EQUAL TO PWP2      ##
644 210   IF (SLWAT2(J) >= PWP2) THEN

```



```

645         GOTO 211
646     END IF
647     SLWAT2(J) = PWP2
648     DRAIN2 = 0.0
649 211    WAT = WJ
650
651     ! TO REDUCE SOIL WATER DURING WINTER I.E AFTER DAY 300      ##
652     ! SOIL WATER IS REDUCED BY 0.3 MM/DAY                      ##
653     IF (GRSTGE == 5) THEN
654         SLWAT1(J) = SLWAT1(J) - 0.3
655     END IF
656     IF (GRSTGE == 5 .AND. SLWAT1(J) < PWP1) THEN
657         SLWAT1(J) = PWP1
658     END IF
659     IF (GRSTGE == 5 .AND. SLWAT1(J) == PWP1) THEN
660         SLWAT2(J) = SLWAT2(J) - 0.1
661     END IF
662     IF (GRSTGE == 5 .AND. SLWAT2(J) < PWP2) THEN
663         SLWAT2(J) = PWP2
664     END IF
665     SLWAT(J + 1) = (SLWAT1(J) * SDP1 + SLWAT2(J) * SDP2) / SDP
666     SLWAT1(J + 1) = SLWAT1(J)
667     SLWAT2(J + 1) = SLWAT2(J)
668     STRESS = 1.0 - FW
669     IF (TRANS2 <= 0.0) THEN
670         TRANS2 = 0.001
671     END IF
672     RFD = RFD / 10.0 ** 6.0
673     ALAI = AL * BCFUNC
674     TDRAIN = TDRAIN + DRAIN2
675
676     WRITE (7,511) JDA, FI, FT, FW, F, LWP / 100.0, GWP / 100.0,
677 &          PE, WHC, SLWAT(J), SLWAT1(J), SLWAT2(J), RAIN(J),
678 &          TRUNOF, TDRAIN, DRAIN1, DRAIN2, SLVAP, TRANS1,
679 &          TRANS2, AE
680     ! *****
681     ! *          END OF WATER SUBSECTION          *
682     ! *****
683
684     ! *****
685     ! *          ENVIRONMENTAL FACTORS AND PRODUCTION          *
686     ! *****
687     ! TO COMPUTE THE INFLUENCE OF SOLAR RADIATION ON THE      ##
688     ! MAX RATE OF PHOTOSYNTHESIS (FI)                        ##
689     ! FI = PERCENTAGE SUNLIGHT ABSORBED BY THE CANOPY        ##
690         TRFD = TRFD + RFD
691         FI = (1.0 - EXP(-0.7 * AL * BCFUNC)) * 100.0
692         TFI = TFI + FI
693
694     ! TO COMPUTE THE INFLUENCE OF TEMP ON THE MAX RATE OF    ##

```

```

695      ! PHOTOSYNTHESIS (FT)                                ##
696      FT = 100.0 * (EXP(-1.0 * ((ATEMP - 37.0)**2.0) / 360.0))
697      IF (ATEMP < BO) THEN
698          FT = 0.0
699      END IF
700      TFT = TFT + FT
701
702      ! TO COMPUTE THE INFLUENCE OF WATER AVAILABILITY ON THE    ##
703      ! MAX RATE OF PHOTOSYNTHESIS (FW)                        ##
704      FW = FW * 100.0
705      TFW = TFW + FW
706
707      ! SHOULD SOIL BE SATURATED REDUCE PHOTOSYNTHETIC RATE BY 20% ##
708      IF (SLWAT2(J) > FC2) THEN
709          FW = 100.0 - 10.0 * (SLWAT2(J) - FC2) / SDP2
710      END IF
711      IF (FW <= 0.0) THEN
712          FW = 0.0
713      END IF
714
715      ! COMPUTE BEGINING AND END, AS WELL AS NUMBER OF          ##
716      ! MOISTURE STRESS DAYS                                    ##
717      IF (GRSTGE < 5) THEN
718          GOTO 6
719      ELSE
720          GOTO 7
721      END IF
722  6      IF (FW < 50.0 .AND. ATEMP > BO) THEN
723          ITTRE = ITTRE + 1
724      END IF
725      ! WPC = CRITICAL LEAF WATER POTENTIAL                    ##
726      IF (FW < 50.0 .AND. ATEMP > BO) THEN
727          WPC = WPC - 15.0
728      END IF
729      IF (WPC <= -3000.0) THEN
730          WPC = -3000.0
731      END IF
732      WPC = -2000.0
733      IF (FW < 50.0 .AND. ATEMP > BO) THEN
734          WRITE (8,512) "STRESS DAY ON ", J, ITTRE, FW
735      END IF
736  7      BOGUS = 1
737
738      ! POTENTIAL EFFICIENCY OF PHOTOSYNTHESIS = EFFMAX        ##
739      ! IN RELATION TO RANGELAND CONDITION SCORE                ##
740      IF (RFDM >= 10.0) THEN
741          GOTO 8
742      END IF
743      EFFMAX = 0.0
744      GOTO 9

```

```

745 8      IF (VCS < 80.0) THEN
746          WRITE (*,*) "NOT CLIMAX VELD - END"
747          STOP
748          END IF
749          EFFMAX = 3.51 * (VCS - 79.6114)
750 9      TFFMAX = TFFMAX + EFFMAX
751
752          ! THE INFLUENCE OF THE ENVIRONMENT ON THE EFFICIENCY OF      ##
753          ! PHOTOSYNTHESIS (F)                                         ##
754          F = (FI / 100.0) * (FT / 100.0) * (FW / 100.0) * 100.0
755          TF = TF + F
756
757          ! ACTUAL EFFICIENCY OF PHOTOSYNTHESIS (EFF)                   ##
758          EFF = EFFMAX * F / 100.0
759          TEFF = TEFF + EFF
760
761          ! THE POTENTIAL OF CO2-ASSIMALATION = P (KG CO2/HA/DAY)      ##
762          IF (RFDM >= 10.0) THEN
763              GOTO 10
764          END IF
765          P = 0.0
766          GOTO 11
767 10      P = EFF / 100.0 * FE * RFDM
768 11      P = P * DALEN(NMNTH) * 3600.0 * 10.0**4.0
769
770          ! CONVERSION OF P (KG CO2/HA/DAY) TO KG CARBOH./HA/DAY = ASSIM      ##
771          ! AND DEDUCTION OF CONSTRUCTION RESPIRATION (1.0-CONS)       ##
772          ASSIM = COMM * P * (1.0 - CONS)
773          TASSIM = TASSIM + ASSIM
774
775          ! CARBOHYDRATE DEMOLATION DUE TO MAINTENANCE RESPIRATION      ##
776          ! OF THE PLANT                                                 ##
777          TNITE = (TMPD + AMN(J)) / 4.0
778          MAIN = (C30 * (0.044 + 0.0019 * TNITE + 0.001 * TNITE**2.0))
779          & * CLIVE
780          RESP = MAIN
781          TRESP = TRESP + RESP
782
783          ! NETTO DRY MATTER GAIN IS THE RESULT OF ASSIMILATION -      ##
784          ! RESPIRATION                                                 ##
785          DMG = ASSIM
786          TDMG = TDMG + DMG
787
788          ! EFFICIENCY OF DRY MATTER = EFFDMG                            ##
789          IF (RFDM == 0.0) THEN
790              GOTO 12
791          END IF
792          EFFDMG = DMG / (COMM * FE * (RFDM * DALEN(NMNTH) * 3600.0))
793 12      TFFDMG = TFFDMG + EFFDMG
794

```

```

795 ! *****
796 ! *                GROWTH STAGES                *
797 ! *****
798
799     SELECT CASE (GRSTGE)
800         CASE (1)
801             GOTO 13
802         CASE (2)
803             GOTO 25
804         CASE (3)
805             GOTO 30
806         CASE (4)
807             GOTO 35
808         CASE (5)
809             GOTO 37
810     END SELECT
811
812 ! *****
813 ! *                GROWTH STAGE ONE                *
814 ! *****
815 ! FIRST GROWTH STAGE IS VEGETATIVE GROWTH (MAKE SURE THE      ##
816 ! WEATHER DATA IS ARRANGED FROM 1ST JULY OF THE FIRST YEAR   ##
817 ! TO THE 30TH JUNE OF THE SECOND YEAR). TRIGGER FOR CHANGE    ##
818 ! TO 2ND GROWTH STAGE IS TEST IF LEAF MASS PER HECTARE AT     ##
819 ! 100% COVER (BL) IS GREATER THAN 4600 KG/HA = BLM AND THE    ##
820 ! HEAT DEMAND (HUCRIT) HAS BEEN SATISFIED                     ##
821
822 13     IF (HU > HUCRIT) THEN
823         GOTO 14
824     ELSE
825         GOTO 15
826     END IF
827 14     IF (BL > BLM) THEN
828         GOTO 24
829     END IF
830 15     IF (TNEXT == 1) THEN
831         GOTO 16
832     ELSE
833         GOTO 17
834     END IF
835 16     IF (J > 154) THEN
836         VCS = VCS
837     END IF
838     IF (BL > BLTT) THEN
839         GOTO 17
840     END IF
841
842 ! SHOULD GROWTH STAGE 1 LAST TO LONG (BEYOND 258 DAYS)      ##
843 ! SWITCH TO NEXT GROWTH STAGE                                  ##
844 ! AND IF TEMP IS TOO LOW TERMINATE GROWTH                     ##

```

```

845 17      IF (J > 258) THEN
846          GOTO 18
847      ELSE
848          GOTO 19
849      END IF
850 18      IF (AMN(J) <= 2.0) THEN
851          GOTO 23
852      END IF
853
854      ! BCON = KG/HA/DAY/°C AT 100% COVER          ##
855 19      BCON = 40.0
856          IF (BL <= BLTT) THEN
857              BCON = BCON * 0.2
858          END IF
859          TGROW = ATEMP
860          IF (TGROW >= 30.0) THEN
861              TGROW = 30.0
862          END IF
863          IF (TGROW <= B0) THEN
864              TGROW = B0
865          END IF
866
867      ! THE FOLLOWING IF-STATEMENT IS TO PREVENT HU FROM BEING          ##
868      ! ACCUMULATED BEFORE THE LEAVES HAVE REACHED A CERTAIN          ##
869      ! MINIMUM MASS                                                  ##
870          IF (BL <= BLTT) THEN
871              GOTO 20
872          END IF
873          HU = HU + (TGROW - B0)
874          HUCRIT = HUCRIT - 3.0 * (100.0 - FW) / 100.0
875          IF (HUCRIT <= HUCRMN) THEN
876              HUCRIT = HUCRMN
877          END IF
878
879      ! CALCULATION OF LEAVE MASS CHANGE DEMAND (KG/HA/DAY)          ##
880 20      DBL = BCON * (TGROW - B0)
881          BBL = BL * BCFUNC
882          BDBL = DBL * BCFUNC
883
884      ! CALCULATE MASS FLOW VARIABLES FOR MASS FLOW FROM LIVING          ##
885      ! PARTS TO DEAD PARTS                                          ##
886          X(1) = 0.001 * SL
887          X(2) = 0.001 * BL
888          X(3) = 0.001 * RL
889          X(4) = 0.0
890          X(8) = 0.0
891          GOTO 38
892 23      WRITE (6,513) "ON DAY = ", JDA, " Tmin = ", AMN(J),
893      & " <<<<>>>> THEREFORE TERMINATE GROWTH"
894 24      WRITE (6,510) "The growth stage is ", STAGE(2),

```

```

895      & " Growth Stage 2 on Julian Day ", JDA
896
897      ! TRANSLOCATION RATES ARE PROPORTIONAL TO DIFFERENCES          ##
898      ! BETWEEN EXISTING AND DESIRED ORGAN PROPORTIONS              ##
899      ! DESIRED PROPORTIONS = DPRO ...FOR REPRODUCTIVE GROWTH STAGE ##
900          DPROG = 0.0
901          DPROC = 0.125
902          DPROB = 0.125
903          DPROS = 0.25
904          DPROR = 0.5
905          GRSTGE = 2
906          MKOUNT = J + 25
907
908      ! *****
909      ! *                      GROWTH STAGE TWO                      *
910      ! *****
911      ! SECOND GROWTH STAGE IS REPRODUCTIVE GROWTH. TRIGGER FOR      ##
912      ! CHANGE TO 3RD GROWTH STAGE IS 25 DAYS OF GROWTH WITH A      ##
913      ! MINIMUM PRODUCTION OF 25% OF THE MASS OF LEAVES FOR A      ##
914      ! THEORETICAL BASAL COVER OF 100%                               ##
915
916      25      IF (CL > (0.25 * BL) .AND. J > MKOUNT) THEN
917          GOTO 29
918      END IF
919      IF (J >= 258) THEN
920          GOTO 26
921      END IF
922      GOTO 27
923      26      IF (AMN(J) <= 2.0) THEN
924          GOTO 28
925      END IF
926
927      ! CALCULATE THE MASS FLOW OF LIVING PLANT MATERIAAL TO DEAD    ##
928      27      X(1) = 0.001 * SL
929          X(2) = 0.001 * BL
930          X(3) = 0.001 * RL
931          GOTO 38
932      28      WRITE (6,513) "ON DAY = ", JDA, " Tmin = ", AMN(J),
933      &          " <<<<>>> THEREFORE TERMINATE GROWTH"
934      29      WRITE (6,510) "The growth stage is ", STAGE(3),
935      &          " Growth Stage 3 on Julian Day ", JDA
936
937      ! DESIRED PROPORTIONS = DPRO ...FOR SEED GROWTH STAGE          ##
938          DPROG = 0.003
939          DPROC = 0.1
940          DPROB = 0.1
941          DPROS = 0.347
942          DPROR = 0.45
943          GRSTGE = 3
944          MKOUNT = J + 50

```

```

945         IKOUNT = MKOUNT - 30
946
947         ! *****
948         ! *                GROWTH STAGE THREE                *
949         ! *****
950         ! THIRD GROWTH STAGE IS SEED FILLING.                ##
951         ! TRIGGER FOR 4TH GROWTH STAGE IS 50 DAYS OF SEED FORMATION. ##
952         ! TERMINATE GROWTH IF BEYOND DAY 258 AND TEMP < 3°C    ##
953
954     30         IF (J > MKOUNT) THEN
955                 GOTO 34
956         END IF
957         IF (J >= 258) THEN
958                 GOTO 31
959         END IF
960         GOTO 32
961     31         IF (AMN(J) < 3.0) THEN
962                 GOTO 33
963         END IF
964     32         X(1) = 0.002 * SL
965                 X(2) = 0.002 * BL
966                 X(3) = 0.003 * RL
967         IF (J >= IKOUNT) THEN
968                 X(8) = 0.15 * GL
969         END IF
970                 X(9) = 0.001 * CL
971                 X(6) = 0.001 * SD
972                 X(7) = 0.001 * BD
973         GOTO 38
974     33         WRITE (6,513) "ON DAY = ", JDA, " Tmin = ", AMN(J),
975         &                 " <<<<>>> THEREFORE TERMINATE GROWTH"
976     34         WRITE (6,510) "The growth stage is ", STAGE(4),
977         & " Growth Stage 4 on Julian Day ", JDA
978
979         ! DESIRED PROPORTIONS = DPRO ...FOR SEEDFALL GROWTH STAGE ##
980                 DPROG = 0.0
981                 DPROC = 0.08
982                 DPROB = 0.08
983                 DPROS = 0.26
984                 DPROR = 0.58
985                 GRSTGE = 4
986                 GLO = GD + GL + 1
987
988         ! *****
989         ! *                GROWTH STAGE FOUR                *
990         ! *****
991         ! FORTH GROWTH STAGE IS SEEDFALL.                ##
992         ! TRIGGER TO FIFTH GROWTH STAGE IS A MINIMUM TEMPERATURE < 3°C ##
993
994     35         IF (AMN(J) < 3.0) THEN

```

```

995         GOTO 36
996     END IF
997     X(1) = 0.002 * SL
998     X(2) = 0.01 * BL
999     X(3) = 0.003 * RL
1000    X(4) = 0.0
1001    IF ((GD + GL) > 0.0) THEN
1002        X(4) = (GLO - (GD + GL)) * 0.3
1003    END IF
1004    IF (X(4) > GD) THEN
1005        X(4) = GD
1006    END IF
1007    IF (X(4) >= GD) THEN
1008        GL = 0.0
1009    END IF
1010    X(5) = 0.005 * CD
1011    X(6) = 0.005 * SD
1012    X(7) = 0.005 * BD
1013    X(8) = 0.5 * GL
1014    X(9) = 0.05 * CL
1015    GOTO 38
1016
1017    ! DESIRED PROPORTIONS = DPRO ...FOR DORMANT GROWTH STAGE      ##
1018    ! IS THE SAME AS FOR THE SEEDFALL GROWTH STAGE                ##
1019 36    GRSTGE = 5
1020        WRITE (6,510) "The growth stage is ", STAGE(5),
1021    & " Growth Stage 5 on Julian Day ", JDA
1022
1023    ! *****
1024    ! *                               GROWTH STAGE FIVE          *
1025    ! *****
1026    ! FIFTH GROWTH STAGE IS DORMANT.                                ##
1027
1028 37    X(1) = 0.02 * SL
1029        X(2) = 0.2 * BL
1030        X(3) = 0.003 * RL
1031        X(4) = 0.5 * GD
1032        X(5) = 0.002 * CD
1033        X(6) = 0.003 * SD
1034        X(7) = 0.005 * BD
1035        X(8) = 0.5 * GL
1036        X(9) = 0.25 * CL
1037
1038    ! DETERMINE WHETHER PRODUCTION HAS BEEN CUT                    ##
1039 38    IF (JDA /= CUT) THEN
1040        GOTO 39
1041    END IF
1042    TP = BTG + BTC + BTB
1043    WRITE (6,515) "A BIOMASS PRODUCTION OF ", TP,
1044    & " (KG/HA) WAS REACHED ON CUTTING DATE ", JDA

```



```

1045      GRSTGE = 1
1046      WPC = -1800.0
1047      VCS = VCS * 0.75
1048      TNEXT = 2
1049      HUCRIT = HUCRIT * 0.8
1050      HUCRMN = HUCRMN * 0.8
1051      HU = 0.0
1052      BLM = BLM * 0.4
1053      BLTT = BLTT * 0.4
1054      IF (CUT == CUT3) THEN
1055          CUT = CUT4
1056      END IF
1057      IF (CUT == CUT2) THEN
1058          CUT = CUT3
1059      END IF
1060      IF (CUT == CUT1) THEN
1061          CUT = CUT2
1062      END IF
1063      IF (J > 258) THEN
1064          GRSTGE = 5
1065      END IF
1066      IF (GRSTGE == 5) THEN
1067          DPROG = 0.0
1068          DPROC = 0.08
1069          DPROB = 0.08
1070          DPROS = 0.26
1071          DPROR = 0.58
1072      END IF
1073      BGL = 0.0
1074      BGD = 0.0
1075      BTB = 100.0 - BTG - BTC
1076      BBL = 0.4 * BTB
1077      BBD = 0.4 * BTB
1078      BCL = 0.1 * BTB + BTC
1079      BCD = 0.1 * BTB
1080      BTC = BCL + BCD
1081      BTB = BBL + BBD
1082      CL = BCL / BCFUNC
1083      CD = BCD / BCFUNC
1084      BL = BBL / BCFUNC
1085      BD = BBD / BCFUNC
1086      GL = 0.0
1087      GD = 0.0
1088
1089      ! *****
1090      ! *                                TRANSLOCATION                                *
1091      ! *****
39      BOGUS = 1
1092
1093      ! *****
1094

```

```

1095      ! *                      SUBSECTION FOR TRANSLOCATION                      *
1096      ! *****
1097      ! TRANSLOCATION RATES ARE PROPORTIONAL TO EXISTING                      ##
1098      ! FRACTIONS OF MAXIMUM POSSIBLE ORGAN SIZE                          ##
1099      ! MAXIMUM (ABSOLUTE) ORGAN SIZE = ABS    (KG/HA)                      ##
1100
1101      ABSG = 300.0
1102      ABSC = 12500.0
1103      ABSB = 12500.0
1104      ABSS = 25000.0
1105      ABSR = 50000.0
1106
1107      ! MAXIMUM GROWTH RATE (TRANSLOCATION) OF ORGANS (KG/HA/DAY)          ##
1108      ! AND = AGR MAXIMUM TRANSLOCATION RATE = MAXIMUM GROWTH RATE          ##
1109      ! MAXIMUM (ABSOLUTE) ORGAN SIZE = ABS    (KG/HA)                      ##
1110      AGRB = 0.0
1111      AGRC = 0.0
1112      AGRS = 0.0
1113      AGRG = 0.0
1114      TLRB = 0.0
1115      TLRG = 0.0
1116      TLRC = 0.0
1117      SELECT CASE (GRSTGE)
1118          CASE (1)
1119              GOTO 311
1120          CASE (2)
1121              GOTO 312
1122          CASE (3)
1123              GOTO 313
1124          CASE (4)
1125              GOTO 314
1126          CASE (5)
1127              GOTO 316
1128      END SELECT
1129
1130      ! MAXIMUM TRANSLOCATION RATES FOR VEGETATIVE GROWTH STAGE              ##
1131      ! R(1) PROPORTIONAL TO BCON, TEMPERATURE AND FW                      ##
1132      311  AGRB = DBL
1133          AGRR = 0.15 * DBL
1134          TLRB = 1.0
1135          TLRR = 1.0
1136          GOTO 318
1137
1138      ! MAXIMUM TRANSLOCATION RATES FOR REPRODUCTIVE GROWTH STAGE          ##
1139      312  AGRC = 420.0
1140          AGRB = 520.0
1141          AGRS = 810.0
1142          AGRR = 1250.0
1143          GOTO 316
1144

```

```

1145      ! MAXIMUM TRANSLOCATION RATES FOR SEED GROWTH STAGE      ##
1146  313  AGRG = 50.0
1147      AGRS = 810.0
1148      AGRR = 1250.0
1149      GOTO 316
1150
1151      ! MAXIMUM TRANSLOCATION RATES FOR SEEDFALL GROWTH STAGE  ##
1152  314  AGRS = 810.0
1153      AGRR = 1250.0
1154      GOTO 316
1155
1156      ! MAXIMUM TRANSLOCATION RATES FOR DORMANT GROWTH STAGE  ##
1157      ! CALCULATE PROPORTION REQUIREMENTS                      ##
1158  316  IF (GRSTGE == 3) THEN
1159      VG = (GL + GD) / C / DPROG
1160      END IF
1161      VC = (CL + CD) / C / DPROC
1162      VB = (BL + BD) / C / DPROB
1163      VS = (SL + SD) / C / DPROS
1164      VR = (RL + RD) / C / DPROR
1165
1166      ! CALCULATE THE DIFFERENT TRANSLOCATION RATES = TLR CONTROLLED  ##
1167      ! BY RATIOS                                              ##
1168      TLRG = (2.0 / (1.0 + EXP(-10.0 * (1.0 - VG)))) - 1.0)
1169      TLRC = (2.0 / (1.0 + EXP(-10.0 * (1.0 - VC)))) - 1.0)
1170      TLRB = (2.0 / (1.0 + EXP(-10.0 * (1.0 - VB)))) - 1.0)
1171      TLRS = (2.0 / (1.0 + EXP(-10.0 * (1.0 - VS)))) - 1.0)
1172      TLRR = (2.0 / (1.0 + EXP(-10.0 * (1.0 - VR)))) - 1.0)
1173
1174      ! CALCULATE MASS FLOW VARIABLES CONCERNED                ##
1175      ! RATE OF TRANSLOCATION IS PROPORTIONAL TO:              ##
1176      !           (I) FW/100                                   ##
1177      !           (II) DEMAND (RATE OF ACTUAL PROPORTION TO C TO ##
1178      !                   DESIRED PROPORTION OF ORGAN)       ##
1179      !           EG. (BL+BD)/C/DPROB                         ##
1180      !           (III) FURTHERMORE THE PLANT IS CAPABLE OF SUPPLYING ##
1181      !                   CARBOHYDRATES AT THE REQUIRED RATE PROVIDED ##
1182      !                   RES > 0                             ##
1183  318  R(5) = TLRG * AGRG * FW / 100.0
1184      R(4) = TLRC * AGRC * FW / 100.0
1185      R(1) = TLRB * AGRB * FW / 100.0
1186      R(2) = TLRS * AGRS * FW / 100.0
1187      R(3) = TLRR * AGRR * FW / 100.0
1188
1189      ! TEST FOR THE AVAILABILTY OF RESERVES                    ##
1190      IF (RES > (R(1) + R(2) + R(3) + R(4) + R(5) + RESP)) THEN
1191      GOTO 317
1192      END IF
1193
1194      ! RESET THE MASS FLOW VARIABLES TO ZERO                  ##

```

```

1195      DO IR = 1,5
1196          R(IR) = 0.0
1197      END DO
1198 317    DRES = DMG - R(1) - R(2) - R(3) - R(4) - R(5)
1199      BL = BL + R(1) - X(2) - (BL / CLIVE) * RESP
1200      BD = BD + X(2) - X(7)
1201      SL = SL - X(1) - (SL / CLIVE) * RESP + DRES
1202      SD = SD + X(1) - X(6)
1203      CL = CL + R(4) - X(9) - (CL / CLIVE) * RESP
1204      CD = CD + X(9) - X(5)
1205      GL = GL + R(5) - X(8) - (GL / CLIVE) * RESP
1206      GD = GD + X(8) - X(4)
1207      RL = RL + R(3) - X(3) - (RL / CLIVE) * RESP
1208      RD = RD + X(3)
1209      RES = RES + DRES - (RES / SD * RESP)
1210      TR = TR + X(4) + X(5) + X(6) + X(7)
1211      C = GL + GD + CL + CD + BL + BD + SL + SD + RL + RD
1212      CLIVE = GL + CL + BL + SL + RL
1213
1214      ! *****
1215      ! *                END OF TRANSLOCATION SUBSECTION                *
1216      ! *****
1217
1218          IF (BL > 0.0) THEN
1219              GOTO 40
1220          END IF
1221          BL = 0.0
1222          BD = BD
1223 40      IF (SL > 0.0) THEN
1224              GOTO 41
1225          END IF
1226          SL = 0.0
1227          SD = SD
1228 41      IF (RL > 0.0) THEN
1229              GOTO 42
1230          END IF
1231          RL = 0.0
1232          RD = RD
1233 42      IF (CL > 0.0) THEN
1234              GOTO 43
1235          END IF
1236          CL = 0.0
1237          CD = CD
1238 43      IF (GL > 0.0) THEN
1239              GOTO 45
1240          END IF
1241          GL = 0.0
1242          GD = GD
1243 45      TFI = TFI / ITERM
1244          TFT = TFT / ITERM

```

```

1245      TFW = TFW / ITERM
1246      TF = TF / ITERM
1247      TFFMAX = TFFMAX / ITERM
1248      TEFF = TEFF / ITERM
1249      TRESP = TRESP / ITERM
1250      TASSIM = TASSIM / ITERM
1251      TRFD = TRFD / ITERM
1252      TDMG = TDMG / ITERM
1253      PNF = TPNF / ITERM
1254      TFFDMG = TFFDMG / ITERM
1255      FI = TFI
1256      FT = TFT
1257      FW = TFW
1258      F = TF
1259      ALAI = AL
1260      CPHA = (C - SL - SD - RL - RD) * BCOVER * BCFUNC
1261      EFFMAX = TFFMAX
1262      EFF = TEFF
1263      P = TP
1264      ASSIM = TASSIM
1265      RESP = TRESP
1266      DMG = TDMG
1267      EFFDMG = TFFDMG
1268      A = J / ITERM
1269      AX = A * 10.0
1270
1271      ! TO EXPRESS PRODUCTION IN TERMS OF THE BASAL COVER
1272      BDBL = DBL * BCFUNC
1273      BRES = RES * BCFUNC
1274      BGL = GL * BCFUNC
1275      BGD = GD * BCFUNC
1276      BCL = CL * BCFUNC
1277      BCD = CD * BCFUNC
1278      BBL = BL * BCFUNC
1279      BBG = BG * BCFUNC
1280      BSL = SL * BCFUNC
1281      BSD = SD * BCFUNC
1282      BRL = RL * BCFUNC
1283      BRD = RD * BCFUNC
1284      BTR = TR * BCFUNC
1285      BDMG = DMG * BCFUNC
1286      BP = P * BCFUNC
1287      BASSIM = ASSIM * BCFUNC
1288      BRESP = RESP * BCFUNC
1289      BTG = BGL + BGD
1290      BTC = BCL + BCD
1291      BTB = BBL + BBG
1292      BTS = BSL + BSD
1293      BTRO = BRL + BRD
1294      TP = BTG + BTC + BTB

```

##

```

1295     PPROD = PPRODO * (1.0 - J / 210.0)
1296     IF (PPROD <= 0.0) THEN
1297         PPROD = 0.0
1298     END IF
1299     TPROD = TP + PPROD
1300     IF (JDA == 211) THEN
1301         ANA = "JUL"
1302     END IF
1303     IF (JDA == 241) THEN
1304         ANA = "AUG"
1305     END IF
1306     IF (JDA == 271) THEN
1307         ANA = "SEP"
1308     END IF
1309     IF (JDA == 301) THEN
1310         ANA = "OCT"
1311     END IF
1312     IF (JDA == 331) THEN
1313         ANA = "NOV"
1314     END IF
1315     IF (JDA == 361) THEN
1316         ANA = "DEC"
1317     END IF
1318     IF (JDA == 26) THEN
1319         ANA = "JAN"
1320     END IF
1321     IF (JDA == 56) THEN
1322         ANA = "FEB"
1323     END IF
1324     IF (JDA == 86) THEN
1325         ANA = "MAR"
1326     END IF
1327     IF (JDA == 116) THEN
1328         ANA = "APR"
1329     END IF
1330     IF (JDA == 146) THEN
1331         ANA = "MAY"
1332     END IF
1333     IF (JDA == 176) THEN
1334         ANA = "JUN"
1335     END IF
1336     IF (OD == "Y") THEN
1337         WRITE (5,516) JDA, BCL, BCD, BBL, BBD, BSL, BSD,
1338 &             TP, PPROD, TPROD, BCON, AL
1339     END IF
1340     IF (TP > TPMAKS) THEN
1341         JDMAKS = JDA
1342         TPMAKS = TP
1343     END IF
1344     TFI = 0.0

```

```

1345      TFT = 0.0
1346      TFW = 0.0
1347      TF = 0.0
1348      TFFMAX = 0.0
1349      TEF = 0.0
1350      TP = 0.0
1351      TRESP = 0.0
1352      TASSIM = 0.0
1353      TRFD = 0.0
1354      TDMG = 0.0
1355      TFFDMG = 0.0
1356      TPNF = 0.0
1357
1358      END DO !End of J-loop starting in line 398
1359      SSLWP1 = SLWAT1(J - 1) / SDP1 * 100.0
1360      SSLWP2 = SLWAT2(J - 1) / SDP2 * 100.0
1361      WHCTEMP = WHC
1362      PRVISC = C * 25.0 / 100.0 * BCOVER / 100.0
1363      WRITE (6,517) "THE MAXIMUM BIOMASS PRODUCTION OF ", TPMAKS,
1364 &      " (KG/HA) WAS REACHED ON DAY ", JDMAKS
1365      WRITE (6,518) "THE NUMBER OF MOISTURE STRESS DAYS = ", ITTRE
1366      WRITE (6,519) "RESERVES (kg/ha) ON 1 JULY = ", PRVISC
1367      WRITE (6,519) "RESIDUAL PRODUCTION ON 1 JULY ", TPROD
1368      WRITE (6,519) "A-HORIZON SWC (%) ON 30 JUNE = ", SSLWP1
1369      WRITE (6,519) "B-HORIZON SWC (%) ON 30 JUNE = ", SSLWP2
1370
1371      ! WRITE THE STATS FILE                                     ##
1372      WRITE (11,527) YEAR, ", TPMAKS = ", TPMAKS, ", PRVISC = ", PRVISC,
1373 &      ", MSD = ", ITTRE, ", DOY = ", JDMAKS
1374
1375      ITTRE = 0
1376      CLOSE (2)
1377      CLOSE (4)
1378      CLOSE (5)
1379      CLOSE (6)
1380      CLOSE (7)
1381      CLOSE (8)
1382
1383      ! *****
1384      ! *                UPDATE SOIL FILE (INFOG)                *
1385      ! *****
1386      SSLWP1 = 19.68
1387      SSLWP2 = 19.68
1388      WHC1 = 41.00
1389      WHC2 = 36.91
1390      WHC3 = 28.61
1391      WHC4 = 19.68
1392      SDP = 1000.0
1393      BCOVER = 10.0
1394      CUT1 = 366

```

1395 CUT2 = 366
1396 CUT3 = 366
1397 CUT4 = 366
1398 ITERM = 1
1399 NN = 0
1400 JDMAKS = 0
1401 GRSTGE = 1
1402 MKOUNT = 35
1403 TNEXT = 1
1404 PO = 3240.0
1405 FE = 0.0000001
1406 COMM = 0.66
1407 BA = 200.0
1408 C30 = 0.01
1409 CONS = 0.5
1410 HUCRIT = 250.0
1411 HUCRMN = 225.0
1412 BO = 12.0
1413 VCS = 97.0
1414 SPL = 500.0
1415 TMPD = 20.0
1416 WPC = -1800.0
1417 LP = 1
1418 HYCON = 0.01
1419 BCON = 40.0
1420 RUNPAR = 0.1
1421 DRAINP = 0.9
1422 PPRODO = 1200.0
1423 OPEN (1, FILE=SOIL)
1424 WRITE (1, 501) STATION
1425 WRITE (1, 501) DAT(1)
1426 WRITE (1, 501) DAT(2)
1427 WRITE (1, 503) SSLWP1
1428 WRITE (1, 503) SSLWP2
1429 WRITE (1, 503) WHC1
1430 WRITE (1, 503) WHC2
1431 WRITE (1, 503) WHC3
1432 WRITE (1, 503) WHC4
1433 WRITE (1, 503) SDP
1434 WRITE (1, 503) BCOVER
1435 WRITE (1, 504) CUT1
1436 WRITE (1, 504) CUT2
1437 WRITE (1, 504) CUT3
1438 WRITE (1, 504) CUT4
1439 WRITE (1, 504) ITERM
1440 WRITE (1, 503) PRVISC
1441 WRITE (1, 504) NN
1442 WRITE (1, 504) JDMAKS
1443 WRITE (1, 503) TPKAKS
1444 WRITE (1, 504) GRSTGE


```

1445 WRITE (1, 504) MKOUNT
1446 WRITE (1, 504) TNEXT
1447 WRITE (1, 503) PO
1448 WRITE (1, 505) FE
1449 WRITE (1, 503) COMM
1450 WRITE (1, 503) BA
1451 WRITE (1, 503) C30
1452 WRITE (1, 503) CONS
1453 WRITE (1, 503) HUCRIT
1454 WRITE (1, 503) HUCRMN
1455 WRITE (1, 503) BO
1456 WRITE (1, 503) VCS
1457 WRITE (1, 503) SPL
1458 WRITE (1, 503) TMPD
1459 WRITE (1, 503) WPC
1460 WRITE (1, 504) LP
1461 WRITE (1, 503) HYCON
1462 WRITE (1, 503) BCON
1463 WRITE (1, 503) RUNPAR
1464 WRITE (1, 503) DRAINP
1465 WRITE (1, 503) PPRODO
1466 CLOSE (1)

```

```

1467
1468 ! *****
1469 ! * RE-INITIALISING VARIABLES *
1470 ! *****
1471 AMX = 0.0
1472 AMN = 0.0
1473 AVET = 0.0
1474 EVAP = 0.0
1475 RAIN = 0.0
1476 SUN = 0.0
1477 SLWAT = 0.0
1478 SLWAT1 = 0.0
1479 SLWAT2 = 0.0
1480 SLWP1 = 0.0
1481 SLWP2 = 0.0
1482 X = 0.0
1483 R = 0.0
1484 A = 0.0
1485 ABSB = 0.0
1486 ABSC = 0.0
1487 ABSG = 0.0
1488 ABSR = 0.0
1489 ABSS = 0.0
1490 AE = 0.0
1491 AECVAP = 0.0
1492 AGRB = 0.0
1493 AGRC = 0.0
1494 AGRG = 0.0

```

1495 AGRR = 0.0
1496 AGRS = 0.0
1497 AI1 = 0.0
1498 AI2 = 0.0
1499 AI3 = 0.0
1500 AL = 0.0
1501 ALAI = 0.0
1502 ALPHA = 0.0
1503 ARGU = 0.0
1504 ASSIM = 0.0
1505 ATEMP = 0.0
1506 AX = 0.0
1507 B = 0.0
1508 BA = 0.0
1509 BASSIM = 0.0
1510 BBD = 0.0
1511 BBL = 0.0
1512 BCD = 0.0
1513 BCFUNC = 0.0
1514 BCL = 0.0
1515 BCON = 0.0
1516 BCOVER = 0.0
1517 BD = 0.0
1518 BDBL = 0.0
1519 BDMG = 0.0
1520 BETA = 0.0
1521 BGD = 0.0
1522 BGL = 0.0
1523 BL = 0.0
1524 BLM = 0.0
1525 BLTT = 0.0
1526 BO = 0.0
1527 BP = 0.0
1528 BRD = 0.0
1529 BRES = 0.0
1530 BRESP = 0.0
1531 BRL = 0.0
1532 BSD = 0.0
1533 BSL = 0.0
1534 BTB = 0.0
1535 BTC = 0.0
1536 BTG = 0.0
1537 BTR = 0.0
1538 BTRO = 0.0
1539 BTS = 0.0
1540 C = 0.0
1541 C30 = 0.0
1542 CD = 0.0
1543 CL = 0.0
1544 CLIVE = 0.0

1545 COEF = 0.0
1546 COMM = 0.0
1547 CONS = 0.0
1548 CPHA = 0.0
1549 DAYFRC = 0.0
1550 DBL = 0.0
1551 DMG = 0.0
1552 DPROB = 0.0
1553 DPROC = 0.0
1554 DPROG = 0.0
1555 DPROR = 0.0
1556 DPROR = 0.0
1557 DRAIN1 = 0.0
1558 DRAIN2 = 0.0
1559 DRAINP = 0.0
1560 DRES = 0.0
1561 DRN1P = 0.0
1562 EE = 0.0
1563 EFF = 0.0
1564 EFFDMG = 0.0
1565 EFFMAX = 0.0
1566 F = 0.0
1567 FC1 = 0.0
1568 FC2 = 0.0
1569 FE = 0.0
1570 FG = 0.0
1571 FI = 0.0
1572 FRACL = 0.0
1573 FT = 0.0
1574 FW = 0.0
1575 GD = 0.0
1576 GL = 0.0
1577 GLO = 0.0
1578 GS = 0.0
1579 GWP = 0.0
1580 GWPST = 0.0
1581 HU = 0.0
1582 HUCRIT = 0.0
1583 HUCRMN = 0.0
1584 HYCON = 0.0
1585 INFIL = 0.0
1586 IRRIG = 0.0
1587 LWP = 0.0
1588 MAIN = 0.0
1589 P = 0.0
1590 PE = 0.0
1591 PECONS = 0.0
1592 PECVAP = 0.0
1593 PNF = 0.0
1594 PO = 0.0

1595 PPROD = 0.0
1596 PPRODO = 0.0
1597 PRVISC = 0.0
1598 PWP1 = 0.0
1599 PWP2 = 0.0
1600 RD = 0.0
1601 RES = 0.0
1602 RESP = 0.0
1603 RFD = 0.0
1604 RFDM = 0.0
1605 RL = 0.0
1606 RUNOF = 0.0
1607 RUNPAR = 0.0
1608 SD = 0.0
1609 SDP = 0.0
1610 SDP1 = 0.0
1611 SDP2 = 0.0
1612 SL = 0.0
1613 SLVAP = 0.0
1614 SOLK = 0.0
1615 SPL = 0.0
1616 STRESS = 0.0
1617 SSLWP1 = 0.0
1618 SSLWP2 = 0.0
1619 TASSIM = 0.0
1620 TDMG = 0.0
1621 TDRAIN = 0.0
1622 TEFF = 0.0
1623 TF = 0.0
1624 TFFDMG = 0.0
1625 TFFMAX = 0.0
1626 TFI = 0.0
1627 TFT = 0.0
1628 TFW = 0.0
1629 TGROW = 0.0
1630 TLRB = 0.0
1631 TLRC = 0.0
1632 TLRG = 0.0
1633 TLRR = 0.0
1634 TLRS = 0.0
1635 TMPD = 0.0
1636 TNITE = 0.0
1637 TP = 0.0
1638 TPMAKS = 0.0
1639 TPNF = 0.0
1640 TPROD = 0.0
1641 TR = 0.0
1642 TRANS1 = 0.0
1643 TRANS2 = 0.0
1644 TRESP = 0.0

```

1645      TRFD = 0.0
1646      TRUNOF = 0.0
1647      VB = 0.0
1648      VC = 0.0
1649      VG = 0.0
1650      VR = 0.0
1651      VS = 0.0
1652      VCS = 0.0
1653      WAT = 0.0
1654      WHC = 0.0
1655      WHC1 = 0.0
1656      WHC2 = 0.0
1657      WHC3 = 0.0
1658      WHC4 = 0.0
1659      WHCTEMP = 0.0
1660      WJ = 0.0
1661      WPC = 0.0
1662      WST = 0.0
1663      XX = 0.0
1664      CNT = 0
1665      CUT = 0
1666      CUT1 = 0
1667      CUT2 = 0
1668      CUT3 = 0
1669      CUT4 = 0
1670      DAG = 0
1671      EX = 0
1672      GRSTGE = 0
1673      IKOUNT = 0
1674      INDEKS = 0
1675      ITERM = 0
1676      ITTRE = 0
1677      J = 0
1678      JDA = 0
1679      JDMAKS = 0
1680      JMAX = 0
1681      JR = 0
1682      LP = 0
1683      MKOUNT = 0
1684      NMNTH = 0
1685      NN = 0
1686
1687      ! *****
1688      ! *                               FORMAT STATEMENTS                               *
1689      ! *****
1690
1691      501  FORMAT (A)
1692      502  FORMAT (A,A,2X,A,A)
1693      503  FORMAT (F10.2)
1694      504  FORMAT (I4)

```

```

1695 505  FORMAT (F11.7)
1696 506  FORMAT (7X,I1,23X,A,1X,I4)
1697 507  FORMAT ( )
1698 508  FORMAT (14X,I2,4X,F4.1,5(3X,F5.1))
1699 509  FORMAT (2X,A,A,A,F6.1,A)
1700 510  FORMAT (A,A,A,I3)
1701 511  FORMAT (I4,20(1X,F6.1))
1702 512  FORMAT (A,I4,I4,F6.1)
1703 513  FORMAT (A,I4,A,F5.1,A)
1704 515  FORMAT (A,F6.1,A,I4)
1705 516  FORMAT (I4,11(1X,F6.1))
1706 517  FORMAT (A,F7.2,A,I4)
1707 518  FORMAT (A,I4)
1708 519  FORMAT (A,F7.2)
1709 527  FORMAT (I4,A,F10.2,A,F10.2,A,I4,A,I4)
1710 999  FORMAT (I4,1X,A)
1711      ! *****
1712
1713 50      READ (15, 999, IOSTAT=DSTAT) YEAR, WDIR
1714      ENDDO
1715      CLOSE(15)
1716      END PROGRAM PUTU VELD

```

APPENDIX B

Table of FORTRAN variable names, their meanings, initial values and units of measure.

VARIABLE	EXPLANATION	VALUE	UNIT
A	Exponent of Co-efficient		
ABSB	Leaves	12500	kg.ha ⁻¹
ABSC	Culms	12500	kg.ha ⁻¹
ABSG	Seeds	300	kg.ha ⁻¹
ABSR	Roots	50000	kg.ha ⁻¹
ABSS	Stubble	25000	kg.ha ⁻¹
AE	Actual evaporation		mm
AECVAP	Ratio of actual evaporation to pan evaporation		
AGRB	Leaves		kg.ha ⁻¹ .d ⁻¹
AGRC	Culms		kg.ha ⁻¹ .d ⁻¹
AGRG	Seeds		kg.ha ⁻¹ .d ⁻¹
AGRR	Roots		kg.ha ⁻¹ .d ⁻¹
AGRS	Stubble		kg.ha ⁻¹ .d ⁻¹
AI1	Exponent of the retention curve intersections		
AI2			
AI3			
AL	Leaf area		ha
ALAI	Leaf area index		
ALPHA	Fraction of net radiation conducted into the soil		
AMN	Average daily minimum temperature		°C
AMX	Average daily maximum temperature		°C
ARGU	Argument of the retention		

ASSIM	Carbohydrate assimilated conversion of P (kg CO ₂ .ha ⁻¹ .d ⁻¹) to kg carboh.ha ⁻¹ .d ⁻¹		kg CHO.ha ⁻¹ .d ⁻¹
ATEMP	Average temperature		°C
AV	Argument for determining end of file		
AVET	Average daily temperature		°C
B	Constant in determining actual evapotranspiration		
B	Total biomass (standing biomass)		kg.ha ⁻¹
BA	Above ground dead biomass	200	kg.ha ⁻¹
BASSIM	Carbohydrate assimilated expressed in terms of BCOVER		
BB	Root biomass		kg.ha ⁻¹
BBD	Leaves dead expressed in terms of BCOVER		
BBL	Leaf mass at the present of basal cover		kg.ha ⁻¹
BCD	Culms dead expressed in terms of BCOVER		
BCFUNC	Basal cover conversion factor		kg.ha ⁻¹
BCL	Culms living expressed in terms of BCOVER		
BCON	Growth rate of the leaves	40	kg.ha ⁻¹ .d ⁻¹
BCOVER	Basal cover of the canopy	10	%
BD	Leaves dead		kg.ha ⁻¹
BDBL	Leaf mass change demand in terms of BCOVER		kg.ha ⁻¹ .d ⁻¹
BDMG	Dry matter gain in terms of BCOVER		
BETHA	Atmosphere permeability		
BGD	Seeds dead in terms of BCOVER		
BGL	Seeds living in terms of BCOVER		
BL	Leaves living		kg.ha ⁻¹
BLM	Minimum leaf size to terminate vegetative growth stage	4600	kg.ha ⁻¹
BLT	Minimum leaf size before heat units are accumulated	2900	kg.ha ⁻¹
BO	Minimum temperature for heat units	12	°C
BP	P expressed in terms of BCOVER		
BRD	Roots dead in terms of BCOVER		

BRES	Reserves expressed in terms of BCOVER		
BRESP	Respiration expressed in terms of BCOVER		
BRL	Roots living expressed in terms of BCOVER		
BSD	Stubble dead expressed in terms of BCOVER		
BSL	Stubble living expressed in terms of BCOVER		
C	Total plant mass at 100% basal cover		kg.ha ⁻¹
C30	Maintenance respiration constant	0.01	
CA	Above ground standing crop		kg.ha ⁻¹
CB	Below ground standing crop		kg.ha ⁻¹
CD	Culms dead		kg.ha ⁻¹
CEVAP	Class A-Pan evaporation		mm
CL	Culms living		kg.ha ⁻¹
CLIVE	All living parts (Roots, leaves, stubble excluding culms)		
CNT	Counter for days after rain		d
COEF	Coefficient of each graph intersection		
COMM	CO ₂ to carbohydrate conversion factor	0.66	
CONS	Construction respiration constant	0.5	
CUT	Cutting dates	365	dos
D	Total dead matter		kg.ha ⁻¹
DA	Above ground dead biomass		kg.ha ⁻¹
DAE	Days in each month		d
DALEN	Day length		h
DAT1	Year simulations begin		
DAT2	Year simulations end		
DAYFRC	Fraction of daily possible sunshine duration		
DB	Root biomass dead		kg.ha ⁻¹
DBL	Leaf mass change demand		kg.ha ⁻¹ .d ⁻¹
DIR	Directory		

DMG	Daily dry matter gain			kg CHO.ha ⁻¹ .d ⁻¹
DPROB	Leaves	} Desired proportions for each component during a specific growth stage		kg.ha ⁻¹
DPROC	Culms			kg.ha ⁻¹
DPROG	Seeds	} Desired proportions for each component during a specific growth stage		kg.ha ⁻¹
DPROR	Roots			kg.ha ⁻¹
DPROS	Stubble			kg.ha ⁻¹
DRAIN1	Drainage from the soil layer 1		0	mm
DRAIN2	Drainage from the soil layer 2		0	mm
DRAINP	Drainage from the whole soil profile		0.9	mm
DRES	Change in plant reserves			kg.ha ⁻¹
EE	Equilibrium evapotranspiration			mm
EFF	Actual efficiency of photosynthesis			%
EFFDMG	Efficiency of DMG			%
EFFMAX	Potential efficiency of photosynthesis			%
EVAP	Total daily evaporation			mm
EXT1	File extension .txt			
EXT2	File extension .out			
F	Influence of the environment on the efficiency of photosynthesis			%
FC1	Field capacity for soil level 1			%
FC2	Field capacity for soil level 2			%
FE	Photochemical equivalent		100	μg.J ⁻¹
FG	Soil water evaporation rate			
FI	Percentage of radiation absorbed by the canopy			%
FT	Influence of temperature on maximum photosynthesis rate			%
FW	Limitations of water availability on photosynthetic efficiency			%
GD	Seeds dead			kg.ha ⁻¹
GL	Seeds living			kg.ha ⁻¹
GLO	Maximum mass seeds reach during the current growth stage			kg.ha ⁻¹
GROWSTAGE	File containing the 5 growth stages			

GRSTGE	Growth stages (1 - vegetative)		
GS	Constant of equilibrium evapotranspiration		
GWP	Ground water potential		kPa
GWPST	Ground water potential status at a specific intersection of the retention curve		kPa
HU	Heat units		°C
HUCRIT	Heat unit demand for the vegetative growth stage	250	dd
HUCRMN	Minimum heat units required	225	dd
HYCON	Hydraulic conductivity constant	0.006	
IBEGIN	Day begin of water stress		d
IEND	Day end of water stress		d
IKOUNT	Length of active seed forming stage		d
INDEKS	Day of growth season		
INFIL	Infiltration		mm
IRRIG	Irrigation		mm
ITERM	Iteration of interval	7	d
ITTRE	Counter for de-incrementing WPC	1	
IUY	Length of water stress period		d
JDA	Julian days		d
JDMAKS	Day which maximum biomass was reached		dd
JMAX	Length of growing season	365	d
JMAXX	Length of growing season		d
LP	Counter for water stress periods	1	
LWP	Leaf water potential		kPa
MAAND	Month		
MAIN	Maintenance respiration		kg CHO.ha ⁻¹ .d ⁻¹
MKOUNT	Length of next growing season	25	d
NMNTH	nth month of the season		
NPL	Number of plants per m ²	90	
OD	Daily output		

P	Potential of CO ₂ assimilation		kg CO ₂ .ha ⁻¹ .d ⁻¹
PE	Potential evaporation		mm
PECONS	Constant for determining potential evapotranspiration	1.28	
PECVAP	Ratio of potential evaporation to pan evaporation		
PLACE	Location of station		
PO	Maximum capacity of CO ₂ exchange	3240	kg.ha ⁻¹ .d ⁻¹
PRIVSC	Previous season's production (reserves on 1 July)	2000	kg.ha ⁻¹
PWP1	Permanent wilting point for soil level 1		%
PWP2	Permanent wilting point for soil level 2		%
R	Mass flow variables with respect to the rate of translocation		kg
RAIN	Total daily rainfall		mm
RD	Roots dead		kg.ha ⁻¹
RES	Carbohydrate reserves		kg.ha ⁻¹
RESP	Respiration		kg CHO.ha ⁻¹ .d ⁻¹
RFD	Radiant flux density		J.m ⁻² .d ⁻¹
RFDM	Mean radiant flux density		W.m ⁻² .s ⁻¹
RL	Roots living		kg.ha ⁻¹
RUNOF	Runoff from soil surface	0	mm
SD	Stubble dead		kg.ha ⁻¹
SDP	Depth of root zone	600	mm
SDP1	Depth of soil level 1	100	mm
SDP2	Depth of soil level 2	500	mm
SL	Stubble living		kg.ha ⁻¹
SLVAP	Soil water evaporation		mm
SLWAT	Soil water content of the whole soil profile		mm
SLWAT1	Soil water content of soil level 1		mm
SLWAT2	Soil water content of soil level 2		mm
SLWP1	A Horizon soil water content on 30 June	19.68	%

SLWP2	B Horizon soil water content on 30 June	19.68	%
SO	File name for soil variables		
SOIL	File containing soil information		
SOLK	Solar constant		J.m ⁻¹ .d ⁻¹
SPL	Specific leaf area ratio	500	kg.ha ⁻¹
STAGE	Growth stage		
STATION	Name of station		
SUN	Total daily sunshine hours		h
TASSIM	Accumulated assimilated carbohydrates		kg CHO.ha ⁻¹ .d ⁻¹
TDMG	Accumulated DMG		kg CHO.ha ⁻¹ .d ⁻¹
TDRAIN	Accumulated drainage		mm
TEFF	Accumulated EFF		%
TELLER	Counter		
TF	Accumulated F		%
TFFDMG	Accumulated EFFDMG		%
TFI	Accumulated FI		%
TFT	Accumulated FT		%
TFW	Accumulated FW		%
TGROW	Average temperature		°C
TLRB	Leaves	Indicates the different translocation rates for each plant component	kg.ha ⁻¹ .d ⁻¹
TLRC	Culms		kg.ha ⁻¹ .d ⁻¹
TLRG	Seeds		kg.ha ⁻¹ .d ⁻¹
TLRR	Roots		kg.ha ⁻¹ .d ⁻¹
TLRS	Stubble		kg.ha ⁻¹ .d ⁻¹
TMXPD	Maximum temperature of the previous day	20	°C
TNEXT	Next = counter for repeating the phenological cycle	1	
TNITE	The average night time temperature for day j		°C
TNSLOC	Translocation		mm
TP	Biomass production		kg.ha ⁻¹

TPMAKS	Maximum biomass production for the growth season	2000	kg.ha ⁻¹
TPROD	Residual production on 1 July		kg.ha ⁻¹
TPTEST	Flag in argument for determining water stress days	3	
TR	Total rainfall		mm
TRANS1	Transpiration from soil level 1	0	mm
TRANS2	Transpiration from soil level 2	0	mm
TRESP	Accumulated respiration		kg.CHO.ha ⁻¹ .d ⁻¹
TRFD	Accumulated RFD		W.m ⁻²
TRUNOF	Accumulated runoff		mm
VCS	Rangeland condition score	90	%
VB	Leaves	Proportional requirements for each plant component	
VC	Culms		
VG	Seeds		
VR	Roots		
VS	Stubble		
WEATHER	File containing weather variables		
WHC	Initial water holding capacity	7.32	%
WHC1	Water holding capacity at 10 kPa	41	%
WHC2	Water holding capacity at 22 kPa	36.91	%
WHC3	Water holding capacity at 148 kPa	28.61	%
WHC4	Water holding capacity at 2440 kPa	19.68	%
WJ	Actual solid water content		%
WPC	Water potential content (for determining stress)	-1800	kPa
WPL	Water potential of the leaf		kPa
WST	Water stress at a specific intersection of the retention curve		%
WX	File name for weather variables		
X	Mass flow variables for mass flow from living plant parts to dead plant parts		kg.ha ⁻¹
XX	Argument in determining the solar constant		

APPENDIX C

Table of program explanation.

STATEMENT NUMBER	EXPLANATION
1 – 17	Start of PUTUVELD Model.
19 – 65	Variable declarations.
67 – 107	File declarations.
78 – 88	Open files.
75 – 79	Read growth stage file.
119 – 200	Comment lines showing the diagram of all plant components and their variable names.
204 – 272	Set initial statuses and parameters (read soil file).
274 – 292	Calculate soil water content and soil depth.
294 – 358	Read weather data file, check for leap years and calculate total rainfall for each month.
361 – 390	Determine the initial masses of the different plant components.
393 – 405	Start of simulations per day for the growth season.
407 – 419	Start of the water balance subsection for calculations of the different soil parameters.
420 – 453	Comment lines declaring the variables and their FORTRAN designation.
45 – 480	Compute the exponents of the retention curve.
482 – 455	Calculate the average temperature and the constant for determining equilibrium evapotranspiration (ET).
486 – 406	Determine the Julian day of the year and radiant flux density.
508 – 525	Calculate the equilibrium ET and the ratio to pan evaporation.
527 – 537	Calculate an index of plant coverage as a result of the leaf area (AL).
539 – 541	Calculate the leaf water potential.
543 – 555	Calculate the limitation of water availability on photosynthesis efficiency.
557 – 574	Calculate evaporation rate of rainfall.
576 – 586	Calculate runoff from the soil surface.
588 – 649	Calculate the soil water evaporation, transpiration from the soil, drainage, recharge and actual water content of both layers.

651 – 674	A means of reducing soil water during winter (after day 300) by 0.3 mm.d^{-1}
676 – 681	Write output data to the appropriate output file.
687 – 713	Calculate the influence of solar radiation (FI), temperature (FT) and water availability (FW) on the maximum rate of photosynthesis.
715 – 736	The beginning and end as well as the number of water stress days are computed for the whole growing season.
738 – 759	The efficiency of photosynthesis in accordance to the maximum efficiency of photosynthesis and the influence of the environment is computed.
761 – 768	Calculation of CO_2 assimilation in accordance to the efficiency previously described.
770 – 793	Convert the CO_2 assimilated to carbohydrates, calculate carbohydrate break down due to respiration and the nett dry matter gain per day is the result of assimilation minus respiration.
799 – 810	Determine the phenological growth stage.
813 – 865	The 1 st growth stage (vegetative) is terminated when the leaf mass per hectare exceeds 4600 kg.ha^{-1} and the heat demand has been met. After Julian day 258, if frost has occurred, then the growth stage is terminated.
867 – 877	Determine the growth rate of the leaves and accumulate the heat units provided that the leaf mass exceeds the critical minimum (BLT).
879 – 891	Calculate the leaf mass change demand and the mass flow variables for mass flow from the living to dead components of the plant.
892 – 906	Set the desired proportions and other parameters for the next growth stage.
909 – 925	The 2 nd growth stage (reproductive) is terminated after 25 days of growth provided that the production of culms exceeds 25% of the mass of the leaves. The same temperature conditions as for the vegetative stage can terminate this growth stage.
927 – 931	Determine the mass flow variables concerned with the reproductive growth stage.
932 – 945	Set the desired proportions, growth stage flag and length of the next growth stage.
948 – 963	The 3 rd growth stage (seed) is terminated after 50 days of seed formation or under the same temperature conditions as stated in the other growth stages.

964 – 973	Determine the mass flow variables concerned with this growth stage.
974 – 986	Set the desired proportions and growth stage flag.
989 – 996	The 4 th growth stage (seed fall) is terminated on the first occurrence of frost.
997 – 1015	Determine the mass flow variables concerned with this growth stage.
1017 – 1021	Set next growth stage flag.
1024 – 1045	The 5 th growth stage (dormancy) is terminated if production has been cut or will persist till the end of the growing season. Set the mass flow variables for this growing season.
1046 – 1087	If the production has been cut reset initial statuses and go back to growth stage 1 only if the growing season does not exceed 258 days.
1097 – 1128	Set the maximum (absolute) growth rates for plant components concerned during each growth stage.
1130 – 1164	Calculate the proportional requirements.
1166 – 1172	Calculate the different translocation rates.
1174 – 1187	Calculate the mass flow variables. i.e. the mass flow from plant reserves to the living components of the plant.
1189 – 1192	Determine the availability of plant reserves and if reserves are insufficient, reset the mass flow variables.
1198 – 1212	Calculate the mass of the different plant components and prepare the output data.
1218 – 1362	Preparing output data and writing average over the iteration interval for the environmental controlling factors and the accumulated values over this interval for the plant variables.
1363 – 1374	Writing data to the output files.
1375 – 1381	Close files.
1384 – 1466	Update soil file (INFOG) with the current TPMAKS and PRVISC values as the new values for both these variables for the beginning of the next simulation year.
1469 – 1685	Re-initializing of variables in order to continuously run the model for consecutive years.
1688 – 1711	Format statements.
1324 – 1337	Close files and end PUTUVELD model.

APPENDIX D

The input file (INFOG) with the variables as used by the PUTU VELD model for the simulations.

VARIABLE	VALUE	VARIABLE	VALUE
BEGIN	2010	TNEXT	1
END	2098	PO	3240
SLWP1	19.68	FE	0.0000001
SLWP2	19.68	COMM	0.66
WHC1	41.00	BA	200
WHC2	36.91	C30	0.01
WHC3	28.61	CONS	0.5
WHC4	19.68	HUCRIT	250
SDP	1000	HUCRMN	225
BCOVER	10	BO	12
CUT1	366	VCS	97
CUT2	366	SPL	500
CUT3	366	TMXPD	20
CUT4	366	WPC	-1800
ITERM	1	LP	1
PRVISC	2000	HYCON	0.01
NN	0	BCON	40
JDMAKS	0	RUNPAR	0.1
TPMAKS	2000	DRAINP	0.9
GRSTGE	1	PPRODO	1200
MKOUNT	35		

APPENDIX E

An example of the format for 1 month's weather data file as used by the PUTU VELD model.

Flag	Latitude	Longitude	Altitude	Station	Month	Year	
1		2925	2612	1371	BFN SW	JUL	2010
	DAY	MAXT	MINT	RAIN	EVAP	SUN	AVE T
	1	15.4	-5.9	0	1.7	10.5	4.8
	2	16.4	-5.4	0	1.8	10.7	5.5
	3	16.4	-6.8	0	1.8	11.2	4.8
	4	17	-6.7	0	1.9	11.3	5.2
	5	17	-7.2	0	1.9	11.5	4.9
	6	17.7	-5	0	1.9	11.1	6.4
	7	19	-3.8	0	2	11.1	7.6
	8	17.5	-1.6	0	1.9	9.7	8
	9	17.7	-4.8	0	2	11	6.5
	10	19.2	-5.3	0	2.1	11.7	7
	11	19.8	-4.7	0	2.1	11.8	7.6
	12	19.2	-3.2	0	2.1	11	8
	13	20.1	-3.7	0	2.2	11.5	8.2
	14	20.1	-4.8	0	2.2	12	7.7
	15	18.8	-3.9	0	2.1	11.2	7.5
	16	19	-2.5	0	2.1	10.7	8.3
	17	17.9	0.7	0	2	9	9.3
	18	17.7	-1.7	0	2	10	8
	19	20.2	0	0	2.2	10.3	10.1
	20	18.8	-4.6	0	2.2	11.6	7.1
	21	22.1	-0.4	0	2.5	11.2	10.9
	22	22.3	-0.2	0	2.5	11.2	11.1
	23	22.2	-0.3	0	2.5	11.2	11
	24	20.9	-0.2	0	2.4	10.7	10.4
	25	22.4	-1.3	0	2.6	11.8	10.6
	26	21.5	-0.4	0	2.5	11.1	10.6
	27	18.7	-1	0	2.2	10.3	8.9
	28	19	-2.2	0	2.3	10.9	8.4
	29	19.4	-1.4	0	2.3	10.7	9
	30	21.6	1.5	0	2.5	10.5	11.6
	31	19.4	8.8	0.8	2	6.1	14.1
1		2925	2612	1371	BFN SW	AUG	2010
	DAY	MAXT	MINT	RAIN	EVAP	SUN	AVE T
	1	23.1	7.5	0.2	2.5	8.7	15.3

9							